



UNIVERSITY OF
LEICESTER

Circadian Regulation Through The
Binding of Heme to *Drosophila*
Melanogaster PER-PAS

A thesis submitted for the degree of
Doctor of Philosophy in Chemistry

By

Raof Jabbar Abbas MaarooF
MSc. Chemistry

Department of Chemistry
University of Leicester
United Kingdom
September 2018

Statement

Unless otherwise acknowledged, the experimental work described in this thesis has been carried out by the author in the Henry Wellcome Laboratories at the University of Leicester between October 2014 and September 2017. The work has not been submitted and is not presently being submitted for any other degree at this or any other university.

Signed:

Name : Raof Jabbar Abbas Maarof

Date : September 2018

Department of Chemistry
University of Leicester
University Road
Leicester, LE1 7RH
UK

Circadian Regulation Through The Binding of Heme to *Drosophila Melanogaster* PER-PAS

Raof Jabbar Abbas Maarof

Abstract

In *Drosophila*, the clock gene period (*per*), is an integral component of the circadian clock and acts via a negative auto regulatory feedback loop. Comparative analyses of *per* genes in insects and mammals have revealed that they may function in similar ways.

PERIOD proteins are central components of the *Drosophila* and mammalian circadian clocks. Their function is controlled by daily changes in synthesis, cellular localization, phosphorylation, degradation, as well as specific interaction with other clock components. A comparison between the *Drosophila* and the mammalian circadian clock system reveals many similarities and differences amongst them.

In *Drosophila* there are two *period* genes (*per1*, *per2*). PERIOD is a transcriptional regulatory factor involved in metazoan circadian rhythms. In *Drosophila melanogaster*, PERIOD2 (dPER2) dimerises with TIMELESS (TIM) and the complex enters the nucleus and disrupts the DNA binding of the transcriptional activator heterodimer CLOCK/CYCLE (or dBMAL1). The dCLOCK/dBMAL1 complex is a transcriptional activator for both *per* and *tim* genes and hence PER and TIM inhibit their own expression through a negative feedback mechanism.

In more recent years, the role of heme in biology appears to also include a regulatory function in the cell; some proteins involved in transcription, like the CLOCK proteins, are known to interact with heme via their PAS domains. This work endeavours to investigate the effect of heme on the dPER protein.

In this work, we have cloned and expressed constructs of *Drosophila per2* in *E. coli*; including the PAS-A, PAS-B, PAS-AB and PAS- AB α domains of the protein. These structures were designed in three trials. In each trial, the different regions of the *per* gene was expressed to identify the heme binding domain and characterise the binding. Constructs were designed with a range of purification tags (His, GST, MBP and trial without tag) to enable soluble protein expression. We have used difference absorption spectroscopy to examine whether the dPER-PAS fragments (dPER-PAS-A, dPER-PAS-B, dPER-PAS-AB and dPER-PAS-AB α) are able to bind heme. The difference absorption spectra obtained after addition of increasing amounts of heme to dPER-PAS-A, dPER-

PAS-B, dPER-PAS-AB and dPER-PAS-AB α show that heme can form a complex with all four domains above with a Soret band at $\sim 423\text{nm}$.

To support the finding of heme binding to these dPER-PAS fragments, Electron Paramagnetic Resonance (EPR) was performed. EPR showed binding between heme and a cysteine within the dPER domain in a 1:1 ratio. There are eight cysteines in the dPER domain. To find out whether this interaction is specific, two single mutants were made for each of dPER-PAS-A (C312A, C369A), dPER-PAS-B (C455A, C467A), dPER-PAS-AB (C312A, C455A) and dPER-PAS-AB α (C312A, C455A). There was no significant change to the heme binding properties of mutant domains as measured by UV-visible spectroscopy. This suggests that the heme binding occurs in one of the cysteines that we have yet to look at in this study. Additionally, we attempted to make dPER-PAS-A, dPER-PAS-B, dPER-PAS-AB, and dPER-PAS-AB crystals complexed with heme to identify the site and the amino acids responsible for heme binding. Conditions resulting in crystalline dPER-PAS-A were discovered.

Overall, in this project we have shown that the dPER protein is capable of binding heme. Each of the domains studied here (PAS-A, PAS-B, PAS-AB) are capable, on their own, of heme binding. We have demonstrated that the binding of heme to dPER is via a cysteine residue, however loss of cysteine through mutagenesis at positions C312, C369, C455, and C467, is not sufficient to ablate the heme binding activity of dPER.

Acknowledgements

First of all, my great thanks are to the Ministry of Higher Education and Scientific Research in Iraq for providing the funding for this PhD.

I gratefully acknowledge my project supervisor Professor Emma Raven for providing the opportunity to work in her research group on this fascinating topic as well as for the time and advice she has offered me throughout.

Many thanks to Dr. Andrew Hudson for his help and for acting as my supervisor over the last part of my PhD.

I would like to give special and big thanks to Dr. Sofia Kapetanaki for dedicating so much time to guiding my work and teaching me a great deal in this area of science. Also great thanks to Dr. Helena Wright, Dr. Nico Portolano and Dr. Ayhan Celik.

Special thanks to Dr. Dima Svistunenko the director of Biomedical of EPR facility (University of Essex) for collecting the EPR data on several protein samples for me and then helping to analyse the spectra and to the late Dr. Xiaowen Yang for his help with cloning into pLEICS vectors at Protein Expression Laboratory (PROTEX).

Many thanks go to my best friends and my colleagues Dr. Samuel Freeman and Dr. Simon Fung.

Finally, I would like to extend my thanks to the rest of the Raven group, namely Dr. Jaswir Basran, Dr. Hanna Kwon.

Raouf Jabbar Abbas Maarouf

Table of Contents

Statement	I
Abstract	II
Acknowledgements	IV
Abbreviations and Acronyms	XI
Amino acids	XI
Chemicals and Materials.....	XII
Techniques	XIII
Proteins	XIII
Units/Symbols.....	XIV
Miscellaneous	XV
1. Introduction.....	2
1.1. Circadian Cycle and Regulation.....	2
1.2. Mammalian Clock.....	8
1.3. <i>Drosophila</i> Clock.....	8
1.4. Transcription Factors	9
1.5. PAS Domains	11
1.5.1. <i>Drosophila Melanogaster</i> CLOCK and <i>Drosophila Melanogaster</i> CYC Complex with E-box DNA	12
1.5.2. <i>Drosophila Melanogaster</i> PER-PAS	13
1.6. Heme	15
1.6.1. Biological Role of Heme with PER Protein	18
1.7. Hemeprotein.....	19
1.7.1. Types of Hemeproteins.....	19
1.8. Aims of Project	21
1.9. References	22

2.	Materials and methods	32
2.1.	Materials.....	32
2.1.1.	Chemicals and equipment.....	32
2.2.	Methods.....	32
2.2.1.	Production of Constructs	32
2.2.1.1.	Cloning of dPER-PAS (either A or B or AB)	32
2.2.2.	Molecular Biology	36
2.2.2.1.	Primers Design	36
2.2.2.2.	Polymerase chain reaction (PCR)	37
2.2.2.3.	The dPer-PAS-A construct	37
2.2.2.4.	The dPer-PAS-B construct	38
2.2.2.5.	The dPer-PAS-AB construct.....	39
2.2.2.6.	Mutant Primer Design.....	40
2.2.2.7.	Mutagenesis of dPER-PAS-A, dPER-PAS-B and dPER-PAS-AB	42
2.2.3.	Transformation.....	42
2.2.4.	Expression trials.....	43
2.2.5.	Bugbuster Protocol	43
2.2.6.	SDS-PAGE Gel.....	43
2.2.7.	Large-scale Expression	45
2.2.8.	Purification.....	46
2.2.8.1.	Purification of GST-tagged Protein.....	46
2.2.8.2.	Size Exclusion Chromatography	46
2.2.9.	Protein Refolding	47
2.2.9.1.	Small-scale Preparation of Inclusion Bodies	47
2.2.9.2.	Protein Refolding Small-scale Trials	47
2.2.9.3.	Large-scale Preparation of Inclusion Bodies	47
2.2.9.4.	Large-scale Protein Refolding (condition 5).....	49
2.2.9.5.	Dialysis of refolded Protein	50
2.2.10.	Nickel Affinity Purification	50

2.2.11.	Purification of MBP tag Protein by Amylose Affinity Chromatography	52
2.2.12.	Small-scale Plasmid DNA Purifications	52
2.2.13.	UV-Visible Absorption Spectroscopy.....	53
2.2.14.	Electron Paramagnetic Resonance (EPR)	53
2.2.15.	Circular Dichroism (CD).....	55
2.2.16.	Protein Heme-Binding Titrations	57
2.2.16.1.	Preparation of Hemin Stock Solution.....	57
2.2.16.2.	UV-visible Hemin Titrations.....	57
2.2.16.3.	Ligand Binding Kinetics.....	57
2.2.17.	Protein Crystallisation	59
2.2.17.1.	Setting of Sitting Drop Crystallisation Plates.....	62
2.3.	References	64
3.	dPER-PAS-A	67
3.1.	Introduction	67
3.2.	Result.....	67
3.2.1.	Construct Design.....	67
3.2.2.	Protein Expression and Purification	69
3.2.2.1.	His/TEV-Tagged Protein	69
3.2.2.2.	His-dPER-PAS-A refolding trial	73
3.2.2.3.	GST Tagged protein	75
3.2.2.4.	MBP Tagged Protein.....	77
3.2.2.5.	No Tagged Protein.....	79
3.3.	Heme Binding Properties	80
3.3.1.	Heme Affinity	80
3.3.2.	UV-Visible Spectroscopy	81
3.3.3.	Electron Paramagnetic Resonance (EPR).....	84
3.3.4.	Circular Dichroism (CD)	85
3.3.5.	Mutant Variants	86

3.4.	Summary	89
3.5.	References	91
4.	dPER-PAS-B	95
4.1.	Introduction	95
4.2.	Result.....	95
4.2.1.	Construct Design.....	95
4.2.2.	Protein Expression and Purification	97
4.2.2.1.	His-dPer-PAS-B refolding trial	97
4.2.3.	Heme Titration	103
4.2.4.	UV-Visible Spectroscopy	105
4.2.5.	Electron Paramagnetic Resonance (EPR).....	107
4.2.6.	Circular Dichroism (CD)	108
4.2.7.	Mutant Variants	108
4.3.	Summary	111
4.4.	References	112
5.	dPER-PAS-AB.....	115
5.1.	Introduction	115
5.2.	Result.....	115
5.2.1.	Construct Design.....	115
5.2.2.	GST-dPER-PAS-AB purification	117
5.2.3.	His-dPER-PAS-AB.....	119
5.2.4.	GST-dPER-PAS-AB.....	122
5.3.	Spectroscopic investigation of the interaction of dPER-PAS-AB with heme	123
5.4.	Electron Paramagnetic Resonance (EPR)	127
5.5.	Circular Dichroism (CD).....	132
5.6.	Summary	140

5.7. References	141
6. Thesis Summary and Future Work	144
6.1. Thesis Summary	144
6.2. Future Work	146
6.3. References	147
7. Appendix.....	149
7.1. Mass spectrometry analysis.....	149
7.2. DNA quantification.....	149
7.3. Bacterial strains	149
7.4. Preparation	149
7.5. Buffers and Media.....	149
7.5.1. 2x YT media	149
7.5.2. LB (Luria-Bertani) Agar	149
7.5.3. Sample loading buffer (SDS-PAGE)	150
7.5.4. 10 x Running Gel Buffer	150
7.5.5. Staining solution	150
7.5.6. Buffers for Ni-NTA column	150
7.5.6.1. Regenerate Ni column.....	150
7.5.6.2. N1 buffer	150
7.5.6.3. N2 buffer	150
7.5.6.4. Dialysis buffer.....	150
7.6. Gel Filtration	151
7.7. Size Exclusion Chromatography.....	151
7.8. Protocols.....	152
7.8.1. Competent cell preparation.....	152
7.8.2. Cell Lysis	152
7.8.3. Denaturing SDS-polyacrylamide gel electrophoresis (SDS-PAGE)	153

7.8.4.	SDS-PAGE gel silver stain protocol.....	153
7.8.5.	Tag Cleavage	156
7.8.6.	Measure of Protein Concentration	156
7.8.6.1.	Bio-Rad Protein assay day reagent concentrate	156
7.9.	Vectors	157
7.9.1.	pLEICS-07	157
7.9.2.	pLEICS-14	158
7.9.3.	pLEICS-05	159
7.9.4.	pLEICS-10	160
7.9.5.	pLEICS-92	161
7.9.6.	pLEICS-93	162
7.9.7.	pLEICS-04	163
7.9.8.	pLEICS-03	164
7.9.9.	pLEICS-01	165
7.10.	Sequence of amino acids for dPER-PAS domains constructs.....	167
7.10.1.	Sequence for the first trial constructs.....	167
7.10.2.	Sequence for the second trial constructs	168
7.10.3.	Sequence for the third trial constructs.....	169

Abbreviations and Acronyms

Amino acids

Ala	A	Alanine
Arg	R	Arginine
Asn	N	Asparagine
Asp	D	Aspartate
Cys	C	Cysteine
Gln	Q	Glutamine
Glu	E	Glutamic acid
Gly	G	Glycine
His	H	Histidine
Ile	I	Isoleucine
Leu	L	Leucine
Lys	K	Lysine
Met	M	Methionine
Phe	F	Phenylalanine
Pro	P	Proline
Ser	S	Serine
Thr	T	Threonine
Trp	W	Tryptophan
Tyr	Y	Tyrosine
Val	V	Valine

Chemicals and Materials

2XYT	2X Yeast extract and Tryptone
Amp	Ampicillin
APS	Ammonium Persulfate
CBB	Coomassie Brilliant Blue
Chlo	Chloramphenicol
CO	Carbon Monoxide
ddH ₂ O	Deionized distilled water
DTT	Dithiothreitol
EDTA	Ethylene Diamine Tetra Acetic acid
HEPES	4-(2-Hydroxyethyl)piperazine-1-ethanesulfonic acid
Im	Imidazole
IPTG	Isopropyl β -D-1-thiogalactopyranoside
Kan	Kanamycin
Ni-NTA	Nickel-Nitrilotriacetic acid
NO	Nitric Oxide
O ₂	Oxygen
PPIX	Protoporphyrin IX
SDS	Sodium dodecylsulphate
TEMED	N,N,N',N'-Tetramethylethylenediamine
Tris	Tris (hydroxyl methyl) amino methane

Techniques

EPR	Electron paramagnetic resonance
PCR	Polymerase chain reaction
SDS-PAGE	Sodium dodecyl sulfate-Polyacrylamide gel electrophoresis
UV-visible	Ultra violet-visible light spectroscopy

Proteins

ARNT	Aryl hydrocarbon Receptor Nuclear Transporter
bHLH	basic Helix-Loop-Helix
BMAL1	Brain and Muscle ARNT-like 1
CLOCK	Circadian Locomotor Output Cycles Kaput
Cry	Cryptochrome
DNase	Deoxyribonuclease
dPER-PAS	<i>Drosophila Melanogaster</i> PERIOD -PAS
EcDOS	<i>E. coli</i> , Direct of Oxygen Sensor
Hb	Haemoglobin
HO	Heme oxygenase
mCLOCK	Mouse Circadian Locomotor Output Cycles Kaput
mNPAS2	Mouse Neuronal PAS domain protein 2
NR	Nuclear Receptor
PAS	PER ARNT Sim
PER	PERIOD protein

Sim	Single-minded protein
SIM	Single-Minded
SwMb	Sperm Whale myoglobin
TEV	Tobacco etch virus protease

Units/Symbols

°C	degree Celsius
A	Absorbance
A_{\max}	Maximum absorbance
A_{\min}	Minimum absorbance
Å	Angstrom
bp	base pair
cm	Centimetre
E_m	mid-point potential
hr	hour
K	Kelvin
K_D	Dissociation constant
kDa	kilo Daltons
L	Litre
M	Molar
mA	Milliampere
min	Minute

ml	Millilitre
mM	Millimolar
PCR	Polymerase chain reaction
rpm	Revolution per minute
Sec	Second
V	Volt
ϵ	Absorption coefficient
μ l	Microliter
μ M	Micro Molar

Miscellaneous

bHLH	base Helix-loop-helix
Cat	Catalog
CD	Circular dichroism
C-terminal	Carboxyl terminal
CV	Column volume
DBD	DNA binding domain
EET	Extracellular electron transfer
FAD	Flavin adenine dinucleotide
HLH	Helix-loop-helix
LBD	Ligand binding domain
MBP	Maltose-binding protein

N-terminal	Amino terminal
PDB	Protein Data Bank
PDB ID	Protein Data Bank identification code
PNACL	Protein and nucleic acid laboratory
PROTEX	Protein expression laboratory
Ref	Reference
ROS	Reactive oxygen species
SCN	Suprachiasmatic nuclei
wt	Wild-type
FPLC	Fast protein liquid chromatography

Chapter One

Introduction

1. Introduction

1.1. Circadian Cycle and Regulation

The phenomenon of the circadian rhythm - or the “day and night” cycle, as it was previously named - has been known for centuries and has been traced back as far as 13th century Chinese medical texts [8]. The term “*Circadian Rhythm*” was first coined by Franz Halberg, one of the fathers of chronobiology, in the 1950s, [9].

The molecular basis of the circadian clock has been studied in such diverse model systems as the fly *Drosophila melanogaster*, the bread mould *Neurospora crassa* and the cyanobacterium *Synechococcus* [10]. Circadian rhythms are the extrinsic manifestations of an endogenous timing system and include approximately 24 hr (*circadian*: Latin approximately one day) rhythms in many physiological and behavioural processes. The aforementioned biological oscillations can be broken down into behavioural, biochemical, physiological, and molecular changes [11]. Developed as an adaptation to the daily light/dark cycle, these rhythms advantageously influence the activity and survival of organisms from all phyla and link regular environmental changes with the (temporal) molecular composition of organisms [11].

According to Konopka and Benzer, the circadian cycle is the control system for energy and nutritional resources in the cell, with temperature having a small influence on the resources [12]. The circadian cycle acts as a local biological clock in various tissues. It works independently within a cell even when the cell is removed from the original tissue. The circadian clock activates nutrition and responds to changes between day and night which is achieved through the control of regulatory hormonal levels in the circadian cycle [13].

The circadian clock is linked to metabolic homeostasis. Indeed, among the rhythmically regulated genes there are a profound number of rate limiting genes involved in for example, glucose homeostasis as well as lipid and xenobiotic metabolism in the liver [14].

Glucose, which resets the circadian clock in cell assays or food stimulated hormones such as Ghrelin, have been discussed to train the peripheral circadian clocks according to feeding cycles [15, 16]. The redox and metabolic state of the cell, which is for example represented by the coenzyme NAD⁺/NADH ratio, impacts the circadian oscillator [17]. Reduced NADH enhances DNA binding of CLOCK/CYC and NPAS2/CYC,

respectively, while oxidized NAD⁺ attenuates at least NPAS2/CYC DNA binding capacity [18].

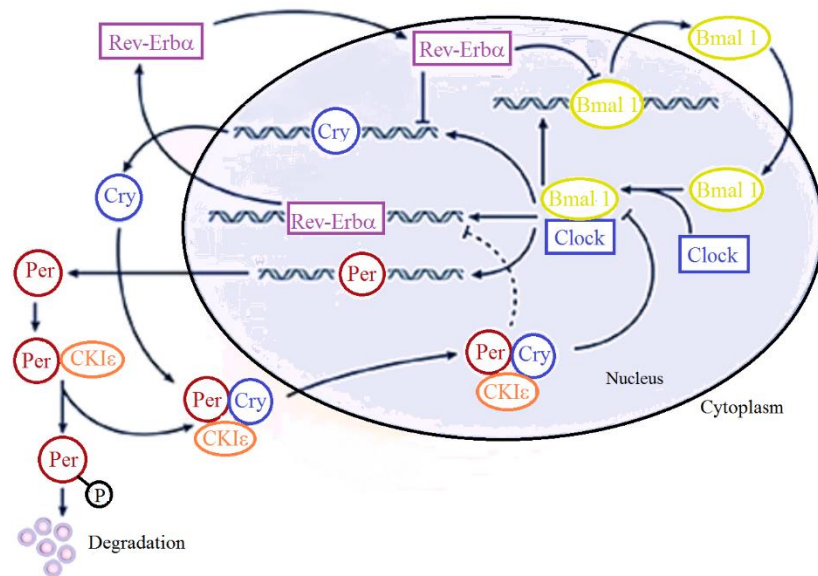


Figure 1-1 Circadian rhythms are generated by the feedback loops of the core circadian genes. In the SCN neurons, the intracellular levels of CLOCK remain steady throughout the 24-hour period, whereas BMAL1 expression levels are high at the beginning of a period [6, 7].

There are many biological daily activities (for example cell growth, damage repair and metabolism) that are controlled by circadian clock [19-22]. The key mechanism which controls all daily activities in different species (mammalian, insects and plants) is the gene expression [23-26] and variation in function for different domains of proteins [27].

PERIOD (PER) is a transcriptional regulatory factor involved in metazoan circadian rhythms. In *Drosophila melanogaster*, PERIOD2 (dPER2) dimerises with TIMELESS (TIM) and the complex enters the nucleus and disrupts the DNA binding of the transcriptional activator heterodimer CLOCK/CYCLE (or dBMAL1). The dCLOCK/dBMAL1 complex is a transcriptional activator for both *PER* and *TIM* genes and hence PER and TIM inhibit their own expression through a negative feedback mechanism [28, 29].

In mammals an analogous negative feedback mechanism is observed where a homologous PER protein dimerises with a cryptochrome (CRY) protein and this dimer in turn has a negative effect on the analogous CLOCK/BMAL transcriptional activator complex. Both mouse PER2 (mPER2) and *Drosophila* PER2 (dPER2) crystal structures show that they consist of two PAS domains and a C-terminal domain [20]. As seen in

Figure 1-2. Both are dimers and require the C-terminal α -helix (α -F) for self-association. The α -F is also suggested to unlatch to allow PER2 to disassociate from itself and interact with Timeless [20].

Recently, mPER2 has been proposed to be a heme-binding protein [30, 31]. It has also been suggested that heme exchange between mPER2 and Neuronal PAS protein 2 (NPAS2) is important in transcription regulation in circadian rhythms [32]. Heme binding characteristics of mPER2-PAS-A and mPER2-PAS-B have been reported [33, 34]. Heme titration assays and mutagenesis on mPER2-PAS-A shows that PAS-A binds Fe (III) protoporphyrin IX complex with a heme: protein stoichiometry of 1:1 [35]. The Fe (III)-bound PAS-A-mPer2 complex is a six coordinated low spin complex with Cys215 as the heme axial ligand. mPER2-PAS-B appears important in homo and heterodimerisation of mPER [31]. Hayasaka *et al.*, [30] suggest that Fe (III) heme binds PAS-B with a 1:1 stoichiometry and a His454 is proposed to be the axial ligand. Airola *et al.*, [31] also examined heme binding to mPER2. However, they have concluded that the heme interactions are non-specific as the heme-binding capabilities of a number of well-characterised proteins with no known biological role with heme were comparable to mPER2. Furthermore, site-directed mutagenesis studies failed to locate a specific heme-binding site on mPer2 [30, 31, 36].

In *Drosophila*, feeding time and temperature determine the period of rest and activity [37, 38]. Besides controlling various behaviours, the *Drosophila* circadian clock also coordinates many rhythms in peripheral organs, such as olfactory and gustatory sensitivity rhythms [39, 40].

The *Drosophila* gene is a member of the bHLH-PAS family which is characterized by the presence of the basic helix-loop-helix (bHLH) and Per-Arnt-Sim (PAS) domains [41, 42]. These domains are shown in Figures 1-3, 1-4, respectively.

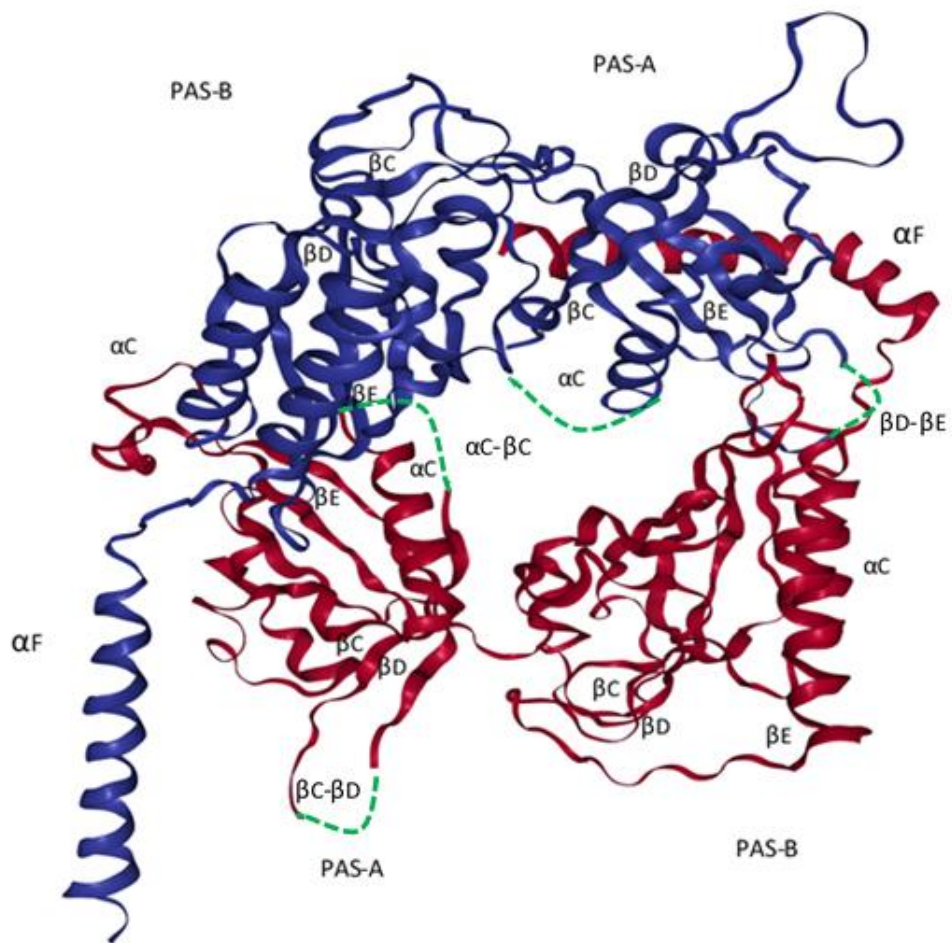


Figure 1-2 Cartoon representation of the dPER homodimer (PDB ID 1WA9). Molecule 1 is shown in blue, molecule 2 in red. The loop insertions of dPER PAS-A (αC - βC , βC - βD , and βD - βE) are labelled, and disordered regions are depicted as green dotted lines.

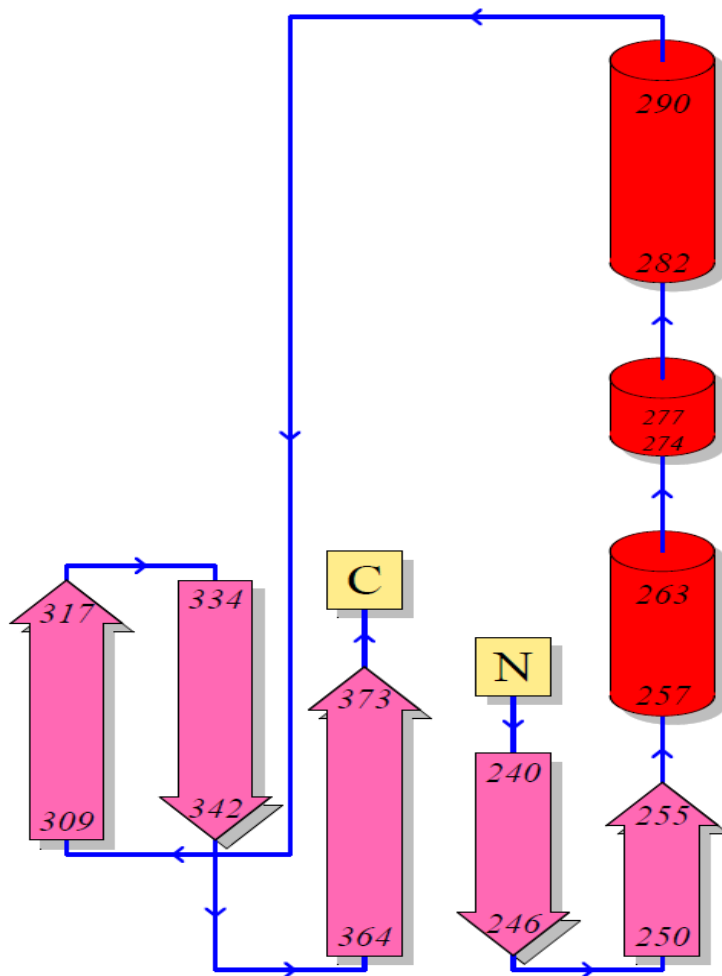


Figure 1-3 PAS-A domain topology schematic. α -Helices and β -sheets are shown as magenta arrows and red cylinders, respectively. PDB sum, UniProt code: P07663 (PER_DROME).

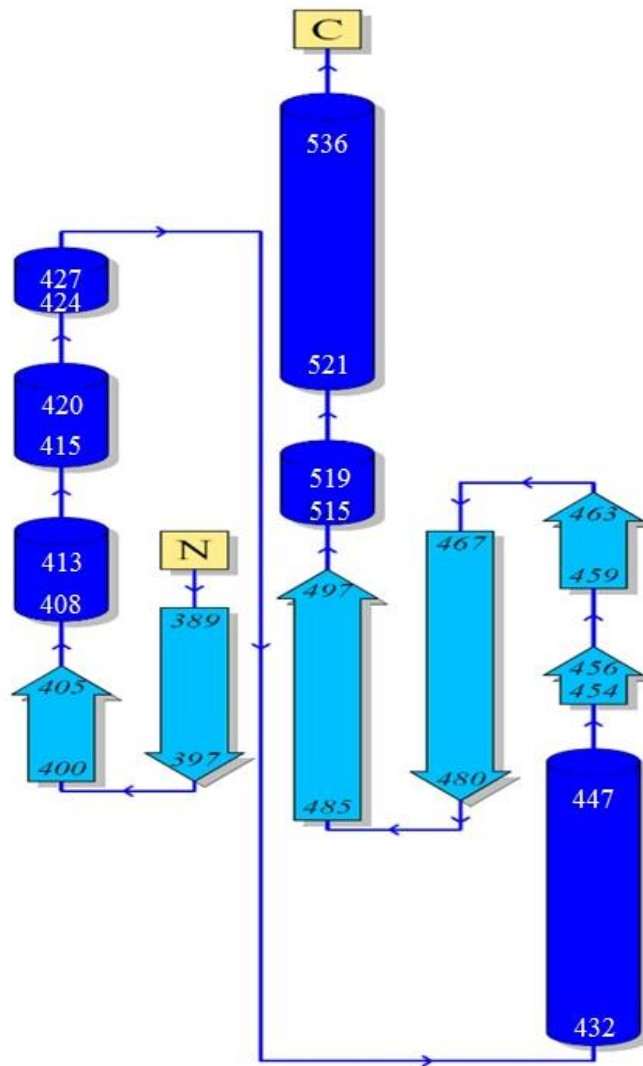


Figure 1-4 PAS-B domain topology schematic. α -Helices and β -sheets are shown as light blue arrows and blue cylinders, respectively. PDB sum UniProt code: P07663 (PER_DROME).

1.2. Mammalian Clock

The circadian rhythm is a fundamental tool used by living organisms to adapt physiological processes to changes in the environment. The circadian time-keeping system, on the one hand, enhances the adaptive ability of the organism by preparing it for the periodical changes in the environment, and on the other hand, allows temporal separation of otherwise conflicting biochemical activities [43]. The most influential models of time perception are inspired by a clock metaphor and propose a dedicated clock mechanism to account for human and animal estimation of time [44-46]. In the mammalian circadian clock there is a set of 14 genes called the core-clock network (CCN) which encodes for other gene groups such as PER (period), CRY (cryptochrome) and BMAL [47]. In mammals there are three types of Period genes (Per1, Per2, and Per3) and two types of cryptochrome genes (Cry1 and Cry2). Both are formed in the suprachiasmatic nucleus or nuclei (SCN), which is a tiny region located in the hypothalamus. The SCN is responsible for controlling circadian rhythms. The SCN has an efferent connection to the pineal gland where it indirectly stimulates secretion of hormones that regulate the molecular clock cycle [48, 49]. The oscillating rhythm of this “master clock” is controlled by a series of transcriptional/translational feedback loops that modulate gene expression and the protein products of these genes are directly involved in the auto regulation of the molecular clock [48].

The PAS region consists of two adjacent degenerate repeats of ~130 amino acids, PAS A and PAS B. The domain is an ancient signalling device conserved through evolution, having been identified in proteins throughout the animal kingdom, in bacteria, fungi and yeast in addition to mammals and flies, where the most commonly studied bHLH/PAS proteins originate. Signals mediated by PAS domains include redox state, hypoglycaemia, oxygen balance and xenobiotic metabolism, and many bacteria contain PAS-like domains that detect light [50, 51].

1.3. *Drosophila* Clock

In *Drosophila*, there are two Period genes (per1, per2) [31]. In *Drosophila*, timeless (tim) plays an analogous role to the cryptochrome (cry) genes in mammalian cells. Joumouille *et al.* [52] have identified different nuclear receptors involved in the transcriptional

control of the *Drosophila* circadian clock [52]. Figure 1-5 compares *Drosophila* to mammalian circadian clock pathways.

There are two types of loops: a negative loop as PER / TIM loop and a positive loop as a clock (CLK) / cycle (CYC) [53, 54]. CLK/CYC activates the transcription of the period (*per*) and timeless (*tim*) genes through binding to E-boxes. Accumulation of PER and TIM proteins leads to a delayed inhibition of the CLK/CYC activity and subsequently genes regulated by CLK/CYC which are usually expressed during the daytime [55, 56].

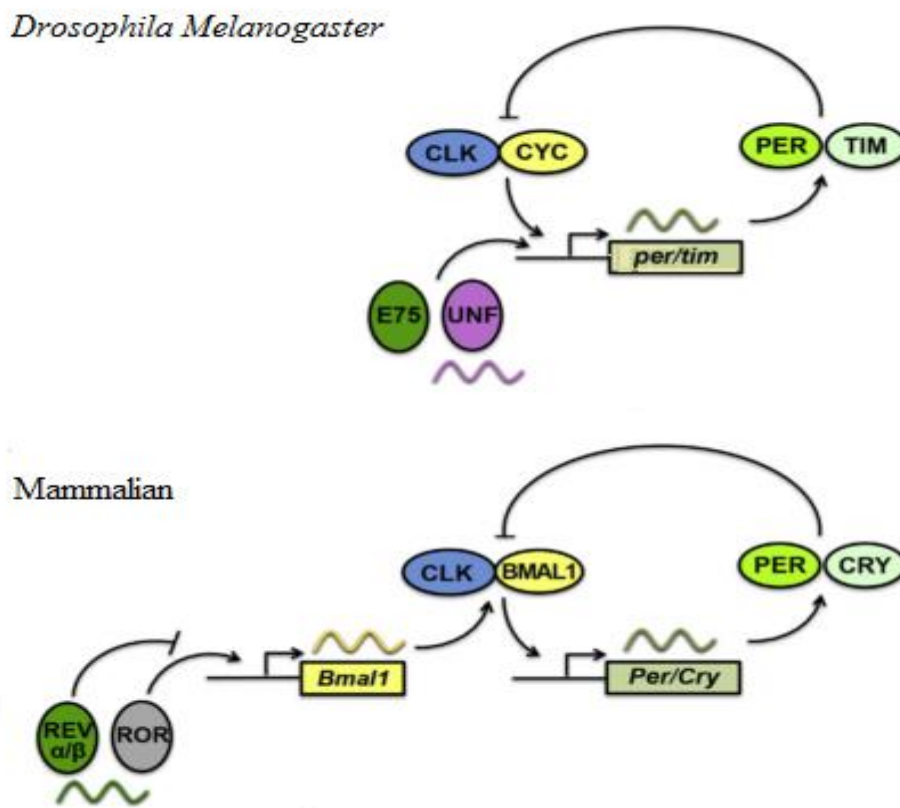


Figure 1-5 Regulation of the circadian clock in *Drosophila* and mammals. PER proteins form a heterodimer, for mouse this is PER/CRY and for *Drosophila* PER/TIM [2, 3].

1.4. Transcription Factors

Circadian rhythms of animal behaviour, physiology, and metabolism are an evolutionary adaptation to the rotation of the earth. There is an underlying transcriptional feedback mechanism, which is modulated by the post-translational modification of key transcription factors [57, 58]. In *Drosophila*, two genes, period (*per*) and timeless (*tim*) *in vitro* involve binding sites on each protein. TIM is essential to the control of circadian

rhythm for the production of the previously described protein interaction domain PAS [12, 59, 60]. In *Drosophila*, the transcription factors CLOCK (CLK) and CYCLE (CYC) activate the transcription of period (*per*) and timeless (*tim*) and other direct target genes during the day. At night, PER and TIM then enter the nucleus and inhibit their own transcription. The activity of CLK/CYC is regulated by a direct interaction with these negative regulators as well as by post-translational modifications, with the focus, to date, being on PER phosphorylation [61, 62]. The PER and TIM are gradually hyperphosphorylated by different kinases during the early night [63, 64]. In the morning after exposure to light, PER and TIM are degraded, which liberates and reactivates CLK/CYC. In addition, hyper phosphorylation of CLK appears to coincide with low transcription activity, suggesting that direct phosphorylation–dephosphorylation may also modulate CLK/CYC activity [65-67].

Drosophila and mammals have highly conserved molecular clocks. At their core lie two transcriptional activators: CLK and CYC in *Drosophila*, and CLK and BMAL1 in mammals [68]. These transcription factors heterodimerize and activate numerous target genes, including those that encode their own inhibitors. In *Drosophila*, *period* (*per*) and *timeless* (*tim*) are direct CLK/CYC targets. PER and TIM proteins dimerize and enter the nucleus, where PER inhibits CLK/CYC activity to complete the negative feedback loop. Similarly, in mammals *mPer1* and *2* and *mCry1* and *2* are direct targets of CLK/BMAL1. mPER/mCRY protein complexes translocate to the nucleus and repress CLK/BMAL1 activity [69]. According to Barnes, [70] the mouse TIMELESS (mTIM) in the brain slices of mouse, like *Drosophila* TIM was found to be required for rhythmicity and to stabilize mPER proteins. Transcription of one transcriptional activator (CLK in *Drosophila* and BMAL1 in mammals) is regulated by the continuous loop between the accumulation of the protein that inhibits the activity of the heterodimer PER/TIM in *Drosophila* and PER/CRY in mammals [71, 72] Figure 1-5.

In contrast to *Drosophila* TIM, mammalian CRY1 and CRY2 are integral, light independent regulators of the circadian clock. Nevertheless, there is an increasing number of reports that include an additional FAD / light dependant function of mammalian cryptochrome. For example, human CRY2 and monarch butterfly type II CRY can rescue magneto sensitivity in the presence of blue-light in mutant flies which lack functional dCRY [73, 74]. Seminal studies of the *Drosophila* circadian clock demonstrated a negative feedback loop mediated by the dPER/dTIM complex. Its formation is both

important for their nuclear localization and repression of its own transcription through interaction with the transcription factors CLOCK and CYCLE [75].

1.5. PAS Domains

The basic helix-loop-helix (bHLH) domain is a highly conserved amino acid motif that defines a group of DNA-binding transcription factors. bHLH proteins play essential regulatory roles in a variety of biological processes in animals, plants, and fungi [76, 77]. Transcription factors of the bHLH class are involved in controlling specification and differentiation of many organs and tissues during development, in vertebrates as well as in invertebrates. In *Drosophila* they play key roles in processes like sex determination and neurogenesis, while in mouse development their function during myogenesis has been particularly well analysed [78, 79]. The PERIOD in transcription regulation is based on the demonstration that it is a member of the bHLH-PAS family of transcription factors [80]. The bHLH domain which mediates protein dimerization and DNA-binding is near the amino terminus and is closely followed by the PAS domain [81, 82]. In bHLH-PAS-containing proteins, the PAS domain is ~230 to 550 amino acids long and contains two well-conserved repeats of approximately 50 amino acids, designated PAS-A and PAS-B [83].

PAS domains are defined as a structural domain with five antiparallel β -sheets arranged in a 3-4-5-1-2 topology of dPER-PAS-A (Figure 1-3), and six antiparallel β -sheets arranged in a 2-1-6-5-4-3 topology of dPER-PAS-B (Figure 1-4). In both, α -helices are inverted into the sequence, generally between the second and third sheet but the length, number and location of these are generally less conserved so do not contribute to the defining qualities of a PAS domain. These helices play an important role by packing onto one side of the β -sheets to create an internal pocket for ligand binding. The external surface created by the β -sheets is then typically involved in protein-protein interactions, meaning that the residues in the β -sheets defining the PAS domain core can alternate between being available for ligand binding and being involved in mediating protein-protein interactions.

Although the homogeneity of the sequence of PAS domains is relatively low, the trigonometry and signalling mechanisms are well preserved [84]. This allows PAS domains with low sequence similarities to form protein-protein interactions with the same binding partners, Figure 1-2. Moreover, with a high degree of conservation among some

PAS domain signalling mechanisms means that these areas, to some extent at least, can be interchangeable, Figure 1-6.

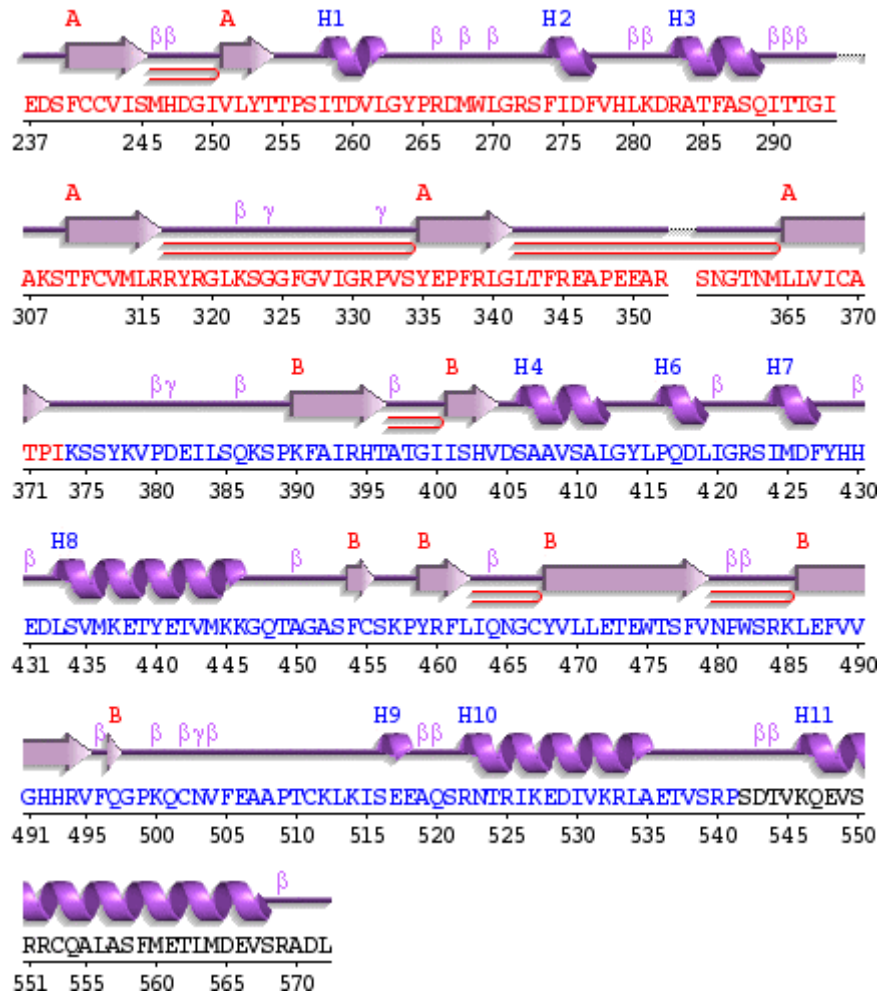


Figure 1-6 Secondary structure for dPER-PAS-AB. This figure has been adapted from PDBsum UniProt code: P07663 (PER-DROME).

1.5.1. *Drosophila Melanogaster* CLOCK and *Drosophila Melanogaster* CYC Complex with E-box DNA

In eukaryotes, the circadian clock keeps time *via* one or more transcriptional feedback loops [6]. Nuclear receptors, the largest superfamily of eukaryotic transcription factors, are involved in almost all physiological processes. They regulate transcription in response to binding of lipophilic hormone ligands such as steroids, thyroid hormones, retinoic acid in mammalian cells, and ecdysone in insect cells [85, 86]. They contain three main functional domains: (1) N-terminal domain A/B, which is highly variable in length and sequence and which has a constitutively active transactivation function, (2) the DNA binding domain (DBD) specific to DNA nucleotide motifs, and (3) the ligand binding

domain (LBD), which is involved not only in binding of the hormone ligand but also in dimerization and binding to coregulatory proteins. The *Drosophila* E75B isoform, does not contain a DBD [87].

In *Drosophila*, a heterodimer formed by CLOCK (CLK) and CYCLE (CYC) binds to an E-box sequence and activates transcription to initiate clock function. In the core loop, CLK-CYC activates *period* (*per*) and *timeless* (*tim*) transcription during mid-day, effecting a rise in *per* and *tim* mRNA levels that peaks during the early evening. PER and TIM proteins then accumulate, form a dimer, and move into the nucleus to bind CLK-CYC during the night, thereby inhibiting their transcriptional activity until PER and TIM are degraded early in the morning [61], Figure 1-1.

PER was previously found inhibit CLK-CYC binding to E-boxes [88, 89], which suggests that the rhythmic transcription of CLK target genes are mediated by PER-dependent rhythms in E-box binding by CLK-CYC. CLK-CYC binds E-boxes in the *per* circadian regulatory sequence (CRS) and the *tim* upstream sequence [90]. The mechanism by which CLK-CYC heterodimers are removed from E-boxes during repression is not well understood. PER is required for the rhythmic binding of CLK complexes, as CLK constantly binds to *per* and *tim* promoters in *per* flies [90, 91].

1.5.2. *Drosophila Melanogaster* PER-PAS

A composite model for the circadian clock in animals consists of four core genes that constitute a negative feedback loop plus two genes that act as checkpoints to regulate procession through the loop [66, 92]. In *Drosophila* the heterodimeric bHLH-PAS-AB is activated the transcription of both PERIOD (dPER) and its interaction partner TIMELESS (dTIM) [93]. The amino acid sequences of dPer-PAS-A, dPer-PAS-B and dPer-PAS-AB (see the Appendix Figures 7-13, 7-14, 7-15) show the sequence for the whole dPER-PAS (dPER-PAS-A, dPER-PAS-B and dPER-PAS-AB domains).

dPER-PAS-A and mPER-PAS-A share of sequence identity (25%) . This allows for a comparison between the heme binding site of the mouse and *Drosophila* proteins

In mouse clock, mouse brain and muscle Arnt-like 1(BMAL1) bind to make a heterodimer; this dimer then binds to the e-box DNA and initiates expression of the PER and CRY [36].

```

sp|P07663|PER_DROME      MEGGESTESTHN--TKVS--DSAYSNCSNSQSQRSQSGSSKSRLSGSHSSGSSGYGKPKST
sp|O15055|PER2_HUMAN    MNGYAEFPSPSPNPTKEPVEPQPSQVPLQEDVDMSSGSSGHETNENCSTGRDSQGSDCDD
sp|O54943|PER2_MOUSE    MNGYVDFSPSPPTSPITKEPGAPQPTQAVLQEDVDMSSGSSG---NENCSTGRDSQGSDCDD
*:* . . . . ** . . . . **** . . . . *:* . . . .

sp|P07663|PER_DROME      QASSSDMI IKRNKDKSRKKKKKNGAGQGAGQAOTLISASTSLEGRDEEKPRPSGTGCV EQ
sp|O15055|PER2_HUMAN    SGKELGMLVEPPDA-----RQSP-DTFSL-----M--MAKSEHNPSTSGCSSD
sp|O54943|PER2_MOUSE    NGKELRMLVESNT-----HSPDDAFRL-----M--MTEAEHNPSTSGCSSE
.... *::: . . . . : : * : : : : .**:*:* .:

sp|P07663|PER_DROME      QICRELQDQQHGEDHSEPOAIEQLQEEEEEDQSGSESEADRVEGVAKSEAAQSFPIPSPL
sp|O15055|PER2_HUMAN    QSSKVDTHKE-----LIKTLKELKVHLPAD-----KKAKGKASTLATLKYALRSVK
sp|O54943|PER2_MOUSE    QSAKADAHKE-----LIRTLKELKVHLPAD-----KKAKGKASTLATLKYALRSVK
* .: . . . . : : : : * . . . . * .: * .: .: .: *

sp|P07663|PER_DROME      SVTIVPPSMG-GCGGVGHAAGLDLSGLAKFDKTWEAGPGKLESMTGVGAAAAGTGQGRERV
sp|O15055|PER2_HUMAN    QVKANEYYQLLMSSEGHPCGADVP-----SYTVEEMESV-----TSEHIVK
sp|O54943|PER2_MOUSE    QVKANEYYQLLMSSESQPCSDVDP-----SYSMEQVEGI-----TSEYIVK
.*. . . . . * . . . . . * .: .: .:

sp|P07663|PER_DROME      KEDSFCCVISMHDGIVLYTTPSITDVLGYPRDMWLGSRFIDFVHLKDRATFASQITTG-I
sp|O15055|PER2_HUMAN    NADMFAVAVSLVSGKILYISDQVASIFHCRRDAFSDAKFVEFLAPHDVGVFHFSFTSPYKL
sp|O54943|PER2_MOUSE    NADMFAVAVSLVSGKILYISNQVASIFHCRRDAFSDAKFVEFLAPHDVSVFHFSYTTPYKL
: * . . . . : * .** : : : : : * : . . . . : * . . . . : :

sp|P07663|PER_DROME      PIA-----ESRGSVPKDAKSTFCVMLRRYRGLKSGGFGVIGRPSVSEYEPFRLGLTFREAP
sp|O15055|PER2_HUMAN    PLWSMCSGADSFTEQCEMEKSFPCRVSVRK-----SHENEIRYHPFRMTPYLVKVR
sp|O54943|PER2_MOUSE    PPWSVCSGLDSFTQCEMEKSFPCRVSVGK-----HHENEIRYQFRMTPYLVKVQ
* . . . . * . . . . * * * * . . . . * .** : :

sp|P07663|PER_DROME      EEARPDNYMVSNGTINMLLVICATPIKSSYKVPDEILSOKSPKFAIRHTAIGIISHVDSAA
sp|O15055|PER2_HUMAN    DQQGAE-----SQLCCLLLAERVHSGYEAPR--IPPEKRIFTTHTPNCLFQDVERA
sp|O54943|PER2_MOUSE    EQQGAE-----SQLCCLLLAERVHSGYEAPR--IPPEKRIFTTHTPNCLFQDVERA
: : . . . . : : * : : * . . . . : : .: * * . . . . * * *

sp|P07663|PER_DROME      VSALGYLPQDLIGRSIMDFYHHEDLSVMKETYETVMKKGQTAGASFCSPKPYRFLIQGCY
sp|O15055|PER2_HUMAN    VPLLGYLPQDLIETPVLVQLHPSDRPLMLAIHKKIL---QSGGQPFDYSPIRFRARNGEY
sp|O54943|PER2_MOUSE    VPLLGYLPQDLIETPVLVQLHPSDRPLMLAIHKKIL---QAGGQPFDYSPIRFRARNGEY
* ***** : : * . * : * : : : : * . . . . * * * * : * * *

sp|P07663|PER_DROME      VLLETWTSFVNPNWRKLEFVVGHHRVFQGPQCNVFEAAPTCKLKISEEQSRNTRIKE
sp|O15055|PER2_HUMAN    ITLDTSWSSFINPWSRKISFIIGRHKVRVGPLNEDVFAAHPCTEEKALHPSI---QELTE
sp|O54943|PER2_MOUSE    ITLDTSWSSFINPWSRKISFIIGRHKVRVGPLNEDVFAAPPCPEEKTPHPSV---QELTE
: * . * . * . * . * . * . * . * . * . * . * . * . * . * . * . * . * . *

sp|P07663|PER_DROME      DIVKRLAETVSRP-----SDTVKQEVSRRCQ-ALASFMETL-
sp|O15055|PER2_HUMAN    QIHRLLLPVPHSGSSGYGLSNGSHEHLMSQTSSSDSNGHEDSRRRRAEICNGNKTK
sp|O54943|PER2_MOUSE    QIHRLLMQPVPHSGSSGYGLSNGSHEHLMSQTSSSDSNGQEESHRRRSRGIKTSKGIQ
: * : * : * : : : : : : : : : : : : : : : : : : : : : : :

sp|P07663|PER_DROME      -----MDEVSRADLKLELPHEN-ELTVSERDSVMLGEISPHHDYDSS-SSSTET
sp|O15055|PER2_HUMAN    NRSHYSHESGEQKKKSVTEMQTNPPAEKKAVPAMEKDS--LGV-----SFPEELACKNQ
sp|O54943|PER2_MOUSE    TKSHVSHESGQKEASVAEMQSSPPAQVKAVTTIERDS--SGASLPKASFPPELAYKNQP
. . * : : : . * : : . * .** * . . . . . : :

sp|P07663|PER_DROME      PPSYNQLNYNENLLRFNSKPVTAPEL--DPPKTEP----PEPRGTCVSGASGPMSPVH
sp|O15055|PER2_HUMAN    TCSYQQISCLDSVIRYLESCNEAATLKRKCEFPANVPALRSSDKRKATVSP--G----PH
sp|O54943|PER2_MOUSE    PCSYQQISCLDSVIRYLESCNEAATLKRKCEFPANIPS-----RKATVSP--G----LH
*:* . . . . : : : : * * : : : * . * . . . * * * * *

```

Figure 1-7 Amino acid sequence of Period including PAS domains A and B for *Drosophila Melanogaster*, human and mouse according to NCBI Reference Sequence: NP_525056.2.

1.6. Heme

Heme derives its name from the Greek word αίμα (haima), which means blood. It is a cofactor consisting of an iron ion contained in the centre of a heterocyclic macrocycle organic compound called a porphyrin, composed of four pyrrole subunits interconnected at their carbon atoms *via* methine bridges (=CH-) [94]. Heme is formed from a tetrapyrrole known as Protoporphyrin, containing an iron ion bound to the centre of the structure. Its full name is iron protoporphyrin and it is found in a number of metalloproteins called heme proteins (Figure 1-8). Heme is biosynthesised in an eight-step process that takes place in both the cytoplasm and mitochondria of cells located in the liver, bone marrow and spleen [95-97]. This molecule has the ability to bind ligands such as oxygen (O₂), carbon monoxide (CO) and nitric oxide (NO). Heme proteins are found in all species (prokaryotic and eukaryotic). One example of a heme protein is haemoglobin which transports oxygen and carbon dioxide in the blood [98].

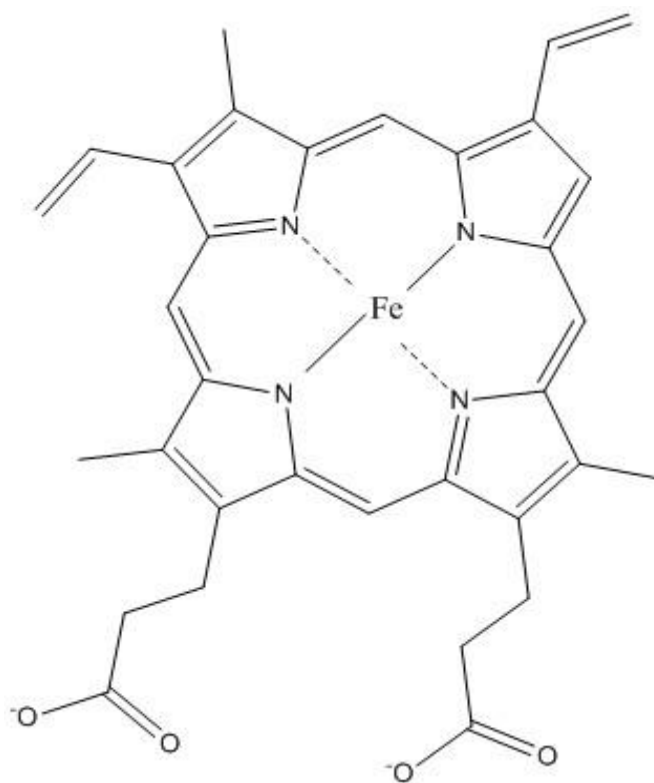


Figure 1-8 Structure of Fe protoporphyrin IX (heme *b*).

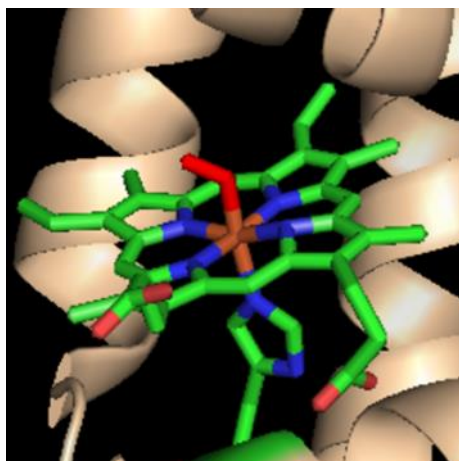


Figure 1-9 Stick model of heme *b* in myoglobin. The iron centre (brown) is bound to: four pyrrolic nitrogens (blue) in the axial plane, histidine (blue and green 5 membered ring) in the proximal position, and O₂ (red) in the distal position [4, 5].

Other hemeproteins, such as cytochromes, have the role of transporting electrons [99]. The iron atom in heme exists as either five coordinate or as a saturated six coordinate metal centre. Four coordination sites are bonded to the nitrogen atoms in the porphyrin macrocycle. The fifth coordination site is bonded to a protein amino acid residue. Only amino acids with atoms that contain a lone pair of electrons such as N, S or O can bind heme [100]. In the six-coordinate heme, the 6th coordination site can be occupied by either another amino acid residue in the protein, a loosely bound water molecule or a tightly bound small molecule such as O₂, CO, or NO [98, 101], Figure (1-9). The iron atom in heme exists in nature primarily as the high spin ferrous Fe²⁺ species [102]. However, binding of a small molecule or protein residue (i.e. going from 5 coordinate heme to 6 coordinate heme) can lead to a change in the oxidation state, electronic configuration, and conformation of both the porphyrin ring and the attached protein. A good example of this is when the iron in haemoglobin binds oxygen [103]. As oxygen binds to the iron, the iron is oxidised from Fe (II) to Fe (III) and switches from a high spin to a low spin electronic configuration. Furthermore, O₂ is reduced to O²⁻ in the process. The consequence of oxygen binding is the conformational flattening of the porphyrin ring, which is transmitted through the proximal ligand to the rest of the protein, resulting in a conformational change in haemoglobin [104].

The binding of a ligand to heme and the associated change in electronic configuration can be rationalised through crystal field theory. Electrons on the heme iron are contained within the five individual metal *d*-orbitals that interact with the surrounding ligands based

on the directionality of their orbitals. The interaction leads to a split of the five d -orbitals into two energy levels: (e_g and t_{2g}), Figure (1-10).

The iron will adopt either a high-spin or a low-spin state depending on the magnitude of the split between the (e_g) and (t_{2g}) orbitals. The splitting is referred to as Δ_E . When the iron atom is surrounded by a ligand field the energy levels of the $3d$ electrons are no longer degenerate and are divided to two groups of orbitals with different energies (the

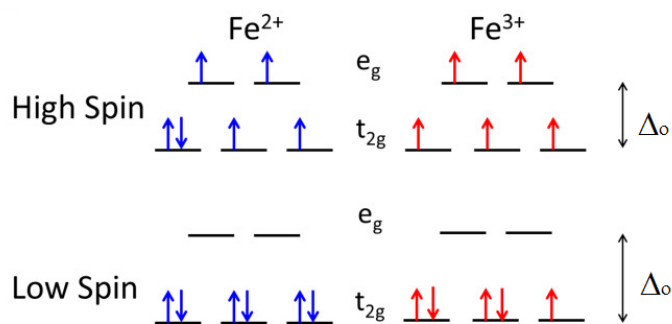


Figure 1-10 Common electron configurations of ferrous and ferric iron.

t_{2g} and e_g orbitals). Depending on the octahedral splitting energy, Δ_o or Δ_E , the iron will adopt either a high-spin or a low-spin state. When the splitting energy is large it is less energetically costly for electrons to pair up in the t_{2g} orbitals than to go into the e_g orbitals and so a low-spin state will be formed.

On the contrary, the iron will adopt a high-spin state, when the splitting energy is small and less than the pairing energy so that the 4th and 5th electrons will occupy the (e_g) orbitals. Below are some ligands from the spectrochemical series



Ordered from left to right by the size of the splitting Δ_o that they produce, going from small Δ_o to large Δ_o [105].

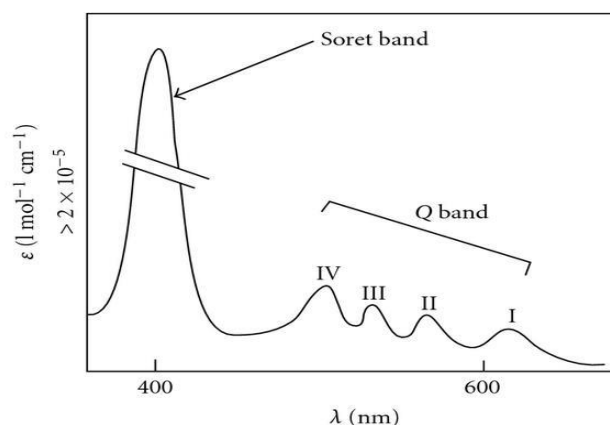


Figure 1-11 Soret band and Q band absorption spectrum [1].

Orbital mixing splits the energy levels of the two excited states, the higher energy state giving rise to the Soret band and lower energy state giving rise to the Q-band. The absorption spectrum of the heme is dominated by the π - π^* transitions [106]. Figure 1-11 shows the absorption spectrum of reduced cytochrome c which illustrates the classical features of metalloporphyrin spectra. Three electronic bands are observed, Q₀ (a), Q_v (b) and B (Soret). They originate from the two π - π orbital excitations, 1 and 2, which are subject to strong configuration interaction, with the transition dipoles adding in the higher energy Soret transitions and nearly cancelling in the lower energy a transition [107]. The b band is the envelope of 0 to 1 vibronic transitions induced by mixing of the Q and B electronic transitions [108].

The oxidation state and the coordination number of the iron centre in heme has a profound effect on the energy of these electronic transitions and therefore any changes in heme binding are reflected in the position and intensity of the Soret Band. Furthermore, heme binding kinetics can be determined by heme titration to the protein of interest using UV-vis spectroscopy. Plotting heme concentration against absorbance at the Soret wavelength allows one to calculate the dissociation constant of the heme-bound protein complex [109, 110].

1.6.1. Biological Role of Heme with PER Protein

In *Drosophila melanogaster*, there is only one gene encoding heme oxygenase (HO) [111] that plays an important role in development and in controlling the signalling pathway of DNA damage. Any other functions of HO in insects are still unknown [112,

113]. In the suprachiasmatic nuclei (SCN), the site of the mammalian circadian pacemaker for behavioural rhythms, HO activity changes during the day, reaching a maximum during the night. This pattern is maintained in constant darkness, suggesting that the activity of HO is controlled by the circadian clock [114]. The changes in the heme level influence the expression of clock genes and the degradation of the clock protein PERIOD (PER) [32, 115]. In *D. melanogaster*, cyclic expression of the (ho) gene has been found in whole head homogenates, although nothing is known about the role of HO in the circadian system [116, 117]. Nuclear Receptors (NR) bind specific DNA motifs in response to small molecule signalling. They generally share conserved domain architecture, with a DNA-binding region containing two zinc fingers, a ligand-binding domain, and activation domains [118].

1.7. Hemeprotein

1.7.1. Types of Hemeproteins

Hemeproteins promote various biochemical events such as oxygen transport/storage, electron transfer, gas sensing, and enzymatic oxidation/oxygenation in biological systems [119]. There are heme-binding proteins in the Nuclear Receptor (NR) superfamily, which is the largest transcription factor superfamily [120]. Circadian rhythms are regulated by feedback loops at transcriptional/translational levels. Heme is critical in this process [32]. The well-organized protein matrix of hemeproteins regulates the redox potential and reactivity of heme as a cofactor. For over a half-century, the chemical and biological properties of many hemeproteins have been investigated, and a number of crystal structures and data now encourage us to modify the various functions of hemeproteins by protein engineering [121]. Several hemeproteins can be used as building blocks for creating artificial protein assemblies because hemeprotein assemblies provide well-ordered metalloporphyrin clusters without aggregation. As a result, hemeprotein assemblies are expected to provide new biomaterials with synergetic or cooperative effects derived from accumulated cofactor functions [122].

There are other roles for heme. Heme can inappropriately bind to various biomolecules and alter their structure and function and can catalyse the formation of deleterious reactive oxygen species (ROS) [123, 124]. Therefore, the concentration and bioavailability of heme must be tightly controlled. Whether heme is synthesized endogenously or acquired from exogenous sources, it must be safely transported and trafficked

to heme proteins located in virtually every subcellular compartment, including the nucleus, ER, mitochondria, cytosol, and peroxisomes [125]. Electron transfer, when coordinated with proton transfer in respiration, charges biological membranes for the synthesis of energy-storing ATP molecules. For many respiratory organisms, maintaining this electron flow depends on the availability of soluble electron donors (food) and acceptors (e.g. O₂) that can enter cells to interact with bioenergetics machinery [126, 127].

1.8. Aims of Project

The aim of this thesis was primarily to examine the heme binding properties and the heme chemistry of the *Drosophila Melanogaster* circadian clock period (PER) protein. For this, constructs corresponding to the PAS domains (dPER-PAS-A, dPER-PAS-B and dPER-PAS-AB) were expressed and purified. The design of new DNA constructs for the domains (dPER-PAS-A, dPER-PAS-B and dPER-PAS-AB) with different suitable tags (His, GST, MBP and trial without tag), was completed in order to purify a suitable amount of soluble protein. Furthermore, protein crystallography was attempted on the heme-bound forms to identify the amino acids involved in heme binding and to potentially investigate the means of signal transduction originating from the heme binding site. The binding between the heme and dPER-PAS-A, dPER-PAS-B and dPER-PAS-AB has been investigated using optical absorbance heme titration assays, measuring heme kinetics using stopped flow apparatus and Circular Dichroism (CD) to determine if the type of binding is specific or nonspecific (i.e. investigate interactions between heme and other binding partners.). Crystallography trials of the complex of heme and proteins (dPER-PAS-A, dPER-PAS-B and dPER-PAS-AB) were performed. Site-directed mutants of dPER proteins have been produced and heme binding studies were carried out.

1.9. References

1. Josefsen, L B and Boyle, R W, "Photodynamic Therapy and the Development of Metal-Based Photosensitisers. Metal-Based Drugs", (2008) 2008
2. Meyer, P; Saez, L, and Young, M W, "Per-Tim Interactions in Living *Drosophila* Cells: An Interval Timer for the Circadian Clock. Science", (2006) 311(5758): 226-229.
3. John, P C S; Hirota, T; Kay, S A, and Doyle, F J, "Spatiotemporal Separation of Per and Cry Posttranslational Regulation in the Mammalian Circadian Clock. Proceedings of the National Academy of Sciences", (2014) 111(5): 2040-2045.
4. Chu, K; Vojtchovský, J; McMahon, B H; Sweet, R M; Berendzen, J, and Schlichting, I, "Structure of a Ligand-Binding Intermediate in Wild-Type Carbonmonoxy Myoglobin. Nature", (2000) 403(6772): 921.
5. Vojtěchovský, J; Chu, K; Berendzen, J; Sweet, R M, and Schlichting, I, "Crystal Structures of Myoglobin-Ligand Complexes at near-Atomic Resolution. Biophysical Journal", (1999) 77(4): 2153-2174.
6. Bell-Pedersen, D; Cassone, V M; Earnest, D J; Golden, S S; Hardin, P E; Thomas, T L, and Zoran, M J, "Circadian Rhythms from Multiple Oscillators: Lessons from Diverse Organisms. Nature Reviews Genetics", (2005) 6(7): 544.
7. Renn, S C; Park, J H; Rosbash, M; Hall, J C, and Taghert, P H, "A Pdf Neuropeptide Gene Mutation and Ablation of Pdf Neurons Each Cause Severe Abnormalities of Behavioral Circadian Rhythms in *Drosophila*. Cell", (1999) 99(7): 791-802.
8. Lu and Needham, N J T M, "Celestial Lancets: History and Rationale of Acupuncture and Moxa". (1980): Cambridge University Press.
9. Halberg, F; Cornélissen, G; Katinas, G; Syutkina, E V; Sothorn, R B; Zaslavskaya, R; Halberg, F; Watanabe, Y; Schwartzkopff, O, and Otsuka, K, "Transdisciplinary Unifying Implications of Circadian Findings in the 1950s. Journal of circadian rhythms", (2003) 1(1): 2.
10. Rosato, E; Piccin, A, and Kyriacou, C P, "Circadian Rhythms: From Behaviour to Molecules. Bioessays", (1997) 19(12): 1075-1082.
11. Loros, J J and Dunlap, J C, "Genetic and Molecular Analysis of Circadian Rhythms in *N Eurospora*. Annual Review of Physiology", (2001) 63(1): 757-794.
12. Konopka, R J and Benzer, S, "Clock Mutants of *Drosophila-Melanogaster*. Proceedings of the National Academy of Sciences of the United States of America", (1971) 68(9): 2112-&.
13. Takahashi, J S, "Molecular Neurobiology and Genetics of Circadian-Rhythms in Mammals. Annual Review of Neuroscience", (1995) 18: 531-553.
14. Panda, S; Antoch, M P; Miller, B H; Su, A I; Schook, A B; Straume, M; Schultz, P G; Kay, S A; Takahashi, J S, and Hogenesch, J B, "Coordinated Transcription of Key Pathways in the Mouse by the Circadian Clock. Cell", (2002) 109(3): 307-320.
15. Hirota, T; Okano, T; Kokame, K; Shirohani-Ikejima, H; Miyata, T, and Fukada, Y, "Glucose Down-Regulates Per1 and Per2 Mrna Levels and Induces Circadian

- Gene Expression in Cultured Rat-1 Fibroblasts. *Journal of Biological Chemistry*", (2002)
16. LeSauter, J; Hoque, N; Weintraub, M; Pfaff, D W, and Silver, R, "Stomach Ghrelin-Secreting Cells as Food-Entrainable Circadian Clocks. *Proceedings of the National Academy of Sciences*", (2009): pnas. 0906426106.
 17. Zhang, E E and Kay, S A, "Clocks Not Winding Down: Unravelling Circadian Networks. *Nature reviews Molecular cell biology*", (2010) 11(11): 764.
 18. Bartok, O; Teesalu, M; Ashwall-Fluss, R; Pandey, V; Hanan, M; Rovenko, B M; Poukkula, M; Havula, E; Moussaieff, A, and Vodala, S, "The Transcription Factor Cabut Coordinates Energy Metabolism and the Circadian Clock in Response to Sugar Sensing. *The EMBO journal*", (2015) 34(11): 1538-1553.
 19. Price, J L; Blau, J; Rothenfluh, A; Abodeely, M; Kloss, B, and Young, M W, "Double-Time Is a Novel *Drosophila* Clock Gene That Regulates Period Protein Accumulation. *Cell*", (1998) 94(1): 83-95.
 20. King, H A; Hoelz, A; Crane, B R, and Young, M W, "Structure of an Enclosed Dimer Formed by the *Drosophila* Period Protein. *Journal of Molecular Biology*", (2011) 413(3): 561-572.
 21. Gatfield, D and Schibler, U, "Circadian Glucose Homeostasis Requires Compensatory Interference between Brain and Liver Clocks. *Proceedings of the National Academy of Sciences*", (2008) 105(39): 14753-14754.
 22. Nakahata, Y; Kaluzova, M; Grimaldi, B; Sahar, S; Hirayama, J; Chen, D; Guarente, L P, and Sassone-Corsi, P, "The Nad⁺-Dependent Deacetylase Sirt1 Modulates Clock-Mediated Chromatin Remodeling and Circadian Control. *Cell*", (2008) 134(2): 329-340.
 23. Goda, T; Mirowska, K; Currie, J; Kim, M-H; Rao, N V; Bonilla, G, and Wijnen, H, "Adult Circadian Behavior in *Drosophila* Requires Developmental Expression of Cycle, but Not Period. *Plos Genetics*", (2011) 7(7)
 24. Zhang, E E and Kay, S A, "Clocks Not Winding Down: Unravelling Circadian Networks. *Nature Reviews Molecular Cell Biology*", (2010) 11(11): 764-776.
 25. Allada, R and Chung, B Y, "Circadian Organization of Behavior and Physiology in *Drosophila*", in *Annual Review of Physiology*. (2010). 605-624.
 26. Son, G H; Chung, S; Choe, H K; Kim, H-D; Baik, S-M; Lee, H; Lee, H-W; Choi, S; Sun, W, and Kim, H, "Adrenal Peripheral Clock Controls the Autonomous Circadian Rhythm of Glucocorticoid by Causing Rhythmic Steroid Production. *Proceedings of the National Academy of Sciences*", (2008) 105(52): 20970-20975.
 27. Efimov, I; Parkin, G; Millett, E S; Glenday, J; Chan, C K; Weedon, H; Randhawa, H; Basran, J, and Raven, E L, "A Simple Method for the Determination of Reduction Potentials in Heme Proteins. *FEBS Letters*", (2014) 588(5): 701-704.
 28. Akashi, M; Okamoto, A; Tsuchiya, Y; Todo, T; Nishida, E, and Node, K, "A Positive Role for Period in Mammalian Circadian Gene Expression. *Cell Reports*", (2014) 7(4): 1056-1064.
 29. Huang, N A; Chelliah, Y; Shan, Y L; Taylor, C A; Yoo, S H; Partch, C; Green, C B; Zhang, H, and Takahashi, J S, "Crystal Structure of the Heterodimeric

- Clock: Bmal1 Transcriptional Activator Complex. *Science*", (2012) 337(6091): 189-194.
30. Hayasaka, K; Kitanishi, K; Igarashi, J, and Shimizu, T, "Heme-Binding Characteristics of the Isolated Pas-B Domain of Mouse Per2, a Transcriptional Regulatory Factor Associated with Circadian Rhythms. *Biochimica Et Biophysica Acta-Proteins and Proteomics*", (2011) 1814(2): 326-333.
 31. Airola, M V; Du, J; Dawson, J H, and Crane, B R, "Heme Binding to the Mammalian Circadian Clock Protein Period 2 Is Nonspecific. *Biochemistry*", (2010) 49(20): 4327-4338.
 32. Kaasik, K and Lee, C C, "Reciprocal Regulation of Haem Biosynthesis and the Circadian Clock in Mammals. *Nature*", (2004) 430(6998): 467-471.
 33. Gustafson, C L and Partch, C L, "Emerging Models for the Molecular Basis of Mammalian Circadian Timing. *Biochemistry*", (2015) 54(2): 134-149.
 34. Hoffmann, A and Roeder, R, "Purification of His-Tagged Proteins in Non-Denaturing Conditions Suggests a Convenient Method for Protein Interaction Studies. *Nucleic Acids Research*", (1991) 19(22): 6337.
 35. Maines, M D, "The Heme Oxygenase System: A Regulator of Second Messenger Gases. *Annual Review of Pharmacology and Toxicology*", (1997) 37: 517-554.
 36. Kitanishi, K; Igarashi, J; Hayasaka, K; Hikage, N; Saiful, I; Yamauchi, S; Uchida, T; Ishimori, K, and Shimizu, T, "Heme-Binding Characteristics of the Isolated Pas-a Domain of Mouse Per2, a Transcriptional Regulatory Factor Associated with Circadian Rhythms. *Biochemistry*", (2008) 47(23): 6157-6168.
 37. Zhang, Y and Emery, P, "Molecular and Neural Control of Insect Circadian Rhythms", in *Insect Molecular Biology and Biochemistry*. (2012), Elsevier. 513-551.
 38. Kaneko, H; Head, L M; Ling, J; Tang, X; Liu, Y; Hardin, P E; Emery, P, and Hamada, F N, "Circadian Rhythm of Temperature Preference and Its Neural Control in *Drosophila*. *Current Biology*", (2012) 22(19): 1851-1857.
 39. Chatterjee, A; Tanoue, S; Houl, J H, and Hardin, P E, "Regulation of Gustatory Physiology and Appetitive Behavior by the *Drosophila* Circadian Clock. *Current Biology*", (2010) 20(4): 300-309.
 40. Krishnan, B; Dryer, S E, and Hardin, P E, "Circadian Rhythms in Olfactory Responses of *Drosophila Melanogaster*. *Nature*", (1999) 400(6742): 375.
 41. Baumann, A; Texada, M; Chen, H; Etheredge, J; Miller, D; Picard, S; Warner, R; Truman, J, and Riddiford, L, "Genetic Tools to Study Juvenile Hormone Action in *Drosophila*. *Sci Rep*", (2017) 7(1): 2132.
 42. Greb-Markiewicz, B; Orłowski, M; Dobrucki, J, and Ożyhar, A, "Sequences That Direct Subcellular Traffic of the *Drosophila* Methoprene-Tolerant Protein (Met) Are Located Predominantly in the Pas Domains. *Molecular and Cellular Endocrinology*", (2011) 345(1-2): 16-26.
 43. Gorea, A, "Ticks Per Thought or Thoughts Per Tick? A Selective Review of Time Perception with Hints on Future Research. *Journal of Physiology-Paris*", (2011) 105(4-6): 153-163.

44. Gu, B-M; van Rijn, H, and Meck, W H, "Oscillatory Multiplexing of Neural Population Codes for Interval Timing and Working Memory. *Neuroscience & Biobehavioral Reviews*", (2015) 48: 160-185.
45. Addyman, C; French, R M, and Thomas, E, "Computational Models of Interval Timing. *Current Opinion in Behavioral Sciences*", (2016) 8: 140-146.
46. Jovanovic, L and Mamassian, P, "Timing in the Absence of a Clock Reset. *Journal of Vision*", (2018) 18(6): 13-13.
47. Lehmann, R; Childs, L; Thomas, P; Abreu, M; Fuhr, L; Herzog, H; Leser, U, and Relogio, A, "Assembly of a Comprehensive Regulatory Network for the Mammalian Circadian Clock: A Bioinformatics Approach. *Plos One*", (2015) 10(5)
48. Ko, C H and Takahashi, J S, "Molecular Components of the Mammalian Circadian Clock. *Human Molecular Genetics*", (2006) 15(suppl_2): R271-R277.
49. Buhr, E D and Takahashi, J S, "Molecular Components of the Mammalian Circadian Clock", in *Circadian Clocks*. (2013), Springer. 3-27.
50. Taylor, B L and Zhulin, I B, "Pas Domains: Internal Sensors of Oxygen, Redox Potential, and Light. *Microbiology and Molecular Biology Reviews*", (1999) 63(2): 479-+.
51. Hosoya, T; Oda, Y; Takahashi, S; Morita, M; Kawauchi, S; Ema, M; Yamamoto, M, and Fujii-Kuriyama, Y, "Defective Development of Secretory Neurons in the Hypothalamus of Arnt2-Knockout Mice. *Genes to Cells*", (2001) 6(4): 361-374.
52. Jaumouille, E; Machado Almeida, P; Stahl, P; Koch, R, and Nagoshi, E, "Transcriptional Regulation Via Nuclear Receptor Crosstalk Required for the *Drosophila* Circadian Clock. *Current biology : CB*", (2015) 25(11): 1502-1508.
53. Matsumoto, A; Ukai-Tadenuma, M; Yamada, R G; Houl, J; Uno, K D; Kasukawa, T; Dauwalder, B; Itoh, T Q; Takahashi, K, and Ueda, R, "A Functional Genomics Strategy Reveals Clockwork Orange as a Transcriptional Regulator in the *Drosophila* Circadian Clock. *Genes & Development*", (2007) 21(13): 000-000.
54. Hardin, P E, "The Circadian Timekeeping System of *Drosophila*. *Current Biology*", (2005) 15(17): R714-R722.
55. Blanchardon, E; Grima, B; Klarsfeld, A; Chélot, E; Hardin, P E; Prémat, T, and Rouyer, F, "Defining the Role of *Drosophila* Lateral Neurons in the Control of Circadian Rhythms in Motor Activity and Eclosion by Targeted Genetic Ablation and Period Protein Overexpression. *European Journal of Neuroscience*", (2001) 13(5): 871-888.
56. Houl, J H; Yu, W; Dudek, S M, and Hardin, P E, "*Drosophila* Clock Is Constitutively Expressed in Circadian Oscillator and Non-Oscillator Cells. *Journal of Biological Rhythms*", (2006) 21(2): 93-103.
57. Caspi, O; Huber, I; Kehat, I; Habib, M; Arbel, G; Gepstein, A; Yankelson, L; Aronson, D; Beyar, R, and Gepstein, L, "Transplantation of Human Embryonic Stem Cell-Derived Cardiomyocytes Improves Myocardial Performance in Infarcted Rat Hearts. *Journal of the American College of Cardiology*", (2007) 50(19): 1884-1893.

58. Orian, A; Grewal, S; Knoepfler, P; Edgar, B; Parkhurst, S, and Eisenman, R. "Genomic Binding and Transcriptional Regulation by the *Drosophila* Myc and Mnt Transcription Factors". in Cold Spring Harbor Symposia on Quantitative Biology. (Year) of Conference.: Cold Spring Harbor Laboratory Press.299-307.
59. Sehgal, A; Price, J L; Man, B, and Young, M W, "Loss of Circadian Behavioral Rhythms and Per Rna Oscillations in the *Drosophila* Mutant Timeless. Science", (1994) 263(5153): 1603-1606.
60. Saez, L and Young, M W, "Regulation of Nuclear Entry of the *Drosophila* Clock Proteins Period and Timeless. Neuron", (1996) 17(5): 911-920.
61. Allada, R and Chung, B Y, "Circadian Organization of Behavior and Physiology in *Drosophila*. Annual Review of Physiology", (2010) 72: 605-624.
62. Doherty, C J and Kay, S A, "Circadian Control of Global Gene Expression Patterns. Annual Review of Genetics", (2010) 44: 419-444.
63. Lin, J-M; Kilman, V L; Keegan, K; Paddock, B; Emery-Le, M; Rosbash, M, and Allada, R, "A Role for Casein Kinase 2 α in the *Drosophila* Circadian Clock. Nature", (2002) 420(6917): 816.
64. Chiu, J C; Ko, H W, and Edery, I, "Nemo/Nlk Phosphorylates Period to Initiate a Time-Delay Phosphorylation Circuit That Sets Circadian Clock Speed. Cell", (2011) 145(3): 357-370.
65. Zhou, J; Yu, W, and Hardin, P E, "Clockwork Orange Enhances Period Mediated Rhythms in Transcriptional Repression by Antagonizing E-Box Binding by Clock-Cycle. Plos Genetics", (2016) 12(11): e1006430.
66. Jindra, M; Uhlirova, M; Charles, J-P; Smykal, V, and Hill, R J, "Genetic Evidence for Function of the Bhlh-Pas Protein Gce/Met as a Juvenile Hormone Receptor. Plos Genetics", (2015) 11(7): e1005394.
67. Schmalen, I; Reischl, S; Wallach, T; Klemz, R; Grudziecki, A; Prabu, J R; Benda, C; Kramer, A, and Wolf, E, "Interaction of Circadian Clock Proteins Cry1 and Per2 Is Modulated by Zinc Binding and Disulfide Bond Formation. Cell", (2014) 157(5): 1203-1215.
68. Taylor, B L and Zhulin, I B, "Pas Domains: Internal Sensors of Oxygen, Redox Potential, and Light. Microbiology and Molecular Biology Reviews", (1999) 63(2): 479-506.
69. Stanewsky, R, "Genetic Analysis of the Circadian System in *Drosophila Melanogaster* and Mammals. Journal of Neurobiology", (2003) 54(1): 111-147.
70. Barnes, J W; Tischkau, S A; Barnes, J A; Mitchell, J W; Burgoon, P W; Hickok, J R, and Gillette, M U, "Requirement of Mammalian Timeless for Circadian Rhythmicity. Science", (2003) 302(5644): 439-442.
71. Sato, T K; Panda, S; Miraglia, L J; Reyes, T M; Rudic, R D; McNamara, P; Naik, K A; FitzGerald, G A; Kay, S A, and Hogenesch, J B, "A Functional Genomics Strategy Reveals Rora as a Component of the Mammalian Circadian Clock. Neuron", (2004) 43(4): 527-537.
72. Collins, B; Mazzoni, E O; Stanewsky, R, and Blau, J, "*Drosophila* Cryptochrome Is a Circadian Transcriptional Repressor. Current Biology", (2006) 16(5): 441-449.

73. Gegear, R J; Foley, L E; Casselman, A, and Reppert, S M, "Animal Cryptochromes Mediate Magnetoreception by an Unconventional Photochemical Mechanism. *Nature*", (2010) 463(7282): 804.
74. Foley, L E; Gegear, R J, and Reppert, S M, "Human Cryptochrome Exhibits Light-Dependent Magnetosensitivity. *Nature communications*", (2011) 2: 356.
75. Dunlap, J C, "Molecular Bases for Circadian Clocks. *Cell*", (1999) 96(2): 271-290.
76. Carretero-Paulet, L; Galstyan, A; Roig-Villanova, I; Martínez-García, J F; Bilbao-Castro, J R, and Robertson, D L, "Genome Wide Classification and Evolutionary Analysis of the Bhlh Family of Transcription Factors in Arabidopsis, Poplar, Rice, Moss and Algae. *Plant Physiology*", (2010): pp. 110.153593.
77. Georgias, C; Wasser, M, and Hinz, U, "A Basic-Helix-Loop-Helix Protein Expressed in Precursors of *Drosophila* Longitudinal Visceral Muscles. *Mechanisms of development*", (1997) 69(1-2): 115-124.
78. Baylies, M K; Bate, M, and Gomez, M R, "Myogenesis: A View from *Drosophila*. *Cell*", (1998) 93(6): 921-927.
79. Jennings, B H; Tyler, D M, and Bray, S J, "Target Specificities of *Drosophila* enhancer of Split Basic Helix-Loop-Helix Proteins. *Molecular and Cellular Biology*", (1999) 19(7): 4600-4610.
80. Crews, S T, "Control of Cell Lineage-Specific Development and Transcription by Bhlh-Pas Proteins. *Genes & Development*", (1998) 12(5): 607-620.
81. Sun, Z S; Albrecht, U; Zhuchenko, O; Bailey, J; Eichele, G, and Lee, C C, "Rigui, a Putative Mammalian Ortholog of the *Drosophila* Period Gene. *Cell*", (1997) 90(6): 1003-1011.
82. Bembenek, J; Itokawa, K; Hiragaki, S; Shao, Q-M; Tufail, M, and Takeda, M, "Molecular Characterization and Distribution of Cycle Protein from *Athalia Rosae*. *Journal of Insect Physiology*", (2007) 53(5): 418-427.
83. Yildiz, O; Doi, M; Yujnovsky, I; Cardone, L; Berndt, A; Hennig, S; Schulze, S; Urbanke, C; Sassone-Corsi, P, and Wolf, E, "Crystal Structure and Interactions of the Pas Repeat Region of the *Drosophila* Clock Protein Period. *Molecular Cell*", (2005) 17(1): 69-82.
84. Kloss, B; Price, J L; Saez, L; Blau, J; Rothenfluh, A; Wesley, C S, and Young, M W, "The *Drosophila* Clock Gene Double-Time Encodes a Protein Closely Related to Human Casein Kinase I ϵ . *Cell*", (1998) 94(1): 97-107.
85. Nobel, S; Abrahmsen, L, and Oppermann, U, "Metabolic Conversion as a Pre-Receptor Control Mechanism for Lipophilic Hormones. *European Journal of Biochemistry*", (2001) 268(15): 4113-4125.
86. Weigel, N L and Zhang, Y, "Ligand-Independent Activation of Steroid Hormone Receptors. *Journal of molecular medicine*", (1998) 76(7): 469-479.
87. Reinking, J; Lam, M M S; Pardee, K; Sampson, H M; Liu, S Y; Yang, P; Williams, S; White, W; Lajoie, G; Edwards, A, and Krause, H M, "The *Drosophila* Nuclear Receptor E75 Contains Heme and Is Gas Responsive. *Cell*", (2005) 122(2): 195-207.

88. Lee, C; Bae, K, and Edery, I, "Per and Tim Inhibit the DNA Binding Activity of a *Drosophila* Clock-Cyc/Dbm11 Heterodimer without Disrupting Formation of the Heterodimer: A Basis for Circadian Transcription. *Molecular and Cellular Biology*", (1999) 19(8): 5316-5325.
89. Hardin, P E, "Molecular Genetic Analysis of Circadian Timekeeping in *Drosophila*", in *Advances in Genetics*. (2011), Elsevier. 141-173.
90. Yu, W; Zheng, H; Houl, J H; Dauwalder, B, and Hardin, P E, "Per-Dependent Rhythms in Clk Phosphorylation and E-Box Binding Regulate Circadian Transcription. *Genes & Development*", (2006) 20(6): 723-733.
91. Kadener, S; Stoleru, D; McDonald, M; Nawathean, P, and Rosbash, M, "Clockwork Orange Is a Transcriptional Repressor and a New *Drosophila* Circadian Pacemaker Component. *Genes & Development*", (2007) 21(13): 000-000.
92. Reiff, T; Jacobson, J; Cognigni, P; Antonello, Z; Ballesta, E; Tan, K J; Yew, J Y; Dominguez, M, and Miguel-Aliaga, I, "Endocrine Remodelling of the Adult Intestine Sustains Reproduction in *Drosophila*. *Elife*", (2015) 4: e06930.
93. Hennig, S; Strauss, H M; Vanselow, K; Yildiz, O; Schulze, S; Arens, J; Kramer, A, and Wolf, E, "Structural and Functional Analyses of Pas Domain Interactions of the Clock Proteins *Drosophila* Period and Mouse Period2. *PLoS Biology*", (2009) 7(4): 836-853.
94. Vasudevan, D M; Sreekumari, S, and Vaidyanathan, K, "Textbook of Biochemistry for Medical Students". (2013): JP Medical Ltd.
95. Ponka, P, "Cell Biology of Heme. *The American journal of the medical sciences*", (1999) 318(4): 241-256.
96. Mochizuki, N; Tanaka, R; Grimm, B; Masuda, T; Moulin, M; Smith, A G; Tanaka, A, and Terry, M J, "The Cell Biology of Tetrapyrroles: A Life and Death Struggle. *Trends in Plant Science*", (2010) 15(9): 488-498.
97. Gozzelino, R; Jeney, V, and Soares, M P, "Mechanisms of Cell Protection by Heme Oxygenase-1. *Annual Review of Pharmacology and Toxicology*", (2010) 50: 323-354.
98. Berg JM, T J, Stryer L. , "Biochemistry. 5th Edition. Book", (2002)(New York: W H Freeman)
99. Barker, P D and Ferguson, S J, "Still a Puzzle: Why Is Haem Covalently Attached in C-Type Cytochromes? Structure with Folding & Design", (1999) 7(12): R281-R290.
100. Spiro, T G; Stong, J D, and Stein, P, "Porphyrin Core Expansion and Doming in Heme Proteins. New Evidence from Resonance Raman Spectra of Six-Coordinate High-Spin Iron (Iii) Hemes. *Journal of the American Chemical Society*", (1979) 101(10): 2648-2655.
101. Kharitonov, V G; Sharma, V S; Magde, D, and Koesling, D, "Kinetics of Nitric Oxide Dissociation from Five-and Six-Coordinate Nitrosyl Hemes and Heme Proteins, Including Soluble Guanylate Cyclase. *Biochemistry*", (1997) 36(22): 6814-6818.

102. Wu, N; Yin, L; Hanniman, E A; Joshi, S, and Lazar, M A, "Negative Feedback Maintenance of Heme Homeostasis by Its Receptor, Rev-Erba. Genes & Development", (2009)
103. Tsai, A-l; Martin, E; Berka, V, and Olson, J S, "How Do Heme-Protein Sensors Exclude Oxygen? Lessons Learned from Cytochrome C', Nostoc Puntiforme Heme Nitric Oxide/Oxygen-Binding Domain, and Soluble Guanylyl Cyclase. Antioxidants & Redox Signaling", (2012) 17(9): 1246-1263.
104. Blomberg, L M; Blomberg, M R, and Siegbahn, P E, "A Theoretical Study on the Binding of O₂, No and Co to Heme Proteins. Journal of Inorganic Biochemistry", (2005) 99(4): 949-958.
105. Noble, A; Olguín, J; Clérac, R, and Brooker, S, "Doubly Pyrazolate-Bridged Dinuclear Complexes of a Highly Constrained Bis-Terdentate Ligand: Observation of a [High Spin-Low Spin] State for [Feii2 (Pmap) 2][Sbf6] 2· 2.25 (C3h8o)(Pmap= 3, 5-Bis {[N-(2-Pyridylmethyl) Amino]-Methyl}-1 H-Pyrazolate). Inorganic Chemistry", (2010) 49(10): 4560-4569.
106. Balan, E; Allard, T; Boizot, B; Morin, G, and Muller, J-P, "Structural Fe 3+ in Natural Kaolinites: New Insights from Electron Paramagnetic Resonance Spectra Fitting at X and Q-Band Frequencies. Clays and Clay Minerals", (1999) 47(5): 605-616.
107. Rimington, C, "Spectral-Absorption Coefficients of Some Porphyrins in the Soret-Band Region. Biochemical Journal", (1960) 75(3): 620.
108. Delos, J B, "Theory of Electronic Transitions in Slow Atomic Collisions. Reviews of Modern Physics", (1981) 53(2): 287.
109. Karnaukhova, E; Rutardottir, S; Rajabi, M; Wester Rosenlöf, L; Alayash, A I, and Åkerström, B, "Characterization of Heme Binding to Recombinant A1-Microglobulin. Frontiers in Physiology", (2014) 5: 465.
110. Kundu, S; Premer, S A; Hoy, J A; Trent III, J T, and Hargrove, M S, "Direct Measurement of Equilibrium Constants for High-Affinity Hemoglobins. Biophysical Journal", (2003) 84(6): 3931-3940.
111. Zhang, X; Sato, M; Sasahara, M; Migita, C T, and Yoshida, T, "Unique Features of Recombinant Heme Oxygenase of *Drosophila Melanogaster* Compared with Those of Other Heme Oxygenases Studied. European Journal of Biochemistry", (2004) 271(9): 1713-1724.
112. Cui, L; Yoshioka, Y; Suyari, O; Kohno, Y; Zhang, X; Adachi, Y; Ikehara, S; Yoshida, T; Yamaguchi, M, and Taketani, S, "Relevant Expression of *Drosophila* Heme Oxygenase Is Necessary for the Normal Development of Insect Tissues. Biochemical and Biophysical Research Communications", (2008) 377(4): 1156-1161.
113. Ida, H; Suyari, O; Shimamura, M; Tai, T T; Yamaguchi, M, and Taketani, S, "Genetic Link between Heme Oxygenase and the Signaling Pathway of DNA Damage in *Drosophila Melanogaster*. The Tohoku journal of experimental medicine", (2013) 231(2): 117-125.
114. Rubio, M a F; Agostino, P V; Ferreyra, G A, and Golombek, D A, "Circadian Heme Oxygenase Actitivity in the Hamster Suprachiasmatic Nuclei. Neuroscience Letters", (2003) 353(1): 9-12.

115. Yang, J; Kim, K D; Lucas, A; Drahos, K E; Santos, C S; Mury, S P; Capelluto, D G, and Finkielstein, C V, "A Novel Heme-Regulatory Motif Mediates Heme-Dependent Degradation of the Circadian Factor Period 2. *Molecular and Cellular Biology*", (2008) 28(15): 4697-4711.
116. Guenther, C J; Bickar, D, and Harrington, M E, "Heme Reversibly Damps Period2 Rhythms in Mouse Suprachiasmatic Nucleus Explants. *Neuroscience*", (2009) 164(2): 832-841.
117. Ceriani, M F; Hogenesch, J B; Yanovsky, M; Panda, S; Straume, M, and Kay, S A, "Genome-Wide Expression Analysis in *Drosophila* reveals Genes Controlling Circadian Behavior. *Journal of Neuroscience*", (2002) 22(21): 9305-9319.
118. Bain, D L; Heneghan, A F; Connaghan-Jones, K D, and Miura, M T, "Nuclear Receptor Structure: Implications for Function. *Annual Review of Physiology*", (2007) 69: 201-220.
119. Bertini, I and Sigel, A, "Handbook on Metalloproteins". (2001): CRC Press.
120. Mukaiyama, Y; Uchida, T; Sato, E; Sasaki, A; Sato, Y; Igarashi, J; Kurokawa, H; Sagami, I; Kitagawa, T, and Shimizu, T, "Spectroscopic and DNA-Binding Characterization of the Isolated Heme-Bound Basic Helix-Loop-Helix-Pas-a Domain of Neuronal Pas Protein 2 (Npas2), a Transcription Activator Protein Associated with Circadian Rhythms. *FEBS Journal*", (2006) 273(11): 2528-2539.
121. Hayashi, T, "Generation of Functionalized Biomolecules Using Hemoprotein Matrices with Small Protein Cavities for Incorporation of Cofactors. *Coordination chemistry in protein cages: Principles, design, and applications*", (2013): 87-110.
122. Fauque, G D and Barton, L L, "Hemoproteins in Dissimilatory Sulfate-and Sulfur-Reducing Prokaryotes", in *Advances in Microbial Physiology*. (2012), Elsevier. 1-90.
123. Atamna, H and Boyle, K, "Amyloid-B Peptide Binds with Heme to Form a Peroxidase: Relationship to the Cytopathologies of Alzheimer's Disease. *Proceedings of the National Academy of Sciences*", (2006) 103(9): 3381-3386.
124. Kumar, S and Bandyopadhyay, U, "Free Heme Toxicity and Its Detoxification Systems in Human. *Toxicology Letters*", (2005) 157(3): 175-188.
125. Reddi, A R and Hamza, I, "Heme Mobilization in Animals: A Metallolipid's Journey. *Accounts of Chemical Research*", (2016) 49(6): 1104-1110.
126. Shi, L; Dong, H; Reguera, G; Beyenal, H; Lu, A; Liu, J; Yu, H-Q, and Fredrickson, J K, "Extracellular Electron Transfer Mechanisms between Microorganisms and Minerals. *Nature Reviews Microbiology*", (2016) 14(10): 651.
127. Liu, J; Chakraborty, S; Hosseinzadeh, P; Yu, Y; Tian, S; Petrik, I; Bhagi, A, and Lu, Y, "Metalloproteins Containing Cytochrome, Iron-Sulfur, or Copper Redox Centers. *Chemical Reviews*", (2014) 114(8): 4366-4469.

Chapter Two

Materials and Methods

2. Materials and methods

2.1. Materials

2.1.1. Chemicals and equipment

All chemicals and reagents were ordered from Sigma-Aldrich, Apollo Scientific, Fischer Scientific, Acros Organics and Melford. The water used was ultra-pure, deionized distilled water (ddH₂O) as prepared using an Elga PureLab Option (DV35) water purifier to prepare the medias, buffers and any type of solution, while TEV protease was expressed and purified in-house. UV-visible spectrophotometry was carried out using a Perkin-Elmer Lambda 40. The pH of solutions was measured using a Hanna's company pH meter. Gravity column chromatography from Econo-Column®. Nanodrop UV-visible was Thermo Scientific, NanoDrop 2000 Spectrophotometer.

2.2. Methods

2.2.1. Production of Constructs

2.2.1.1. Cloning of dPER-PAS (either A or B or AB)

Constructs were produced for *Drosophila melanogaster* Period PAS-A (dPER-PAS-A), PASB (dPER-PAS-B) and PAS-A and B (dPER-PAS-AB) by the Protein Expression Laboratory (PROTEX) at the University of Leicester. Primers were designed against (*per*) gene sequence and are listed in Table 2-2 of the appendix. Amino-terminal affinity tags were spaced from the inserts with a TEV protease recognition sequence and in addition to a selective antibiotic resistance gene, which is lethal to the bacterial cells expressing it in sucrose agar plates. Genes were amplified by PCR and fused into the expression vectors shown in Table 1 to allow for the expression of the protein with an additional His tag, GST tag or no tag [4]. All constructs were sequenced by the Protein Nucleic Acid Chemistry Laboratory (PNAACL) at the University of Leicester.

In this study, different length of constructs was used for the same domains (either dPER-PAS-A or dPER-PAS-B) according to (Tables 2-1, 2-9 and Figure 2-1). Three trials were made; one for each construct.

Table 2-1 Cloning and Expression vectors used for this study.

No.	Plasmid	Characteristics	Source/ Reference
1.	pLEICS-03	Cloning vector with Kan resistance, C-His6 tag and TEV protease cleavage site	Protex
2.	pLEICS-04	Cloning vector with Kan resistance, N-GST tag and TEV protease cleavage site	Protex
3.	pLEICS-05	Cloning vector with Amp resistance, C-His6 tag and TEV protease cleavage site	Protex
4.	pLEICS-07	Cloning vector with Kan resistance, N-His6/S tag and TEV protease cleavage site	Protex
5.	pLEICS-10	Cloning vector with Amp resistance, N-MBP tag and TEV protease cleavage site	Protex
6.	pLEICS-14	Cloning vector with Amp resistance, N-GST tag and TEV protease cleavage site	Protex
7.	pLEICS-92	Cloning vector with Amp resistance, N-GST tag and TEV protease cleavage site	Protex
8.	pLEICS-93	Cloning vector with Amp resistance, C-His6 tag and TEV protease cleavage site	Protex
9.	pHis-dPER-PAS-A	Expression of N-terminal His-tagged dPER-PAS-A cloned into pLEICS-07	This study, 1 st trial
10.	pHis-dPER-PAS-B	Expression of N-terminal His-tagged dPER-PAS-B cloned into pLEICS-07	This study, 1 st trial
11.	pHis-dPER-PAS-AB	Expression of N-terminal His-tagged dPER-PAS-AB cloned into pLEICS-07	This study, 1 st trial
12.	pGST-dPER-PAS-A	Expression of N-terminal GST-tagged dPER-PAS-A cloned into pLEICS-14	This study, 1 st trial
13.	pGST-dPER-PAS-B	Expression of N-terminal GST-tagged dPER-PAS-B cloned into pLEICS-14	This study, 1 st trial
14.	pGST-dPER-PAS-AB	Expression of N-terminal GST-tagged dPER-PAS-AB cloned into pLEICS-14	This study, 1 st trial
15.	pNO-dPER-PAS-A	Expression dPER-PAS-A cloned into pLEICS-05 with no tag.	This study, 1 st trial
16.	pNO-dPER-PAS-B	Expression of dPER-PAS-B cloned into pLEICS-05 with no tag.	This study, 1 st trial
17.	pMBP-dPER-PAS-A	Expression of N-terminal MBP-tagged dPER-PAS-A cloned into pLEICS-10	This study, 1 st trial
18.	pMBP-dPER-PAS-A	Expression of N-terminal MBP-tagged dPER-PAS-Af cloned into pLEICS-10	This study, 2 nd trial

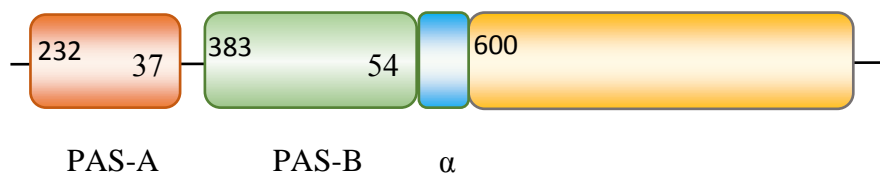
19.	pMBP-dPER-PAS-A	Expression of N-terminal MBP-tagged dPER-PAS-As cloned into pLEICS-10	This study, 2nd trial
20.	pMBP-dPER-PAS-B	Expression of N-terminal MBP-tagged dPER-PAS-B cloned into pLEICS-10	This study, 2nd trial
21.	pGST-dPER-PAS-AB	Expression of N-terminal GST-tagged dPER-PAS-B cloned into pLEICS-92	This study, 2nd trial
22.	pGST-dPER-PAS-AB	Expression of N-terminal GST-tagged dPER-PAS-ABs cloned into pLEICS-92	This study, 2nd trial
23.	pHis-dPER-PAS-AB	Expression dPER-PAS-ABf cloned into pLEICS-93 with His-tag.	This study, 2nd trial
24.	pHis-dPER-PAS-AB	Expression of dPER-PAS-ABs cloned into pLEICS-93 with His-tag.	This study, 2nd trial
25.	pGST-dPER-PAS-A	Expression of N-terminal GST-tagged dPER-PAS-A cloned into pLEICS-04	This study, 3rd trial
26.	pHis-dPER-PAS-A	Expression of N-terminal His-tagged dPER-PAS-A cloned into pLEICS-03	This study, 3rd trial
27.	pGST-dPER-PAS-B	Expression of N-terminal GST-tagged dPER-PAS-B cloned into pLEICS-04	This study, 3rd trial
28.	pHis-dPER-PAS-B	Expression of N-terminal His-tagged dPER-PAS-B cloned into pLEICS-03	This study, 3rd trial
29.	pGST-dPER-PAS-AB	Expression of N-terminal GST-tagged dPER-PAS-AB cloned into pLEICS-04	This study, 3rd trial
30.	pHis-dPER-PAS-AB	Expression of N-terminal His-tagged dPER-PAS-AB cloned into pLEICS-03	This study, 3rd trial
31.	pGST-dPER-PAS-B α	Expression dPER-PAS-B α cloned into pLEICS-04 with GST tag.	This study, 3rd trial
32.	pHis-dPER-PAS-B α	Expression of dPer-PAS-3B α cloned into pLEICS-03 with His tag.	This study, 3rd trial
33.	pGST-dPER-PAS-AB α	Expression dPer-PAS-3T cloned into pLEICS-04 with GST tag.	This study, 3rd trial
34.	pHis-dPER-PAS-AB α	Expression of dPer-PAS-3T cloned into pLEICS-01 with His tag.	This study, 3 rd trial



dPER construct of first trial



dPER construct of second trial



dPER construct of third trial

Figure 2-1 Scheme for period of *Drosophila Melanogaster* which was designed in this work.

2.2.2. Molecular Biology

2.2.2.1. Primers Design

Primers were manually designed using the Enzyme X software and purchased either from Invitrogen or Eurofins MWG Operon and were dissolved in sterile water to give a stock concentration of 100 μ M and stored at -20 °C. They were designed to have a 21 bp annealing region to the gene of interest plus a vector homology region (16 bp on forward primers and an 18 bp on reverse primers) for cloning the PCR product into an expression vector.

Table 2-2 5' to 3' sequence of forward and reverse primers used to generate alternative constructs of domains of dPER-PAS. Keys (F: forward, R: reverse, no: no tag, His: His tag, MBP: MBP tag and GST: GST tag).

Primer	Sequence 5'-3'	Target	Trial No.
Per-Pas-A F	TATTTTCAGGGCGCCC GCGGGGAGCGGGTGA AGGAG	pHis-dPER-PAS-A pHis-dPER-PAS-AB pGST-dPER-PAS-A pGST-dPER-PAS-AB	1 st trial
Per-Pas-B F	TATTTTCAGGGCGCCA AGGTTCCCGACGAGA TTCTC	pHis-dPER-PAS-B pGST-dPER-PAS-B	1 st trial
Per-Pas-A R	GACGGAGCTCGAATTT TAGCCCGTGGTGATCT CACT	pHis-dPER-PAS-A pGST-dPER-PAS-A	1 st trial
Per-Pas-B R	GACGGAGCTCGAATTT TAGGACACCGTCTCCG CCAG	pHis-dPER-PAS-B pGST-dPER-PAS-B pHis-dPER-PAS-AB pGST-dPER-PAS-AB	1 st trial
Per-Pas-A-no tag F	AGGAGATATACATAT GCGCGGGGAGCGGGT GAAGGA	pNO-dPER-PAS-A	1 st trial
Per-Pas-A-no tag R	GAAGTACAGGTTCTCT CAGCCCGTGGTGATCT CACT	pNO-dPER-PAS-A	1 st trial
Per-Pas-B-no tag F	AGGAGATATACATAT GAAGGTTCCCGACGA GATTCT	pNO-dPER-PAS-B	1 st trial
Per-Pas-B-no tag R	GAAGTACAGGTTCTCT CAGGACACCGTCTCCG CCAG	pNO-dPER-PAS-B	1 st trial
Per-Pas-A F	GTATTTTCAGGGCGCC ATGGAGGGCGGCGAG TCCAC	pMBP-dPER-PAS-A pHis-dPER-PAS-AB pGST-dPER-PAS-AB	2 nd trial
Per-Pas-A F	GTATTTTCAGGGCGCC ATGGAGGAGGATCAG TCCGG	pMBP-dPER-PAS-A pHis-dPER-PAS-AB pGST-dPER-PAS-AB	2 nd trial
Per-Pas-A R	GACGGAGCTCGAATTT CACTGTGAGAGAATCT CGTC	pMBP-dPER-PAS-A pMBP-dPER-PAS-A	2 nd trial

Per-Pas-B F	GTATTTTCAGGGCGCC ATGAAGAGCCCCAAG TTCGC	pMBP-dPER-PAS-B	2 nd trial
Per-Pas-B R	GACGGAGCTCGAATTT CAGTGGTGCGGCGAA ATCTCG	pHis-dPER-PAS-AB pGST-dPER-PAS-AB pHis-dPER-PAS-AB pGST-dPER-PAS-AB	2 nd trial
Per-Pas-A F	TACTTCCAATCCATGG GGGAGCGGGTGAAGG AGGAC	pHis-dPER-Pas-A pGST-dPER-Pas-A pHis-dPER-PAS-AB pGST-dPER-PAS-AB pHis-dPER-PAS-AB α pGST-dPER-PAS-AB α	3 rd trial
Per-Pas-A R	TATCCACCTTTACTGT CAGCTCTTGATCGGAG TGGCG	pHis-dPER-PAS-A pGST-dPER-PAS-A	3 rd trial
Per-Pas-B F	TACTTCCAATCCATGA TTCTCTCACAGAAGAG CCCC	pHis-dPER-PAS-B pGST-dPER-PAS-B pHis-dPER-PAS-B α pGST-dPER-PAS-B α	3 rd trial
Per-Pas-B R	TATCCACCTTTACTGT CACGGACGGGACACC GTCTCC	pHis-dPER-PAS-B pGST-dPER-PAS-B pHis-dPER-PAS-AB pGST-dPER-PAS-AB	3 rd trial
Per-Pas-B α R	TATCCACCTTTACTGT CAGTGGTGCGGCGAA ATCTCGCC	pHis-dPER-Pas-B α pGST-dPER-Pas-B α pHis-dPER-PAS-AB α pGST-dPER-PAS-AB α	3 rd trial

2.2.2.2. Polymerase chain reaction (PCR)

Cloning of dPER-PAS-A, dPER-PAS-B and dPER-PAS-AB were performed by Dr Xiaowen Yang at the PROTEX facility, University of Leicester.

2.2.2.3. The dPer-PAS-A construct

Table 2-3 The dPer-PAS-A with details tags, types of vectors was used for each construct and weight of construct by kDa.

No.	Domain	Sequence of residues	Length of residues	Sequence of trial	Type of tag	Type of vector	Total weight kDa
1.	dPER-PAS-A	231-293	63	first trial	GST	pLEICS-14	32.74
					His	pLEICS-7	7.45
					without tag	pLEICS-5	7.15
					MBP	pLEICS-10	47.77
2.	dPER-PAS-A	1-386	386	second trial	MBP	pLEICS-10	84.75
3.	dPER-PAS-A	145-386	242	second trial	MBP	pLEICS-10	68.4
4.	dPER-PAS-A	232-375	144	third trial	GST	pLEICS-4	42.91
					His	pLEICS-3	17.63

Table 2-4 Mutant dPer-PAS-A with details tags, types of vectors was used for each construct and weight of construct by kDa.

No.	Mutated construct	Mutation	Length of residues	Type of vector	Total weight kDa
1.	His-dPer-PAS-A	C312A	144	pLEICS-3	17.63
2.	His-dPer-PAS-A	C369A	144	pLEICS-3	17.63

2.2.2.4. The dPer-PAS-B construct

Table 2-5 The dPer-PAS-B with details tags, types of vectors was used for each construct and weight of construct by kDa.

No.	Domain	Sequence of residues	Length of residues	Sequence of trial	Type of tag	Type of vector	Total weight kDa
1.	dPER-PAS-B	378-539	162	first trial	GST	pLEICS-14	45.29
					His	pLEICS-7	20.01
					without tag	pLEICS-5	19.705
2.	dPER-PAS-B	387-599	213	second trial	MBP	pLEICS-10	60.32
3.	dPER-PAS-B	383-541	159	third trial	GST	pLEICS-4	44.96
					His	pLEICS-3	19.67
4.	dPER-PAS-B with α -Helix	383-599	217	third trial	GST	pLEICS-4	52.09
					His	pLEICS-3	26.80

Table 2-6 Mutant dPer-PAS-B with details tags, types of vectors was used for each construct and weight of construct by kDa.

No.	Mutated construct	Mutation	Length of residues	Type of vector	Total weight kDa
1.	His-dPer-PAS-B	C455A	159	pLEICS-3	19.67
2.	His-dPer-PAS-B	C467A	159	pLEICS-3	19.67

2.2.2.5. The dPer-PAS-AB construct

Table 2-7 The dPer-PAS-AB with details tags, types of vectors was used for each construct and weight of construct by kDa.

No.	Domain	Sequence of residues	Length of residues	Sequence of trial	Type of tag	Type of vector	Total weight kDa
1.	dPER-PAS-AB	231-539	309	first trial	GST	pLEICS-14	61.35
					His	pLEICS-7	35.12
2.	dPER-PAS-AB	1-599	599	second trial	GST	pLEICS-92	95.16
					His	pLEICS-93	70.46
3.	dPER-PAS-AB	145-599	455	second trial	GST	pLEICS-92	78.80
					His	pLEICS-93	54.10
4.	dPER-PAS-AB	232-541	310	third trial	GST	pLEICS-4	62.55
					His	pLEICS-3	37.85
5.	dPER-PAS-AB with α -Helix	232-599	368	third trial	GST	pLEICS-4	70.17
					His	pLEICS-1	44.97

2.2.2.6. Mutant Primer Design

PCR is a technique used to multiply DNA sequences for stock, to study or ligate into host cells and cultivate proteins. This technique requires primers which are short sequences of DNA typically 18-22 bp complimentary to the 3' end of the DNA to be multiplied. Primers were designed based on the genetic sequence, ligation sites of restriction enzymes and any mutations.

Table 2-8 Mutant dPer-PAS-AB and (dPer-PAS-AB with α -Helix) with details tags, types of vectors was used for each construct and weight of construct by kDa.

No.	mutated construct	mutation	Length of residues	type of vector	total weight kDa
1.	His-dPer-PAS-AB	C312A	310	pLEICS-3	37.85
2.	His-dPer-PAS-AB	C369A	310	pLEICS-3	37.85
3.	His-dPer-PAS-AB	C455A	310	pLEICS-3	37.85
4.	His-dPer-PAS-AB	C467A	310	pLEICS-3	37.85
5.	His-dPer-PAS-AB with α -Helix	C312A	368	pLEICS-3	44.97
6.	His-dPer-PAS-AB with α -Helix	C369A	368	pLEICS-3	44.97
7.	His-dPer-PAS-AB with α -Helix	C455A	368	pLEICS-3	44.97
8.	His-dPer-PAS-AB with α -Helix	C467A	368	pLEICS-3	44.97

Table 2-9 Details dPER domains constructs for all trials in this work.

No.	Domain	First & last Residue	Length of Domain by Residues	Notes	No. of Trials
1.	dPER-PAS-A	R231 to G293	63		Constructs of first trial
2.	dPER-PAS-B	K378 to S539	162		
3.	dPER-PAS-AB	R231 to S539	309		
4.	dPER-PAS-A	M1 to Q386	386		Constructs of second trial
5.	dPER-PAS-A	E145 to Q386	242		
6.	dPER-PAS-B	K387 to H599	213		
7.	dPER-PAS-AB	M1 to H599	599		
8.	dPER-PAS-AB	E145 to H599	455		
9.	dPER-PAS-A	G232 to S 375	144		Constructs of third trial
10.	dPER-PAS-B	I383 to P541	159		
11.	d-Per-PAS-B α	I383 to H599	217	B domain + α Helix	
12.	dPER-PAS-AB	G232 to P 541	310		
13.	dPER-PAS-AB α	G232 to H599	368	A+B domains + α Helix	

2.2.2.7. Mutagenesis of dPER-PAS-A, dPER-PAS-B and dPER-PAS-AB

One of the main aims of this project was to investigate the heme binding mechanism with dPER-PAS domains, with the specific aim of identifying the exact amino acid residues involved in the binding of dPER-PAS domains to heme through UV-vis heme titrations. An experiment was designed based on the basic principle: removal or mutation of the distal residue will lead to a decrease in the binding capacity of dPER-PAS domains. Deletion of a residue in a protein, however, is a drastic a change that can lead to protein misfolding or conformational changes that could potentially obscure the heme binding, according to the EPR data (for heme binding with PAS domains) and the stereochemistry for the dPER-PAS molecule. Four mutagenesis were performed for C312A and C369A in dPER-PAS-A and C455A and C467A in dPER-PAS-B (for the third trial only). The same primers for the third trial were used to make the mutations (Table 2-2). All mutagenesis were made in the PROTEX laboratory at the University of Leicester (Dr. Xiaowen Yang). The sequences of all mutageneses after PCR were verified by the Protein and Nucleic Acid Laboratory (PNACL), University of Leicester.

2.2.3. Transformation

The constructs presented in Table 2-1 were transformed into expression strains of *E. coli*. The strains used were *BL21 DE3* (Novagen) and *Rosetta* (Novagen). *Rosetta* is a *BL21DE3* derivative and contains a chloramphenicol-resistant gene on a plasmid. This plasmid also encodes for t-RNAs that are rarely used in *E. coli*. Both strains express a T7 polymerase upon IPTG induction which allows for regulated, high levels of protein expression. An aliquot of 1 µl of plasmid DNA was mixed with 50 µl of *BL21 DE3* or *Rosetta* competent cells and incubated on ice for 30 min. Cells were then heat-shocked at 42 °C for 1 min and placed on ice for 2 min. A volume of 200 µl of 2XYT media was pipetted on to the cells, which were then rescued by an incubator at 37 °C for 1 hr in an orbital-shaker incubator running at 190 rpm. An aliquot of 50 µl of the sample were spread on a LB-agar plate containing a suitable antibiotic (the type of antibiotic depends on the vector which is used). Table 2-2. The plate was then incubated at 37 °C overnight and bacterial colonies containing the plasmid were observed the following day.

2.2.4.Expression trials

An aliquot of 10 ml of 2XYT was inoculated with one colony from the transformation plates and grown to an OD_{600 nm} of 1.0-1.2. The culture was then divided into two tubes. One tube was induced by adding a 1 mM final concentration of isopropyl β-D-1-thiogalactopyranoside (IPTG). IPTG is a lactose analogue that cannot be degraded by the bacteria [5], it binds to the lactose repressor region on the plasmid (Lac I on vectors, see vectors maps in the appendix, figure 7-4 to figure 7-12) which causes the release of a tetrameric repressor unit from the lactose operator, thereby allowing T7 RNA polymerase to be transcribed and translated. T7 RNA polymerase binds to the T7 promoter sequence upstream of the *dper-pas* domain gene and transcribes the gene [5]. After allowing an incubation period of about 12 hr at low temperature, the target protein was expected to be abundant in the culture. The culture was grown overnight in an orbital-shaker incubator at 20 °C and 180 rpm. There are trials to expression without using IPTG that occur due to a self-induction technique. A comparison of the results for normal induction and self-induction shows no difference for either mechanism.

2.2.5.Bugbuster Protocol

An aliquot of 1 ml culture (Which is coming from step 2.2.6.) was centrifuged at 13,000 rpm (F-45-12-11 rotor) for 5 min. The pellet was resuspended in 100 µl of Bugbuster and was kept at room temperature for 5 mins. Samples were then spun at 13,000 rpm (F-45-12-11 rotor) for 10 min and the supernatant removed and kept on ice as a soluble fraction. The pellet, which represented the insoluble fraction, was washed twice in 100 µl of buffer (50 mM Tris pH 8.0, 100 mM NaCl). The same buffer (50 mM Tris pH 8.0, 100 mM NaCl) was used to re-suspend the pellet. The samples were there relocated to SDS-PAGE gel analysis.

2.2.6.SDS-PAGE Gel

An SDS-PAGE gel analyses were used to check protein availability and purity. An SDS-PAGE gel is run over three key stages: after the sample has passed through the nickel column, after the tag has been cleaved, and after the protein has been subject to size exclusion chromatography.

SDS-PAGE gel will separate the components of a protein sample based on their size, as reliant on the basic principles of electrophoresis: a charged molecule will migrate in an

electric field towards an electrode of opposite charge. This will auto-polymerize over time, bonding head to tail with neighbouring molecules. Bis-acrylamide is required to cross-link the acrylamide chains, resulting in the formation of a gel. Ammonium persulfate (APS) (source of a free radical to initiate polymerization at a faster rate). *N, N,*

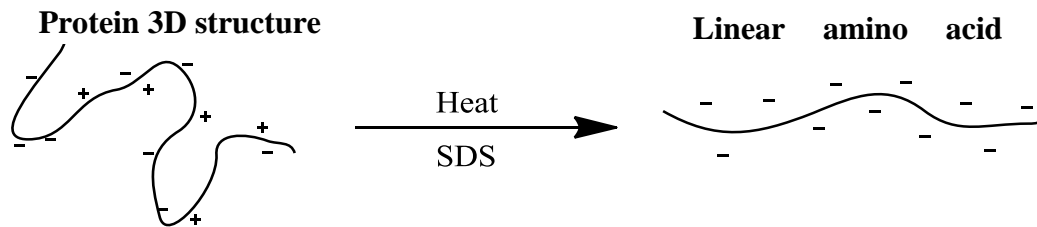


Figure 2-2 Artistic impression of the effect heat and SDS has on protein structure.

N, N'- tetramethylethylenediamine (TEMED) stabilizes free radicals there by greatly improving the rate of polymerization and gel formation. The protein sample was diluted in a protein loading buffer which contained sodium dodecyl sulphate (SDS), which is a detergent that denatures proteins and coats them with a negative charge. The sample was heated to disrupt the intermolecular interactions responsible for the protein's structural conformation. This eliminated other parameters that could potentially affect the electrophoretic mobility such as shape and charge. Any protein in the mixture will at this point have been converted from a multi-charged complicated 3D structure to a negatively charged linear amino acid chain (Figure 2-2). The polyacrylamide gel has a molecular sieving effect, which will slow down the migration of the denatured protein fragments depending on their size resulting in protein separation [6, 7].

Normally, 10-12% polyacrylamide resolving gels (the percentage was varied according to the molecular weight) containing 0.1% SDS were used for this study. A layer of 4% polyacrylamide stacking gel containing 0.1% SDS was poured onto the resolving gel to compress the protein sample and make sure it would enter the resolving layer as a single band [1]. A volume of 20 μ l protein samples were obtained by mixing 16 μ l of protein with 4 μ l of sample loading buffer (1:10 DTT from stock 1M solution) and heated for 3 min at 100 $^{\circ}$ C. Gels were run in an SDS running buffer for approximately one hr at 180 V until the dye front reached the bottom of the gel.

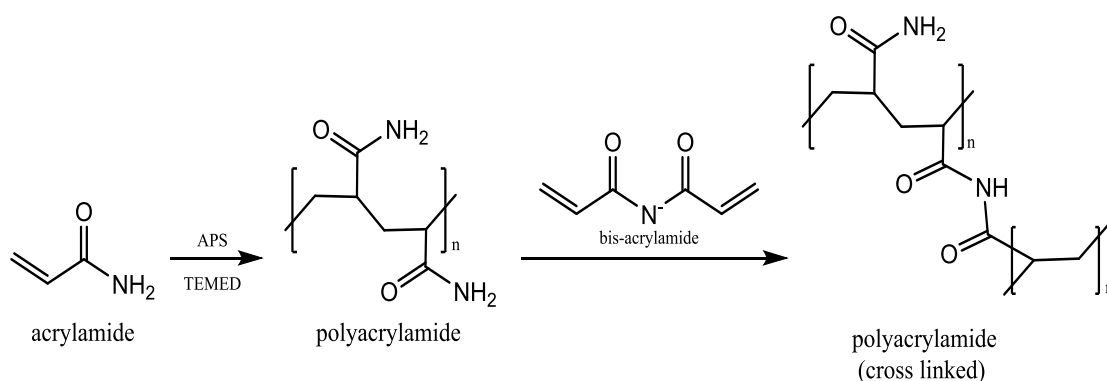


Figure 2-3 Reaction of acrylamide with APS and TEMED to form a cross-linked gel.

After the gels were run, they were stained with Coomassie Brilliant Blue G-250, which left the protein bands visible to the naked eye.

Protein sizes were estimated using a pre-stained molecular ladder as a reference (Figure 2-4). Excess stain was removed by soaking in PAGE-distain overnight (water) [8].

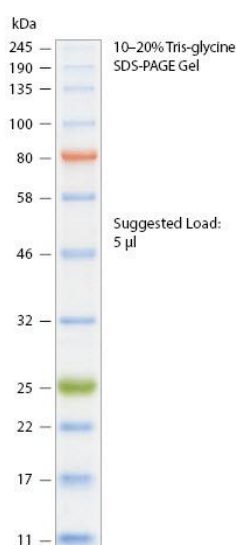


Figure 2-4 Protein ladder used to determine the mass of protein during SDS-PAGE gel analysis. Provided by New England Biolabs®, Biolabs N. Protein Standards, <http://www.bio-rad.com/en-uk/category/protein-ladders-standards-markers?ID=09507551-2848-4bd1-a3c1-650b4d41aa48>.

2.2.7. Large-scale Expression

An aliquot of 2 ml from an overnight starter culture was added to 700 ml of 2XYT with a suitable antibiotic depending on type of *E. coli.*, and type of plasmid resistance (the concentration of antibiotic used was dependent on the type of antibiotic see Appendix Table 7-2). The culture was grown to an OD_{600nm} of 0.6-0.8 and induced with IPTG (100

μM final concentration). The culture was incubated overnight at 15-37 °C (insoluble at 37 °C, soluble at 15 °C) and at 180 rpm. Cells were harvested the next day and centrifuged at 4000 rpm (SLC-6000 rotor), 4 °C and 20 min, after which the pellets were stored at -80 °C.

2.2.8. Purification

2.2.8.1. Purification of GST-tagged Protein

Pellets produced from 0.5 L bacterial cultures expressing dPER-PAS-AB were taken from the freezer at -80 °C and re-suspended with 40 ml of sonication buffer (50mM Tris buffer pH 7.5, 150 mM NaCl) and 1 Roche tablet of protease inhibitor. The solution was sonicated for a total time of 4 min. by alternating 20 s of sonication and 20 s of rest on ice to avoid sample heating. The cell crude lysate was centrifuged in a SS-34 rotor at 18,000 rpm and 4 °C for 30 min.

An aliquot of 2 ml of Glutathione Sepharose 4B packed in a column was washed with 10 times the resin volume of ddH₂O to remove the 20% storage ethanol. A volume of 20 ml of the supernatant from the previous step was added to the column and left for 1 hr. The column was then washed with 10 times the resin volume of GST buffer (GST buffer: 50 mM Tris buffer pH 7.5 and 150 mM NaCl). A volume of 28 μl of TEV protease (7.5 U/ μl) were mixed with 4ml of GST buffer, added to the column, and left overnight. The supernatant was collected which contained the cleaved dPER-PAS-AB. This was concentrated to 5 ml for gel filtration.

To elute any uncleaved protein Glutathione Elution Buffer (10 mM reduced glutathione, 50 mM Tris, pH 8.0, 150 mM NaCl) was added to the column and left in cold room (4 °C) overnight. The next day, 2 ml fractions were collected and then run on SDS-PAGE gel to check for any uncleaved protein.

2.2.8.2. Size Exclusion Chromatography

Size exclusion chromatography was performed at room temperature using a Superdex 75 16/60 column mounted on an ÄKTA purifier P-900 (GE Healthcare LifeSciences). The column was equilibrated with 120 ml of 0.22 μm -filtered gel filtration buffer (50 mM Tris pH 7.5, 150 mM NaCl, 1 mM DTT). The protein, which was concentrated to 5 ml by centrifugal filtration, was injected onto the column and run at a flow rate of 0.5 ml/min. The fractions for 1 ml were collected.

2.2.9. Protein Refolding

2.2.9.1. Small-scale Preparation of Inclusion Bodies

Inclusion bodies were prepared using 1 ml pellets of induced overnight cultures of His-tagged dPER-PAS-A and dPER-PA-SB grown at 37 °C. Pellets were resuspended in 200 µl Bugbuster master mix, incubated at room temperature for 10 min and centrifuged (at 13,000 rpm (F-45-12-11 rotor) for 15 min at 4 °C). The supernatant was removed and the Bugbuster step was repeated. The pellet was resuspended in 200 µl Wash Buffer 1 (25 mM Tris pH 7.5, 0.5 M NaCl, 1 M urea, 1 mg/ml sodium deoxy cholate, 1 mM EDTA), incubated for 5 min at room temperature and centrifuged at 13,000 rpm (F-45-12-11 rotor) for 15 min at 4 °C, and the supernatant discarded. This was repeated using Wash Buffer 2 (25 mM Tris pH 7.5, 0.5 M NaCl, 1 mM EDTA, 0.25% Triton X-100). The pellet was washed with 200 µl of 20 mM Tris pH 7.0, and the Bugbuster step was repeated once more. The pellet was washed and resuspended in 100 µl 20 mM Tris pH 7.0, and 16 µl was loaded on a SDS-PAGE gel to verify the purity.

2.2.9.2. Protein Refolding Small-scale Trials

The inclusion body pellet was resuspended in 200 µl of Solubilisation Buffer (25 mM Tris pH 7.5, 6 M guanidine hydrochloride, 5 mM DTT) and was incubated at 37 °C for 10 min. After centrifugation at 13,000 rpm (F-45-12-11 rotor) for 15 min, 4 °C, the protein concentration was determined using a Nanodrop (Thermo Scientific). The concentration required was between 1-2 mg/ml. A Quick-Fold Protein Refolding Kit (Athena Enzyme Systems) was used for the refolding trials. Buffers 2, 5, 10 and 15 from the kit were used for the initial trials. An aliquot of 50 µl of solubilised inclusion bodies were added dropwise with gentle vortexing to 0.95 ml of each refolding buffer condition containing 1 mM of DTT and were incubated overnight at 4 °C. Refolded protein samples were centrifuged at 13,000 rpm (F-45-12-11 rotor), 15 min, 4 °C, prior to loading on a Superdex 200 10/300 GL column pre-equilibrated with 20 ml of 20 mM Tris pH 7.5, 150 mM NaCl, 1 mM DTT. The column was run at a flow rate of 0.5 ml/min at room temperature and 0.5 ml fractions were collected.

2.2.9.3. Large-scale Preparation of Inclusion Bodies

Induced pellets from 1 L cultures expressing His-tagged protein were taken from the freezer (-80 °C) and re-suspended using 100 ml lysis buffer (25 mM Tris pH 8.0, 150 mM NaCl, 0.5 mg/ml lysozyme, 0.5% Triton-x-100, 1 mM EDTA), and 1 tablet of Protease

inhibitor cocktail per litre of bacterial culture. The mixture was incubated at room temperature on an orbital shaker for 20-30 min. An aliquot of 5 mM of MgCl₂ and DNase at 5 µg/ml were added, and the sample was incubated at room temperature on an orbital shaker for 15 min. The solution was sonicated for 20 s and stored for 20 s on ice in cycles for 4 min. This was then centrifuged at 20,000 rpm (SS-34 rotor) and 4 °C for 20 min. The pellets were resuspended in 40 ml of buffer 2 (25 mM Tris, pH 8.0, 0.5 M NaCl, 0.5 % Triton-X-100, 1 mM EDTA) then sonicated and centrifuged. After that, the pellet was resuspended in buffer 3 (25 mM Tris, pH 8.0, 0.5 M NaCl, 1 mg/ml sodium deoxy cholate 1 M urea), sonicated and centrifuged and then resuspended in buffer 4 (25 mM Tris, pH 8.0). At this stage, a 16 µl aliquot was taken and analysed via SDS-PAGE gel. Sonication and centrifugation steps were repeated twice more.

After addition of buffer 4, the resultant was divided into Eppendorf tubes, which were then centrifuged at 13,000 rpm (F-45-12-11 rotor). Supernatants were discarded and the pellets snap frozen in liquid nitrogen and stored at -80 °C. The pellets were suspended in 200 µl Bugbuster and incubated for 15 min at room temperature. An aliquot of 800 µl of ddH₂O was added to each sample and then centrifuged at 13,000 rpm (F-45-12-11 rotor), 15 min at 4 °C. Solubilisation buffer (25 mM Tris, pH 8.0, 6 M Guanidine HCl, 5 mM DTT) was prepared and used to re-suspend inclusion body pellets (1 ml of buffer for each pellet). These were then incubated at 37 °C for 15 min. The pellets were then centrifuged at 13,000 rpm (F-45-12-11 rotor) 4 °C. The supernatant were transferred carefully into new Eppendorf tubes as soluble inclusion bodies.

The absorbance spectrum (at 280 nm) for solubilised inclusion bodies was measured using a Nanodrop UV-visible (Thermo Scientific, NanoDrop 2000 Spectrophotometer). The absorbance for the buffer solution was subtracted from that measured for the inclusion bodies.

2.2.9.4. Large-scale Protein Refolding (condition 5)

Refolding buffer condition 5 from the Quick Fold Protein Refolding Kit (50 mM MES, pH 6.0, 240 mM NaCl, 10 mM KCl, 1 mM EDTA, 0.4 M sucrose, 0.75 M guanidine HCl, 1 mM DTT) was prepared and a drop wise refolding experiment was set up at 4 °C as shown in Figure (2-5).



Figure 2-5 Dropwise refolding of solubilised inclusion bodies into the refolding buffer.

Solubilised inclusion bodies were placed in a syringe, and the syringe supported above the refolding buffer. The solubilised inclusion bodies were left to enter the refolding buffer by gravity for 1 h and incubated at 4 °C with gentle stirring for 2 days (Figure 2-5).

2.2.9.5. Dialysis of refolded Protein

The protein in refolding buffer solution was placed in a dialysis tube (SLS dialysis tube Inf Dia 36/32” – 28.6 mm MWCO 12,000-14,000 Da, 3 M, TBU2016) and placed in a cylinder containing dialysis buffer (20 mM Tris, pH 7.5, 140 mM NaCl). This buffer was replaced twice in one day. After 24 hr, the dialysed protein was filtered to remove any unfolded protein (white precipitate) and loaded onto a nickel affinity column, as below.

2.2.10. Nickel Affinity Purification

To remove impurities (consisting of *E.coli* soluble proteins) from the sample, further purification was required. The first purification step was nickel-affinity chromatography. In this technique, the crude lysate was passed through a Ni-nitrilotriacetic agarose (NTA) column. The poly-His tag on the target protein has a high affinity for nickel ions and binds strongly to the NTA column (unlike the impurities, which will flow through).

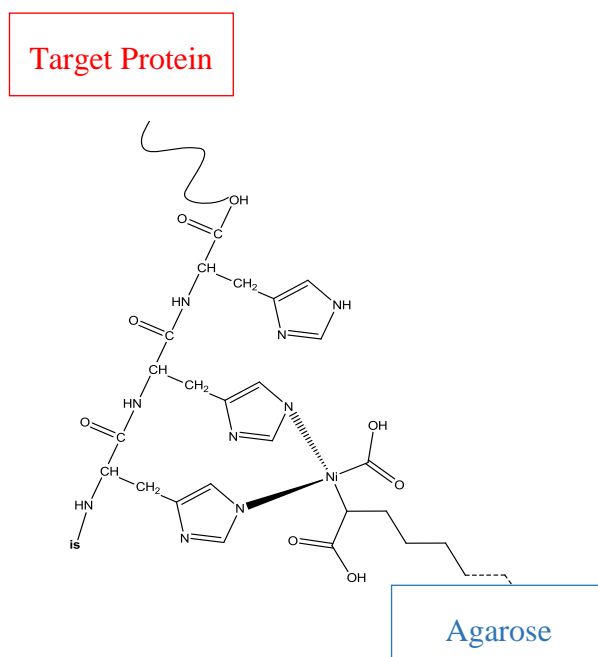


Figure 2-6 Binding mechanism of the poly His-tag on the NTA resin.

Target proteins were then eluted using increasing amounts of imidazole, a molecule that is structurally similar to histidine and will compete with the His-tagged proteins to bind to the nickel ions.

Powdered imidazole was added to a 10 mM final concentration of the filtered protein. An aliquot of 5 ml of Ni²⁺-NTA agarose (nickel-nitrilotriacetic acid) was packed into a gravity column chromatography and washed with ddH₂O (10 times resin volume) and buffer N1 (25 mM Tris, pH 7.5, 140 mM NaCl, and 10 mM imidazole), (2 times resin volume). Next, the sample was loaded into the column. The sample was reapplied to the column to ensure maximum binding. The resin was then washed with five resin volumes of N1. The bound protein was eluted with 50 ml buffer N2 (25 mM Tris, pH 7.5, 140 mM NaCl, 500 mM imidazole, and pH adjusted to 7.5) and 10X 5 ml fractions were collected. To regenerate the nickel column, the column was stripped by applying 5 resin volumes of 500 mM EDTA (the flow-through was collected in a separate container because of the high toxicity of nickel to the environment). The column was then washed with 20 resin volumes of ddH₂O and loaded with 3 resin volumes of 100 mM NiSO₄. The column was finally washed with 10 volumes of ddH₂O.

Fractions were run on a SDS-PAGE to check for protein purity and availability (Figure 2-7). Relevant fractions were pooled and His-tagged TEV protease was added. The digestion was conducted overnight at 4 °C in a dialysis tube in dialysis buffer (50 mM NaCl, 20 mM Tris, pH 7.5, 0.5 mM TCEP, and 0.2 mM EDTA) to dispose of or reduce the imidazole concentration sufficiently and give time to cleave His-tag by TEV protease. The following day His-tagged TEV protease and the cleaved tag was removed by a second round of nickel affinity purification. The sample was then concentrated to 5 mL using a centrifugal filter unit with a 10 kDa molecular weight cut-off and passed through a size exclusion chromatography column.

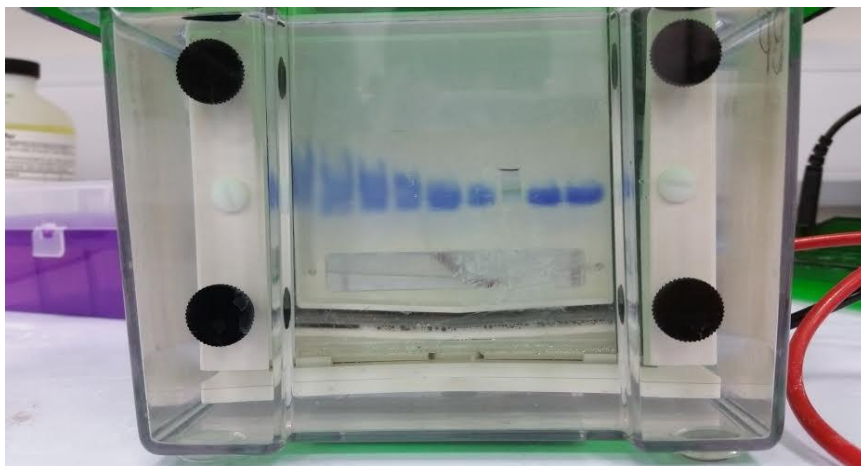


Figure 2-7 SDS-PAGE gel, the figure shows the setting of an electrophoresis apparatus with an SDS-PAGE gel each blue band represents a protein sample.

2.2.11. Purification of MBP tag Protein by Amylose Affinity Chromatography

Pellets derived from 0.75 L bacterial cultures expressing dPER-PAS-A or dPER-PAS-B with an MBP (maltose-binding protein) tag were taken from the freezer at -80 °C and re-suspended with 40 ml of sonication buffer (20 mM Tris buffer, pH 7.5, 200 mM NaCl, 1 mM EDTA, 1 protease inhibitor tablet). The solution was sonicated for a total time of 10 min by alternating 30 s of sonication and 30 s of resting in ice to avoid sample heating. The cell crude lysate was centrifuged in a SS-34 rotor at 18,000 rpm and 4 °C for 30 min. A volume of 5 ml of amylose was packed in a column were washed with 5 times the resin volume of ddH₂O to remove the 20% storage ethanol. An aliquot of 2 times the resin volume of binding buffer (20 mM Tris buffer, pH 7.5, 200 mM NaCl, 1 mM EDTA) was used to equilibrate the column, after which the supernatant from the previous step was added to the column, which was then left for 1 h with gentle rocking and in a cold atmosphere to keep the protein in good condition. To elute the protein from the column, 5 ml of elution buffer (10 mM maltose monohydrate, 20 mM Tris buffer, pH 7.5, 200 mM NaCl, and 1 mM EDTA) was added as fractions. According to the vector map (vector pLIES-10, see appendix figure 7-7), TEV-tag was used to cleave MBP tag. The sample was then concentrated to 5 ml using a centrifugal filter unit with a 10 kDa molecular weight cut-off and passed through a size exclusion chromatography column and then run on SDS-PAGE gel to check for any uncleaved protein.

2.2.12. Small-scale Plasmid DNA Purifications

An aliquot of 100 µl of Top 10 cells stored at -80°C were defrosted on ice for 20 s and subsequently incubated on ice for 30 s with 1 µl of plasmid DNA which wanted to multiplication. The cells were then heat-shocked at 42 °C for 60 s and rested for 2 min on ice. A volume of 200 µl 2XYT (31 gm/L) was added to the mixture (Top 10 cells and plasmid) then rescued by an incubator at 37 °C for 1 h in an orbital-shaker incubator running at 190 rpm. An aliquot of 50 µl of the sample were spread on a LB-agar plate containing a suitable antibiotic (the type of antibiotic depends on the vector which is used). Table 2-2. The plate was then incubated at 37 °C overnight and bacterial colonies containing the plasmid were observed the next day.

One colony was taken and added to a sterile tube with 5 ml of 2XYT that included 5 µl of antibiotic (the type of antibiotic was dependent on the type of plasmid). The tube was placed in an orbital-shaker incubator running at 190 rpm overnight [9].

An aliquot of 1 ml of the culture from incubator was placed in an Eppendorf, which was spun at 13,000 rpm (F-45-12-11 rotor) for 1 min at room temperature. Then, this process was repeated with the remainder of the media (4 ml) in the same Eppendorf which was using in the previous step by repeat the same protocol for the first ml. After which the standard instructions for the protocol's kit were followed (Plasmid DNA Purification Using QIAperp Spin Miniprep Kit 250). The resulting plasmid was stored in a freezer at -20 °C.

2.2.13. UV-Visible Absorption Spectroscopy

A Perkin Elmer Lambda 40 UV-Visible spectrophotometer was used under room temperature environment to the absorption of spectrophotometer between 200-700 nm. In Heme, the protoporphyrin ring IX made heme a strongly conjugated system (natively containing 18π electrons). The absorption of light according to π -system in two distinct areas: the first area near the UV region and the second absorption within the area of visible region. This diversity in absorption region comes from two main absorption transitions from $S_0 \rightarrow S_2$ (Soret) and $S_0 \rightarrow S_1$ (Q bands). Where the absorption of the most intense transitions is at 380-500 nm is called the Soret band, and then followed by absorption of weaker transitions at 500-750 nm called the Q band. The metal centre and its relevant oxidation state influence the distinctive transitions and lead to their differences, with each oxidation state providing a distinct spectrum [10].

2.2.14. Electron Paramagnetic Resonance (EPR)

EPR technique was used to study the relationship between the electronic nature the heme Fe species and distinguish the effect of surrounding ligands on the paramagnetic electrons of the Fe. By comparing the effect of known ligands to the paramagnetic heme Fe centre with that from protein samples with unknown ligation, it is possible to identify the nature of the unknown ligands. The EPR spectra allows the calculation of principal g-factors which contain information about the electronic structure of a heme protein [11].

All heme proteins exhibit a rhombic signal in the $g=2$ region of the spectra. The three-principal g-factors differ slightly in their g values, this difference represents the rhombicity of the protein heme complex (see figure 2-8) [1, 12].

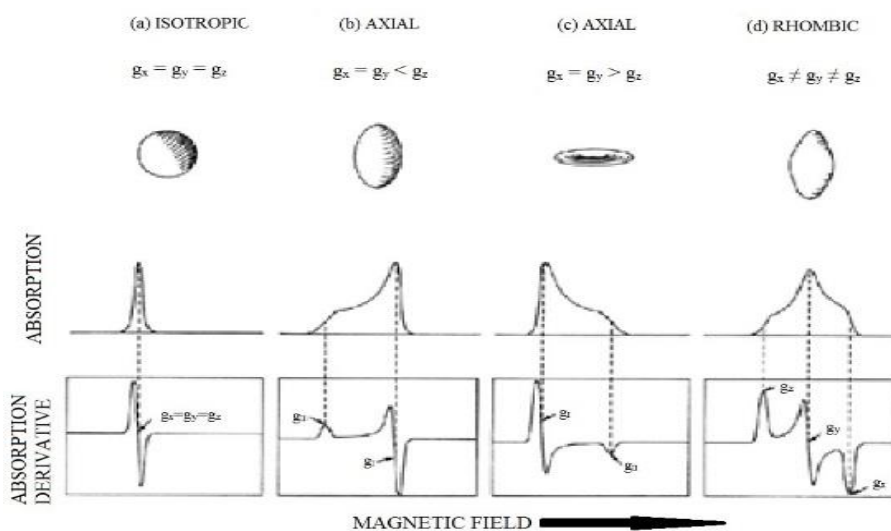


Figure 2-8 The absorption curve and corresponding EPR derivative curve for a Rhombic magnetic moment [1].

EPR spectra were recorded on a Bruker's EMX EPR spectrometer by Dr Dimitri Svistunenko at the University of Essex, UK.

$$\text{Eq 2-1} \quad \Delta E = h \nu = g_e \mu_B B_0$$

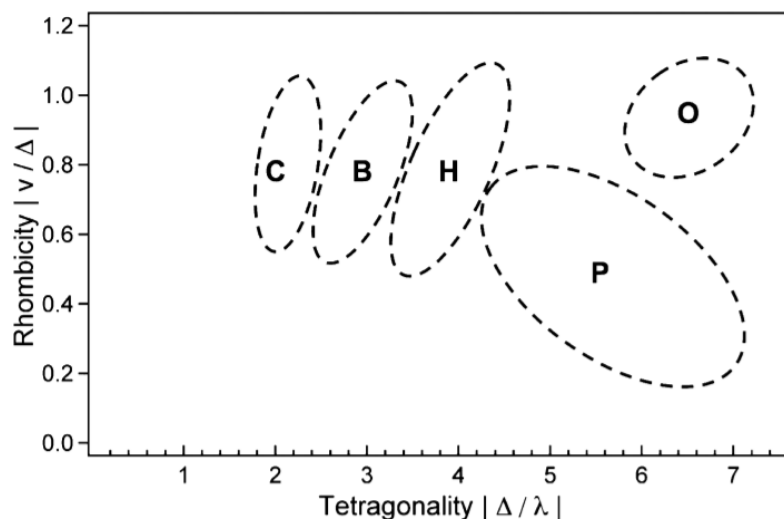


Figure 2-9 Blumberg-Peisach correlation diagram for low-spin heme centres. Regions C, B, H, O and P are designated to His/Met, His/His(N⁻), His/His, His/OH⁻ and Cys(S⁻)/X heme environments, respectively [2].

In an EPR spectrometer, a paramagnetic sample is placed in a large uniform magnetic field which splits the energy levels of the ground state by an amount as described by Equation 2-1. Where

h : is Planck's constant.

ν : the frequency of radiation.

g_e : is g-factor, =2.0023 for the free electron.

μ_B : is Bohr magneton $9.2740 \times 10^{-24} \text{ JT}^{-1}$ or $4.6686 \times 10^{-5} \text{ cm}^{-1} \text{ G}^{-1}$.

B_0 : the strength of magnetic field in Tesla.

One of the objectives of this study was to determine the nature of binding between heme and dPER-PAS domains. Samples of ferric protein were examined by EPR by Dr. Dimitri Svistunenko at the EPR Research Facility (University of Essex) using a Bruker EMX EPR spectrometer X-band (9.38 GHz) equipped with a spherical high quality resonator ER 4122 and an Oxford Instruments liquid helium system for the low-temperature measurements electron paramagnetic resonance spectroscopy. Samples of wild type and mutant for dPER-PAS domains were placed in Wilmad SQ EPR tubes to a final volume of 250 μl , frozen in methanol kept on dry ice, wiped and then transferred to liquid nitrogen and prepared in Tris/HCl buffer at (pH 7.5). The sample in Tris/HCl buffer did produce some interesting results.

2.2.15. Circular Dichroism (CD)

Circular dichroism (CD spectra were obtained with a Chirascan plus CD spectrometer at room temperature) experiments were carried out to qualitatively compare secondary structures of Wild-Type (wt) for dPER-PAS domains and mutants with and without heme bound.

This technique gathers the structural information by measuring differences in circularly polarised light which - if present - gives rise to elliptically polarised light. A depiction of this is given in figure 2-10 which shows how the vector for circularly polarised light changes from plane polarised to elliptically polarised depending on chiral absorption. This difference in chiral absorption arises due to typically right-handed α -helices that absorb right-handed circularly polarised light preferentially in π - π^* transitions. Different types of transitions in relation to structure are observed for α -helices and β -sheets (parallel and antiparallel) giving peaks at different wavelengths that appear in the spectrum. Examples

of proteins with different secondary structure components and their relevant CD spectra can be shown in figure 2-11[13].

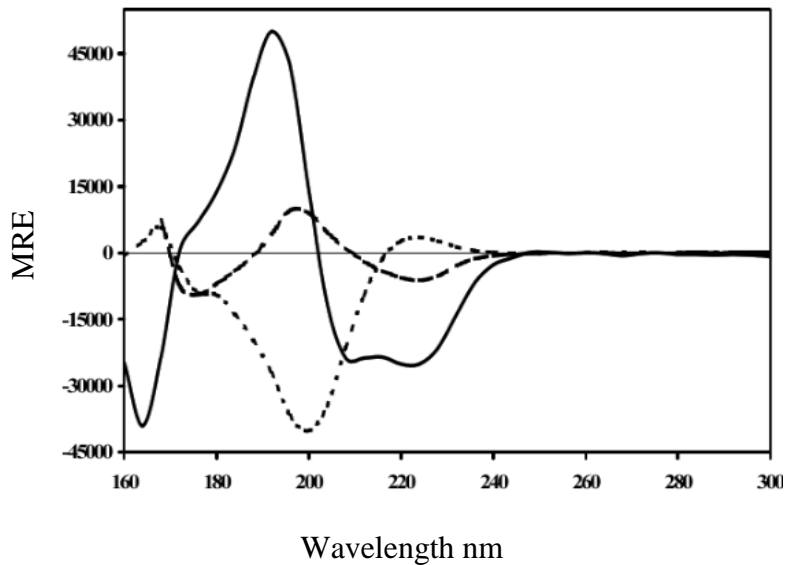


Figure 2-10 Depiction of electronic vectors in circularly polarised light. a) Plane-polarised light arises as a sum of equal and opposing left and right-circularly polarised lights. b) Circularly polarised light unequally absorbed by a sample resulting in an elliptically polarised path. c) Representation of the elasticity that the CD measures.

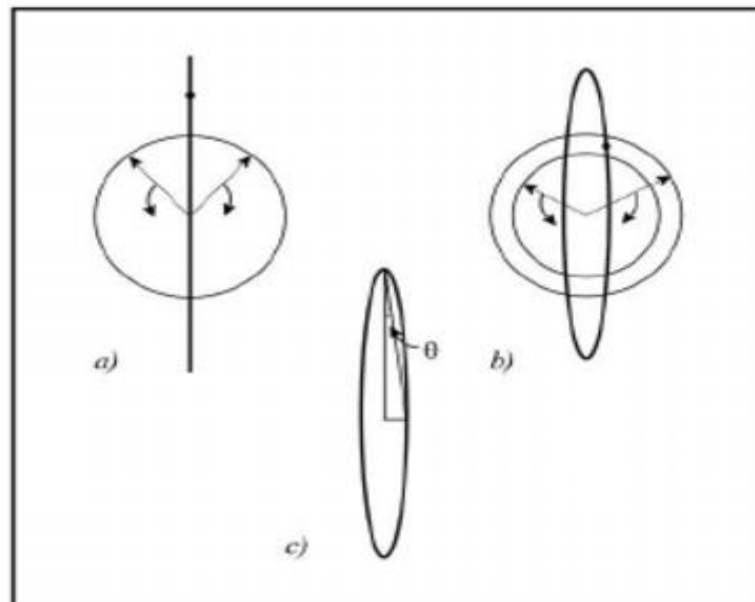


Figure 2-11 CD spectra of three proteins with varying predominant types of secondary structure. The solid line is mainly α -helical, dashed line mainly β -sheet and dotted line a protein containing mostly polyproline-II structures.

2.2.16. Protein Heme-Binding Titrations

2.2.16.1. Preparation of Hemin Stock Solution

A hemin stock was prepared by dissolving some hemin in 100 μl NaOH 0.1 M. The solution was vortexed for 30 s. and wrapped in aluminium foil as hemin is light sensitive. An aliquot of 50 μl of hemin solution was then added to 500 μl of gel filtration buffer (50 mM of NaCl, and 20 mM Tris, pH 7.5) then mixed and centrifuged for 1 min at 13,000 rpm (F-45-12-11 rotor). To determine the concentration of the hemin stock solution, 1 ml of gel filtration buffer was mixed with 20 μl of hemin stock in a cuvette (type Q7) and the absorbance at 385 nm was measured [14]. The concentration of the stock solution was calculated using the Beer-Lambert law:

$$A = c * \epsilon * l$$

A: absorption

C: concentration

ϵ : Extinction coefficient, for heme at 385 nm = 58.44 $\text{mM}^{-1}\text{cm}^{-1}$, (for dPER-PAS-AB at 280 nm = 31150 $\text{M}^{-1}\text{cm}^{-1}$ and would be different in another domain).

l: the length of cuvette (absorption path length)

The resulting concentration was then normalised for a 51-fold dilution. Then two different concentrations of hemin (50 μM and 200 μM) were prepared.

2.2.16.2. UV-visible Hemin Titrations

For the titration assays, heme was added to two cuvettes, one containing gel filtration buffer only (used as a reference) and the other containing the protein of interest (sample). The absorbances were measured and the data was plotted as represented in Figure 3-22.

2.2.16.3. Ligand Binding Kinetics

One way to quantify the affinity with which a protein binds a ligand is the dissociation constant, K_D . If one considers an experiment where a ligand is titrated (such as heme) against a fixed concentration of protein (Equation 1) and the following relationships are observed in Equation 2. This system can then be described by an equilibrium dissociation constant, as shown in Equation 3.



$$\text{Eq 2} \quad [\text{P}]_{\text{tot}} = [\text{P}]_{\text{f}} + [\text{PL}]$$

and

$$[L]_{\text{tot}} = [L]_{\text{f}} + [PL]$$

In Equation 3 the K_d value is expressed as a proportion of free protein ($[P]_{\text{f}}$) and free ligand ($[L]_{\text{f}}$) to a protein-ligand complex $[PL]$. When a term is introduced representing the total amount of protein in equilibrium ($[P]_{\text{tot}}$), Equation 3 can be manipulated to give Equation 4. This equation was then fitted to the absorbance (concentration) of the heme-dPER-PAS domain complex as a function of hemin concentration, from which k_d was then derived. The behaviour that this equation describes is known as hyperbolic binding or, when applied to enzyme kinetics, is known as the Michaelis-Menten equation [15, 16].

$$\text{Eq 3} \quad K_D = \frac{[P]_{\text{f}} [L]_{\text{f}}}{[PL]}$$

$$\text{Eq 4} \quad [PL] = \frac{[P]_{\text{tot}} [L]_{\text{f}}}{K_D + [L]_{\text{f}}}$$

However, Equation 4 can only be used when heme binding is relatively weak and the concentration of free hemin is assumed to be similar to total hemin (free ligand approximation). However, as the binding becomes tighter, and the K_D becomes comparable to the total protein concentration ($[P]_{\text{tot}}$), this assumption is not valid and the apparent binding curve deviates from a hyperbola. This is the case for CO binding to the dPER-PAS domain-heme complex. In this circumstance, free CO compared to total CO needs to be accounted for, resulting in the following quadratic binding (Equation 5) which was used [17] to measure K_D in the tight binding scenario observed in the CO binding titrations [18].

In all the graphs in this study, the K_D value coming from the equation

$$\text{Eq 5} \quad Y = \frac{P_1 * X}{P_2 + X}$$

P_1 : V_{max}

P_2 : K_D

2.2.17. Protein Crystallisation

For the purpose of obtaining the per domains crystals there are a several attempts were made to get crystal suitable to study in X-ray crystallography in order to deduce the three-dimensional structure of the domain and to determine the type (specific or nonspecific) of the heme binding in case of crystallization of the complex protein with heme. The principle of crystallisation depend on the precipitation of a molecule from solution which

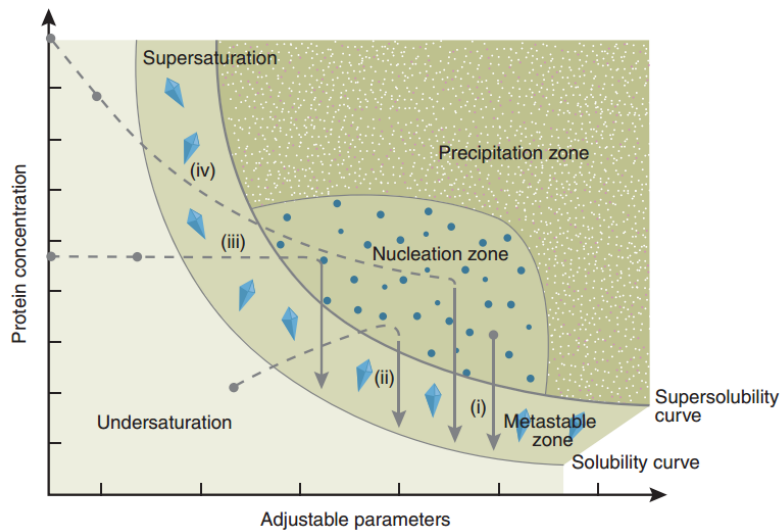


Figure 2-12 Scheme Phase representing different stages of protein crystallisation and effect of different parameters such as pH, buffer, salt, in relation with protein concentration. Profiles of crystallisation techniques include: (i) microbatch (ii) vapour diffusion (iii) dialysis (iv) free interface diffusion [3].

itself involve intermolecular interactions and solvation. These variables are inherently difficult to understand and utilise in protein crystallisation due to the variability of primary, secondary and tertiary structures in large proteins. Therefore, the process of crystallisation is conducted on a trial and error basis, but was aided in this case by the use of pre-determined crystal screens consisting of 96 varying conditions that were tested against the protein using the sitting-drop vapour diffusion technique. This technique is one of the four most commonly used techniques in protein crystallisation which have different saturation profiles, as shown in figure 2-12.

The aim of the protein crystallisation trials was to find a suitable protein concentration and crystallisation parameters to induce nucleation of the protein. In order to screen different parameters, different crystal screens were used including crystal I and II (Hampton Research), JCSG, PACT-Premier, Stura-Macrosol and ProPlex (Molecular Dimensions). These screens were transferred to a 96-well sitting drop crystallisation plate as displayed in figure 2-13, and the protein mixed with a range of parameters using an Oryx 8 protein crystallisation robot. These crystal screens were varied in three key parameters which are important for the following reasons [19].

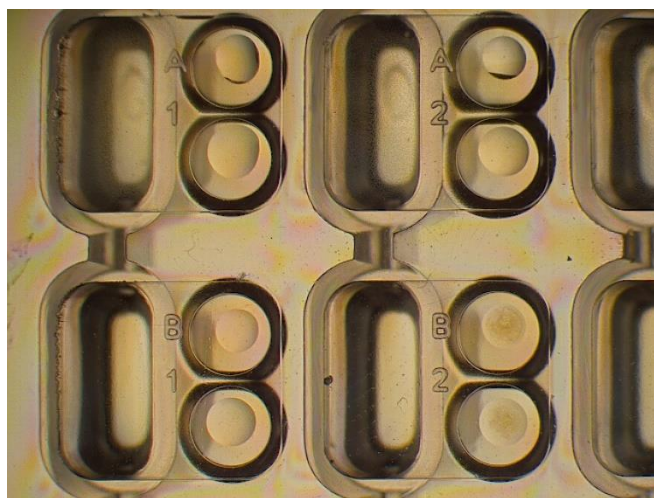


Figure 2-13 Sitting drop vapour diffusion crystallisation plate displaying four conditions. Each condition consisted of a reservoir and two nearby wells screening two protein conditions.

Buffer and pH influence the surface charge distribution on the protein. The pH should be near the pI of the protein (see Table 2-3), resulting in a net charge of zero. Therefore, two neighbouring molecules can interact with one another by cancelling local charges.

Table 2-10 pI value for each domain estimated by (Protein Calculator v3.4), dPER-PAS-Af it is mean A domain contain 386 a.a start with Met1 to the Gln386, dPER-PAS-As it is mean A domain contain 242 a.a start with Glu145 to the Gln386, dPER-PAS-ABf it is mean AB domain contain 599 a.a stat with Met1 to the His599, dPER-PAS-ABs it is mean AB domain contain 455 a.a stat with Glu145 to the His599.

No.	Domain	pI value	Extinction Coefficient ϵ ($M^{-1} cm^{-1}$)	Classified trial
1.	dPER-PAS-A	5.23	8250	1st trial
2.	dPER-PAS-B	8.43	17780	1st trial
3.	dPER-PAS-AB	6.56	31150	1st trial
4.	dPER-PAS-A	6.46	21620	2nd trial
5.	dPER-PAS-A	5.69	19060	2nd trial
6.	dPER-PAS-B	7.23	17780	2nd trial
7.	dPER-PAS-AB	6.84	39400	2nd trial
8.	dPER-PAS-AB	6.66	36840	2nd trial
9.	dPER-PAS-A	8.48	12090	3rd trial
10.	dPER-PAS-B	8.9	17780	3rd trial
11.	dPER-PAS-AB	8.69	31150	3rd trial
12.	dPER-PAS-B α	7.23	17780	3rd trial
13.	dPER-PAS-AB α	7.68	31150	3rd trial

Salt was used to shield charges between proteins or form salt bridges promoting intermolecular interactions. Salts can also have a higher affinity for water molecules therefore promoting protein-protein interactions, *c.f.* protein-water interactions.

Precipitants (polymers) such as polyethylene glycol were used to trap water molecules in inaccessible regions in the protein, therefore driving protein supersaturation. Certain salts with higher affinities for water molecules were also used such as ammonium sulphate. Temperature can also influence protein crystallisation as it can change protein solubility and affect crystallisation thermodynamics.

This 96-well crystallisation plate was used for sitting drop vapour diffusion trials. This method of crystallisation was most commonly used throughout this work and micro batches were also trialled, which consisted of the same 96 different conditions being screened however, the nanodroplets are left under a layer of paraffin oil. The conditions trialled throughout this work are displayed in Table 2-1 alongside their respective protein parameters.

2.2.17.1. Setting of Sitting Drop Crystallisation Plates

For dPER-PAS domains purified in third trial, the crystallisation trials were conducted in duplicate MRC 96-well sitting drop crystallisation plates that were set up using a manual way according to Yildiz [20]. Each reservoir well of the plate was manually filled with 500 μ l of 500 mM of CaCl_2 . Then, equal amount from the reservoir and protein with mixture (5 mg/ml of protein, 20 mM HEPES pH 7.5, 200 mM ammonium carbonate and 5 mM DTE) were mixed (1 μ l, 2 μ l, 3 μ l, 4 μ l and 5 μ l from each). To trial crystallisation conditions for producing a complex of protein with heme drops were set with a ratio of 1:1:2 (protein mixture: heme 5 mg/ml: reservoir). The same ratio for mutant domain (dPER-PAS-A C312A, dPER-PAS-B C455A, The plates were then manually sealed and storage at 4 °C with a transparent sheet that allowed for the formation of protein crystals to be verified (or otherwise) with the aid of an optical microscope. The result was a number of crystalline structures of different concentrations, but the time could not be studied during this study. The recommendation is to be considered in the future.

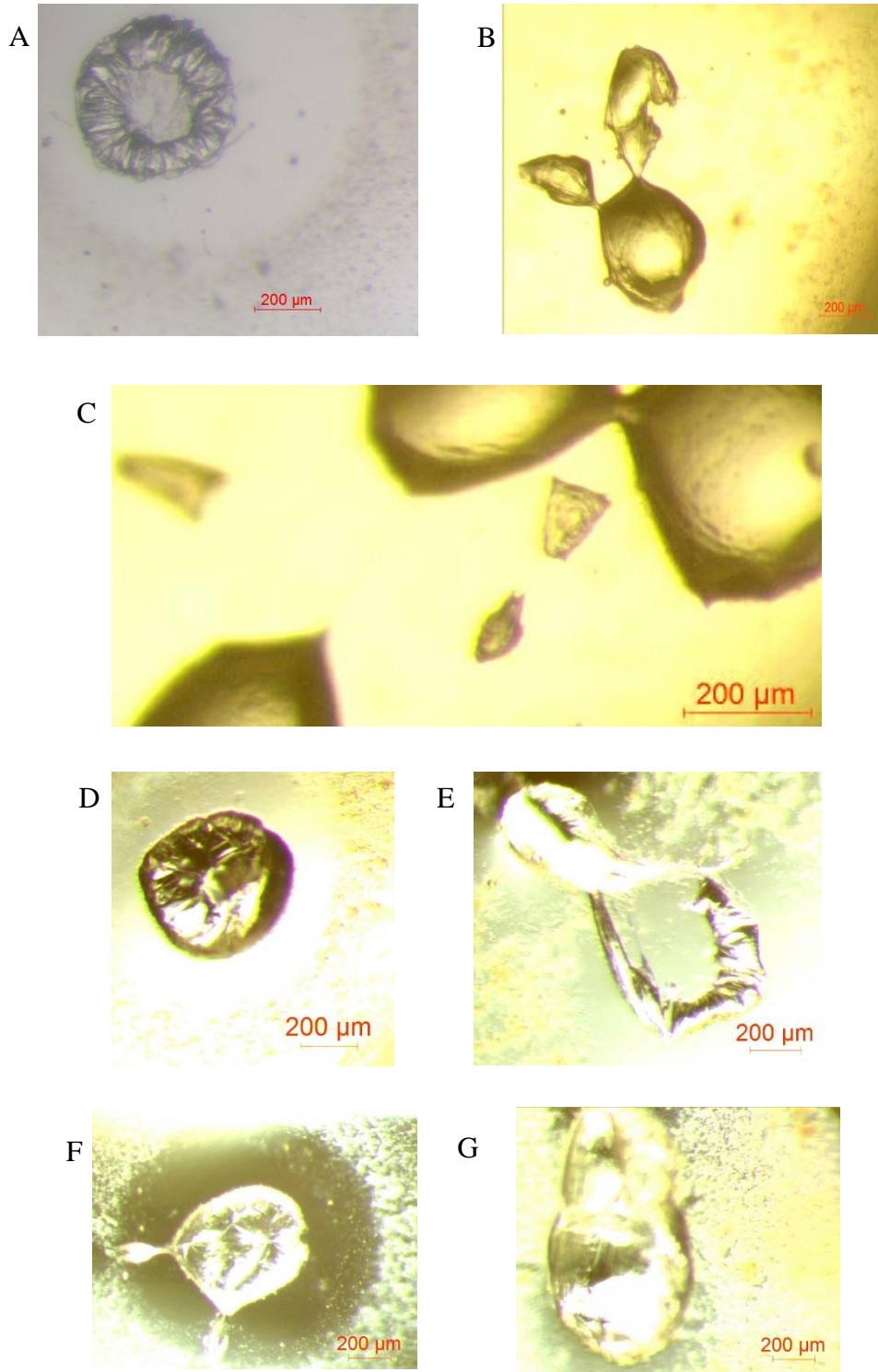


Figure 2-14 crystals by follow setting drop technic **A.** 5 mg/ml of dPER-PAS-AB α . **B.** 4 mg/ml of dPER-PAS-AB α with 4 mg/ml of heme. **C.** 5 mg/ml of mutant dPER-PAS-AB α with 5 mg/ml of heme. **D.** 2 mg/ml of dPER-PAS-AB with 2 mg/ml of heme. **E.** 2 mg/ml of dPER-PAS-A with 2 mg/ml of heme. **F.** 1mg/ml of dPER-PAS-A with 1 mg/ml of heme. **G.** 3 mg/ml of dPER-PAS-B

2.3. References

1. Junk, M J, "Electron Paramagnetic Resonance Theory", in *Assessing the Functional Structure of Molecular Transporters by Epr Spectroscopy*. (2012), Springer. 7-52.
2. Smith, A T; Pazicni, S; Marvin, K A; Stevens, D J; Paulsen, K M, and Burstyn, J N, "Functional Divergence of Heme-Thiolate Proteins: A Classification Based on Spectroscopic Attributes. *Chemical Reviews*", (2015) 115(7): 2532-2558.
3. Chayen, N E and Saridakis, E, "Protein Crystallization: From Purified Protein to Diffraction-Quality Crystal. *Nature Methods*", (2008) 5(2): 147.
4. Hoffmann, A and Roeder, R, "Purification of His-Tagged Proteins in Non-Denaturing Conditions Suggests a Convenient Method for Protein Interaction Studies. *Nucleic Acids Research*", (1991) 19(22): 6337.
5. Dioum, E M; Rutter, J; Tuckerman, J R; Gonzalez, G; Gilles-Gonzalez, M A, and McKnight, S L, "Npas2: A Gas-Responsive Transcription Factor. *Science*", (2002) 298(5602): 2385-2387.
6. Maizel Jr, J V, "Sds Polyacrylamide Gel Electrophoresis. *Trends in Biochemical Sciences*", (2000) 25(12): 590-592.
7. Weber, L; Meigel, W N, and Rauterberg, J, "Sds-Polyacrylamide Gel Electrophoretic. *Archives of Dermatological Research*", (1977) 258(3): 251-257.
8. Wilson, K and Walker, J, "Principles and Techniques of Biochemistry and Molecular Biology". (2018): Cambridge university press.
9. Stadler, J; Lemmens, R, and Nyhammar, T, "Plasmid DNA Purification. *The Journal of Gene Medicine: A cross-disciplinary journal for research on the science of gene transfer and its clinical applications*", (2004) 6(S1): S54-S66.
10. Giovannetti, R, "The Use of Spectrophotometry Uv-Vis for the Study of Porphyrins", in *Macro to Nano Spectroscopy*. (2012), InTech
11. Weil, J A and Bolton, J R, "Electron Paramagnetic Resonance: Elementary Theory and Practical Applications". (2007): John Wiley & Sons.
12. Lu and Needham, N J T M, "Celestial Lancets: History and Rationale of Acupuncture and Moxa". (1980): Cambridge University Press.
13. Wallace, B A and Janes, R W, "Modern Techniques for Circular Dichroism and Synchrotron Radiation Circular Dichroism Spectroscopy". Vol. 1. (2009): IOS press.
14. Antonini, E and Brunori, M, "Hemoglobin and Myoglobin". (1971): Elsevier.
15. Pulkkinen, O and Metzler, R, "Variance-Corrected Michaelis-Menten Equation Predicts Transient Rates of Single-Enzyme Reactions and Response Times in Bacterial Gene-Regulation. *Scientific reports*", (2015) 5: 17820.
16. Yung-Chi, C and Prusoff, W H, "Relationship between the Inhibition Constant (K_i) and the Concentration of Inhibitor Which Causes 50 Per Cent Inhibition (I₅₀)

- of an Enzymatic Reaction. *Biochemical Pharmacology*", (1973) 22(23): 3099-3108.
17. Stelson, A and Seinfeld, J H, "Relative Humidity and Temperature Dependence of the Ammonium Nitrate Dissociation Constant. *Atmospheric Environment (1967)*", (1982) 16(5): 983-992.
 18. Speer, T W, "Dissociation Constant (Kd)", in *Encyclopedia of Radiation Oncology*. (2013), Springer. 157-158.
 19. Einspahr, H and Weiss, M S, *Acta Crystallographica Section F: Structural Biology Communications*. (2013), International Union of Crystallography
 20. Yildiz, O; Doi, M; Yujnovsky, I; Cardone, L; Berndt, A; Hennig, S; Schulze, S; Urbanke, C; Sassone-Corsi, P, and Wolf, E, "Crystal Structure and Interactions of the Pas Repeat Region of the *Drosophila* Clock Protein Period. *Molecular Cell*", (2005) 17(1): 69-82.

Chapter Three

dPER-PAS-A

3. dPER-PAS-A

3.1. Introduction

Different species such as cyanobacteria, fungi, flies, mice and human keep biological time (the circadian clock) by PAS-containing proteins [1, 2]. PAS proteins regulate responses to environmental changes by interacting with signalling molecules [3]. Little is known about the heme binding properties of either of the PAS domains in PER. Some predictions can be made based on results seen for the mouse NPAS2 protein by combining results from the mutagenesis studies of mNPAS2 PAS-A [4].

As the PAS-A is important for directing homodimerization and heterodimerization within the ARNT cluster, we sought to identify dimerization interfaces in ARNT PAS-A, to determine whether a common interface is used for all ARNT hub PAS-A interactions, and if the partner proteins use different dimerization interfaces [5, 6]. In this study, the length of PAS-A had been changed according to Table 3-1

Table 3-1 Details of constructs of dPER-PAS-A used in this study.

No.	Domain	First and last residue	Number of residues	Sequence of trial	HLH domain present	MW (kDa)
1.	dPER-PAS-A	R231-G293	63	1 st trial	No	7.15
2.	dPER-PAS-A	M1-Q386	386	2 nd trial	Yes	44.15
3.	dPER-PAS-A	E145-Q386	242	2 nd trial	No	27.80
4.	dPER-PAS-A	G232-S375	144	3 rd trial	No	17.33

3.2. Result

3.2.1. Construct Design

There are eight constructs for dPER-PAS-A, containing a different tag from a variety of vectors (His tag, GST tag and MBP tag) and different length of sequence of amino acids (See chapter 2 table 2-3). All of them were produced by Dr. Xiaowen Yang at PROTEX in University of Leicester. The target of this was to find the best construct which is soluble and stable in solution for further studies. The construct in first trial starts from amino acid

Arginine 231 to amino acid Glycine 293 with different affinity tags (His, GST, MBP and also without tag).

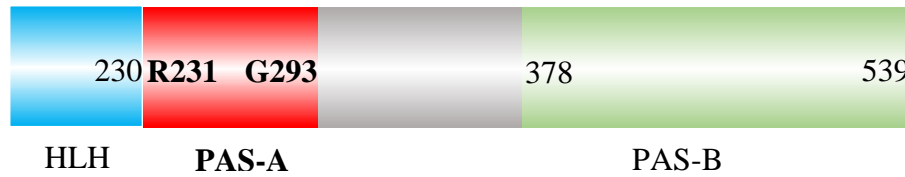


Figure 3-1 First trial construct of dPER-PAS-A full length with the HLH (blue), PAS-A (red) and PAS-B (green) domains labelled.

In the second trial, constructs of two different length of the dPER-PAS-A, domain were made. The first one starts from amino acid number 1 Methionine until amino acid number 386 Glutamine. The second one starts from amino acid number 145 Glutamic acid until amino acid number 386 Glutamine. The second trial's constructs were designed depending on the comparison between mouse Per-PAS-A with *Drosophila* Per-PAS-A (Figure 7-14) [7, 8]. The tags used with this trial were MBP.

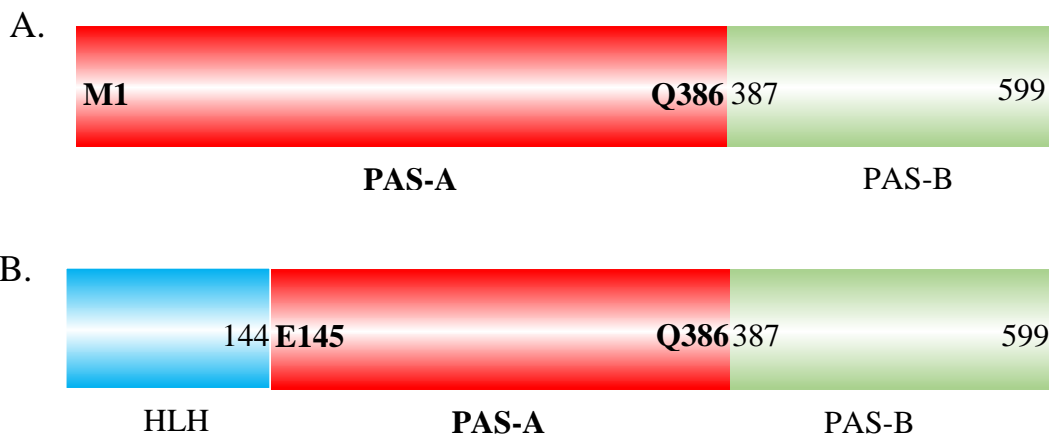


Figure 3-2 Second trial construct dPER-PAS-A constructs produced the top bar illustrates the full length dPER protein PAS-A (red) and PAS-B (green) domains labelled.

The third trial constructs for dPER-PAS-A domain start from amino acid number 232 Glycine until amino acid number 375 Serine with two type of tags (GST and His).



Figure 3-3 Third trial construct dPER-PAS-A constructs produced. Top bar illustrates the full length dPER protein with the HLH (blue), PAS-A (red), PAS-B (green) and α helix in purple domains labelled.

The DNA sequence for each construct were confirmed by Sanger sequencing by PNACL (Protein Nucleic Acid Chemistry Laboratory) at the University of Leicester.

In all the trials in this thesis was established to looking for the stable forms for each domain against purification, tag cleavage and activity to bind with heme. Therefore, the first trial was designed on choose the first β -sheet until the end of α -Helices. This design was not succeed for the aim of this experiment. The second trial designed according to mPER-PAS-A (Figure 1-7) and the result was similar to first trial. The third trial adopted the Yaldiz [9] crystal shape (in PUBmed under code 1WA9) was succeed in purification, cleavage of tags and heme binding.

3.2.2. Protein Expression and Purification

3.2.2.1. His/TEV-Tagged Protein

In the first trial, the R231-G293 part of dPer-PAS-A was expressed in various constructs with and without tags (GST tag, His tag and MBP tag) in *Escherichia coli* (*Rosetta* and *BL21DE3*) cells, figure 3-4. The product of expression was different in terms of the amount of protein and stability (soluble or insoluble), from each of the trials. Protein was found to be expressed in all constructs.

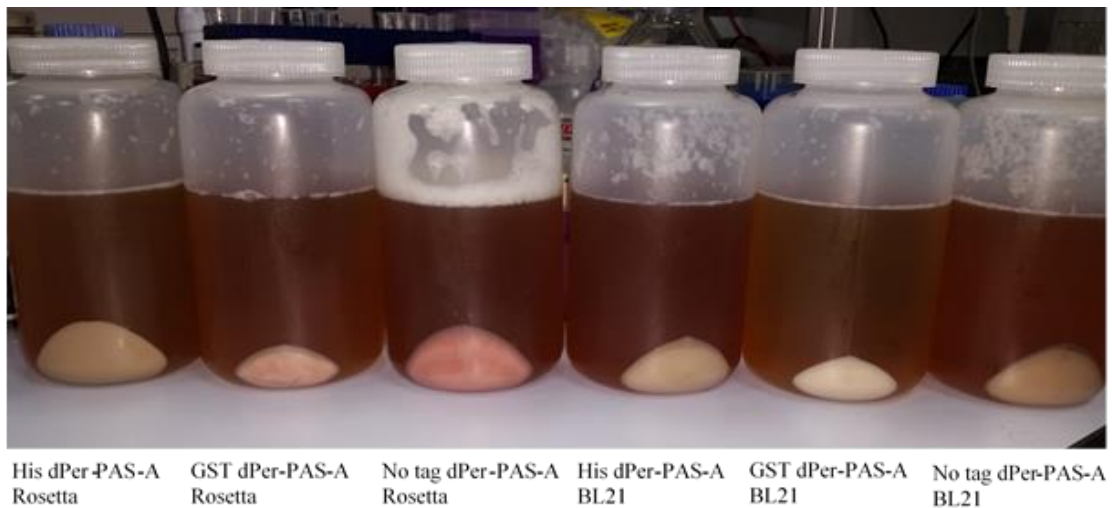


Figure 3-4 Cell pellets obtained under various expression conditions (type of *E. coli* and type of tag).

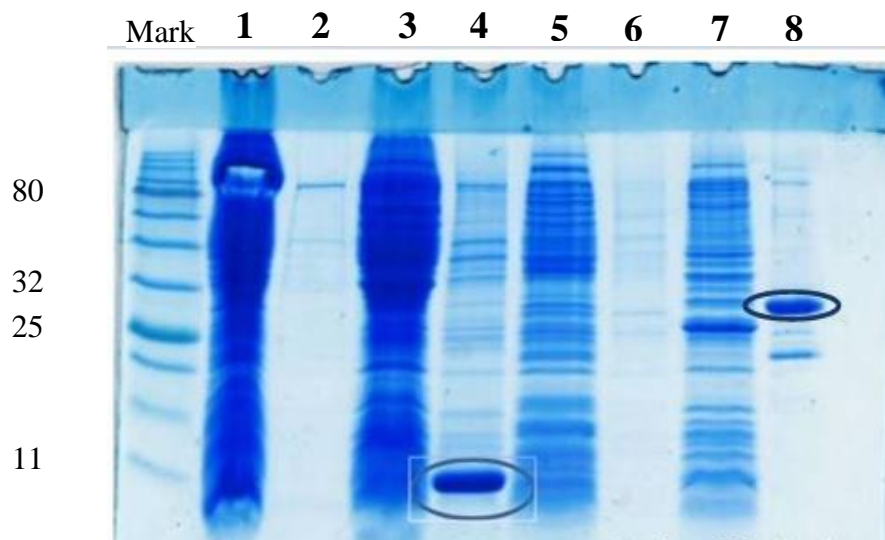


Figure 3-5 Coomassie blue stained 12% SDS-PAGE gel of the soluble and insoluble fractions after cell lysis. Color Protein Standard marker. His-dPER-PAS-A represent in lane 1 (soluble) and lane 2 (insoluble) by using *E. coli, Rosetta* type, His-dPER-PAS-A represent in lane 3 (soluble) and lane 4 (insoluble) by using type *E. coli, BL21DE3*. GST-dPER-PAS-A represent in lane 5 (soluble) and lane 6 (insoluble) by using *E. coli, Rosetta* type, GST-dPER-PAS-A represent in lane 7 (soluble) and lane 8 (insoluble) by using type *E. coli, BL21DE3*. The ring in lane 4 represent the band of His-dPER-PAS-A and the ring in lane 8 represent the band of GST-dPER-PAS-A.

There are several reasons for these differences, mainly the difference in the sequence of amino acids for each trial, the type of tag connected and the temperature for incubation after IPTG addition (16 °C, 18 °C, 20 °C and 22 °C), figure 3-5.

The Ni-NTA column was used to purify (see chapter two 2.2.10) and a gel filtration column using AKTA was used as a second and final step, figures 3-6, 3-7 and 3-8.

The high ability of His tag to bind with heme, makes its cleavage necessary in after purification. His-TEV (Tobacco Etch Virus protease) was used to cleave the His-tag. The majority of the protein expression (by using *E. coli* type *BL21D3*, tag was His and GST for dPER-PAS-A start with R231-G293 and induce by IPTG in 20 °C) was found in the insoluble fraction. Therefore, attempts were made to refold the protein.

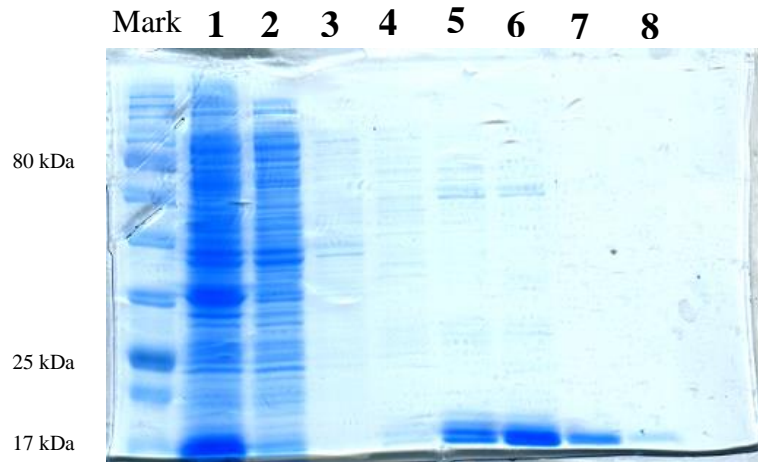


Figure 3-6 Coomassie blue stained 12% SDS-PAGE gel of the soluble fractions after cell lysis. Color Protein Standard marker. His-dPER-PAS-A (G232-S375) 17.63 KDa, represent in lane 1 (dPER-PAS-A domain after sonycation), lane 2 (flow through from Ni-NTA column), lane 3 (washing solution for the column) and lanes 4 to 8 (dPER-PAS-A domain fractions by using Imidazole buffer 50 mM, 100 mM, 250 mM, 300 mM and 500 mM respectively).

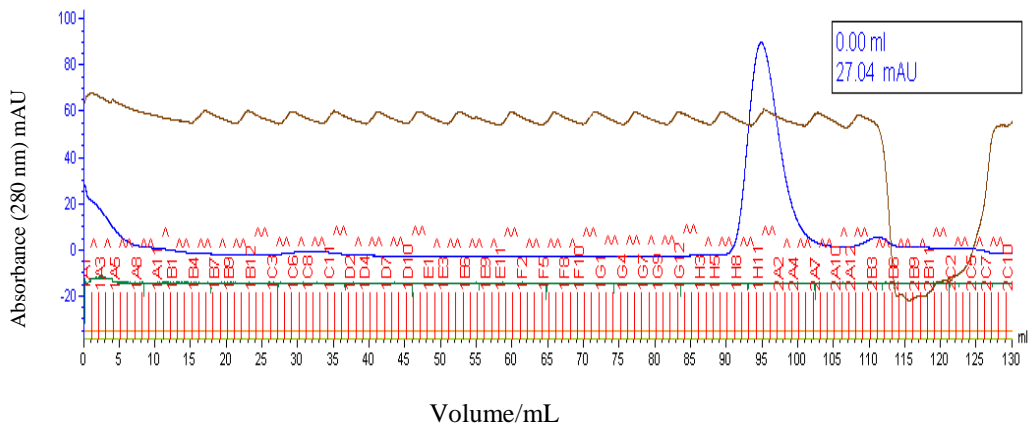


Figure 3-7 Q Sepharose FPLC elution chromatogram run at 1 mL/min. Traces shown are the absorption reading at 280 nm His-dPER-PAS-A (G232-S375). The conductivity of the solution measured in ml siemens per centimetre (mS/cm, brown). The vertical axis corresponds to the absorbance at 280 nm (blue line). The fractions are labelled on the chromatogram in red, of which fractions 1H9 to 2A6 were collected and pooled for further purification in this instance.

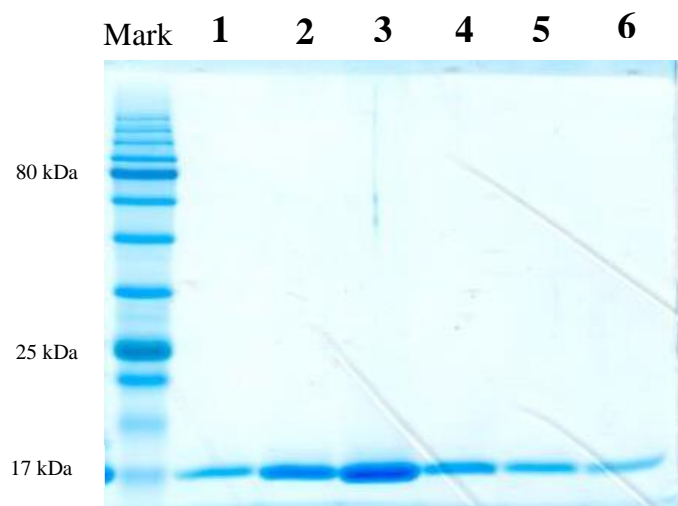


Figure 3-8 Coomassie blue stained 12% SDS-PAGE gel of dPER-PAS-A (G232-S375) 17.3 KDa. Color Protein Standard marker. dPER-PAS-A represent in lanes 1 to 6 as AKTA fractions 1H8, 1H9, 1H12, 2A4, 2A5 and 2A6.

3.2.2.2. His-dPER-PAS-A refolding trial

Protein refolding trials were performed for His-dPER-PAS-A as described in Chapter 2 section 2.2.8. Inclusion bodies were suitably clean as seen in figure 3-9 prior to solubilisation and refolding steps.

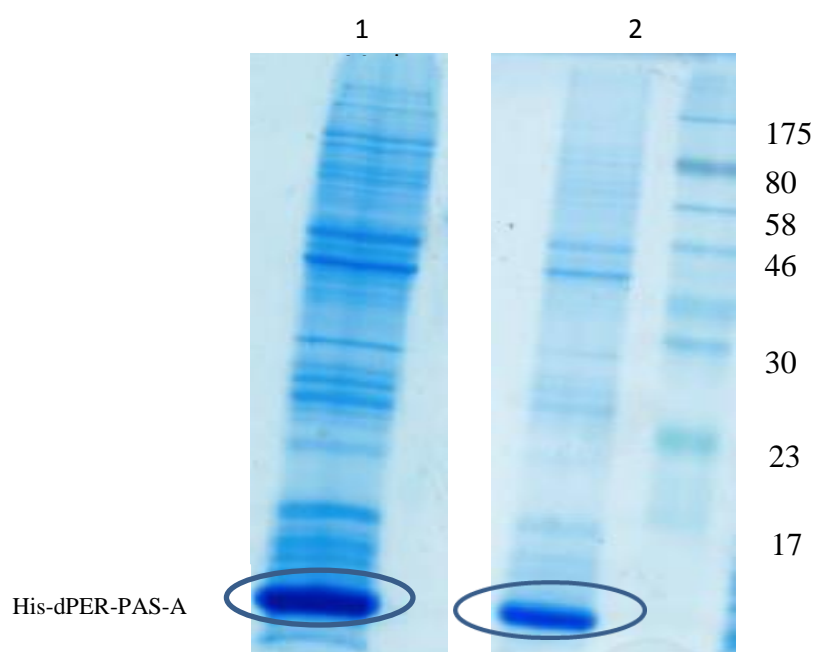


Figure 3-9 Inclusion bodies pre (lane 1) and post (lane 2) clean-up protocol. ColorPlus prestained protein Marker broad rangeis (7-175 kDa) in lane 3. His-dPer-Pas-A is 7.45 kDa.

Elution profiles for His-dPER-PAS-A loaded onto a Superdex 200 gel filtration column after overnight incubation in refolding conditions 2 and 5 from the Quickfold Protein refolding kit are shown in figures 3-10 and 3-11, respectively. Although more than one of refolding technique was used (condition 2 and 5), the protein was lost during the refolding process. The absorbance changes are very small, obviously a peak around 18 ml for both conditions 2 and 5.

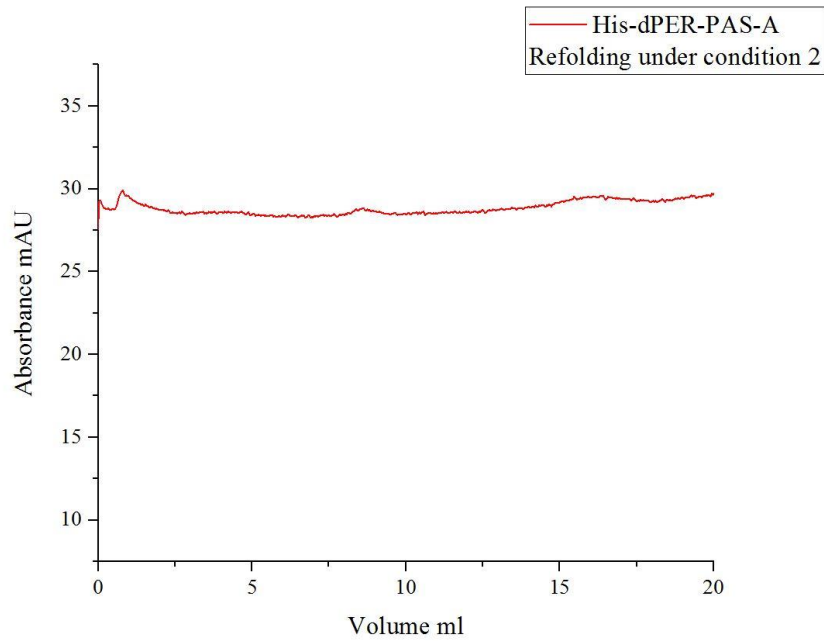


Figure 3-10 Gel filtration elution profiles for His-dPER-PAS-A after refolding trials using condition 2 of the Quickfold protein refolding kit. No peak is observed at 18 ml.

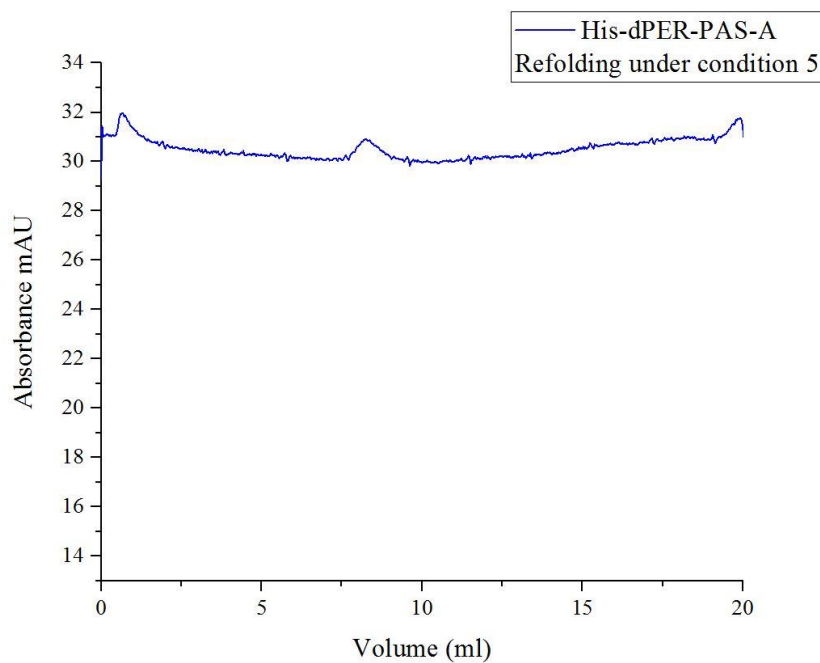


Figure 3-11 Gel filtration elution profiles for His-dPER-PAS-A after refolding trials using condition 5 of the Quickfold protein refolding kit. No peak is observed at 18 ml.

3.2.2.3. GST Tagged protein

The vectors pLEICS-14 and pLEICS-4 were used to build constructs of dPER-PAS-A domain with GST tag (for dPER-PAS-A, R231-G293 and G232-S375 respectively) (Figures 3-12, and 3-13), there is a TEV protease cleavage site in both vectors. For the cell was used for expression and all variables such as yield of expression and stability, physical properties of A domain (Chapter two 2.2.13).

The GST column was used to purification (see Chapter 2.2.7.1.) and AKTA with gel filtration column (Figure 3-14). The GST-TEV was used to cleavage the tag. It is obviously there is no protein after purification by AKTA (Figure 3-15).

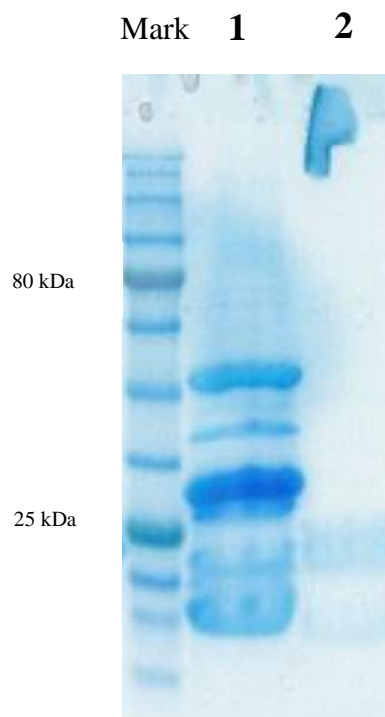


Figure 3-12 Coomassie blue stained 12% SDS-PAGE gel of the soluble fractions after cell lysis. Color Protein Standard marker. GST-dPER-PAS-A (R231-G293) 32.74 KDa are shown in lane 1 (insoluble) and lane 2 (soluble), respectively.

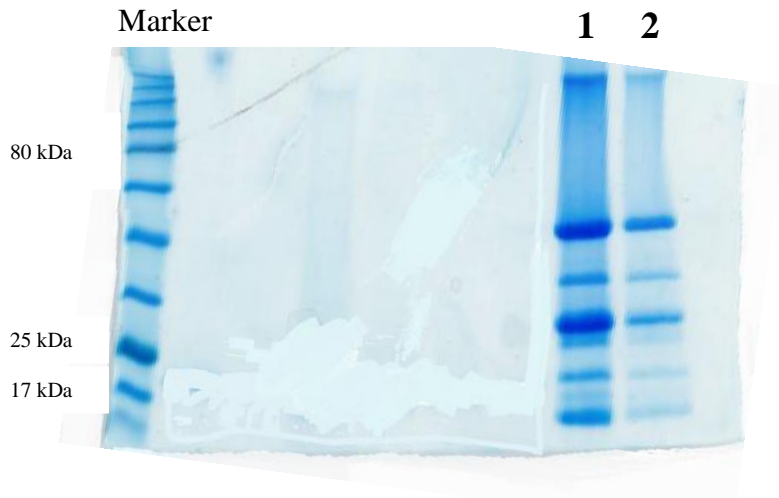


Figure 3-13 Coomassie blue stained 12% SDS-PAGE gel of the soluble fractions after cell lysis. GST-dPER-PAS-A (G232-S375) 42.91 kDa are shown in lane 1 (soluble) and lane 2 (insoluble), respectively.

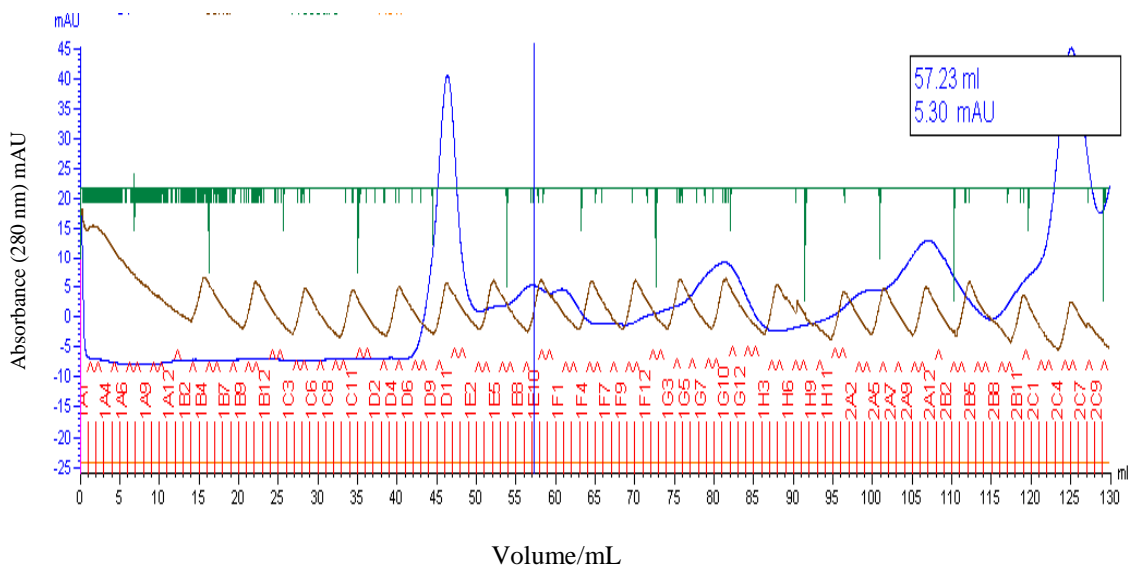


Figure 3-14 Q Sepharose FPLC elution chromatogram run at 1 mL/min. Traces shown are the absorption reading at 280 nm for GST-dPER-PAS-A (R231-G293) after a refolding trial. The conductivity of the solution is measured in ml siemens per centimetre (mS/cm, brown line). The vertical axis corresponds to the absorbance of the 280 nm (blue line). The fractions are labelled on the chromatogram in red, of which fractions (1H11) to (2B6) were collected and pooled for further purification in this instance. Pressure represent in green line.

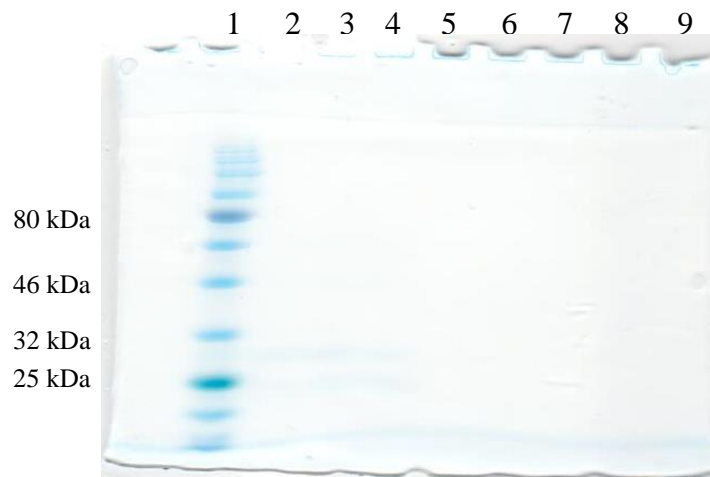


Figure 3-15 Coomassie blue stained 12% SDS-PAGE gel of dPER-PAS-A (R231-G293) 7.15 KDa. Color Protein Standard marker represent in lanes 1 and lanes 2 to 9 represent AKTA fractions 1H12, 2A2, 2A4, 2A7, 2A9, 2A12, 2B2 and 2B6 (Figure 3-14) respectively. There is no protein in all fractions.

3.2.2.4. MBP Tagged Protein

pLEICS-10 was used as a vector for dPER-PAS-A domain construct with an MBP tag. This vector contains a TEV protease cleavage site therefore, it was possible to use either GST-TEV or His-TEV.

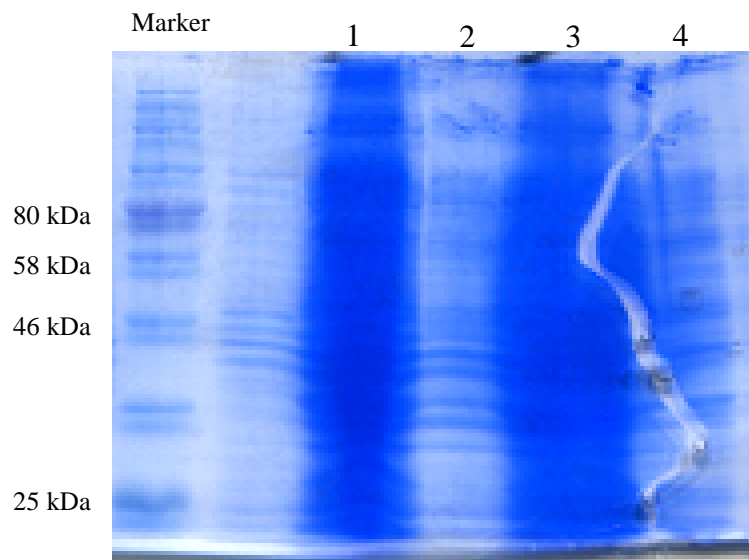


Figure 3-16 Coomassie blue stained 12% SDS-PAGE gel of the soluble and insoluble fractions after cell lysis for MBP-dPer-PAS-A (R231-G293) 47.77 KDa. Lane 1 represent soluble and lane 2 represent insoluble with induced by IPTG then incubated under 20 °C. Lane 3 represent soluble and lane 4 represent insoluble with induced then incubated under 16 °C.

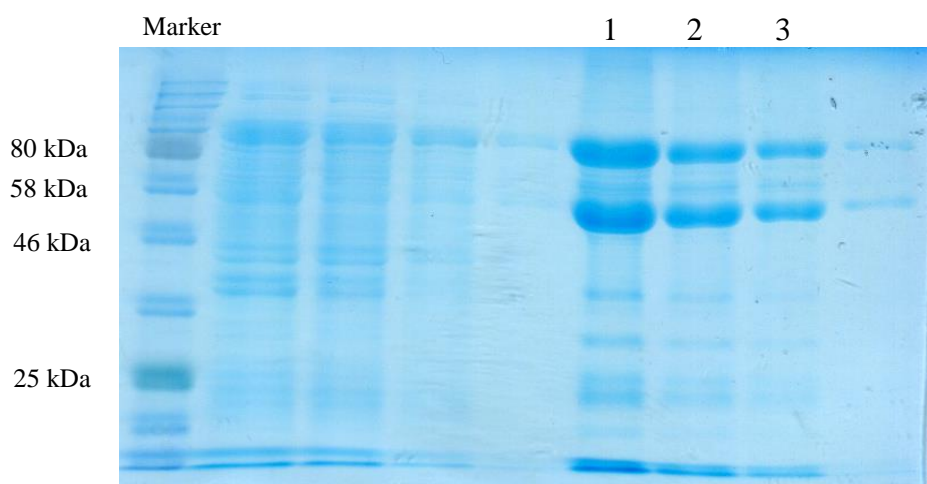


Figure 3-17 Coomassie blue stained 12% SDS-PAGE gel of the soluble and insoluble fractions after cell lysis for MBP-dPer-PAS-A (M1-Q386) 84.75 KDa. Lane 1 represents soluble with induced by IPTG then incubated under 16 °C, lane 2 represents soluble with induced by IPTG then incubated under 20 °C and lane 3 represents soluble with induced by IPTG then incubated under 24 °C.

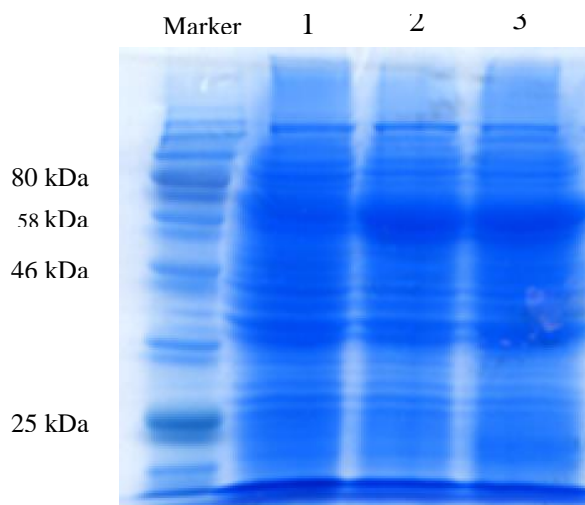


Figure 3-18 Coomassie blue stained 12% SDS-PAGE gel of the soluble and insoluble fractions after cell lysis for MBP-dPer-PAS-A (E145-Q386) 68.4 KDa. Lane 1 represent soluble without induced and incubated under 20 °C, lane 2 represent soluble with induced by IPTG then incubated under 20 °C and lane 3 represent soluble with induced by IPTG then incubated under 37 °C [2].

3.2.2.5. No Tagged Protein

One of ways to make expression of protein in this thesis was design the plasmid without tag. The same technique was used for transformation and expression which is used for other constructs. Q sepharose™ fast flow was used as purification resin because it is a strong anion exchanger. The result of expression of this construct there is no protein (Figure 3-19).

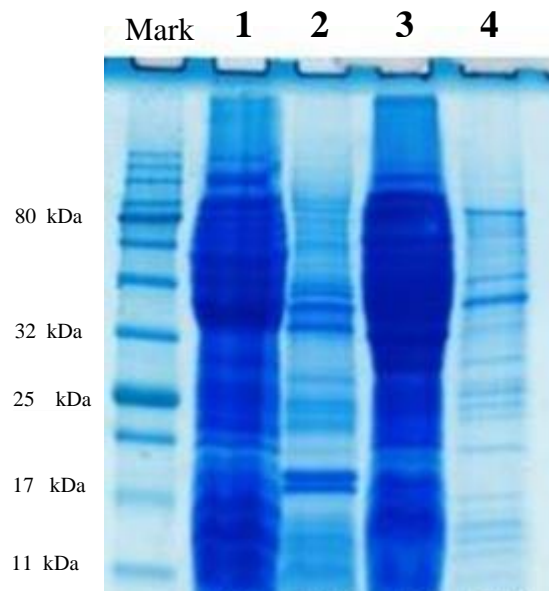


Figure 3-19 Coomassie blue stained 12% SDS-PAGE gel of the soluble and insoluble fractions after cell lysis for dPer-PAS-A (R231-G293). Lane 1 represent soluble dPer-PAS-A without tag expressed by using *Rosetta*. Lane 2 represent insoluble dPer-PAS-A without tag expressed by using *Rosetta*. Lane 3 represent soluble dPer-PAS-A without tag expressed by using *BL21D3*. Lane 4 represent insoluble dPer-PAS-A without tag expressed by using *BL21D3*.

3.3. Heme Binding Properties

3.3.1. Heme Affinity

Binding between heme and dPer-PAS-A was tested using a construct from the third trial (A.A G232-S375). In this heme titration assay, difference spectrophotometry was used to determine the dissociation constant (K_D) of heme binding. The calculation of K_D depends on the changes in absorbance at the Soret band at 424 nm and was calculated to be $5.999 \pm 0.719 \mu\text{M}$ (Figure 3-20 and 3-21). The heme titration technique was also used to determine heme affinity for mCLOCK PAS-A and was found to be $1 \mu\text{M}$ [10]. The binding of heme with the PAS-A domain of mNPAS2 was ($K_D = 160 \text{ pM}$) much tighter than hCLOCK PAS-A [11]. The K_D value for PAS-A domain from mPER was 17.5 pM [7]. The binding was relatively weak when comparing the heme binding of dPER-PAS-A to a traditional heme protein such as Sperm Whale myoglobin (SwMb) which has a $K_D = 13 \mu\text{M}$. And the K_D for hCLOCK PAS-A for heme affinity was $3.7 \pm 0.59 \mu\text{M}$ [12].

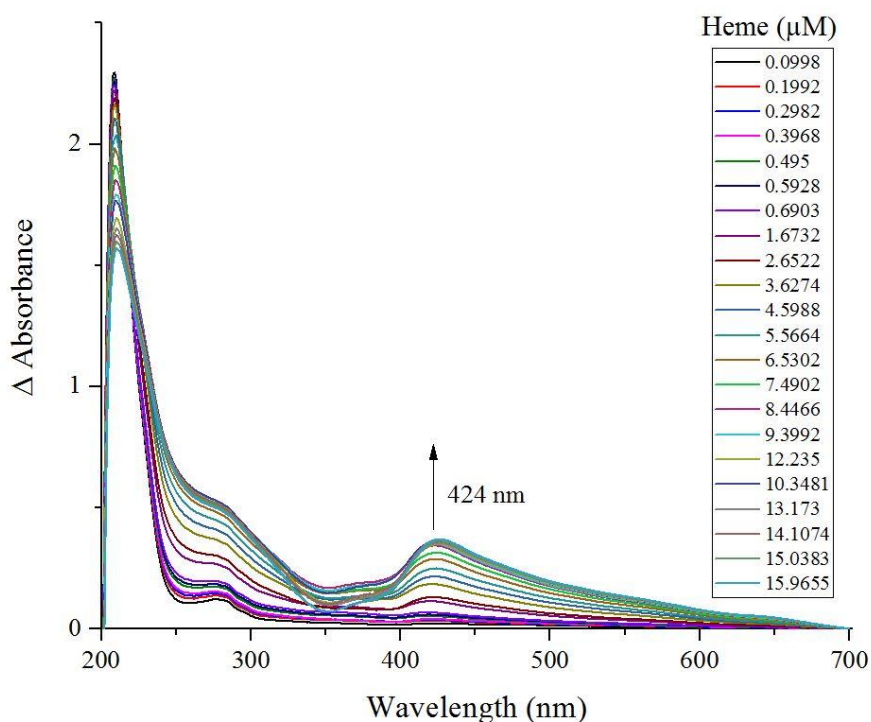


Figure 3-20 UV-visible difference spectrum of heme bound to dPER-PAS-A. Reaction ratio heme to dPER-PAS-A domain is 1:1, the concentration of hemin was $9.255 \mu\text{M}$ and concentration of dPER-PAS-A domain was $10.12 \mu\text{M}$. Legend shows the final concentration of heme used in the titration.

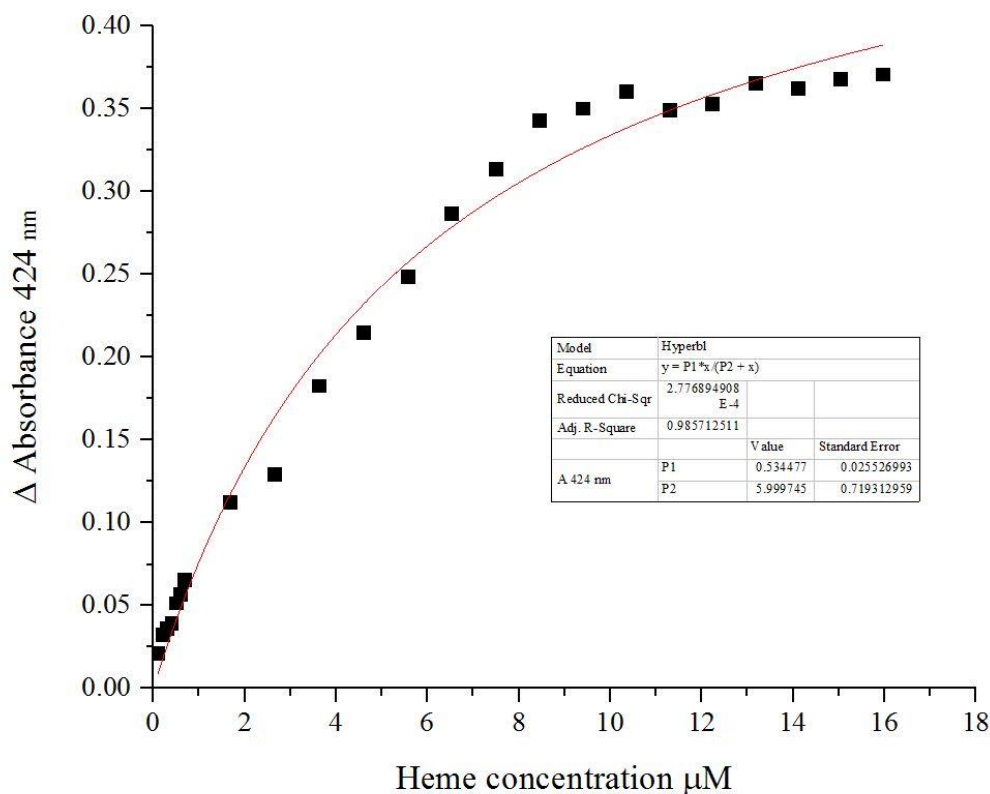


Figure 3-21 The relative absorbance changes to the difference spectrum at 424nm fit to a hyperbolic. $K_D = 5.999745 \pm 0.7193 \mu\text{M}$.

3.3.2. UV-Visible Spectroscopy

dPER-PAS-A domain was purified without tag to avoid any incidental binding with heme. There is a big affinity difference between tags such as MBP and His with heme. The ferric heme spectrum of reconstituted protein had absorbance maxima at 424 nm (Figure 3-22). This is different from the spectra for the PAS-A domain of mNPAS2 which has a peak at 412 nm [13] and mCLOCK which has a peak at 413 nm [10].

According to Koudo [14] resonance Raman spectra of mNPAS2 mutants suggested that this protein binds heme via a His / Cys ligation. In mammalian (mouse and human), CLOCK PAS-A lies somewhere between those of mNPAS2 PAS-A and the PAS domain of EcDOS (*E. coli*, Direct of Oxygen Sensor). The binding of heme in the PAS domain of EcDOS was 416 nm in His/H₂O [15, 16]. This suggests that dPER-PAS-A may bind heme via either a His ligation, a His/H₂O ligation or be present as a mixture of the two.

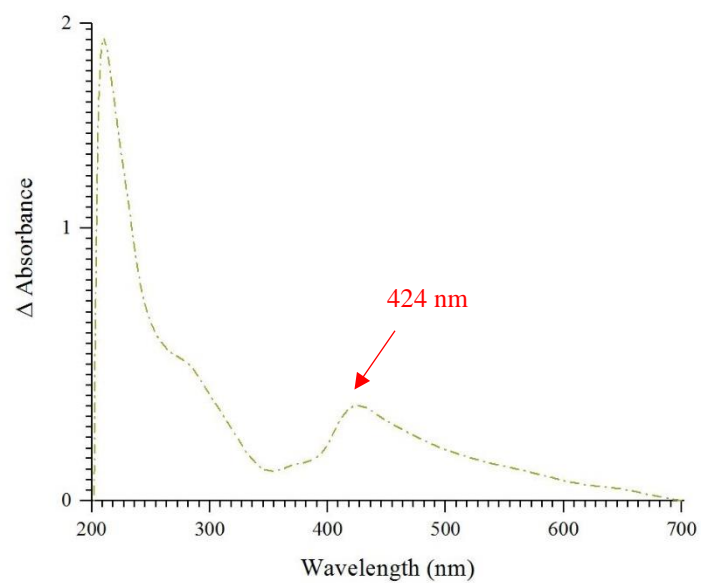


Figure 3-22 UV-Visible absorbance spectra of heme (ferric) bound to dPER-PAS-A at 424 nm.

Table 3-2 Spectral characteristics and axial ligands of various heme proteins.

Protein	Cys	Cys/His	Cys/?	His/?	other	unknown	Soret	Q bands	References
dPER-PAS-A						•	424	-	this work
Clock PAS-A						•	412	535, 565	[10]
NPAS2-PAS-A		•					412	538	[11, 13]
mPER2-PAS-A			•				421	536	[7]
EcDOS-PAS					His/H₂O		416	530, 564	[15, 17, 18]
RmFixLN					His		412	543, 579, 604	[19]
Bach 1	•	•					423 371	540, 580 521, 541, 650	[20] [20]
hCLOCK				•			416	536	[12]

3.3.3. Electron Paramagnetic Resonance (EPR)

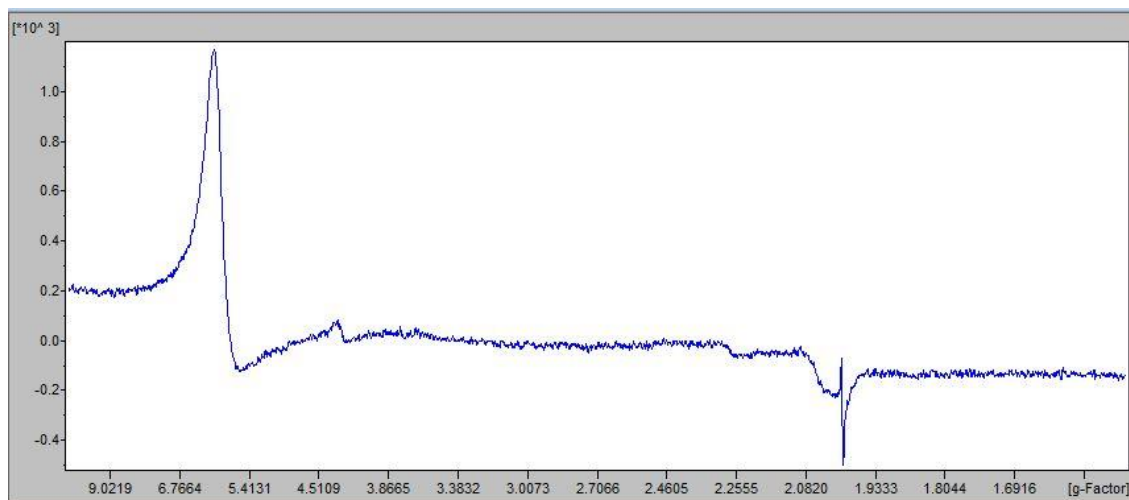


Figure 3-23 EPR spectra for dPER-PAS-A 100 μ M with 30 μ M hemin in pH 7.5, HS haem signal, also much lower of a low spin.

EPR Spectra of the heme Complex of dPER-PAS-A. Crystal field parameters of EPR spectra of Fe (III) low-spin complexes have been successfully used to identify axial ligands of the heme iron [21, 22]. To further investigate the mode of heme binding employed by dPER-PAS-A, samples of ferric protein were tested and analysed with help of Dr. Dimitri Svistunenko at the EPR Research Facility (University of Essex) for a Bruker EMX EPR spectrometer (X-band) equipped with a spherical high quality resonator ER 4122 and an Oxford Instruments liquid helium system for the low-temperature measurements. Samples were placed in Wilmad SQ EPR tubes to a final volume of 250 μ l, frozen in methanol kept on dry ice, wiped and then transferred to liquid nitrogen. EPR spectra were measured at 10 K. There was a clear signal at $g = 2.43$ likely corresponding to a Cys residue. In addition to this, signals have also been observed in other proteins that are similar to g -value signals identified for hCLOCK PAS-A, hCLOCK PAS-A H144A and mPER-PAS-A which were 2.45, 2.45 and 2.44 respectively.

Table 3-3 EPR g-values for hemeproteins.

No.	Protein	Wild-type and mutant domain	ligands	g values	Ref.
1.	dPER	PAS-A	Cys	2.43	this study
2.	hCLOCK	PAS-A	His/?	2.45	[12]
3.	hCLOCK	PAS-A H144A		2.45	[12]
4.	mPER2	PAS-A	Cys/?	2.44	[7]

3.3.4. Circular Dichroism (CD)

Magnetic circular dichroism (CD spectra were obtained with a Chirascan plus CD spectrometer at room temperature) spectral band at the Soret region of heme-bound domain dPer-PAS-A. There is a non-significant difference in optical absorption band between dPer-PAS-A and dPer-PAS-A band heme.

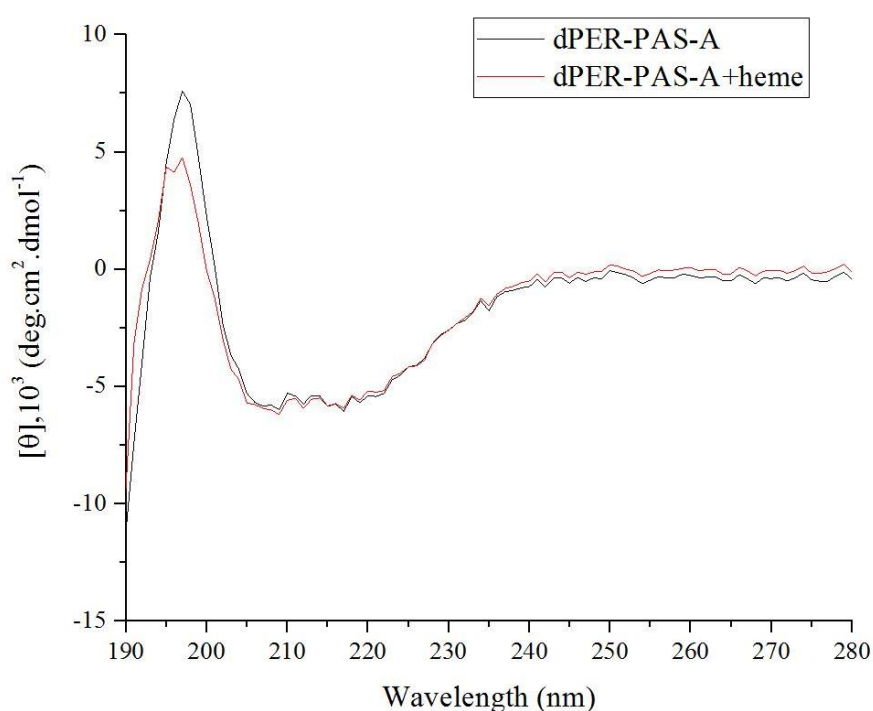


Figure 3-24 Magnetic circular dichroism spectra for dPER-PAS-A (black) and dPER-PAS-A binding with heme (red) in buffer.

3.3.5. Mutant Variants

According to the UV-visible result and the result of EPR (Figure 3-23 and see Chapter five figure 5-26) on the binding between dPER-PAS-A domain and heme, it was decided to mutate the cysteine in dPER-PAS-A domain that align to the proposed heme ligands. There are four Cysteines residues in the dPER-PAS-A chain (C241, C242, C312, and C369). Residues C312 and C369 were mutated to Alanine in separate constructs (see Chapter 2 table 2-4). The expression and purification were carried out in the same way as with wild type dPER-PAS-A. The C312A and C369A mutant binding with heme (ferric) produced UV-visible spectra and a ferric EPR spectrum with absorbance maxima and g values like that of wild type of dPER-PAS-A domain (Figure 3-23). This is not what would be expected if this residue binds directly to the heme iron in the wild type domain and therefore it is likely that dPER-PAS-A does not use Cys 369 to bind heme (Figures 3-25 and 3-27).

However, the Cys 312 mutant did show substantial spectral changes from the wild type. The heme UV-Visible spectrum was shifted, showing that heme is binding to protein (Figures 3-26 and 3-28).

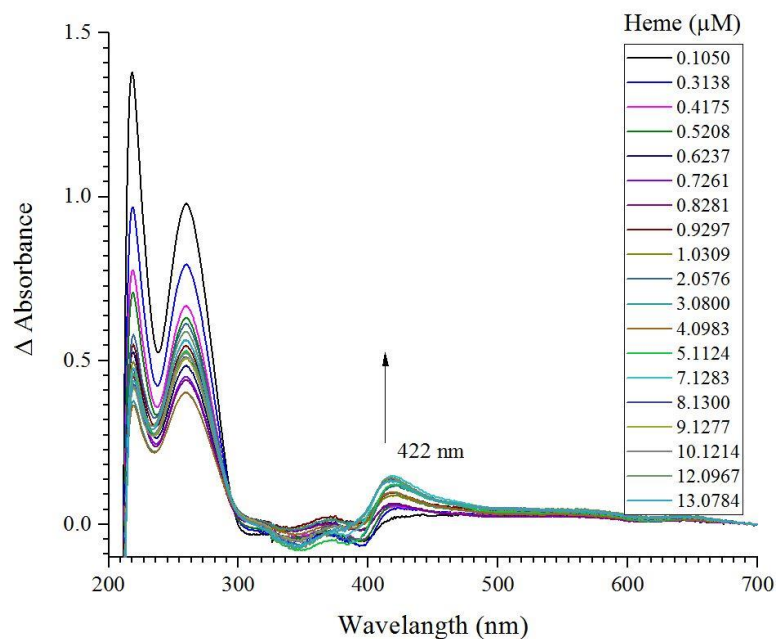


Figure 3-25 UV-visible difference spectrum of heme bound to mutant dPER-PAS-A (Cys369Ala). Legend shows the final concentration of heme used in the titration.

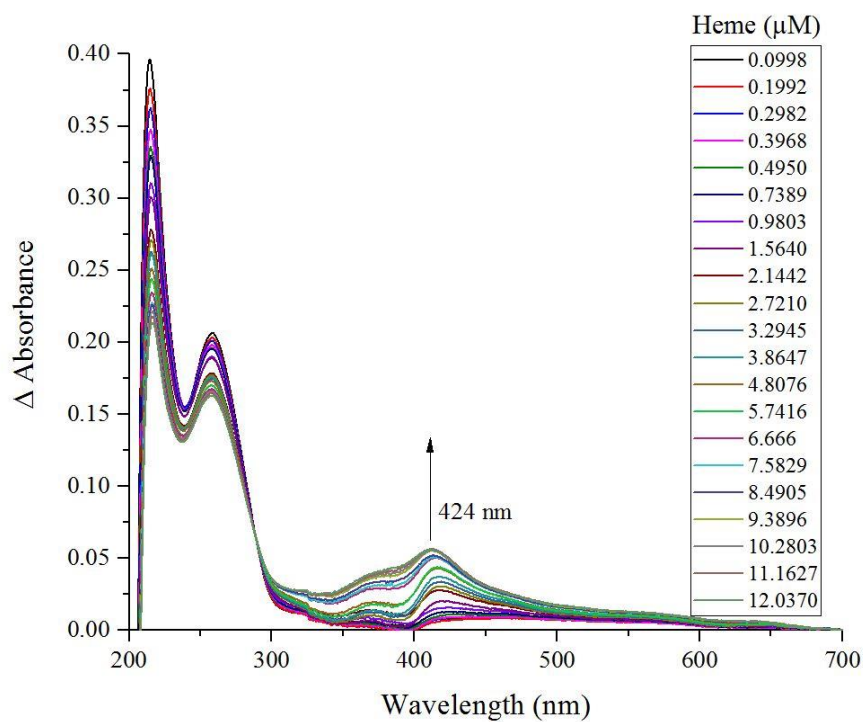


Figure 3-26 UV-visible difference spectrum of heme bound to mutant dPER-PAS-A (Cys312Ala). Legend shows the final concentration of heme used in the titration.

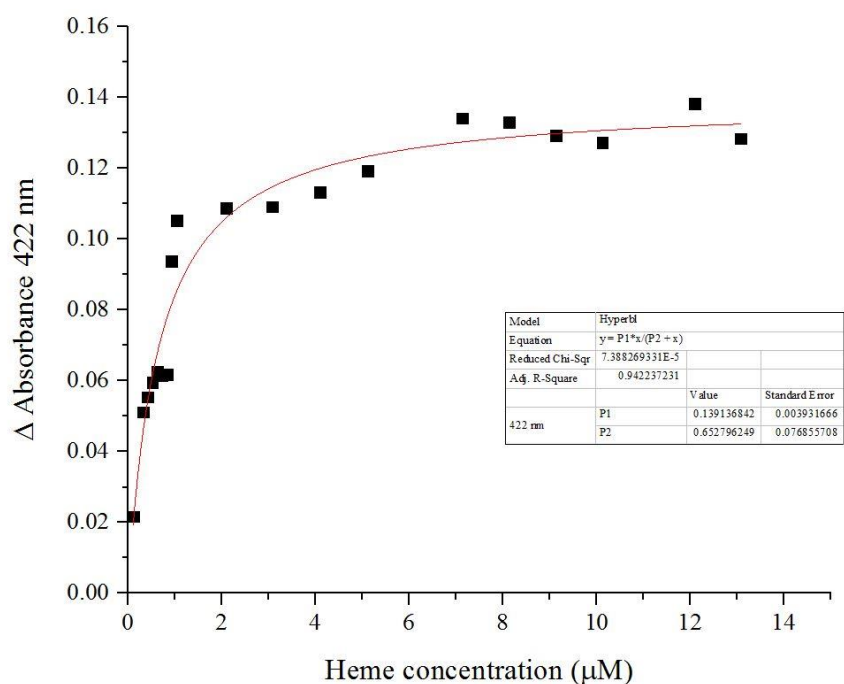


Figure 3-27 The relative absorbance changes to the difference spectrum for mutant Cys369Ala at 422 nm fit to a hyperbolic. $K_D = 0.6527 \pm 0.0768 \mu\text{M}$.

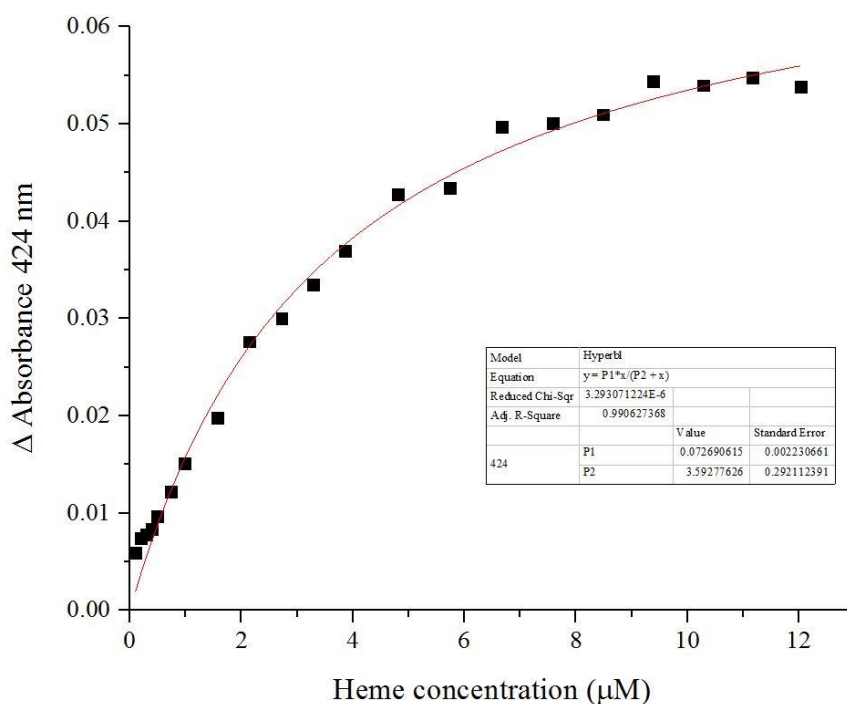


Figure 3-28 The relative absorbance changes to the difference spectrum for mutant Cys312Ala at 424nm fit to a hyperbolic. $K_D = 3.592 \pm 0.292 \mu\text{M}$.

3.4. Summary

dPER-PAS-A was studied starting from the design of the constructs of dPER-PAS-A in three trials that differ in the number of amino acids present in the domain with different tags (GST, His and MBP). Then constructs were expressed using *E. coli* (*Rosetta* and *BL21DE3*). Recombinant dPER-PAS-A domain, purified from *E. coli*, displayed some interesting characteristics. The examination of the ferric form of dPER-PAS-A by EPR spectroscopy (see 3.3.3.) further supported the evidence that the protein bound heme in a 6-coordinate manner. Furthermore, the EPR spectrum showed evidence for one form of ligation with signals generally characteristic of a Cys/Heme ligation.

The heme/Cys binding site was also investigated using mutagenesis in an attempt to identify the heme binding residue. Based on the results of EPR experiments on dPER-PAS-A and the stereochemistry of the protein molecule that allows the binding between the heme and Cysteine residues (there are four residues: Cys241, Cys242, Cys312 and Cys369), it was decided that the most likely heme binding residue in the dPER-PAS-A domain were Cys312 and Cys369.

According to the result of the heme binding assays in this work, UV-visible spectral changes are observed upon addition of heme. Spectral changes were predominantly centred on a peak at 424 nm for dPER-PAS-A wild type domain and 422 nm and 424 nm for the Cys321 and Cys369 mutants respectively. There is no obvious differences in the optical absorption spectral changes induced by adding Heme Iron complexes to the mutants. Spectral changes were observed for the Fe (III) complex titration experiment (monitored at 424 nm). This peak reflects heme binding to dPER-PAS-A.

In wild type, the K_D determined from the heme titration was around 6 μM ; the binding between heme and dPER-PAS- was weak.

To confirm the type of link (specific or nonspecific binding) between the protein and the heme, it is necessary to form crystals of the heme complex (see chapter two) and try to create new mutations for other amino acids expected to be associated with the heme at molecules (Cys241 and Cys242) because there is no significant difference in the absorption spectrum between wild type and mutants investigated in this study.

Table 3-4 Absorbance band for PAS domain to different proteins.

No.	Protein	Absorbance band (nm)	Reference
1.	mPER2-PAS-A C215A	418	[7]
2.	mPER2-PAS-A C270A	417	[7]
3.	Isolated PAS-A	412	[13]
4.	bHLH-PAS-A WT	421	[13]
5.	bHLH-PAS-A C170A	421	[23]

3.5. References

1. McIntosh, B E; Hogenesch, J B, and Bradfield, C A, "Mammalian Per-Arnt-Sim Proteins in Environmental Adaptation. Annual Review of Physiology", (2010) 72: 625-645.
2. King, H A; Hoelz, A; Crane, B R, and Young, M W, "Structure of an Enclosed Dimer Formed by the *Drosophila* Period Protein. Journal of Molecular Biology", (2011) 413(3): 561-572.
3. Wang, G L; Jiang, B-H; Rue, E A, and Semenza, G L, "Hypoxia-Inducible Factor 1 Is a Basic-Helix-Loop-Helix-Pas Heterodimer Regulated by Cellular O₂ Tension. Proceedings of the National Academy of Sciences", (1995) 92(12): 5510-5514.
4. Militi, S; Maywood, E S; Sandate, C R; Chesham, J E; Barnard, A R; Parsons, M J; Vibert, J L; Joynson, G M; Partch, C L, and Hastings, M H, "Early Doors (Edo) Mutant Mouse Reveals the Importance of Period 2 (Per2) Pas Domain Structure for Circadian Pacemaking. Proceedings of the National Academy of Sciences", (2016) 113(10): 2756-2761.
5. Erbel, P J; Card, P B; Karakuzu, O; Bruick, R K, and Gardner, K H, "Structural Basis for Pas Domain Heterodimerization in the Basic Helix-Loop-Helix-Pas Transcription Factor Hypoxia-Inducible Factor. Proceedings of the National Academy of Sciences", (2003) 100(26): 15504-15509.
6. Amezcua, C A; Harper, S M; Rutter, J, and Gardner, K H, "Structure and Interactions of Pas Kinase N-Terminal Pas Domain: Model for Intramolecular Kinase Regulation. Structure", (2002) 10(10): 1349-1361.
7. Kitanishi, K; Igarashi, J; Hayasaka, K; Hikage, N; Saiful, I; Yamauchi, S; Uchida, T; Ishimori, K, and Shimizu, T, "Heme-Binding Characteristics of the Isolated Pas-a Domain of Mouse Per2, a Transcriptional Regulatory Factor Associated with Circadian Rhythms. Biochemistry", (2008) 47(23): 6157-6168.
8. Hayasaka, K; Kitanishi, K; Igarashi, J, and Shimizu, T, "Heme-Binding Characteristics of the Isolated Pas-B Domain of Mouse Per2, a Transcriptional Regulatory Factor Associated with Circadian Rhythms. Biochimica Et Biophysica Acta-Proteins and Proteomics", (2011) 1814(2): 326-333.
9. Yildiz, O; Doi, M; Yujnovsky, I; Cardone, L; Berndt, A; Hennig, S; Schulze, S; Urbanke, C; Sassone-Corsi, P, and Wolf, E, "Crystal Structure and Interactions of the Pas Repeat Region of the *Drosophila* Clock Protein Period. Molecular Cell", (2005) 17(1): 69-82.
10. Lukat-Rodgers, G S; Correia, C; Botuyan, M V; Mer, G, and Rodgers, K R, "Heme-Based Sensing by the Mammalian Circadian Protein Clock. Inorganic Chemistry", (2010) 49(14): 6349-6365.
11. Uchida, T; Sato, E; Sato, A; Sagami, I; Shimizu, T, and Kitagawa, T, "Co-Dependent Activity-Controlling Mechanism of Heme-Containing Co-Sensor Protein, Neuronal Pas Domain Protein. Journal of Biological Chemistry", (2005) 280(22): 21358-21368.

12. Efimov, I; Parkin, G; Millett, E S; Glenday, J; Chan, C K; Weedon, H; Randhawa, H; Basran, J, and Raven, E L, "A Simple Method for the Determination of Reduction Potentials in Heme Proteins. FEBS Letters", (2014) 588(5): 701-704.
13. Mukaiyama, Y; Uchida, T; Sato, E; Sasaki, A; Sato, Y; Igarashi, J; Kurokawa, H; Sagami, I; Kitagawa, T, and Shimizu, T, "Spectroscopic and DNA-Binding Characterization of the Isolated Heme-Bound Basic Helix-Loop-Helix-Pas-a Domain of Neuronal Pas Protein 2 (Npas2), a Transcription Activator Protein Associated with Circadian Rhythms. FEBS Journal", (2006) 273(11): 2528-2539.
14. Koudo, R; Kurokawa, H; Sato, E; Igarashi, J; Uchida, T; Sagami, I; Kitagawa, T, and Shimizu, T, "Spectroscopic Characterization of the Isolated Heme-Bound Pas-B Domain of Neuronal Pas Domain Protein 2 Associated with Circadian Rhythms. FEBS Journal", (2005) 272(16): 4153-4162.
15. Delgado-Nixon, V M; Gonzalez, G, and Gilles-Gonzalez, M-A, "Dos, a Heme-Binding Pas Protein from *Escherichia Coli*, Is a Direct Oxygen Sensor. Biochemistry", (2000) 39(10): 2685-2691.
16. Park, H; Suquet, C; Satterlee, J D, and Kang, C, "Insights into Signal Transduction Involving Pas Domain Oxygen-Sensing Heme Proteins from the X-Ray Crystal Structure of *Escherichia Coli* Dos Heme Domain (Ec Dosh). Biochemistry", (2004) 43(10): 2738-2746.
17. Sato, A; Sasakura, Y; Sugiyama, S; Sagami, I; Shimizu, T; Mizutani, Y, and Kitagawa, T, "Stationary and Time-Resolved Resonance Raman Spectra of His77 and Met95 Mutants of the Isolated Heme Domain of a Direct Oxygen Sensor from *E. Coli*. Journal of Biological Chemistry", (2002)
18. Tomita, T; Gonzalez, G; Chang, A L; Ikeda-Saito, M, and Gilles-Gonzalez, M-A, "A Comparative Resonance Raman Analysis of Heme-Binding Pas Domains: Heme Iron Coordination Structures of the B_j Fixl, A_x Pdea1, Ec Dos, and Mt Dos Proteins. Biochemistry", (2002) 41(15): 4819-4826.
19. Lukat-Rodgers, G S; Rexine, J L, and Rodgers, K R, "Heme Speciation in Alkaline Ferric Fixl and Possible Tyrosine Involvement in the Signal Transduction Pathway for Regulation of Nitrogen Fixation. Biochemistry", (1998) 37(39): 13543-13552.
20. Hira, S; Tomita, T; Matsui, T; Igarashi, K, and Ikeda-Saito, M, "Bach1, a Heme-Dependent Transcription Factor, Reveals Presence of Multiple Heme Binding Sites with Distinct Coordination Structure. IUBMB life", (2007) 59(8-9): 542-551.
21. Igarashi, J; Sato, A; Kitagawa, T; Yoshimura, T; Yamauchi, S; Sagami, I, and Shimizu, T, "Activation of Heme-Regulated Eukaryotic Initiation Factor 2 α Kinase by Nitric Oxide Is Induced by the Formation of a Five-Coordinate No-Heme Complex Optical Absorption, Electron Spin Resonance, and Resonance Raman Spectral Studies. Journal of Biological Chemistry", (2004) 279(16): 15752-15762.
22. Miksanova, M; Igarashi, J; Minami, M; Sagami, I; Yamauchi, S; Kurokawa, H, and Shimizu, T, "Characterization of Heme-Regulated Eif2 α Kinase: Roles of the N-Terminal Domain in the Oligomeric State, Heme Binding, Catalysis, and Inhibition. Biochemistry", (2006) 45(32): 9894-9905.

23. Uchida, T; Sagami, I; Shimizu, T; Ishimori, K, and Kitagawa, T, "Effects of the Bhlh Domain on Axial Coordination of Heme in the Pas-a Domain of Neuronal Pas Domain Protein 2 (Npas2): Conversion from His119/Cys170 Coordination to His119/His171 Coordination. *Journal of Inorganic Biochemistry*", (2012) 108: 188-195.

Chapter Four

dPER-PAS-B

4. dPER-PAS-B

4.1. Introduction

The constructs of dPER-PAS-B domain protein was designed in three trials based on changes in the number of amino acids in the protein chain. As discussed in the introduction to Chapter 3 the dPER-PAS-B domain of eukaryotic proteins are often less important in regulating the protein's function than the dPER-PAS-A domains [1, 2] but until now the role of the PAS-B domain in the regulation of the circadian cycle is not certain.

Table 4-1 Details of constructions dPER-PAS-B.

No.	Domain	First and last residue	Number of residues	Sequence of trail	HLH domain present	MW (kDa)
1.	dPER-PAS-B	K378-S539	162	1st trail	No	19.71
2.	dPER-PAS-B	K387-H599	213	2nd trail	Yes	26.00
3.	dPER-PAS-B	I383-P541	159	3rd trial	No	19.40
4.	dPER-PAS-B α	I383-H599	217	3rd trial	No	26.50

4.2. Result

4.2.1. Construct Design

According to the possible assumptions, the length of the amino acid chain of the expression domain (three trials) was changed with various tags. Eight constructs were designed, which contain different numbers of residues and tags (See chapter 2, table 2-5). All these constructs were created at the PROTEX laboratory by Dr. Xiaowen Yang in University of Leicester.

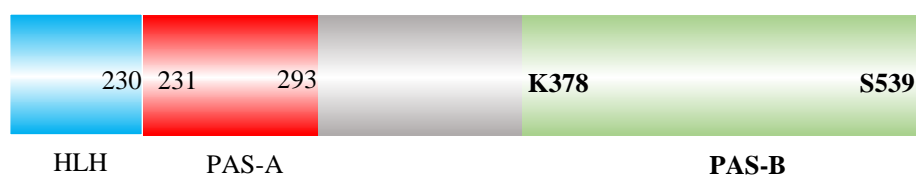


Figure 4-1 First trail construct dPer-PAS-B constructs produced Top bar illustrates the full length dPer protein with the HLH (blue), PAS-A (green) and PAS-B (red) domains labelled.

The dPER-PAS-B construct from first trial was two types of tags (GST, His produced with and without tags). This construct started at residue number 378 (Lysine) and finished at Serine 539 (162 residue). (See chapter 2, table 2-5).

In the second trial, the sequence for mPER-PAS-B was used (213 residues, Lysine 387 to Histidine 599). MBP tag was used (relatively large 40.615 kDa) to give more stability to the domain [3, 4].



Figure 4-2 Second trial construct dPER-PAS-B constructs produced Top bar illustrates the full length dPER protein PAS-A (red) and PAS-B (green) domains labelled.

Then, the third trial is based on the crystal structure defined in codes 1WA9 from the website PDBsum. According to the shape of crystal, dPER-PAS-B domain started from Isoleucine 383 and finished at Proline 541 (159 residues), figure 4-3 A, and another construct including α helix Isoleucine 383 to Histidine 599 (217 residues) figure 4-3 B [5].

GST, His, MBP and without tag were used with all constructs in the three trails (See chapter 2, table 2-5).

To study the type of binding between heme with the domain, two mutants were made separately, C455A and C467A (single mutant, see chapter 2, table 2-6) [6].



Figure 4-3 Third trail construct dPER-PAS-B constructs produced Top bar illustrates the full length dPER protein with the HLH (blue), PAS-A (red), PAS-B (green) and α helix in purple domains labelled.

4.2.2. Protein Expression and Purification

4.2.2.1. His-dPer-PAS-B refolding trial

In first trial construct, the K378-S539 dPER-PAS-B expression resulted in insoluble protein figure 4-4. Therefore, refolding technique was attempted to change the state from insoluble to soluble by using suitable condition.

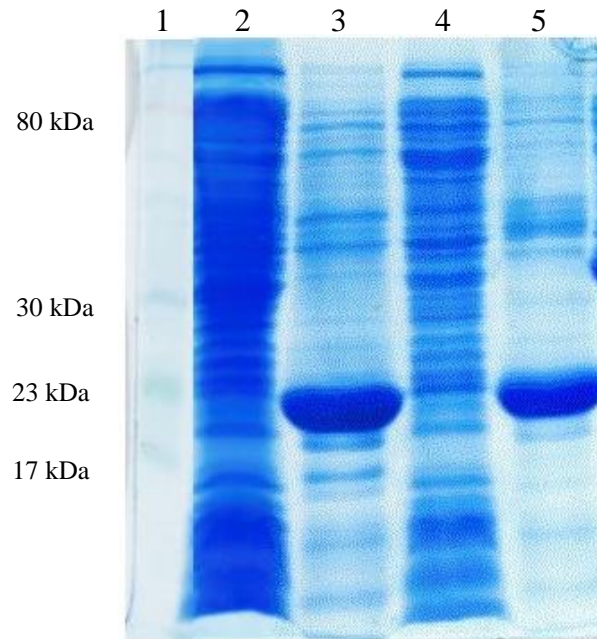


Figure 4-4 Coomassie blue stained 12% SDS-PAGE gel of the His-dPER-PAS-B (K378-S539) (19.7 KDa). Lane 1 corresponds to the SeeBlue Plus2 marker, lane 2 corresponds to the His-dPER-PAS-B soluble, lanes 3 correspond to the His-dPER-PAS-B insoluble by using *E. coli*, *Rosetta* type. Lane 4 corresponds to the His-dPER-PAS-B soluble, lanes 5 correspond to the His-dPER-PAS-B insoluble by using type *E. coli*, *BL21DE3*.

Refolding trials on His-dPER-PAS-B were performed using conditions 2, 5 and 15 from the Quickfold Protein Refolding Kit. Although no peak was seen in condition 2 (data not shown), a peak around 17.5 ml could be detected for both conditions 5 and 15 (Figures 4-5 and 4-6). This peak corresponds to monomeric His-dPer-Pas-B. Fractions collected for the 17.5 ml peaks in these conditions were concentrated using the acetone precipitation method described in Chapter 2 and were analysed using SDS-PAGE (Figure 4-7).

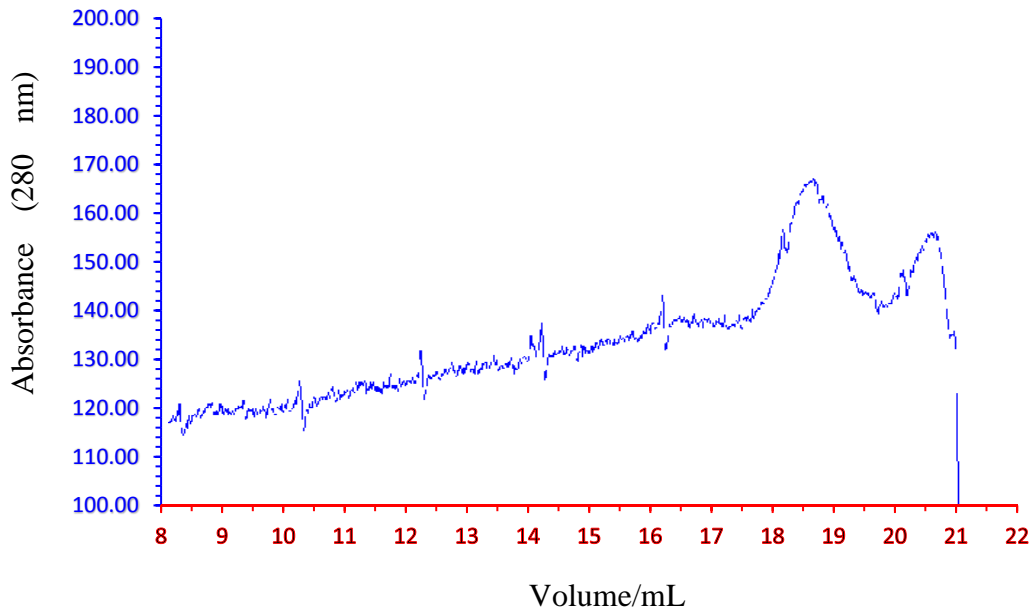


Figure 4-5 Q Sepharose FPLC elution chromatogram run at 1 mL/min. Traces shown are the absorption reading at 280 nm for His-dPer-PAS-B (K378-S539) after refolding trials using condition 5 of the Quickfold protein refolding kit. The vertical axis corresponds to the absorbance of the 280 nm (blue line).

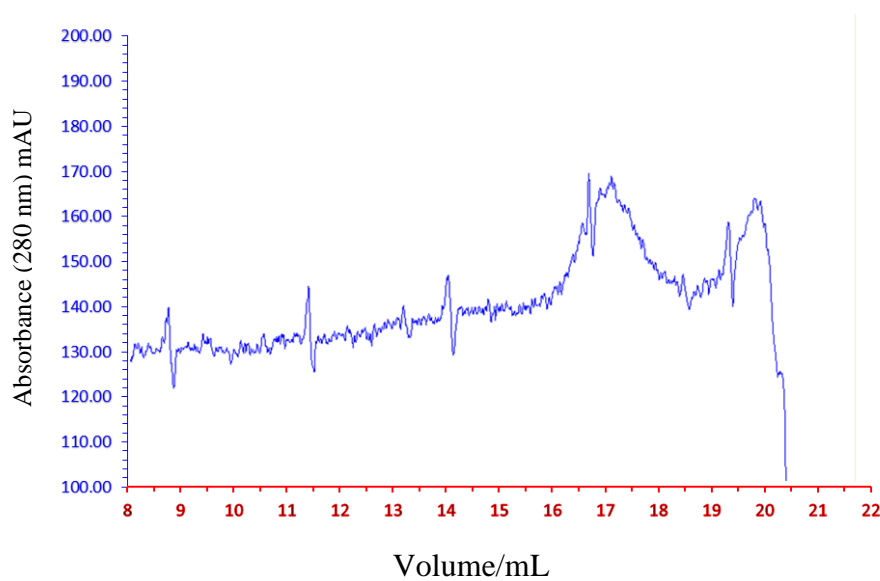


Figure 4-6 Sepharose FPLC elution chromatogram run at 1 mL/min. Traces shown are the absorption reading at 280 nm for His-dPER-PAS-B (K378-S539) after refolding trials using condition 15 of the Quickfold protein refolding kit. The vertical axis corresponds to the absorbance of the 280 nm (blue line).

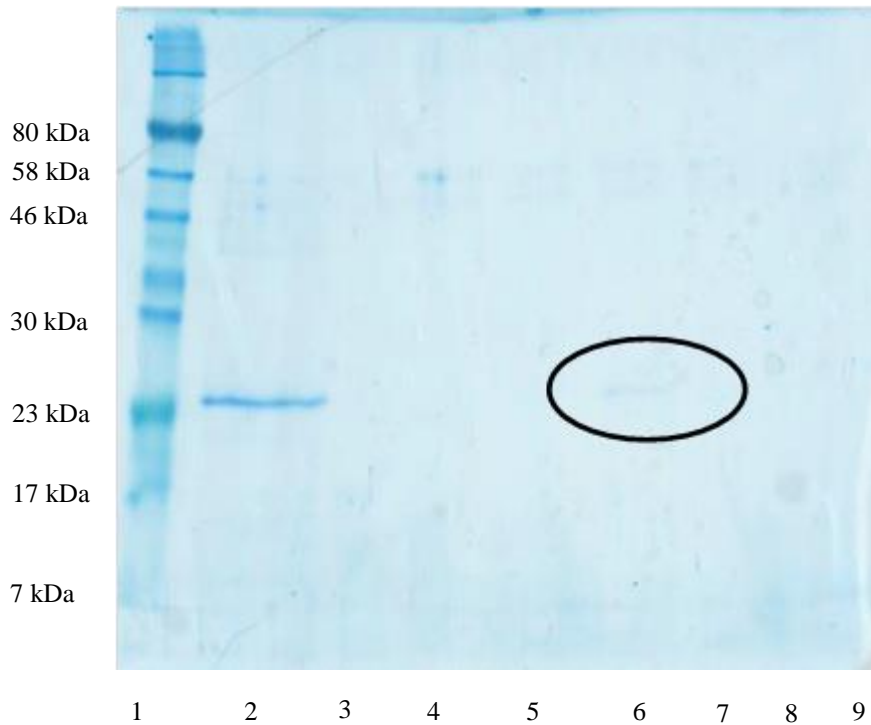


Figure 4-7 Coomassie blue stained 12% SDS-PAGE gel of dPER-PAS-B (K378-S539) after refolding in conditions 5 and 15. Lane 1 corresponds to the Colorplus prestained marker, lane 2 corresponds to solubilized His-dPER-PAS-B inclusion bodies, lanes 3-6 correspond to fractions from refolding condition 5 post acetone precipitation and lanes 7-9 to fractions from refolding condition 15 post acetone precipitations. Circled is a faint band around 22 kDa and there is very small quantities or near to no protein yield.

A very faint band can be visualised in figure 4-5 only for His-dPer-Pas-B condition 5. The lack of bands on the SDS gels for the other peaks are most likely due to the very small quantities of refolded protein recovered and losses during the protein concentration method. These findings suggest that **condition 5** is suitable for a large inclusion body refolding purification.

The elution profile corresponds to the gel filtration of the **large scale** refolding preparation of His-dPer-PAS-B using condition 5. The protein is eluted at around 70 ml using a Superdex-75 16/60 gel filtration column.

As a summation for above, the expression for dPER-PAS-B domain in first trial was Insufficient to this study. The, new plasmid was designed as a second trial with different tag (MBP-dPER-PAS-B) figure 4-8.

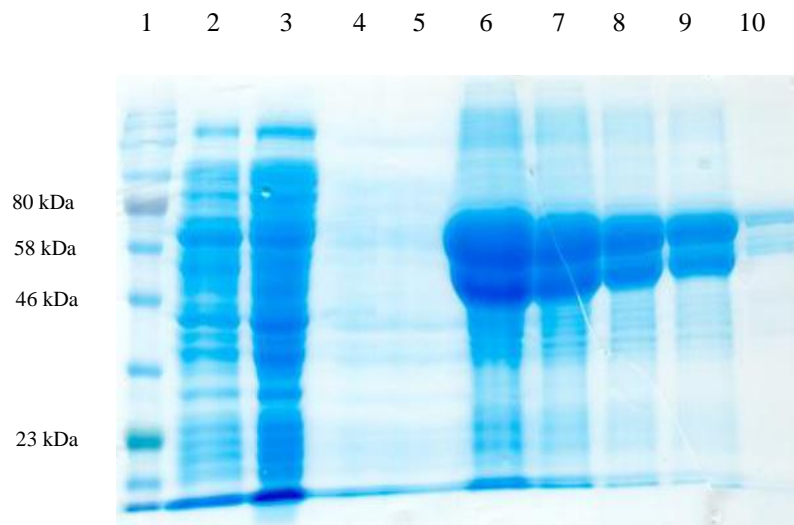


Figure 4-8 Shows the Coomassie blue stained 12% SDS-PAGE gel of the MBP-dPER-PAS-B (K387-H599) fractions from second trial (60.32 kDa). Lane 1 corresponds to the Colorplast prestained marker, lane 2 corresponds to the elution fraction of MBP-dPER-PAS-B after sonication. Lane 3 represent through flow. The washing resin result in lanes 4 and 5. Lanes 6-10 correspond to the MBP-dPER-PAS-B fractions from the Ni-NTA affinity chromatography.

In the second trial, the expression of dPR-PAS-B with MBP tag resulted output a good yield (Figure 4-8). In order to do heme titration, the MBP tag which linked with dPER-PAS-B is required to remove up because of the high efficiency of the MBP to binding with heme which is resulting a false result. His-TEV was used to separate the MBP but the results did not give the free dPER-PAS-B.

New constructs were designed with different tags (His-dPER-PAS-B, GST-dPER-PAS-B) as a third trial (Figures 4-9 and 4-10). It is very obviously from gel figures 4-9 and 4-10 the expression was succeed for both constructs.

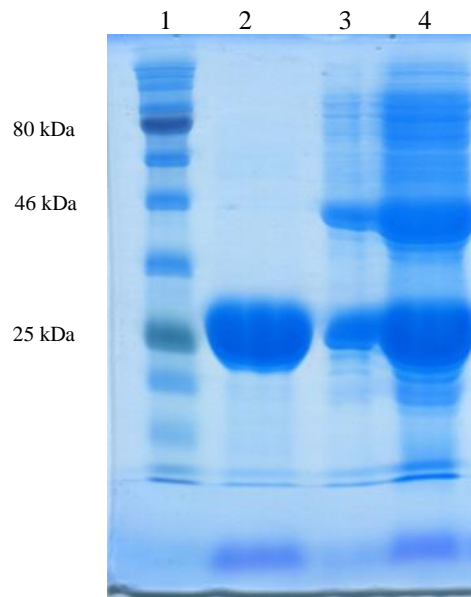


Figure 4-9 Shows the Coomassie blue stained 12% SDS-PAGE gel of the GST-dPER-PAS-B fractions from third trial (44.37 kDa). Lane 1 corresponds to the Color Protein Standard marker, lane 2 corresponds to the GST tag. Lane 3 represent through flow. Lane 4 correspond to the GST-dPER-PAS-B fractions from the GST affinity chromatography.

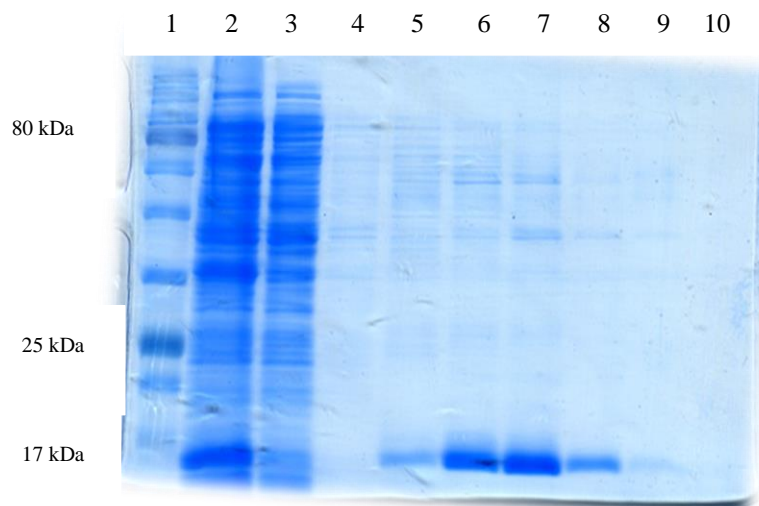


Figure 4-10 Shows the Coomassie blue stained 12% SDS-PAGE gel of the His-dPER-PAS-B fractions from third trial (19.67 kDa). Lane 1 corresponds to the Color Protein Standard marker, lane 2 corresponds to the elution fraction of His-dPER-PAS-B after sonication. Lane 3 represent through flow. The washing resin result in lane 4. Lanes 5-10 correspond to the His-dPER-PAS-B fractions from the Ni-NTA affinity chromatography.

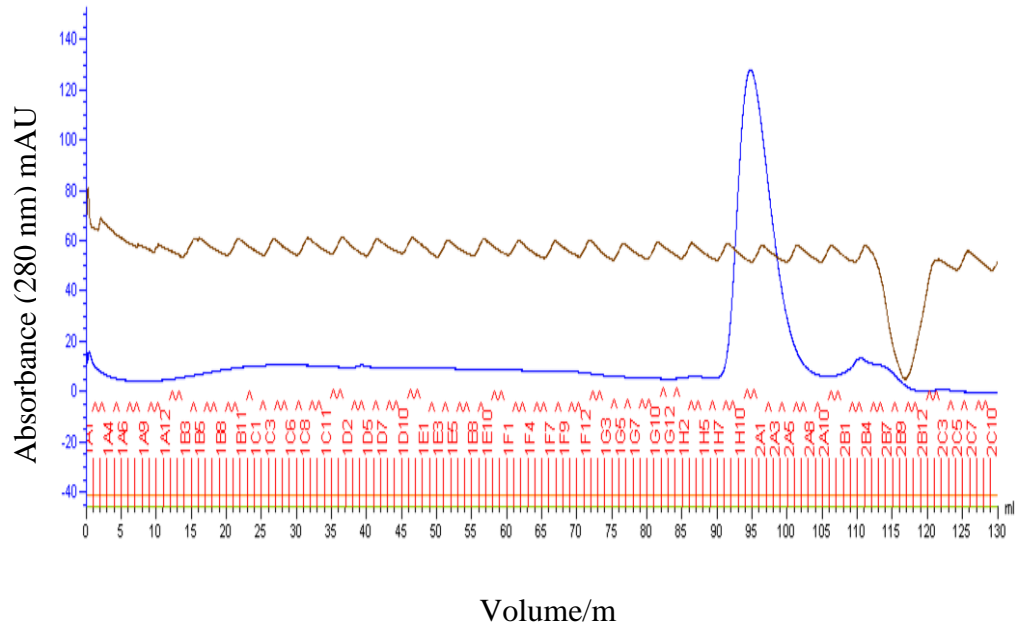


Figure 4-11 Sepharose FPLC elution chromatogram run at 1 mL/min. Traces shown are the absorption reading at 280 nm for His-dPER-PAS-B (I383-P541) on a Superdex-75 16/60 pre-packed column using an Äkta purifier P-900 (GE Healthcare LifeSciences). The conductivity of the solution measured in ml siemens per centimetre (mS/cm, brown line). The vertical axis corresponds to the absorbance of the 280 nm (blue line). The fractions are labelled on the chromatogram in red, of which fractions 1H9 to 2A5 were collected and pooled for further purification in this instance.

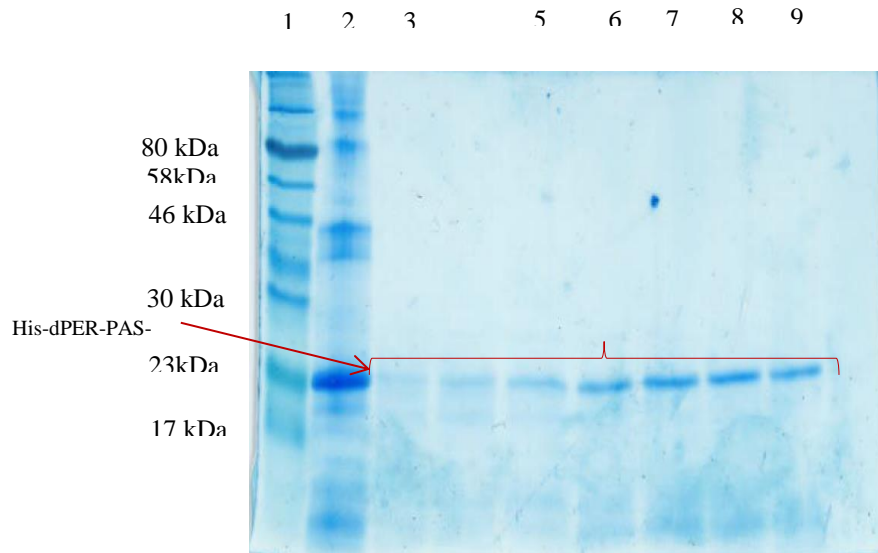


Figure 4-12 Coomassie blue stained 12% SDS-PAGE gel of the His-dPER-PAS-B fractions post refolding. Lane 1 corresponds to the SeeBlue Plus2 marker, lane 2 corresponds to the elution fraction of His-dPER-PAS-B from the Ni-NTA affinity chromatography. Lanes 3 to 9 represent AKTA fractions 1H9, 1H10, 1H12, 2A1, 2A3, 2A4 and 2A5 (Figure 4-11) respectively. Arrow points the His-dPER-PAS-B bands under the red bracket around 18 kDa.

The SDS-PAGE corresponding to the above eluted peak is shown below. A band around 19.37 kDa can be seen which is consistent with the calculated molecular weight of dPER-PAS-B. Typical yields from protein refolding experiments are less than 20 % from the starting quantity of solubilized inclusion bodies added to the refolding buffer. Large losses were observed when the His-tag protein was digested with TEV protease, resulting in a lack of material for further characterisation. The un-tagged protein was item expressed and refolded to minimize these losses.

4.2.3.Heme Titration

According to stability and behaviour (soluble or insoluble) of expression for dPER-PAS-B, the construct from the third trial was used to represent the dPER-PAS-B domain. The binding of heme resulted in a Soret band at 422 nm (Figure 4-15). Difference spectrophotometry was then used to determine a dissociation constant (K_D). The calculation of K_D depends on the changes in absorbance at the Soret band 422 nm and was calculated at $4.8653 \pm 0.5321 \mu\text{M}$ (Figures 4-13 and 4-14). The comparison between dissociation constant rate for dPER-PAS-B in this study and other dissociation constant rate studies such as mNPAS2-PAS-B was 3.2×10^{-3} , $3.0 \times 10^{-4} \text{ s}^{-1}$ [7]. The dPER-PAS-B binds heme with high similar affinities to mNPAS2-PAS-B.

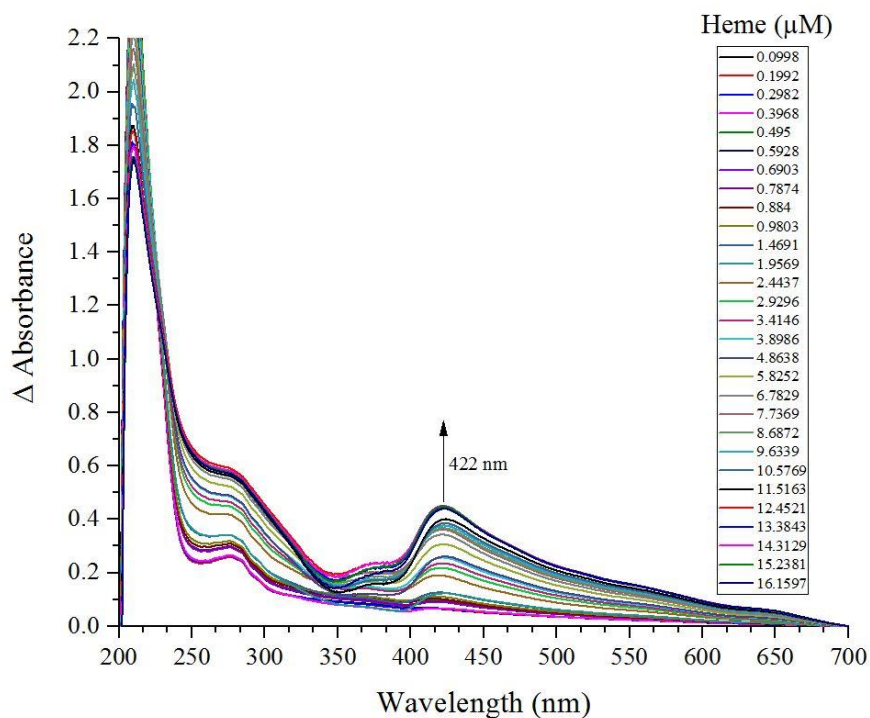


Figure 4-13 UV-visible difference spectrum of heme bound to dPER-PAS-B. Reaction ratio heme to dPER-PAS-B domain is 1:1, the concentration of hemin was $8.654 \mu\text{M}$ and concentration of dPER-PAS-B domain was $8.904 \mu\text{M}$. Legend shows the final concentration of heme used in the titration.

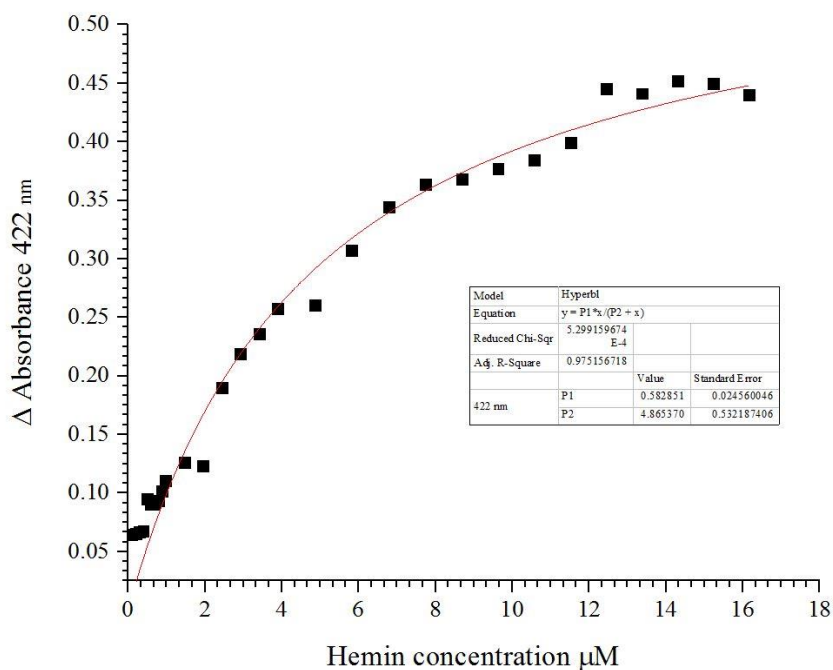


Figure 4-14 The relative absorbance changes to the difference spectrum at 422nm fit to a hyperbolic. $K_D = 4.865 \pm 0.532 \mu\text{M}$.

4.2.4. UV-Visible Spectroscopy

The condition to purified dPER-PAS-B (remove the tag) was similar to dPER-PAS-A, to avoid the wrong binding between tag and heme.

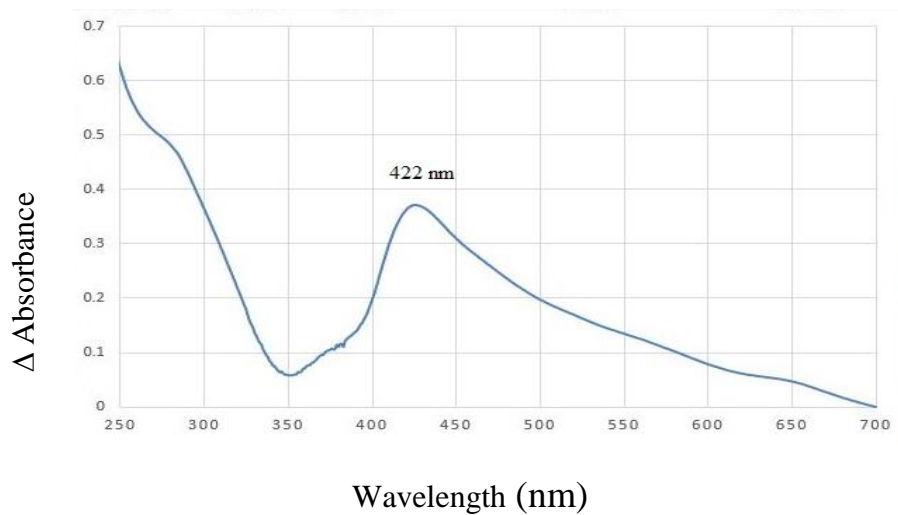


Figure4-15 UV-Visible absorbance spectra of heme (ferric) bound to dPER-PAS-B (422 nm).

Table 4-2 Spectral characteristics and axial ligands of various heme proteins (dPER-PAS-B).

Protein	Cys	Cys/His	Cys/?	His/?	other	unknown	Soret	Q bands	References
dPER-PAS-B						•	422	537	this work
NPAS2-PAS-B				•			419	536	[7]
mPER2-PAS-B			•				412	536,564,630	[8]
EcDOS-PAS					His/H ₂ O		416	530,564	[9-11]
RmFixLN					His		412	543,579,604	[12]
Bach 1	•	•					423 371	540,580 521,541,650	[13]
hCLOCK				•			416	536	[14]

4.2.5. Electron Paramagnetic Resonance (EPR)

EPR Spectra of the heme Complex of dPER-PAS-B. Samples of ferric protein were tested and analysed with the help of Dr. Dimitri Svistunenko at the EPR Research Facility (University of Essex) for a Bruker EMX EPR spectrometer (X-band) equipped with a spherical high quality resonator ER 4122 and an Oxford Instruments liquid helium system for the low-temperature measurements. Samples were placed in Wilmad SQ EPR tubes to a final volume of 250 μ l, frozen in methanol kept on dry ice, wiped and then transferred to liquid nitrogen. EPR spectra were measured at 10 K. Crystal field parameters of EPR spectra of Fe (III) low-spin complexes have been successfully used to identify axial ligands of the heme iron [15, 16].

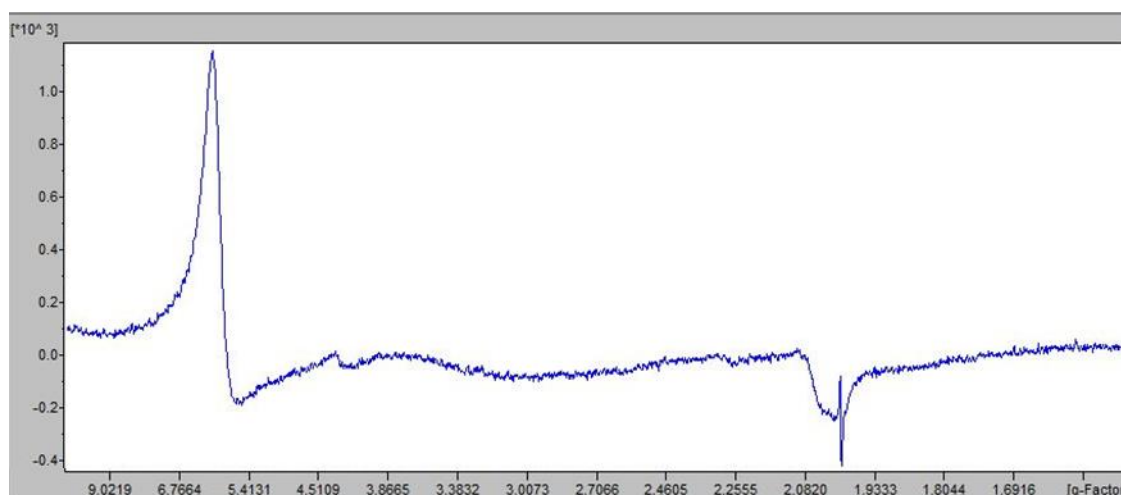


Figure 4-16 EPR spectra for dPER-PAS-B 100 μ M with 30 μ M hemin in pH 7.5, HS haem signal, also much lower of a low spin.

Table 4-3 EPR g values and heme ligands for ferric proteins and a model ferric heme complex.

No.	Protein	Wild-type and mutant domain	ligands	g values	Ref.
1.	dPER	PAS-B	Cys	2.27	this study
2.	hCLOCK	PAS-B	Cys	2.28	[14]
3.	P450		Cys	2.26	[17]

4.2.6. Circular Dichroism (CD)

Magnetic circular dichroism (CD spectra were obtained with a Chirascan plus CD spectrometer at room temperature) spectral band at the Soret region of heme-bound domain dPER-PAS-B. There is a non-significant difference in optical absorption band between dPER-PAS-B and dPER-PAS-B band heme.

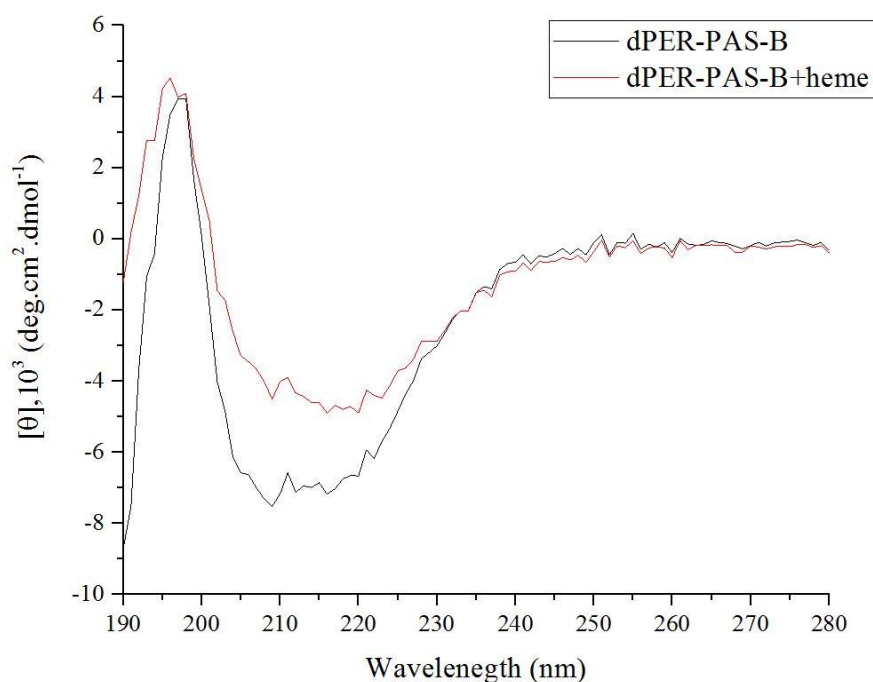


Figure 4-17 Magnetic circular dichroism spectra for dPER-PAS-B (black) and dPER-PAS-B binding with heme (red).

4.2.7. Mutant Variants

The results of EPR experiments suggest that dPER-PAS-B binds heme via a cysteine residue. There are four residues (Cysteine) in dPER-PAS-B supposedly at least one of them binds heme. These residues C455, C467, C502, and C511. Two residues were chosen (C455, C467) to be mutated by changing Cysteine to Alanine (See chapter 2, table 2-6).

The result of heme titration for mutant dPER-PAS-B was very similar to the wild type see figures 4-18 and 4-19.

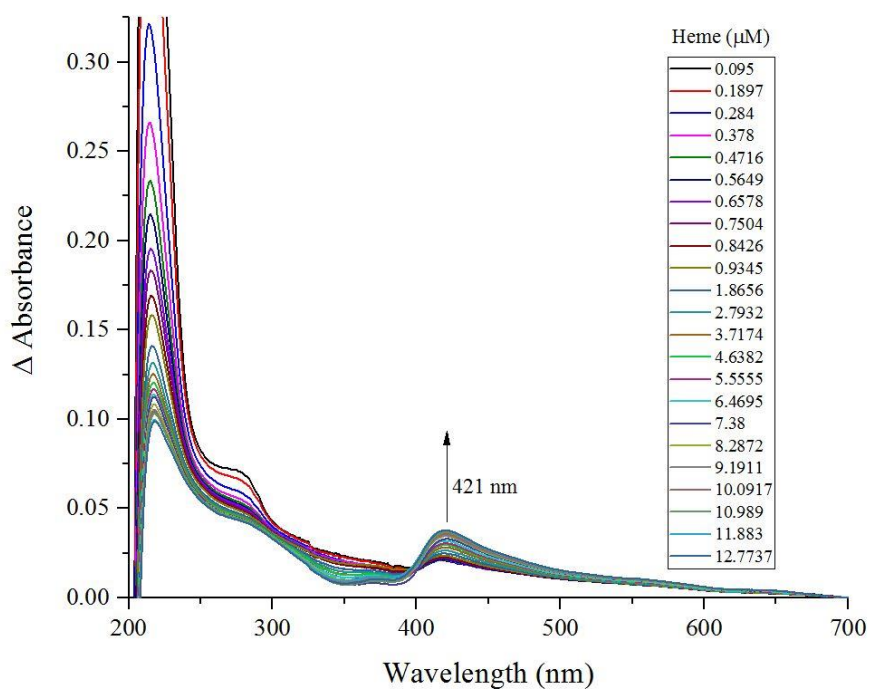


Figure 4-18 UV-visible difference spectrum of heme bound to mutant dPER-PAS-B (Cys455Ala). Legend shows the final concentration of heme used in the titration.

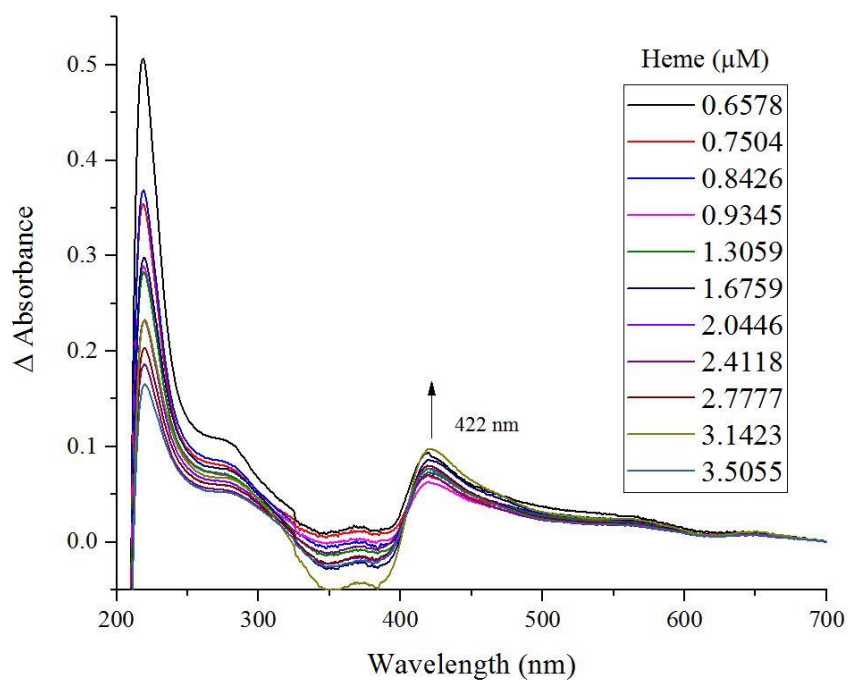


Figure 4-19 UV-visible difference spectrum of heme bound to mutant dPER-PAS-B (Cys467Ala). Legend shows the final concentration of heme used in the titration.

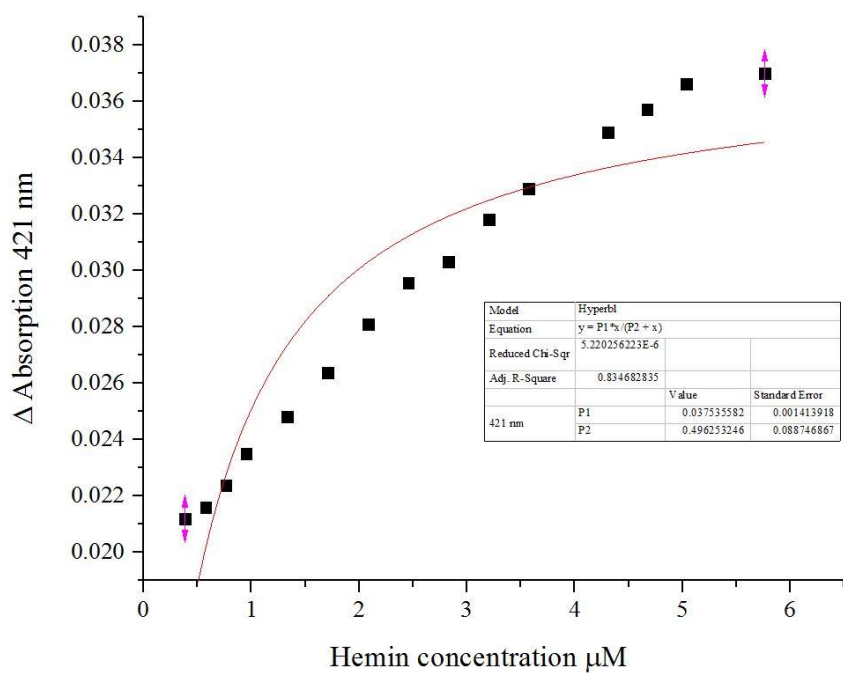


Figure 4-20 The relative absorbance changes to the difference spectrum for mutant Cys455Ala at 421 nm fit to a hyperbolic. $K_D = 0.4962 \pm 0.0887 \mu\text{M}$.

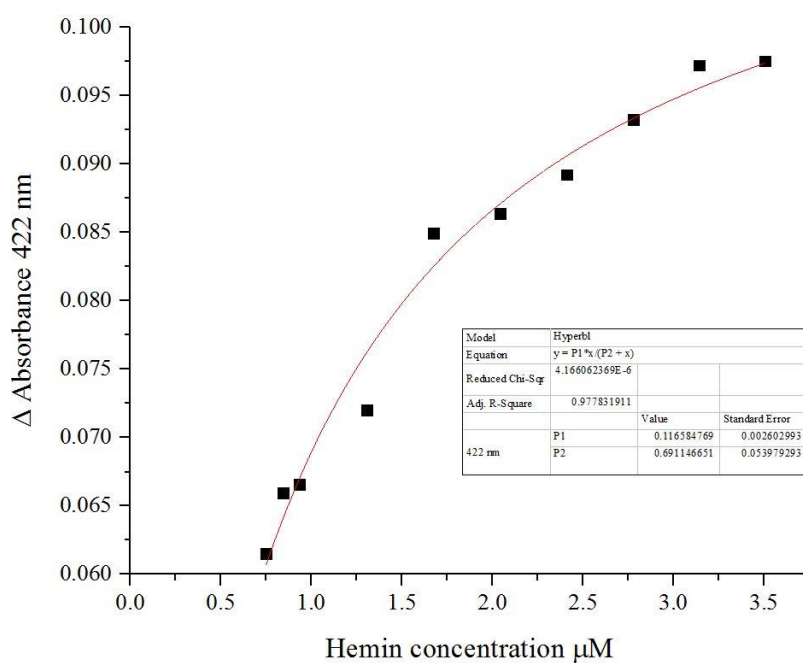


Figure 4-21 The relative absorbance changes to the difference spectrum for mutant Cys467Ala at 422nm fit to a hyperbolic. $K_D = 0.6911 \pm 0.0539 \mu\text{M}$.

4.3. Summary

In this Chapter another domain (dPER-PAS-B) from dPER-PAS was studied. Initially, different constructs in three trials which were different in the length of amino acid sequence with different types of tags (GST, His and MBP). *E. coli* (*Rosetta* and *BL21DE3*) were used as a competent cells under different conditions from temperature and induction. The examination of the ferric form of dPER-PAS-B by EPR spectroscopy (see chapter six) further supported the evidence that the protein bound heme in a 6 coordinate manner. Furthermore, the EPR spectrum showed evidence for one form of ligation with signals generally characteristic of a Cys/Heme ligation.

According to the result of EPR tests on this domain and shape of molecule (stereochemistry) of the protein molecule that allows the binding between the heme and Cysteine molecules (there are four molecules: Cys455, Cys467, Cys502 and Cys511), led to the selection of Cys455 and Cys467 for mutant and replace them with Alanine.

The absorption spectra of molecular of heme and protein complexes were studied for both wild type and mutant type which was found there are no significant difference in absorption peak. This similarity in absorption spectra between wild type and mutant type indicates the possibility that the binding did not occur between the Cys455 and Cys467 in dPER-PAS-B with hem molecule or the binding was not significant.

As a result for above and as a future work to determine the type of binding (specific or unspecified), make a mutation of cysteine 502 and cysteine 511 in dPER-PAS-B. Then study of the binding between dPER-PAS-B and the mutant dPER-PAS-B by absorption spectrometry study and EPR.

4.4. References

1. Masetti, M; Falchi, F, and Recanatini, M, "Protein Dynamics of the Hif-2 Alpha Pas-B Domain Upon Heterodimerization and Ligand Binding. Plos One", (2014) 9(4)
2. Rogers, J L; Bayeh, L; Scheuermann, T H; Longgood, J; Key, J; Naidoo, J; Melito, L; Shokri, C; Frantz, D E; Bruick, R K; Gardner, K H; MacMillan, J B, and Tambar, U K, "Development of Inhibitors of the Pas-B Domain of the Hif-2 Alpha Transcription Factor. Journal of Medicinal Chemistry", (2013) 56(4): 1739-1747.
3. Nallamsetty, S; Austin, B P; Penrose, K J, and Waugh, D S, "Gateway Vectors for the Production of Combinatorially- Tagged His6- Mbp Fusion Proteins in the Cytoplasm and Periplasm of Escherichia Coli. Protein Science", (2005) 14(12): 2964-2971.
4. Needle, D and Waugh, D S, "Rescuing Aggregation-Prone Proteins in Escherichia Coli with a Dual His 6-Mbp Tag", in Protein Affinity Tags. (2014), Springer. 81-94.
5. King, H A; Hoelz, A; Crane, B R, and Young, M W, "Structure of an Enclosed Dimer Formed by the Drosophila Period Protein. Journal of Molecular Biology", (2011) 413(3): 561-572.
6. Lindebro, M; Poellinger, L, and Whitelaw, M, "Protein-Protein Interaction Via Pas Domains: Role of the Pas Domain in Positive and Negative Regulation of the Bhlh/Pas Dioxin Receptor-Arnt Transcription Factor Complex. The EMBO journal", (1995) 14(14): 3528-3539.
7. Koudo, R; Kurokawa, H; Sato, E; Igarashi, J; Uchida, T; Sagami, I; Kitagawa, T, and Shimizu, T, "Spectroscopic Characterization of the Isolated Heme-Bound Pas-B Domain of Neuronal Pas Domain Protein 2 Associated with Circadian Rhythms. FEBS Journal", (2005) 272(16): 4153-4162.
8. Hayasaka, K; Kitanishi, K; Igarashi, J, and Shimizu, T, "Heme-Binding Characteristics of the Isolated Pas-B Domain of Mouse Per2, a Transcriptional Regulatory Factor Associated with Circadian Rhythms. Biochimica Et Biophysica Acta-Proteins and Proteomics", (2011) 1814(2): 326-333.
9. Sato, A; Sasakura, Y; Sugiyama, S; Sagami, I; Shimizu, T; Mizutani, Y, and Kitagawa, T, "Stationary and Time-Resolved Resonance Raman Spectra of His77 and Met95 Mutants of the Isolated Heme Domain of a Direct Oxygen Sensor from *E. Coli*. Journal of Biological Chemistry", (2002)
10. Tomita, T; Gonzalez, G; Chang, A L; Ikeda-Saito, M, and Gilles-Gonzalez, M-A, "A Comparative Resonance Raman Analysis of Heme-Binding Pas Domains: Heme Iron Coordination Structures of the Bj Fixl, Ax Pde1, Ec Dos, and Mt Dos Proteins. Biochemistry", (2002) 41(15): 4819-4826.
11. Delgado-Nixon, V M; Gonzalez, G, and Gilles-Gonzalez, M-A, "Dos, a Heme-Binding Pas Protein from Escherichia Coli, Is a Direct Oxygen Sensor. Biochemistry", (2000) 39(10): 2685-2691.

12. Lukat-Rodgers, G S; Rexine, J L, and Rodgers, K R, "Heme Speciation in Alkaline Ferric Fixl and Possible Tyrosine Involvement in the Signal Transduction Pathway for Regulation of Nitrogen Fixation. *Biochemistry*", (1998) 37(39): 13543-13552.
13. Hira, S; Tomita, T; Matsui, T; Igarashi, K, and Ikeda-Saito, M, "Bach1, a Heme-Dependent Transcription Factor, Reveals Presence of Multiple Heme Binding Sites with Distinct Coordination Structure. *IUBMB life*", (2007) 59(8-9): 542-551.
14. Efimov, I; Parkin, G; Millett, E S; Glenday, J; Chan, C K; Weedon, H; Randhawa, H; Basran, J, and Raven, E L, "A Simple Method for the Determination of Reduction Potentials in Heme Proteins. *FEBS Letters*", (2014) 588(5): 701-704.
15. Igarashi, J; Sato, A; Kitagawa, T; Yoshimura, T; Yamauchi, S; Sagami, I, and Shimizu, T, "Activation of Heme-Regulated Eukaryotic Initiation Factor 2 α Kinase by Nitric Oxide Is Induced by the Formation of a Five-Coordinate No-Heme Complex Optical Absorption, Electron Spin Resonance, and Resonance Raman Spectral Studies. *Journal of Biological Chemistry*", (2004) 279(16): 15752-15762.
16. Miksanova, M; Igarashi, J; Minami, M; Sagami, I; Yamauchi, S; Kurokawa, H, and Shimizu, T, "Characterization of Heme-Regulated Eif2 α Kinase: Roles of the N-Terminal Domain in the Oligomeric State, Heme Binding, Catalysis, and Inhibition. *Biochemistry*", (2006) 45(32): 9894-9905.
17. Schünemann, V; Jung, C; Trautwein, A; Mandon, D, and Weiss, R, "Intermediates in the Reaction of Substrate- Free Cytochrome P450cam with Peroxy Acetic Acid. *FEBS Letters*", (2000) 479(3): 149-154.

Chapter Five

dPER-PAS-AB

5. dPER-PAS-AB

5.1. Introduction

The other type of domain in this study which is dPER-PAS-AB which includes dPER-PAS-A and dPER-PAS-B in same construct. These constructs are different from each other (in three trails) by the number of residues in the sequence of amino acids. This point based on the circadian rhythm in *Drosophila melanogaster* includes binding between PERIOD (PER) and TIMELESS (TIM). The mechanism of this binding still unknown and in this trial we aim to understand the mechanism by finding the role of heme [1-3].

Table 5-1 Details of constructions dPER-PAS-AB used in this study.

No.	Domain	First and last residue	Length of residues	Sequence of trail	HLH domain present	MW (kDa)
1.	dPER-PAS-AB	R231-S539	309	1 st trail	No	37.45
2.	dPER-PAS-AB	M1-H599	599	2 nd trail	Yes	70.16
3.	dPER-PAS-AB	E145-H599	455	2 nd trail	No	53.81
4.	dPER-PAS-AB	G232-P541	310	3 rd trial	No	37.55
5.	dPER-PAS-AB	G232-H599	368	3 rd trial	No	44.68

5.2. Result

5.2.1. Construct Design

Based on constructs dPER-PAS-A and dPER-PAS-B designed in all the three trials, the dPER-PAS-AB was designed. In first trail, there is one construct of dPER-PAS-AB domain start from first amino acid of dPER-PAS-A (Arginine231) until the last amino acid for dPER-PAS-B (Serine539) including group of amino acid between dPER-PAS-A and dPER-PAS-B, 84 a.a (start from Isoleucine 294, ended in Tyrosine 377) with molecular weight 37.45 kDa.

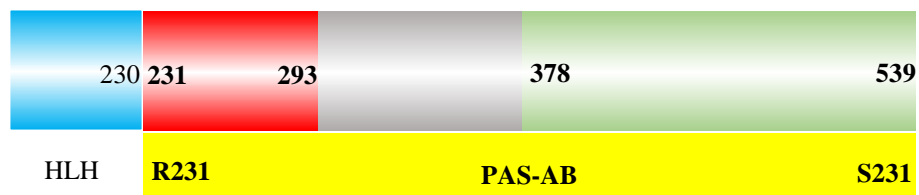


Figure 5-1 First trial construct dPER-PAS-AB constructs produced Top bar illustrates the full length dPer protein with the HLH (blue), PAS-A (green), PAS-B (red) domains labelled and dPER-PAS-AB in yellow colour.

In the second trial, there are two constructs according to dPER-PAS-A (there are two constructs different in number of a.a, first one start in Methionine1 and another one start in Glutamic acid 145, both been ended in Glutamine 386). The longer one with weight 70.16 kDa and the shorter one with weight 53.81 kDa.

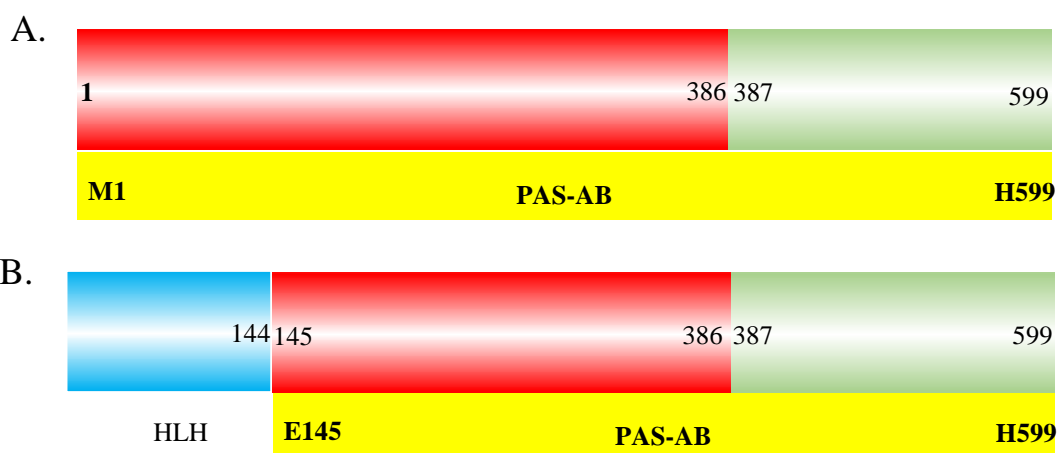


Figure 5-2 Second trial construct dPER-PAS-AB constructs produced Top bar illustrates the full length dPER protein PAS-A (red), PAS-B (green) domains labelled and dPER-PAS-AB in yellow colour.

The first constructs in third trial consists of dPER-PAS-A and dPER-PAS-B with seven a.a (start with Serine376 to Glutamic 382) with molecular weight 37.55 kDa. The second construct extra a.a in C terminal (α -Helix) with molecular weight 44.78 kDa.



Figure 5-3 Third trail construct dPER-PAS-AB constructs produced Top bar illustrates the full length dPER protein with the HLH (blue), PAS-A (red) , PAS-B (green), α - Helix in purple domains labelled and dPER-PAS-AB in yellow colour.

5.2.2. GST-dPER-PAS-AB purification

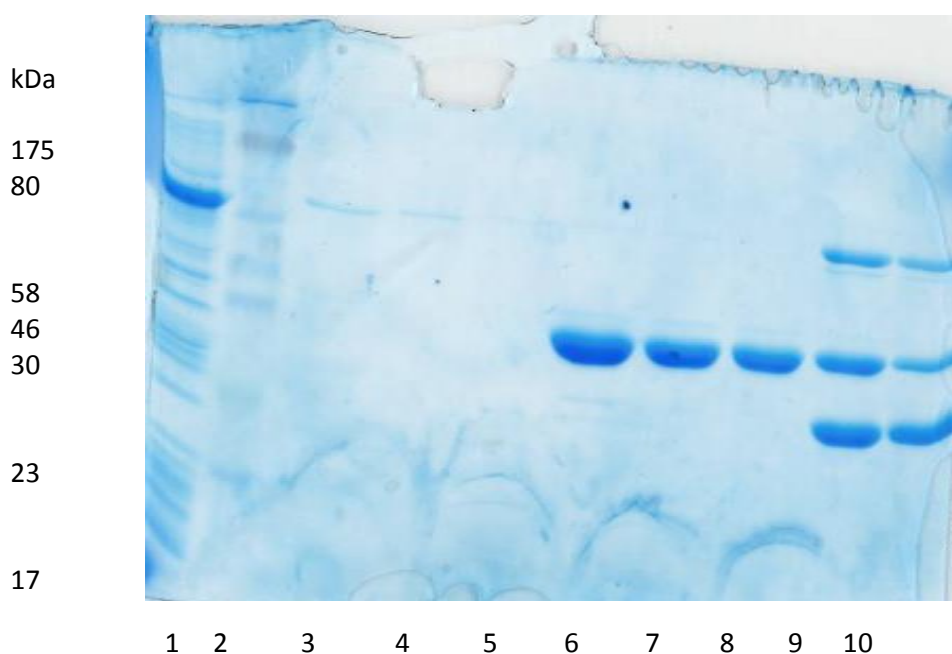


Figure 5-4 Coomassie blue stained 12% SDS-PAGE from the GST-dPER-PAS-AB (R231-S539) purification using Glutathione Sepharose 4B and TEV protease digestion. Lane 1 is the flow through of dPER-PAS-AB supernatant post glutathione sepharose. ColorPlus™ Prestained Protein Marker, Broad Range (7-175 kDa) is in Lane 2. Lanes 3-5 are washes. Lanes 6-8 correspond to elution of dPer-PAS-AB post overnight digestion with GST-tagged TEV protease. Lanes 9-10 are overnight elution of undigested dPER-PAS-AB with reduced glutathione elution buffer. Molecular weight of dPER-PAS-AB is 34.7 kDa, GST 26 kDa and GST-dPer-PAS-AB 61.3 kDa.

GST-tagged dPER-PAS-AB was expressed soluble and purified using Glutathione Sepharose according to standard methods described in Materials and Methods (Chapter 2). The GST-tag was cleaved from the dPER-PAS-AB whilst bound to the column and remaining uncleaved protein was eluted with the reduced glutathione elution buffer. The following gel clearly demonstrates the purity of the protein.

Fractions containing GST-tag cleaved dPer-PAS-AB were pooled and run on a gel filtration column. Figure 5-5 shows the elution of the protein as a single broad peak around 62 ml. According to the manufacturer's column calibration recommendations, this corresponds to a monomer.

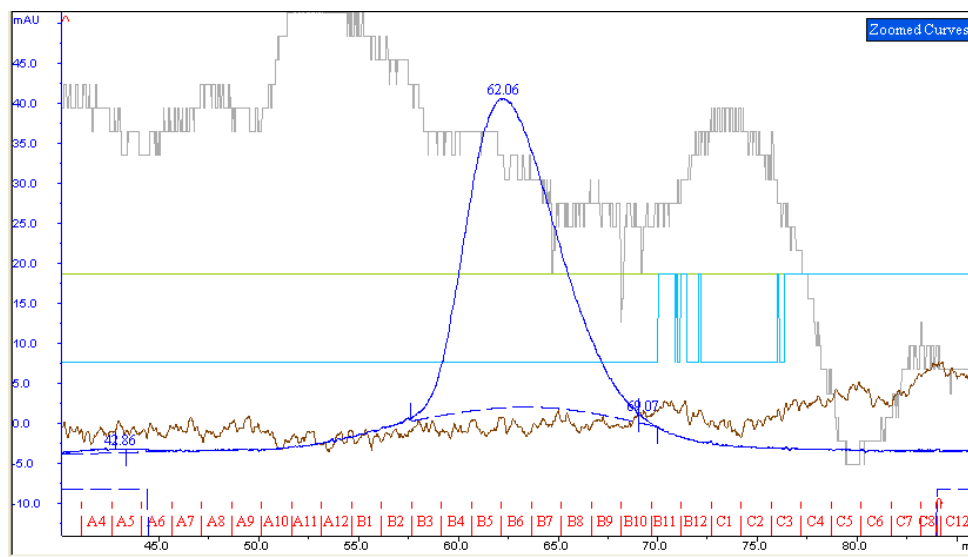


Figure 5-5 Q Sepharose FPLC elution chromatogram run at 1 mL/min. Traces shown are the absorption reading at 280 nm dPER-PAS-AB (R231-S539). The conductivity of the solution measured in ml Siemens per centimeter (mS/cm, brown) and the conductivity percentage (light blue line). Gray line represent pH. Light green line represent concentration. The vertical axis corresponds to the absorbance at 280 nm (blue line). The fractions are labelled on the chromatogram in red, of which fractions 1H9 to 2A6 were collected and pooled for further purification in this instance.

The fractions from the eluted peak were subjected to SDS-PAGE (Figure 5-6). The protein is more than 95% pure.

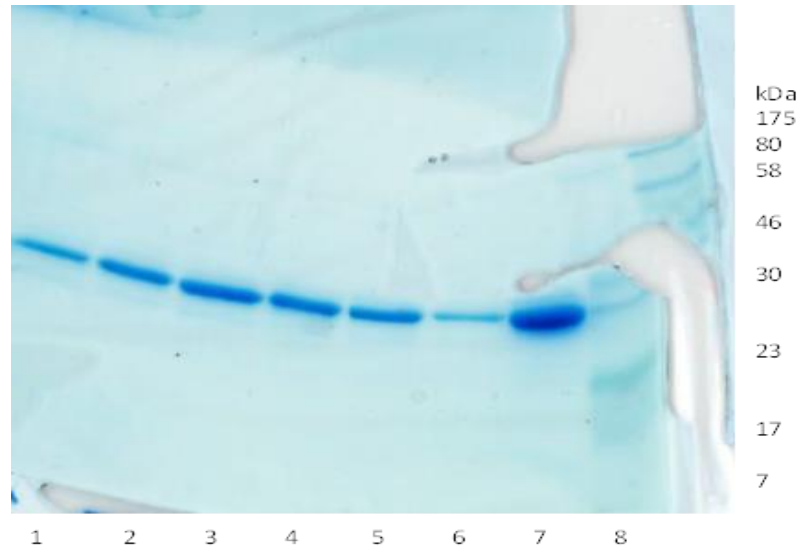


Figure 5-6 Coomassie Blue stained 12% SDS-PAGE showing eluted dPER-Pas-AB fractions from Superdex 75 (Figure 5-5). Lanes 1-6 show fractions B10-B4, dPER-Pas-AB preloading onto Superdex 75 is in lane 7. ColorPlus™ Prestained Protein Marker, Broad Range (7-175 kDa) is in lane 8.

5.2.3. His-dPER-PAS-AB

His-dPER-PAS-AB is one of constructs in the trials which was used to make expression and purification of dPER-PAS-AB by Ni-NTA column.

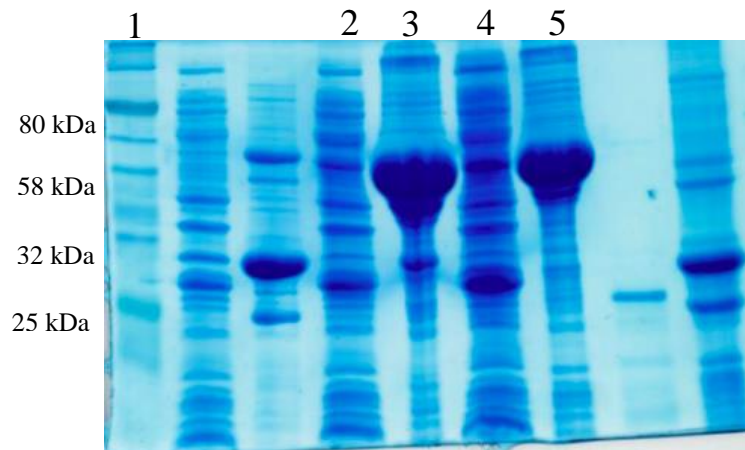


Figure 5-7 Coomassie blue stained 12% SDS-PAGE gel of the His-dPER-PAS-AB (R231-S539) 37.74 kDa fractions post refolding. Lane 1 corresponds to the Color Prestained Protein Standard marker, lanes 2 and 4 corresponds to the soluble of His-dPER-PAS-AB from the Ni-NTA affinity chromatography. Lanes 3 and 5 corresponds to insoluble of His-dPER-PAS-AB from the Ni-NTA affinity chromatography.

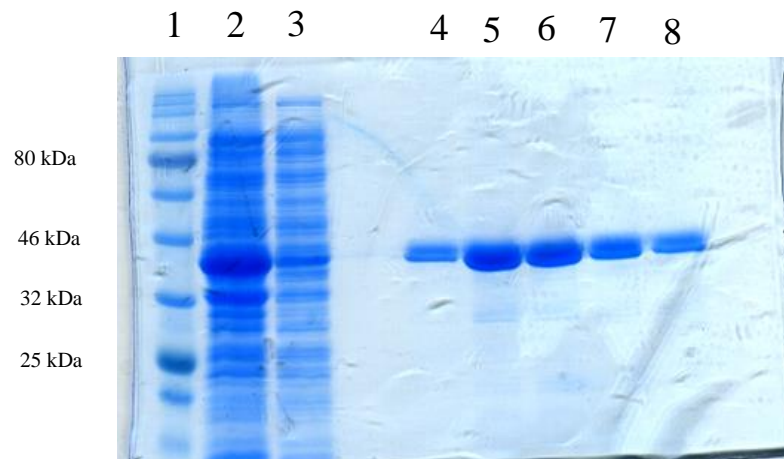


Figure 5-8 Coomassie blue stained 12% SDS-PAGE gel of the His-dPER-PAS-AB (G232-H599) 44.67 KDa fractions post refolding. Lane 1 corresponds to the Color Prestained Protein Standard marker, lane 2 corresponds to the flow through of His-dPER-PAS-AB from the Ni-NTA affinity chromatography, lane 3 corresponds to solution of washing the column and lanes 4-8 corresponds to the elution fraction of His-dPER-PAS-AB from the Ni-NTA affinity chromatography.

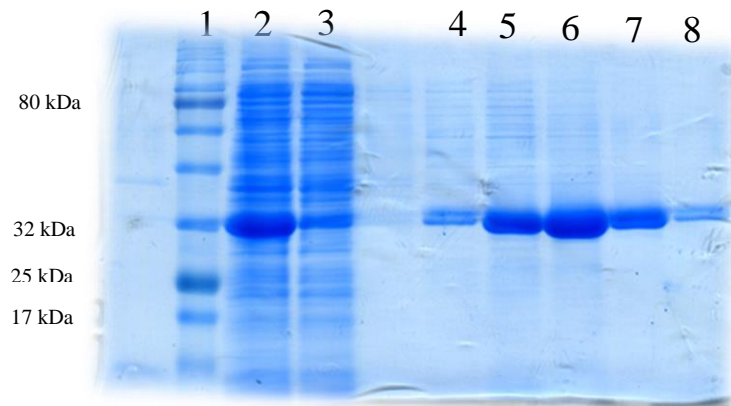


Figure 5-9 Coomassie blue stained 12% SDS-PAGE from the GST-dPER-PAS-AB (R231-S539) purification using Glutathione Sepharose 4B and TEV protease digestion. Lane 1 is the flow through of dPER-PAS-AB supernatant post glutathione sepharose. ColorPlus™ Prestained Protein Marker, Broad Range (7-175 kDa) is in Lane 2. Lanes 3-5 are washes. Lanes 6-8 correspond to elution of dPer-PAS-AB post overnight digestion with GST-tagged TEV protease. Lanes 9-10 are overnight elutions of undigested dPER-PAS-AB with reduced glutathione elution buffer. Molecular weight of dPER-PAS-AB is 34.7 kDa, GST 26 kDa and GST-dPer-PAS-AB 61.3 kDa.

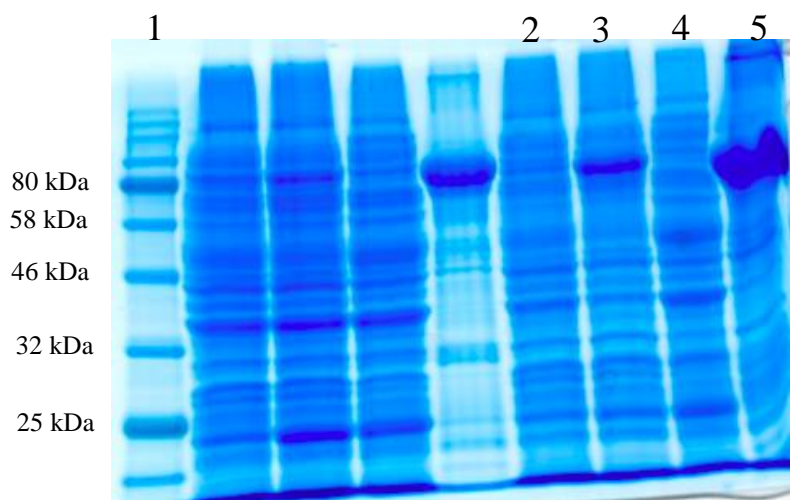


Figure 5-10 Coomassie blue stained 12% SDS-PAGE gel of the His-dPER-PAS-AB (M1-H599) 70.46 KDa fractions post refolding. Lane 1 corresponds to the Color Prestained Protein Standard marker, lanes 2 and 4 corresponds to the no induce of His-dPER-PAS-AB (in 20 °C and 37 °C respectively) from the Ni-NTA affinity chromatography. Lanes 3 and 5 corresponds to induce of His-dPER-PAS-AB (in 20 °C and 37 °C respectively) from the Ni-NTA affinity chromatography.

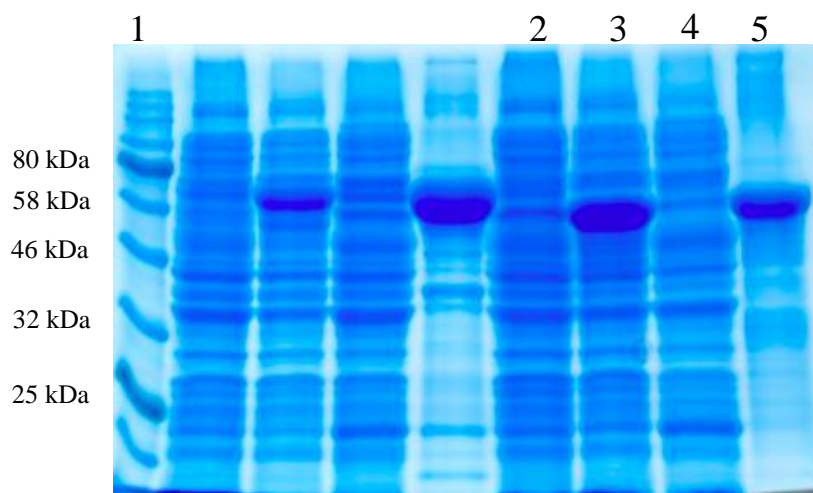


Figure 5-11 Coomassie blue stained 12% SDS-PAGE gel of the His-dPER-PAS-AB (E145-H599) 54.1 KDa fractions post refolding. Lane 1 corresponds to the Color Prestained Protein Standard marker, lanes 2 and 4 corresponds to the no induce of His-dPER-PAS-AB (in 20 °C and 37 °C respectively) from the Ni-NTA affinity chromatography. Lanes 3 and 5 corresponds to induce of His-dPER-PAS-AB (in 20 °C and 37 °C respectively) from the Ni-NTA affinity chromatography.

5.2.4. GST-dPER-PAS-AB

The GST tag was used for the expression and purification of the dPER-PAS-AB domain for the constructions in the three trials. Glutathione Sepharose 4 Fast Flow was used as an affinity resin to purification.

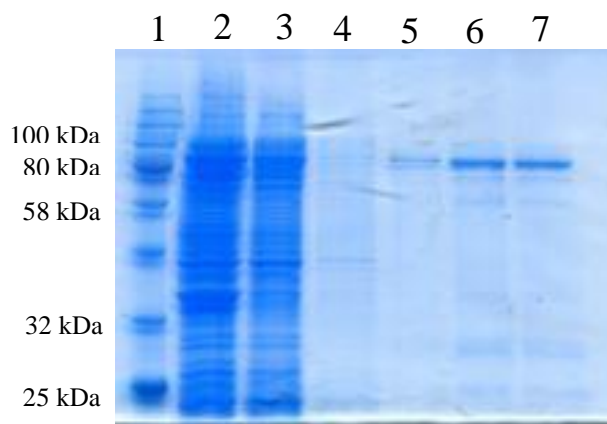


Figure 5-12 Coomassie blue stained 12% SDS-PAGE gel of the GST-dPER-PAS-AB (M1-H599) 95.16 kDa fractions post refolding. Lane 1 corresponds to the Color Prestained Protein Standard marker, lane 2 corresponds to the flow through of GST-dPER-PAS-AB from the Glutathione Sepharose 4 Fast Flow. Lane 3 corresponds to solution of washing the column and lanes 4-7 corresponds to the elution fraction of GST-dPER-PAS-AB from the Glutathione Sepharose 4 Fast Flow affinity chromatography.

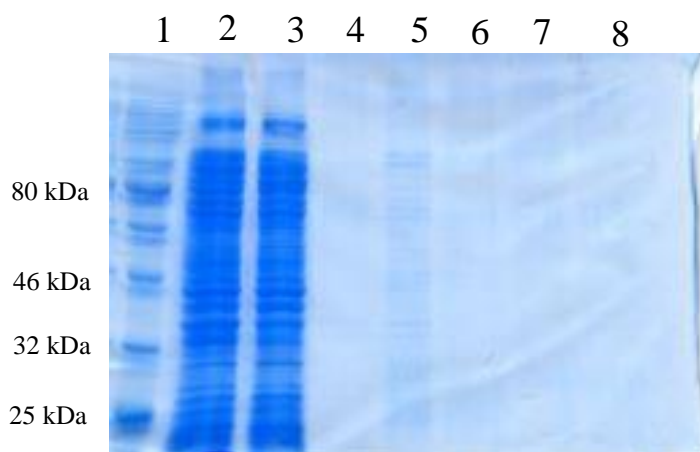


Figure 5-13 Coomassie blue stained 12% SDS-PAGE gel of the GST-dPER-PAS-AB (E145-H599) 78.8 kDa fractions post refolding. Lane 1 corresponds to the Color Prestained Protein Standard marker, lane 2 corresponds to the flow through of GST-dPER-PAS-AB from the Glutathione Sepharose 4 Fast Flow, and lane 3 corresponds to solution of washing the column and lanes 4-8 corresponds to the elution fraction of GST-dPER-PAS-AB from the Glutathione Sepharose 4 Fast Flow affinity chromatography.

5.3. Spectroscopic investigation of the interaction of dPER-PAS-AB with heme

To examine whether dPER-PAS-AB is a heme-binding protein and, if so, the number of bound heme molecules, we examined the spectral changes caused by adding heme. Figure 5-14 shows the difference absorption spectra obtained after addition of increasing amounts of heme to dPER-PAS-AB. dPER-PAS-AB binds heme and forms a complex with a Soret band at 423 nm which is characteristic for a predominantly six-coordinate low-spin iron [4-6] and Table (5-1).

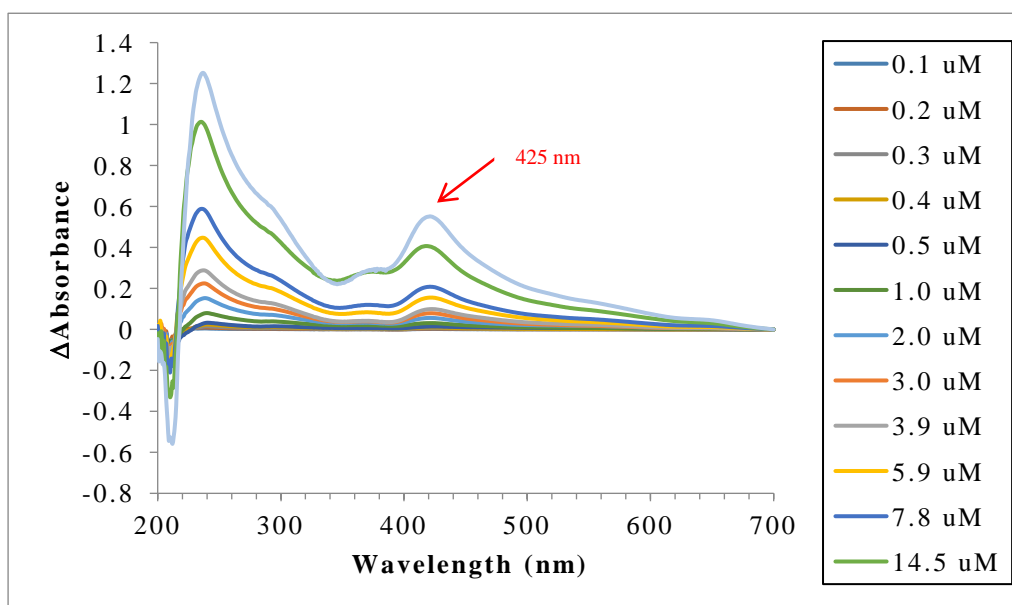


Figure 5-14 UV-visible absorption spectra of dPer_PasAB (11 μM) titrated with ferric heme (0.1, 0.2, 0.3, 0.4, 0.5, 1.0, 2.0, 3.0, 3.9, 5.9, 7.8, 14.5, 21.2 μM).

Spectral changes for the Fe (III) complex titration experiment (monitored at 423 nm) seem to be composed of two phases (Figure 5-15). Based on similar studies on mPER2 PAS-A [6], the first phase is suggested to reflect heme binding to the apo-protein and the second phase may represent nonspecific binding. From the spectral data, a 0.8:1 heme: protein complex is suggested to be formed. However, more spectral points are necessary to be collected in order to unequivocally establish a stoichiometry. In addition, we need to investigate different conditions due to a precipitation problem at higher heme concentrations.

Next, heme binding was examined under reduced conditions and in the presence of carbon monoxide. Figure (5-16) shows the absorption spectra of the ferric, ferrous and ferrous-CO bound forms of dPER-PAS-AB domain. The ferrous form displays a broad Soret band centred at 422 nm. Addition of carbon monoxide to the ferrous form results in the formation of a species with a Soret band at 420 nm. Inspection of the Q-bands region Figure (5-17) reveals the characteristic doublet with bands at 538 nm and 565 nm for a CO-bound complex. We have also recorded the absorption spectrum of the free-heme CO complex which exhibits a Soret band at 410 nm Figure (5-18).

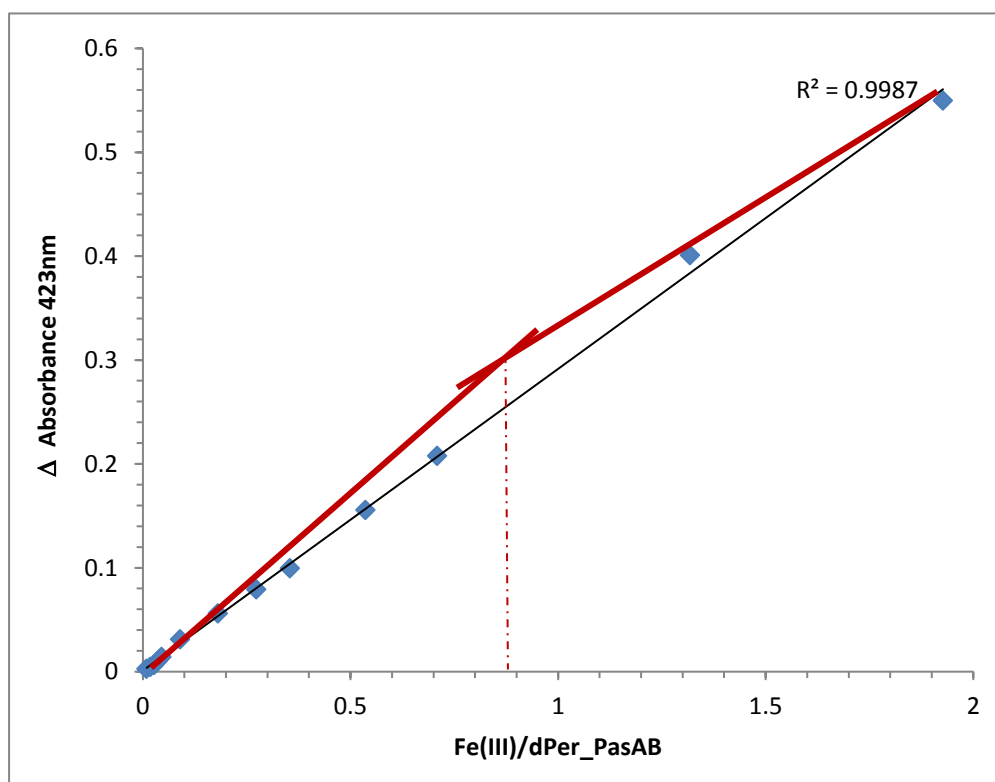


Figure 5-15 Intensity changes of spectra monitored at 423 nm for the ferric hemin complex of dPER-PAS-AB.

The differences in the absorption characteristics of the free heme-CO and the ferrous CO complex of dPER-PAS-AB further support our finding that dPER-PAS-AB is a heme binding protein.

Table 5-1 summarizes the absorption features of various heme binding PAS domains. The coordination structure of the ferric complex is similar to that of PAS domains where Cys thiolate and His imidazole are the heme axial ligands. The Soret absorption band at 422 nm for the ferrous complex is possibly derived from coordination with a non-thiolate residue as a five-coordinate thiolate-bound complex is known to display a Soret

absorption at around 410 nm. The absence of thiolate coordination for the reduced species is also confirmed by the absorption at 420 nm for the Fe (II)-CO complex. Heme-CO complexes with His as the trans ligand and a Soret at 420 nm have been reported for many Cys-ligated hemoproteins [7].

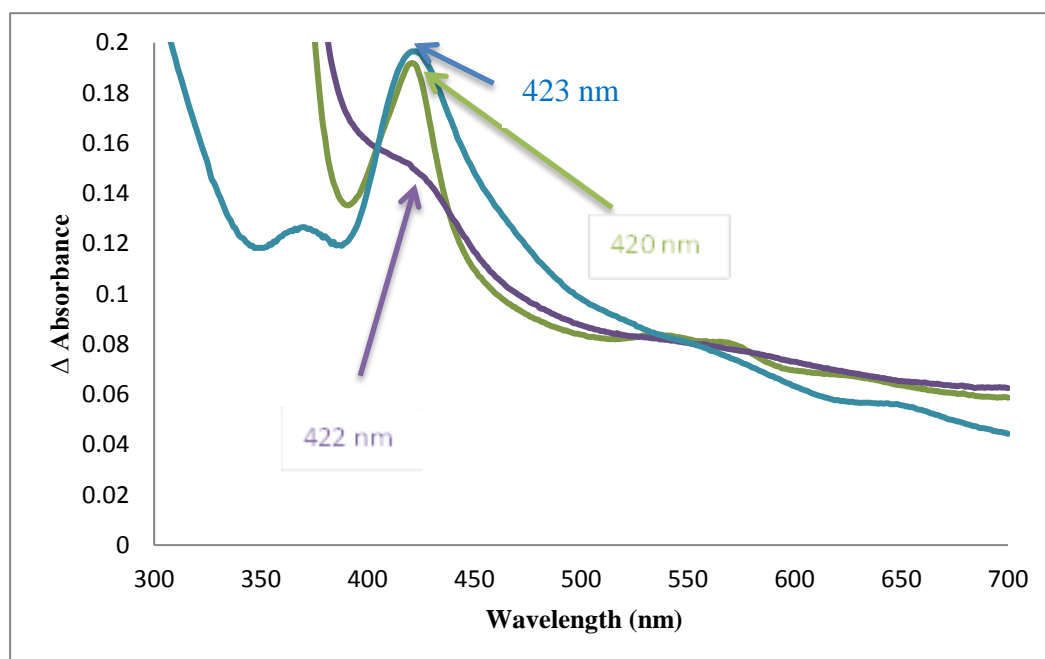


Figure 5-16 Absorption spectra of Fe(III) (blue line), Fe(II) purple line and Fe(II)-CO (green line) complexes (11 μ M) of dPER-PAS-AB in 20 mM Tris-HCl, 150 mM NaCl, 1 mM DTT pH 7.5.

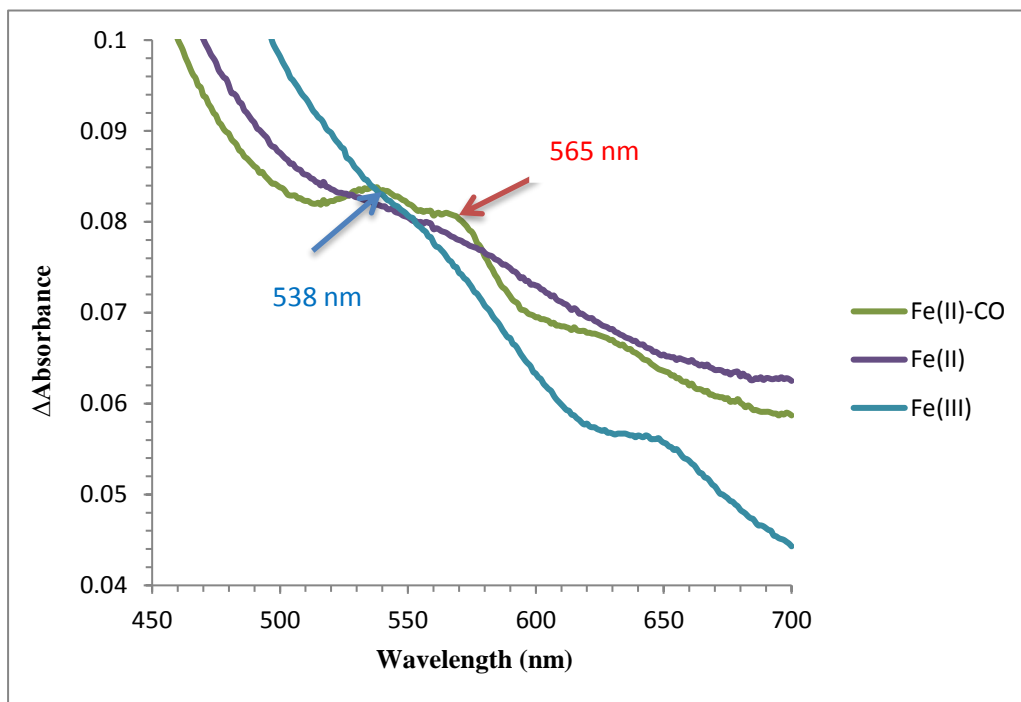


Figure 5-17 Enlargement of absorption spectra between 450–700 nm of Fe(III) (blue line), Fe(II) purple line and Fe(II)-CO (green line) complexes (11 μ M) of dPER-PAS-AB in 20 mM Tris-HCl, 150 mM NaCl, 1 mM DTT pH 7.5.

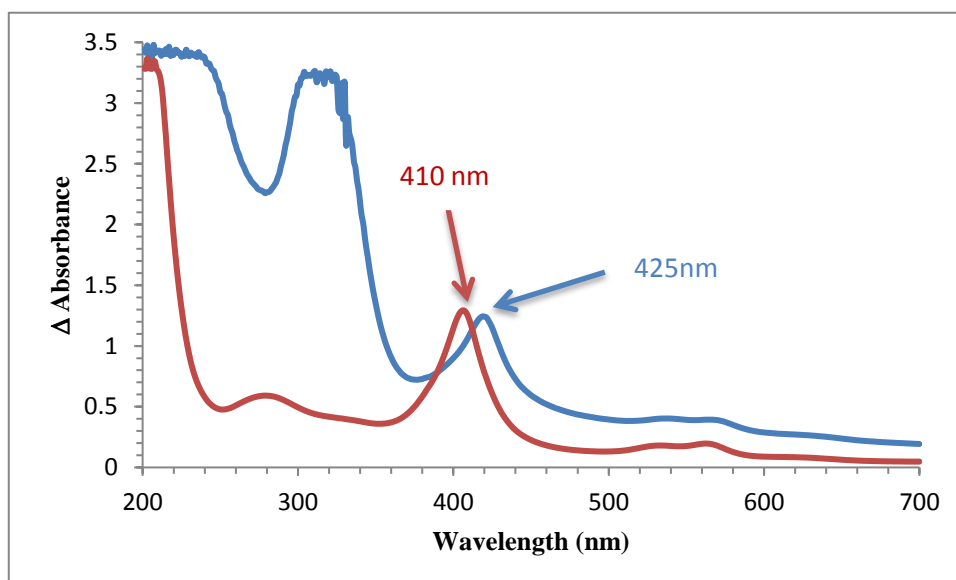


Figure 5-18 Absorption spectra of free heme Fe(II)-CO (red line) and Fe(II)-CO complexed with dPER-PAS-AB (blue line).

Table 5-2 Optical Absorption spectra of various heme binding PAS domains.

Protein	Fe(III)	Heme coordination	Fe(II)	Fe(II)-CO	Reference
dPER PAS AB	425	Cys?/His?	422		This work
mPER2 PASA	421	Cys/?	425	420	[6]
NPAS2 PAS A	412	Cys/His	423	420	[8]
NPAS2 PASB	419	His/?	424	420	[9]
bHLH PASA NPAS2	421	Cys/?	426	420	[10]

5.4. Electron Paramagnetic Resonance (EPR)

EPR Spectra of the heme Complex of dPER-PAS-B. Crystal field parameters of EPR spectra of Fe (III) low-spin complexes have been successfully used to identify axial ligands of the heme iron [11, 12].

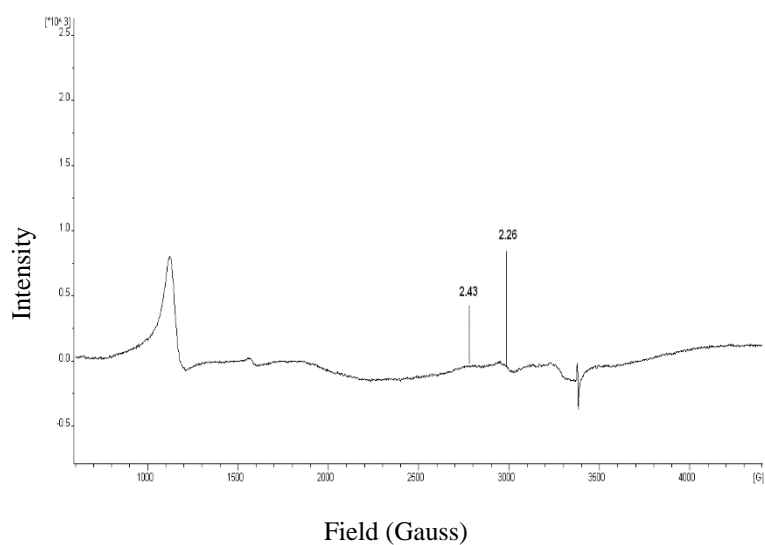


Figure 5-19 these g-factors of the LS ferric haem are consistent with a Cys ligand, see entry 16 in my Haem g-factors table on-line.

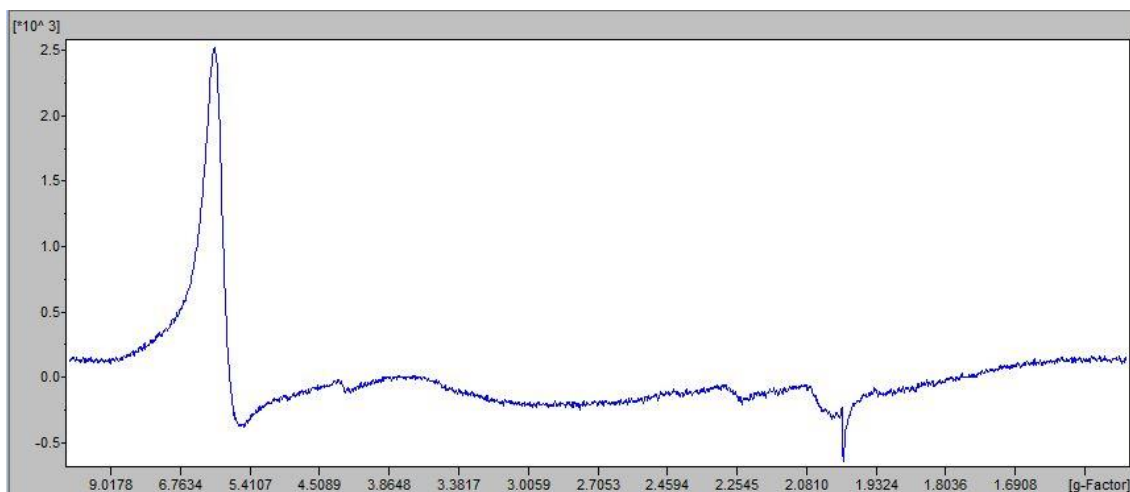


Figure 5-20 EPR spectra for dPER-PAS-AB 300 μM with 100 μM hemin in pH 7.5, HS haem signal, also a little bit of a low spin.

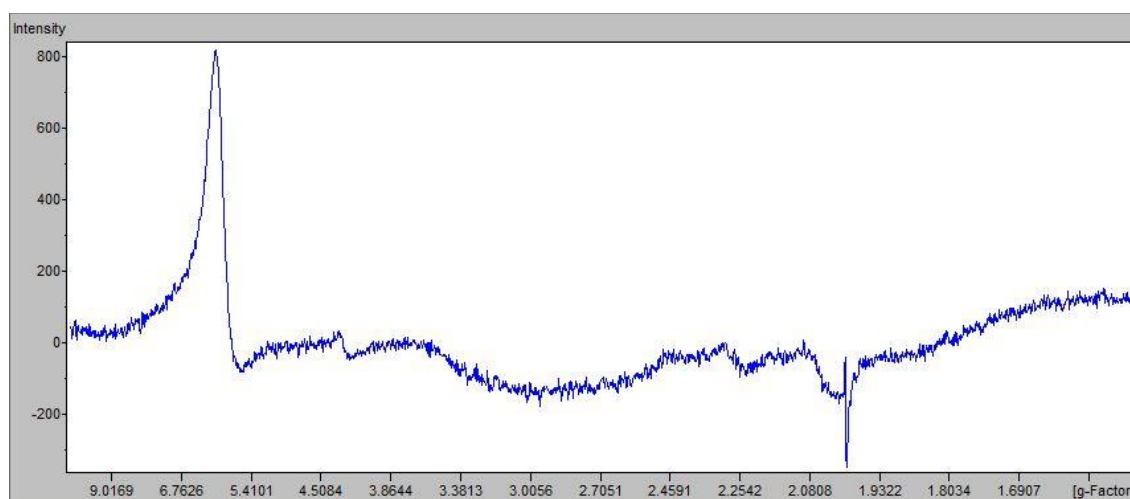


Figure 5-21 EPR spectra for dPER-PAS-AB 300 μM with 30 μM hemin in pH 7.5.

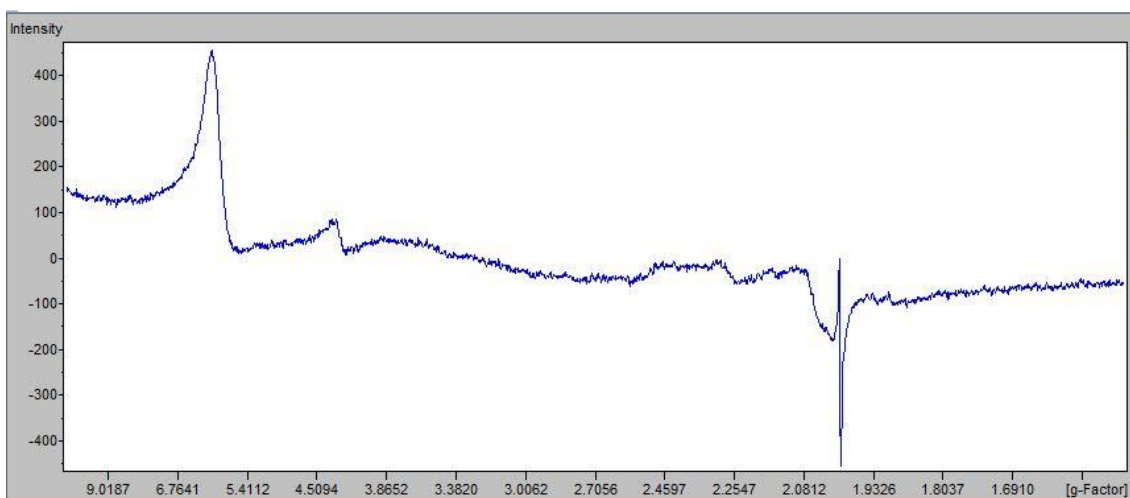


Figure 5-22 EPR spectra for dPER-PAS-AB 33 μM with 10 μM hemin in pH 7.5.

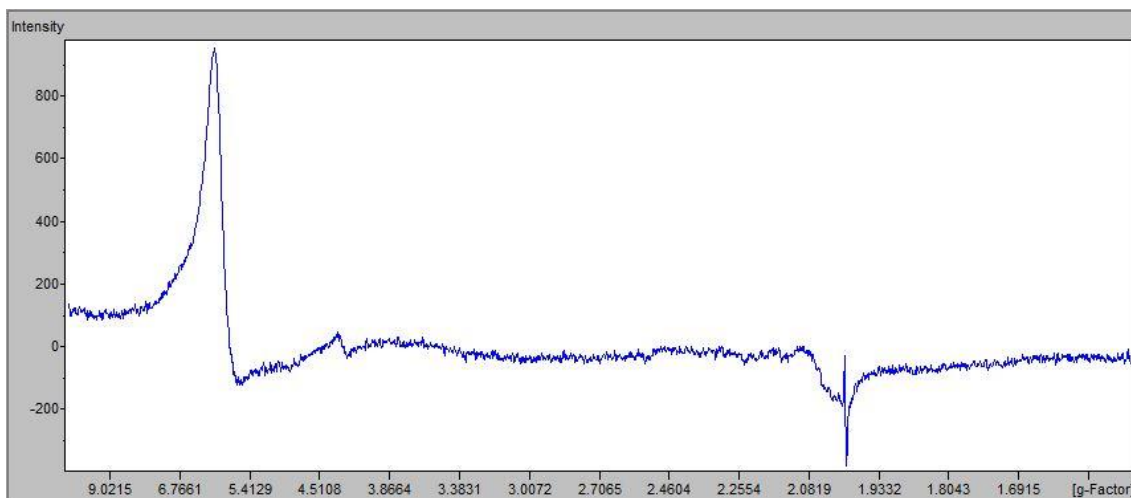


Figure 5-23 EPR spectra for dPER-PAS-AB α 100 μ M with 30 μ M hemin in pH 7.5, HS haem signal, also much lower of a low spin.

.

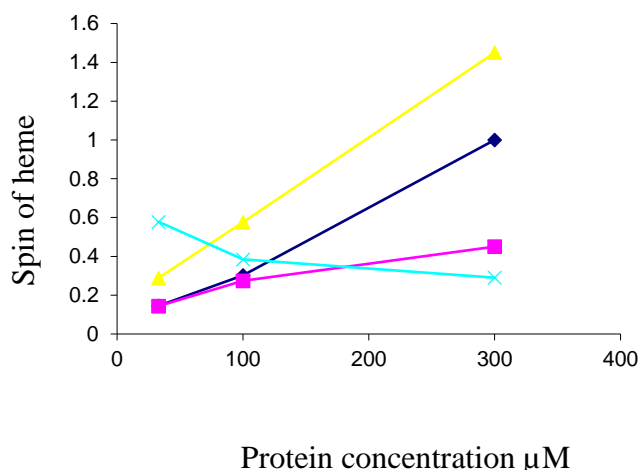


Figure 5-24 Protein concentration grows, at the same sub-stoichiometric concentration of hemin (1/3), the partial fraction of the HS increases. Low spin represent by pink colour. High spin represent by deep blue and the summation of high and low spin represent in yellow colour. Light blue represent per heme x20.

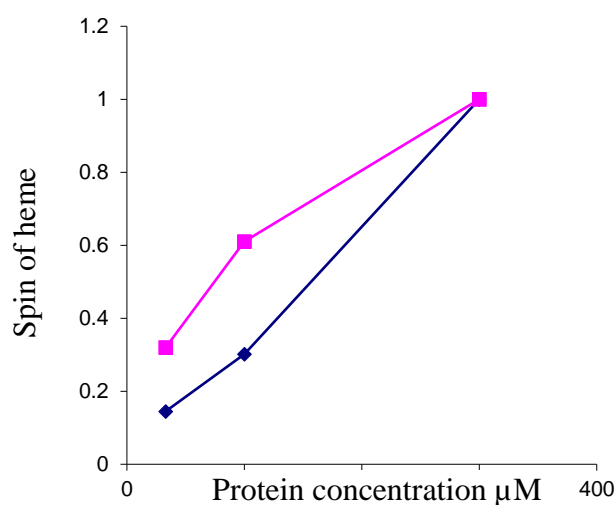


Figure 5-25 The difference between high span and low span. High spin represent by deep blue and low spin represent by pink colour.

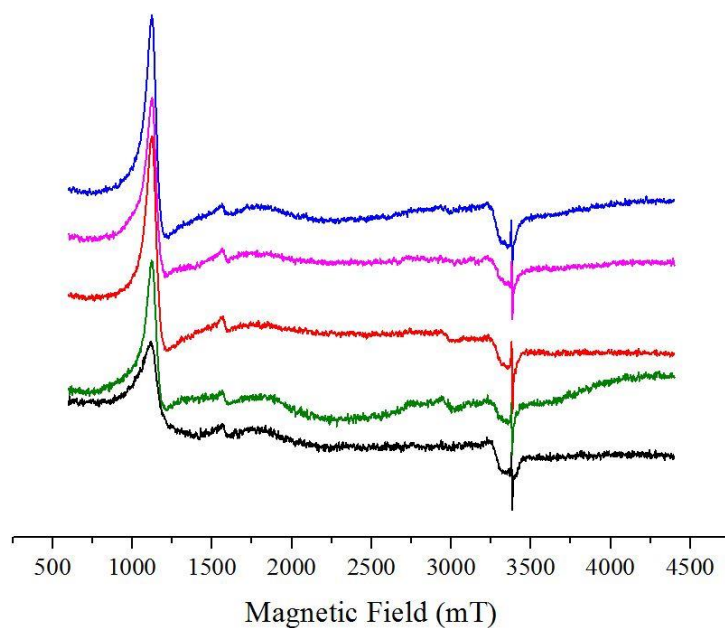


Figure 5-26 X-band (9.38 GHz) electron paramagnetic resonance spectrum of heme bound to wild types domains of dPER-PAS-A 100μM with heme 30 μM (red), dPER-PAS-B 100μM with heme 30 μM (blue), dPER-PAS-AB 100μM with heme 30 μM (pink), dPER-PAS-ABα 100μM with heme 30 μM (green) and heme 30μM (black).

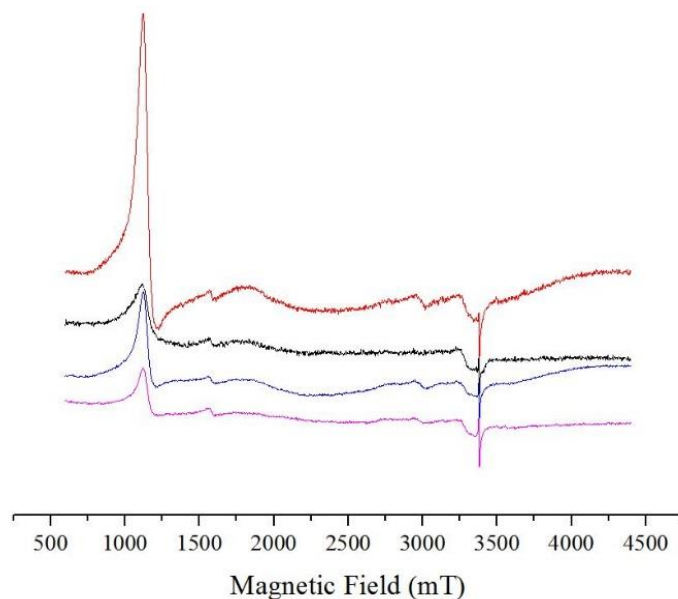


Figure 5-27 X-band (9.38 GHz) electron paramagnetic resonance spectrum of heme bound to wild type domain of dPER-PAS-AB α 300 μ M with heme 100 μ M (red), dPER-PAS- AB α 100 μ M with heme 30 μ M (blue), dPER-PAS- AB α 33 μ M with heme 30 μ M (pink) and heme 30 μ M (black).

Table 5-3 EPR g-values and heme ligands for ferric proteins and a model ferric heme complex.

No.	Protein	Wild-type and mutant domain	ligands	g-values	Ref.
1.	dPER	PAS-AB	Cys	2.44	this study
2.	dPER	PAS-AB α	Cys	2.43	this study
3.	hCLOCK	PAS-A	His/?	2.98/2.45	[13]
4.	hCLOCK	PAS-A H144A		2.45	[13]
5.	mPER2	PAS-A	Cys/?	2.44	[6]
6.		P450	Cys/H ₂ O	2.45	[14]
7.	hCLOCK	PAS-B		2.45	[13]

The EPR spectra of heme with dPER-PAS domains (See figures 5-26 and 5-27). And, the EPR spectrum of heme-bound dPER-PAS-AB was characteristic of a low-spin heme complex with g-values of 0.32, 0.61, and 1.00 (Figure 5-25) and high -spin 0.145, 0.302 and 1.000 (See chapter five, figure 5-25). The summation of high and low spin when use the 1/3 heme concentration were 0.289, 0.576 and 1.450 (Figure 5-24). Crystal field parameters of the dPER-PAS domains complex were located in the region for the axial ligands Cys/OH-[15].

To further investigate the mode of heme binding employed by domains (dPER-PAS-A, dPER-PAS-B, dPER-PAS-AB, and dPER-PAS-AB α), samples of ferric protein were did and analysed with the help of Prof. Dima Svistunenko at Biomedical EPR Facility (University of Essex) for X-band (9.38 GHz) electron paramagnetic resonance spectroscopy. Samples of wild type PAS domains were prepared Tris/HCl buffer at pH 7.5.

5.5. Circular Dichroism (CD)

Magnetic circular dichroism (CD spectra were obtained with a Chirascan plus CD spectrometer at room temperature) spectral band at the Soret region of heme-bound domain dPer-PAS-AB and dPer-PAS-AB α . There is a non-significant difference in optical absorption band between dPer-PAS-AB and dPer-PAS-AB band heme (Figure 5-28), dPer-PAS-AB and dPer-PAS-AB band heme (Figure 5-29).

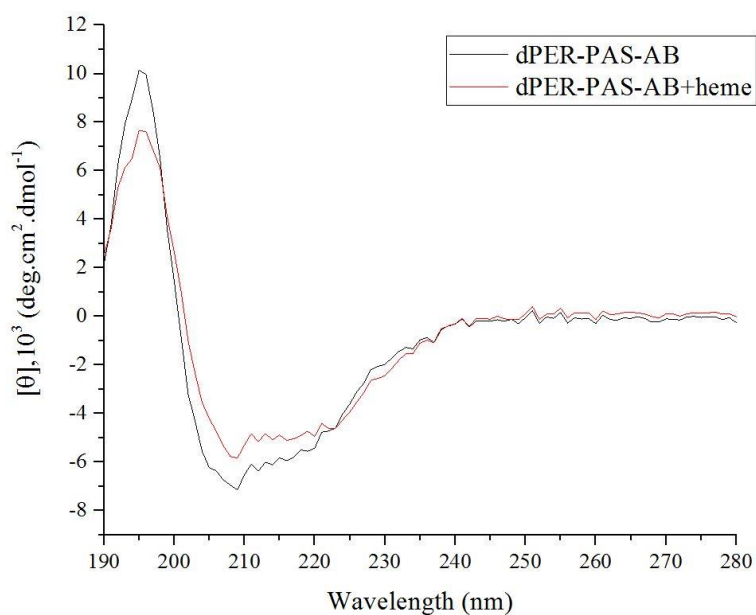


Figure 5-28 Circular dichroism spectra for dPER-PAS-AB (black) and dPER-PAS-AB binding with heme (red).

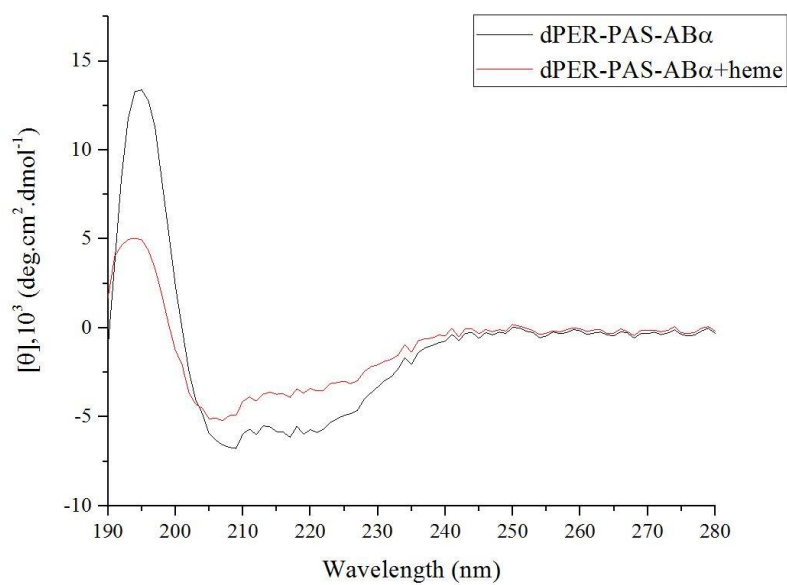


Figure 5-29 Circular dichroism spectra for dPER-PAS-AB α (black) and dPER-PAS-AB α binding with heme (red).

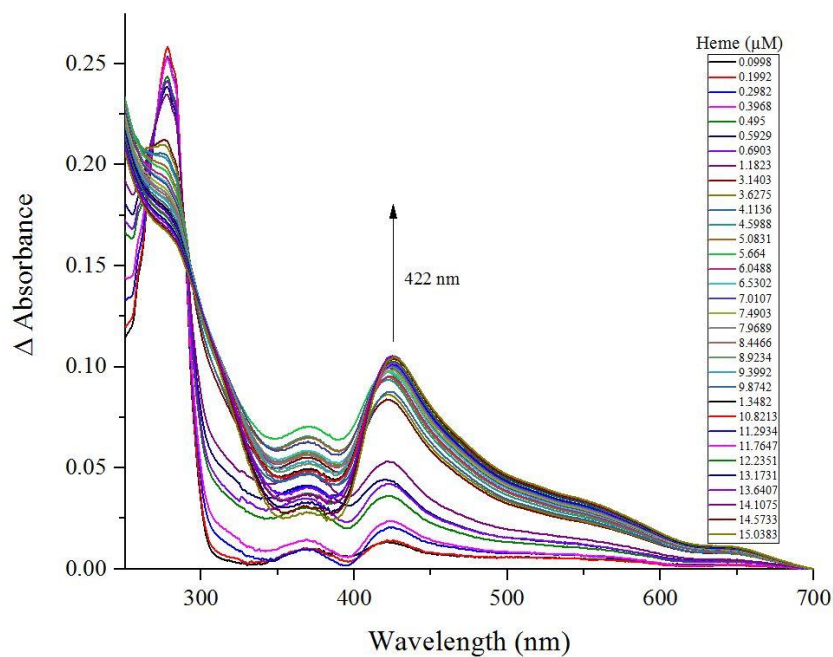


Figure 5-30 UV-visible difference spectrum of heme bound to dPER-PAS-AB. Legend shows the final concentration of heme used in the titration.

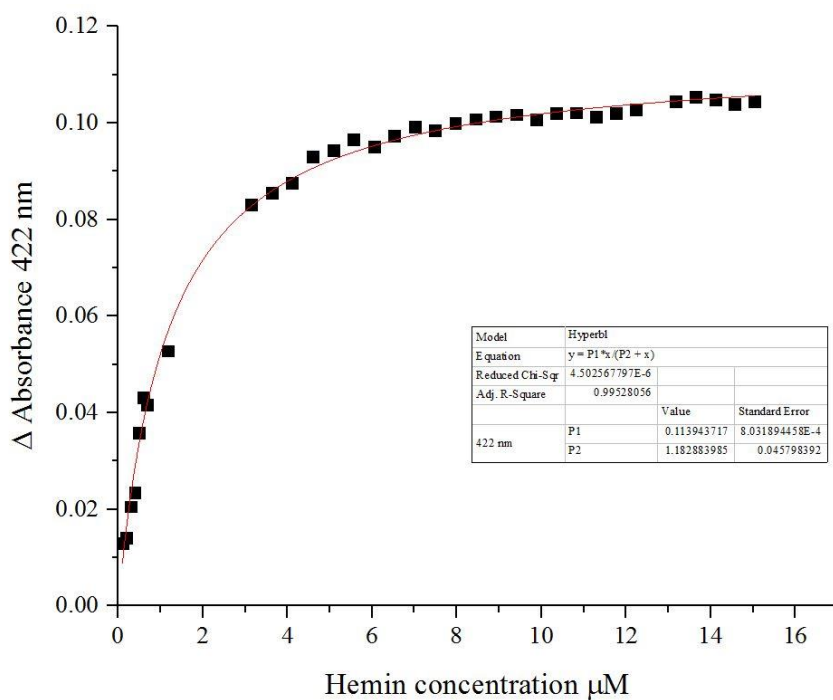


Figure 5-31 The relative absorbance changes to the difference spectrum at 422nm fit to a hyperbolic. $K_D = 1.182 \pm 0.0457$

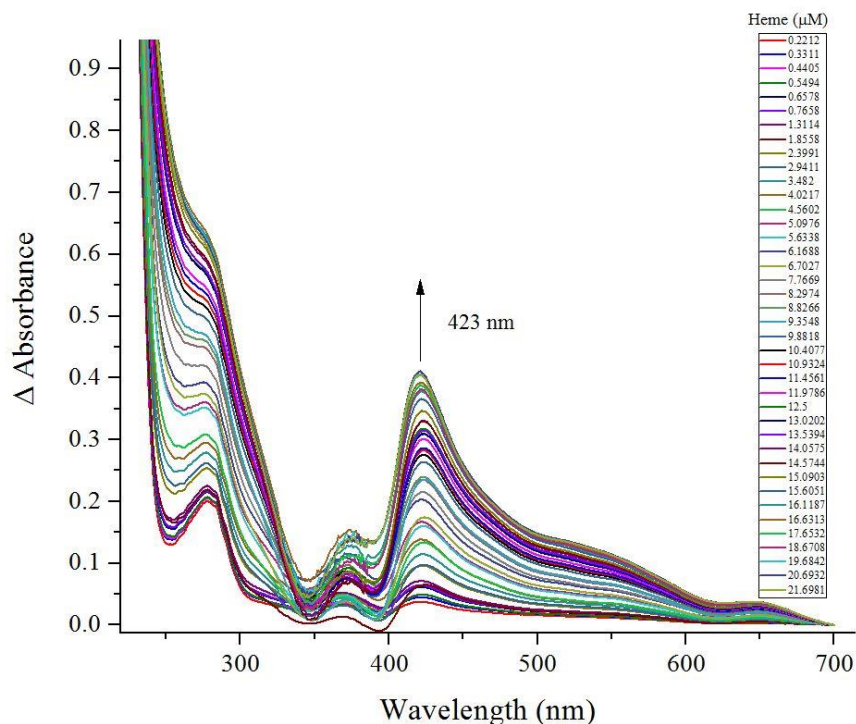


Figure 5-32 UV-visible difference spectrum of heme bound to dPER-PAS-AB α . Legend shows the final concentration of heme used in the titration.

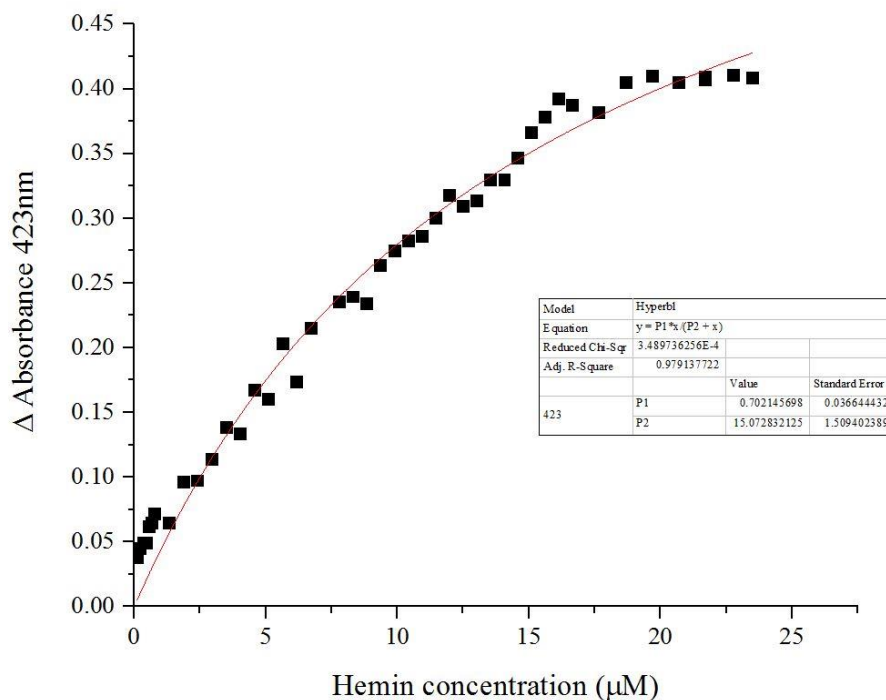


Figure 5-33 the relative absorbance changes to the difference spectrum at 423 nm fit to a hyperbolic. $K_D = 15.0728 \pm 1.509$

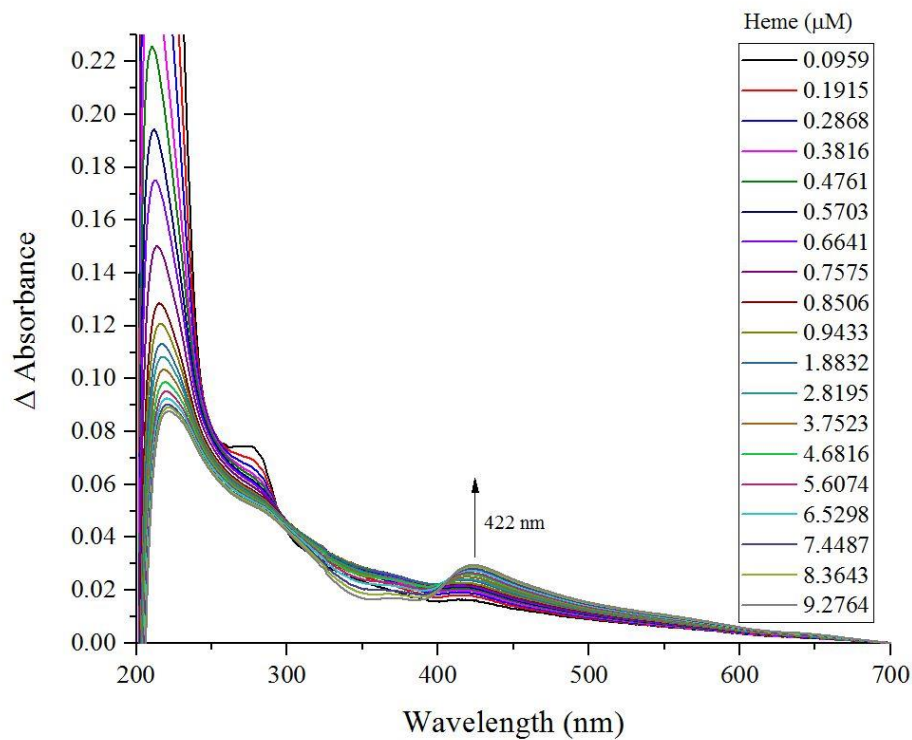


Figure 5-34 UV-visible difference spectrum of heme bound to mutant dPER-PAS-AB (Cys312Ala), Legend shows the final concentration of heme used in the titration.

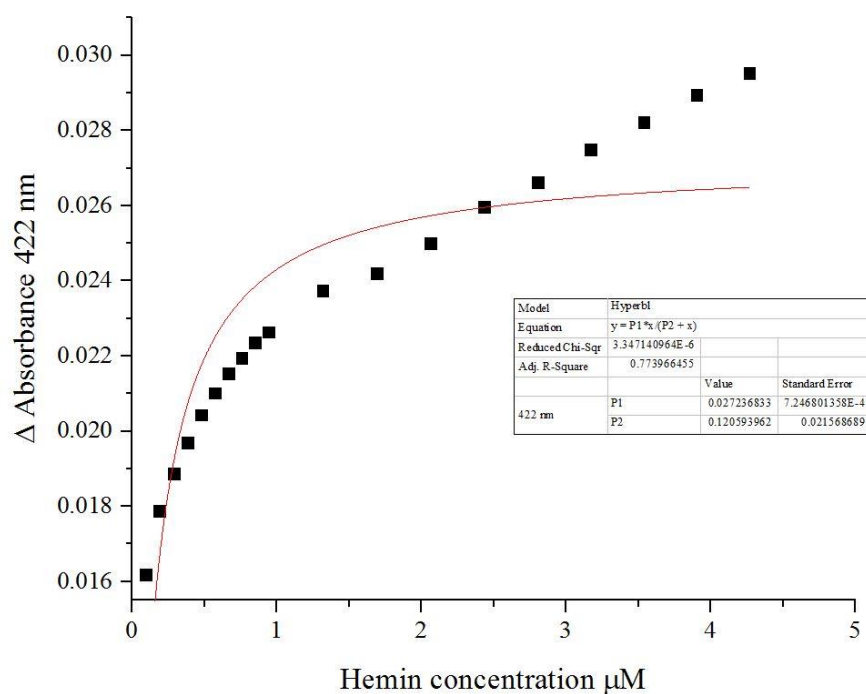


Figure 5-35 the relative absorbance changes to the difference spectrum for mutant Cys312Ala at 422nm fit to a hyperbolic. $K_D = 0.120 \pm 0.021 \mu$ M.

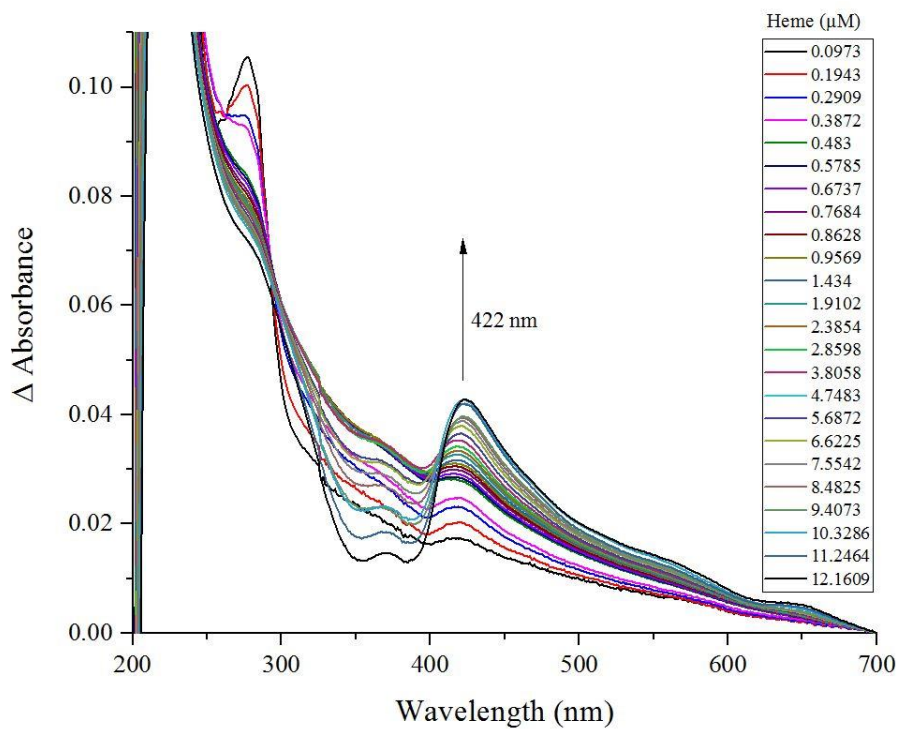


Figure 5-36 UV-visible difference spectrum of heme bound to mutant dPER-PAS-AB (Cys455Ala). Legend shows the final concentration of heme used in the titration.

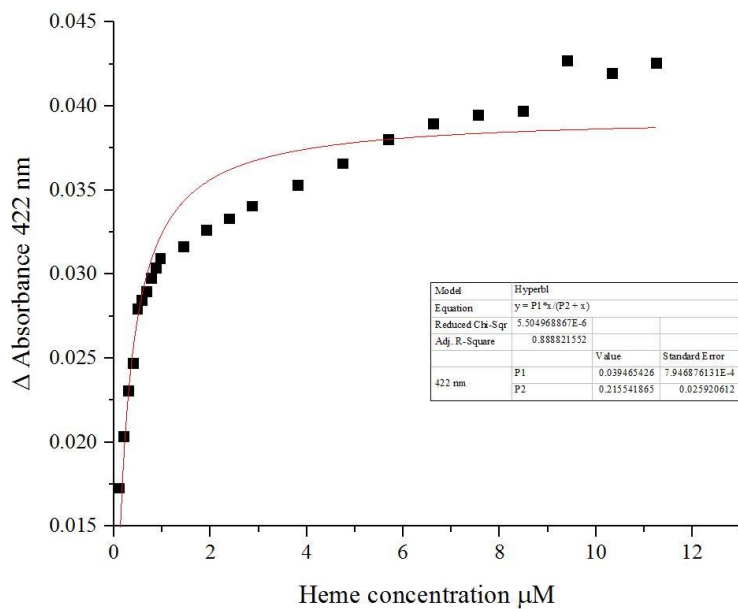


Figure 5-37 The relative absorbance changes to the difference spectrum for mutant Cys455Ala at 422nm fit to a hyperbolic. $K_D = 0.215 \pm 0.0259 \mu\text{M}$.

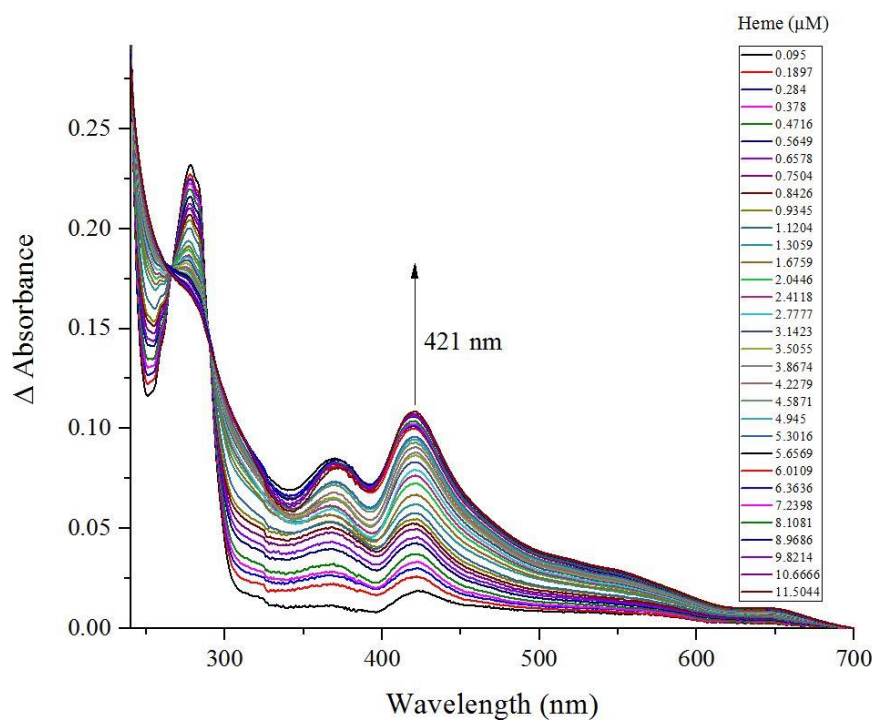


Figure 5-38 UV-visible difference spectrum of heme bound to mutant dPER-PAS-AB α (Cys312Ala). Legend shows the final concentration of heme used in the titration.

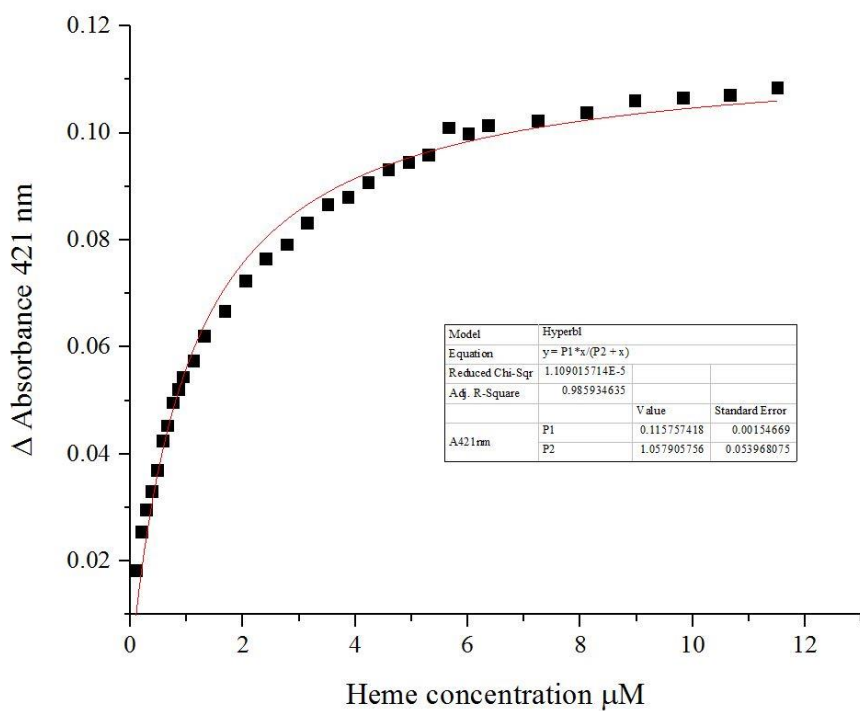


Figure 5-39 The relative absorbance changes to the difference spectrum for mutant Cys312Ala at 421nm fit to a hyperbolic. $K_D = 1.0579 \pm 0.0539 \mu\text{M}$.

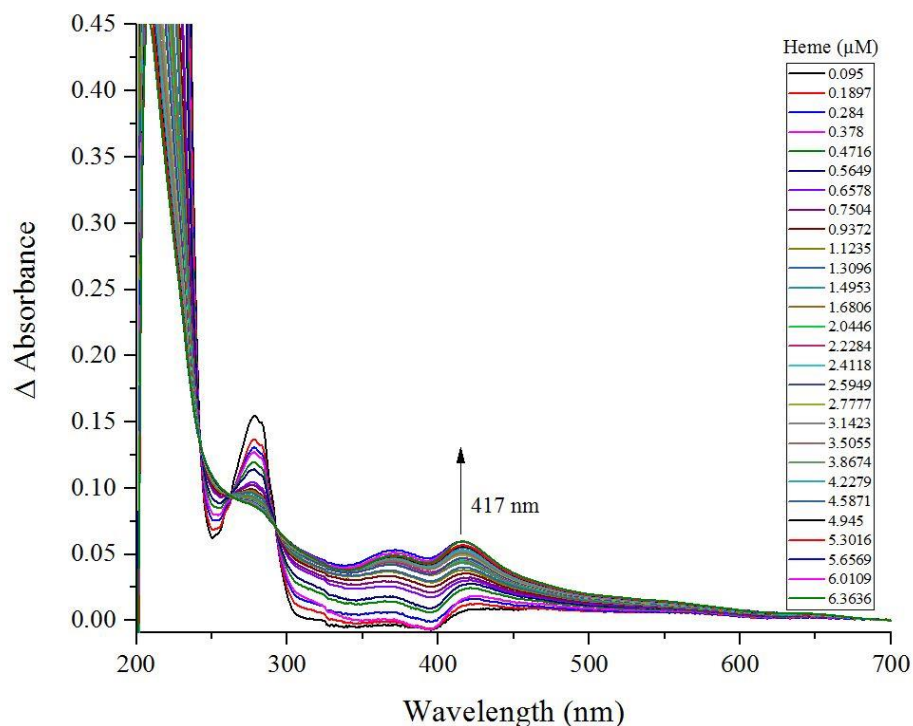


Figure 5-40 UV-visible difference spectrum of heme bound to mutant dPER-PAS-AB α (Cys455Ala). Legend shows the final concentration of heme used in the titration.

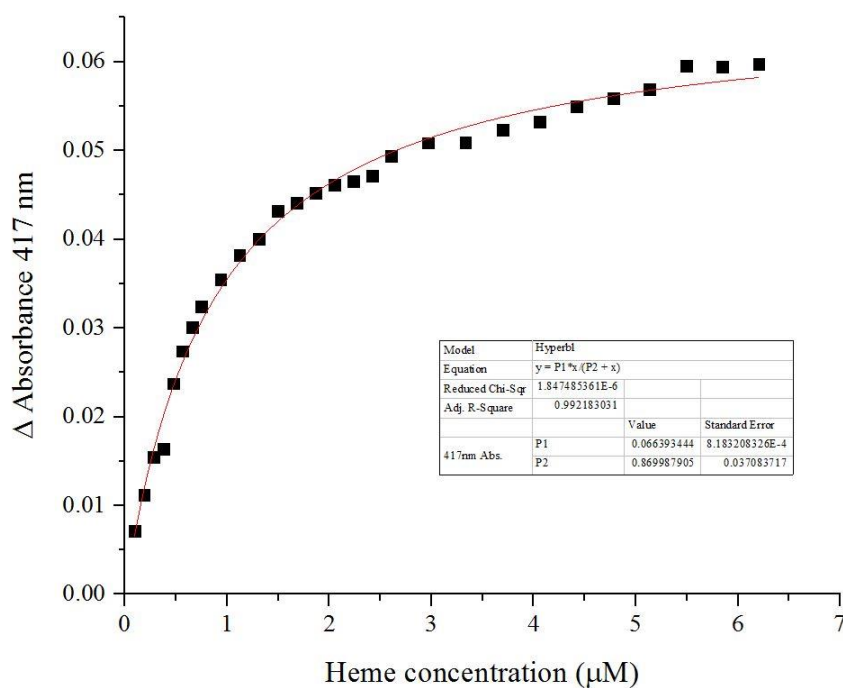


Figure 5-41 The relative absorbance changes to the difference spectrum for mutant Cys455Ala at 417nm fit to a hyperbolic. $K_D = 0.8699 \pm 0.037 \mu$ M.

5.6. Summary

dPER-PAS-AB, the biggest protein in this study, which included both domains dPER-PAS-A and dPER-PAS-B. dPER-PAS-AB makes a homodimer (see chapter one figure 1-2) that increases the stability of protein [16]. Constructs of different amino acid sequence length were made, and fused with different purification tags (GST, His, MBP and no tag in some constructs). The constructs were expressed using *E. coli* (*Rosetta* and *BL21DE3*) with the induction and temperature regulation. Depending on the type of tags, different types of resins were used (Ni-NTA, Glutathione sepharose 4 Fast flow and SP sepharose Fast flow). The tags were removed from dPER-PAS-AB to avoid the binding between heme and tag which would result in false positives.

According to the result of heme assay by using absorption spectrum, there is a binding between heme and dPER-PAS-AB and by using EPR, it was determined that the binding was between heme and Cysteine (there are eight molecules: Cys241, Cys242, Cys312, Cys369, Cys455, Cys467, Cys502 and Cys511). Cys312 and Cys455 were chosen to make mutations for dPER-PAS-AB and dPER-PAS-AB α . The result of spectrum absorption for mutant constructs were similar for wild types.

As a recommendation for the future work of this study, for the purpose of determining the type of binding (specific or unspecific) other mutations should be made (single or double) and studied using absorption spectroscopy.

5.7. References

1. Montelli, S; Mazzotta, G; Vanin, S; Caccin, L; Corrà, S; De Pittà, C; Boothroyd, C; Green, E W; Kyriacou, C P, and Costa, R, "Period and Timeless Mrna Splicing Profiles under Natural Conditions in *Drosophila Melanogaster*. Journal of Biological Rhythms", (2015) 30(3): 217-227.
2. Beaver, L M and Giebultowicz, J M, "Regulation of Copulation Duration by Period and Timeless in *Drosophila Melanogaster*. Current Biology", (2004) 14(16): 1492-1497.
3. Kotwica, J; Larson, M K; Bebas, P, and Giebultowicz, J M, "Developmental Profiles of Period and Doubletime in *Drosophila Melanogaster* Ovary. Journal of Insect Physiology", (2009) 55(5): 419-425.
4. Airola, M V; Du, J; Dawson, J H, and Crane, B R, "Heme Binding to the Mammalian Circadian Clock Protein Period 2 Is Nonspecific. Biochemistry", (2010) 49(20): 4327-4338.
5. Hayasaka, K; Kitanishi, K; Igarashi, J, and Shimizu, T, "Heme-Binding Characteristics of the Isolated Pas-B Domain of Mouse Per2, a Transcriptional Regulatory Factor Associated with Circadian Rhythms. Biochimica Et Biophysica Acta-Proteins and Proteomics", (2011) 1814(2): 326-333.
6. Kitanishi, K; Igarashi, J; Hayasaka, K; Hikage, N; Saiful, I; Yamauchi, S; Uchida, T; Ishimori, K, and Shimizu, T, "Heme-Binding Characteristics of the Isolated Pas-a Domain of Mouse Per2, a Transcriptional Regulatory Factor Associated with Circadian Rhythms. Biochemistry", (2008) 47(23): 6157-6168.
7. Shimizu, T, "Binding of Cysteine Thiolate to the Fe(Iii) Heme Complex Is Critical for the Function of Heme Sensor Proteins. Journal of Inorganic Biochemistry", (2012) 108: 171-177.
8. Uchida, T; Sato, E; Sato, A; Sagami, I; Shimizu, T, and Kitagawa, T, "Co-Dependent Activity-Controlling Mechanism of Heme-Containing Co-Sensor Protein, Neuronal Pas Domain Protein. Journal of Biological Chemistry", (2005) 280(22): 21358-21368.
9. Koudo, R; Kurokawa, H; Sato, E; Igarashi, J; Uchida, T; Sagami, I; Kitagawa, T, and Shimizu, T, "Spectroscopic Characterization of the Isolated Heme-Bound Pas-B Domain of Neuronal Pas Domain Protein 2 Associated with Circadian Rhythms. FEBS Journal", (2005) 272(16): 4153-4162.
10. Mukaiyama, Y; Uchida, T; Sato, E; Sasaki, A; Sato, Y; Igarashi, J; Kurokawa, H; Sagami, I; Kitagawa, T, and Shimizu, T, "Spectroscopic and DNA-Binding Characterization of the Isolated Heme-Bound Basic Helix-Loop-Helix-Pas-a Domain of Neuronal Pas Protein 2 (Npas2), a Transcription Activator Protein Associated with Circadian Rhythms. FEBS Journal", (2006) 273(11): 2528-2539.
11. Igarashi, J; Sato, A; Kitagawa, T; Yoshimura, T; Yamauchi, S; Sagami, I, and Shimizu, T, "Activation of Heme-Regulated Eukaryotic Initiation Factor 2 α Kinase by Nitric Oxide Is Induced by the Formation of a Five-Coordinate No-Heme Complex Optical Absorption, Electron Spin Resonance, and Resonance Raman Spectral Studies. Journal of Biological Chemistry", (2004) 279(16): 15752-15762.

12. Miksanova, M; Igarashi, J; Minami, M; Sagami, I; Yamauchi, S; Kurokawa, H, and Shimizu, T, "Characterization of Heme-Regulated Eif2 α Kinase: Roles of the N-Terminal Domain in the Oligomeric State, Heme Binding, Catalysis, and Inhibition. *Biochemistry*", (2006) 45(32): 9894-9905.
13. Efimov, I; Parkin, G; Millett, E S; Glenday, J; Chan, C K; Weedon, H; Randhawa, H; Basran, J, and Raven, E L, "A Simple Method for the Determination of Reduction Potentials in Heme Proteins. *FEBS Letters*", (2014) 588(5): 701-704.
14. Schünemann, V; Jung, C; Trautwein, A; Mandon, D, and Weiss, R, "Intermediates in the Reaction of Substrate-Free Cytochrome P450cam with Peroxy Acetic Acid. *FEBS Letters*", (2000) 479(3): 149-154.
15. Shimizu, T; Hikage, N; Kitanishi, K; Murase, M; Iizuka, A; Ishikawa, K; Ishitsuka, Y; Saiful, I; Yamauchi, S, and Tanaka, A. "Structure–Function Relationships of the Thiol-Coordinating Heme Proteins, Hri, Associated with Protein Synthesis, and Npas2, a Regulator of Circadian Rhythms". in *Proceedings of 15th International Conference on Cytochromes P450 Biochemistry, Biophysics and Functional Genomics, Bled, Slovenia, Monduzzi Editore International*. (Year) of Conference.31-38.
16. Yildiz, O; Doi, M; Yujnovsky, I; Cardone, L; Berndt, A; Hennig, S; Schulze, S; Urbanke, C; Sassone-Corsi, P, and Wolf, E, "Crystal Structure and Interactions of the Pas Repeat Region of the *Drosophila* Clock Protein Period. *Molecular Cell*", (2005) 17(1): 69-82.

Chapter Six
Thesis Summary
And
Future Work

6. Thesis Summary and Future Work

6.1. Thesis Summary

PAS is involved in the regulation of Circadian Rhythm for different species (animals or plant)[1, 2]. In *Drosophila*, there are two Period genes (*per1*, *per2*) and *timeless* (*tim*) plays an analogous role to the cryptochrome (*cry*) genes in mammalian cells [3, 4]. The transcription factors CLOCK (CLK) and CYCLE (CYC) activate the transcription of period (*per*) and *timeless* (*tim*) and other direct target genes during the day. At night, PER and TIM then enter the nucleus and inhibit their own transcription [5, 6]. A heterodimer formed by CLOCK (CLK) and CYCLE (CYC) binds to an E-box sequence and activates transcription to initiate clock function. PER and TIM proteins then accumulate, form a dimer, and move into the nucleus to bind CLK-CYC during the night, thereby inhibiting their transcriptional activity until PER and TIM are degraded early in the morning [7].

Heme is formed from a tetrapyrrole known as Protoporphyrin, containing an iron ion bond to the centre of the structure. Its full name is iron protoporphyrin and it is found in a number of metalloproteins called hemoproteins. Hemoproteins promote various biochemical events such as oxygen transport/storage, electron transfer, gas sensing, and enzymatic oxidation /oxygenation in biological systems [8]. Circadian rhythms are regulated by feedback loops at transcriptional/translational levels. Heme is critical in this process [9]. This research is attempt to find the binding between heme (hemin) with PER-PAS domains (A, B, and AB) for *Drosophila melanogaster*.

In this study, different lengths of constructs were produced for the dPER-PAS-A, dPER-PAS-B and dPER-PAS-AB domains three trials were made one for each construct. The constructs were designed according the sequence in PUBMed under the code (1WA9). The constructs were transformed into expression strains of *E. coli*. The strains used were *BL21 DE3* and Rosetta. Both strains express a T7 polymerase upon IPTG induction which allows for regulated, high levels of protein expression. The constructs conjugated with different tags (GST, MBP and His) by using different vectors (see Appendix) to make the purification easier. The result of some expressions were insoluble proteins which led to attempts at refolding. When starting to study the binding between protein and heme, and to avoid accidental binding between the heme and the tag, the tags were removed by

suitable TEV-tag. During the purification process the stability and amount of dPER-PAS-AB and dPER-PAS-AB α were more than dPER-PAS-A and dPER-PAS-B.

The dPER-PAS-A, dPER-PAS-B and dPER-PAS-AB domains examined in this thesis showed similar heme binding characteristics. Soret bands observed for all domains with UV-vis spectroscopy show that there is binding with heme. This Soret band around 424 nm, 422 nm, 422 and 423 nm for dPER-PAS-A, dPER-PAS-B, dPER-PAS-AB and dPER-PAS-AB α respectively. The K_D values for heme binding were 5.999 ± 0.719 , 4.86 ± 0.53 , 1.182 ± 0.0457 and 15.0728 ± 1.509 μ M for dPER-PAS-A, dPER-PAS-B, dPER-PAS-AB and dPER-PAS-AB α respectively, (See Chapters 3, 4 and 5 for more details). The values of K_D are divided into two groups, first with a high of K_D (for dPER-PAS-A and dPER-PAS-B) and second with a low of K_D (for dPER-PAS-AB and dPER-PAS-AB α). The Soret bands for wildtype domains were similar (422-424 nm). The K_D values, however, differ significantly. The K_D values showed stronger binding from the full length dPER-PAS-AB compared to just the single domains (dPER-PAS-A and dPER-PAS-B) but the weakest binding was with dPER-PAS-AB α (15.07 ± 1.51). The K_D value for mPER1-PAS domain homodimers is ($K_D = 0.15$ μ M) compared to mPER2 ($K_D = 1.34$ μ M) and mPER3 ($K_D = 1.72$ μ M) [10]. The K_D value for mPER2 is very near to the K_D value for dPER-PAS-AB in this study. The results of EPR determined that the binding was between heme and a Cysteine residue. The protein contains contain eight Cysteine molecules (C241, C242, C312, C369, C455, C467, C502 and C511). Four of these Cysteine molecules were replaced by Alanine residues to make four single mutants (C312, C369, C455 and C467).

Table 6-1 Wildtypes and Mutations, spectral absorption values and their respective values.

No.	Domain	Mutant	absorbance band		K_D (μ M)	
			Wildtype	Mutant	Wildtype	Mutant
1.	dPER-PAS-A	C369A	424 nm	422 nm	5.99 ± 0.72	0.65 ± 0.08
		C312A		424 nm		3.73 ± 0.33
2.	dPER-PAS-B	C455A	422 nm	421 nm	4.86 ± 0.53	0.49 ± 0.08
		C467A		422 nm		0.69 ± 0.05
3.	dPER-PAS-AB	C312A	422 nm	422 nm	1.18 ± 0.046	0.12 ± 0.02
		C455A		422 nm		0.22 ± 0.03
4.	dPER-PAS-AB α	C312A	423 nm	421 nm	15.07 ± 1.51	1.06 ± 0.05
		C455A		417 nm		0.87 ± 0.04

Cysteine mutations did not change the Soret band. Comparison between the values of K_D for the wildtype and the mutant type showed that there is a significant difference between them for all the domains. The binding between heme and domains for mutants were stronger. One explanation for this difference in binding could be due to the poor fitting of data points for figures (3-27), (4-20), (5-35) and (5-37) with the fitted curved resulting in inaccurate K_D values. The difference in the case of dPER-PAS-AB α is much greater than the rest of domains (see table 6-1).

For study and determined the nature of the binding between heme and wild type of domain and mutant domain, attempts were made to make crystals of the heme complex with domain or mutant domain by using the sitting drop technique (See figure 2-14). The same changes in spectral features were observed as with the mutant domain. Thus, heme binding to dPER-PAS can occur at multiple sites. In mouse, Cys215 is the axial ligand for the Fe (III) complex and Redox-dependent ligand switching from Cys to another amino acid occurs when the Fe (III) complex is reduced to the Fe (II) complex [11].

6.2. Future Work

Although there has been significant advances in the understanding of dPER-PAS domains in recent years, there's still a lot to learn. The following are crucial to our understanding of dPER-PAS and it's regulation by heme:

- Using spectrophotometry like UV-visible, Raman, EPR and CD to study the behaviour of more mutant dPER-PAS constructs (C241, C242, C312, C369, C455, C467, C502 and C511) through binding with heme. Single, double, triple and quadruple mutants may be required because the binding may move or change between Cysteine molecules depend on which molecule is available.
- Study the crystals formed in this study (see 2.2.13.1), by using x - rays to draw the molecule by using the drawing applications (e.g. PyMOL, WinCoot, PhenixCoot), to explain the differences in K_D values for wild type, which were higher than mutant dPER-PAS proteins.

6.3. References

1. Son, G H; Chung, S; Choe, H K; Kim, H-D; Baik, S-M; Lee, H; Lee, H-W; Choi, S; Sun, W, and Kim, H, "Adrenal Peripheral Clock Controls the Autonomous Circadian Rhythm of Glucocorticoid by Causing Rhythmic Steroid Production. *Proceedings of the National Academy of Sciences*", (2008) 105(52): 20970-20975.
2. Binder, M D; Hirokawa, N, and Windhorst, U, "Encyclopedia of Neuroscience. (2009)
3. Airola, M V; Du, J; Dawson, J H, and Crane, B R, "Heme Binding to the Mammalian Circadian Clock Protein Period 2 Is Nonspecific. *Biochemistry*", (2010) 49(20): 4327-4338.
4. Jaumouille, E; Machado Almeida, P; Stahli, P; Koch, R, and Nagoshi, E, "Transcriptional Regulation Via Nuclear Receptor Crosstalk Required for the *Drosophila* Circadian Clock. *Current biology : CB*", (2015) 25(11): 1502-1508.
5. Allada, R and Chung, B Y, "Circadian Organization of Behavior and Physiology in *Drosophila*", in *Annual Review of Physiology*. (2010). 605-624.
6. Doherty, C J and Kay, S A, "Circadian Control of Global Gene Expression Patterns. *Annual review of genetics*", (2010) 44: 419-444.
7. Kadener, S; Stoleru, D; McDonald, M; Nawathean, P, and Rosbash, M, "Clockwork Orange Is a Transcriptional Repressor and a New *Drosophila* Circadian Pacemaker Component. *Genes & development*", (2007) 21(13): 000-000.
8. Bertini, I and Sigel, A, "Handbook on Metalloproteins". (2001): CRC Press.
9. Kaasik, K and Lee, C C, "Reciprocal Regulation of Haem Biosynthesis and the Circadian Clock in Mammals. *Nature*", (2004) 430(6998): 467-471.
10. Hennig, S; Strauss, H M; Vanselow, K; Yildiz, O; Schulze, S; Arens, J; Kramer, A, and Wolf, E, "Structural and Functional Analyses of Pas Domain Interactions of the Clock Proteins *Drosophila* Period and Mouse Period2. *PLoS Biology*", (2009) 7(4): 836-853.
11. Kitanishi, K; Igarashi, J; Hayasaka, K; Hikage, N; Saiful, I; Yamauchi, S; Uchida, T; Ishimori, K, and Shimizu, T, "Heme-Binding Characteristics of the Isolated Pas-a Domain of Mouse Per2, a Transcriptional Regulatory Factor Associated with Circadian Rhythms. *Biochemistry*", (2008) 47(23): 6157-6168.

Appendix

7. Appendix

7.1. Mass spectrometry analysis

Protein bands from Coomassie stained SDS PAGE gels were excised and submitted to the Protein and Nucleic Acid Chemistry Laboratory of University of Leicester (PNACL) where they were analysed either by MALDI-ToF or LCMS/MS.

7.2. DNA quantification

DNA concentration was calculated by an Implen NanoPhotometer® that was operated according to the manufacturer's instructions.

7.3. Bacterial strains

Competent (*Escherichia coli* strain *BL21 (DE3)* cells (Novagen) used for protein expression. Rosetta (Novagen). This is a derivative of BL21 and contains codons rarely used in *E. coli* were kindly provided by Dr. Sofia Kapetanaki.

tRNAs for the codons AUA, AGG, AGA, CUA, CCC, GGA are supplied on a chloramphenicol resistant plasmid and is used for protein expression.

Top10 *E. coli* strain used to produce high copy numbers of constructs.

7.4. Preparation

A Class II microbiological safety cabinet BioMAT2 hood (MedicalAirTechnology) was utilized as sterilizing environment for transformation. Both the hood and the required working materials were carefully sterilised with 70% ethanol.

7.5. Buffers and Media

7.5.1. 2x YT media

(All types of media were autoclaved at 123°C for three hours prior to use) Solution of 16 g/L Casein Digest Peptone, 10 g/L Yeast Extract and 5 g/L Sodium Chloride. Made up to 1 L with distilled water. The solution was sterilized in an autoclave.

7.5.2.LB (Luria-Bertani) Agar

20 gm LB (Melford : 1% w/v tryptone, 1% w/v NaCl and 0.5% w/v yeast extract) media and 10 gm Agar made up to 1 L with distilled water. The solution was sterilized in an autoclave.

7.5.3. Sample loading buffer (SDS-PAGE)

Solution of 1 x Electrode running buffer (50 mM Tris-HCl pH 8.8, 0.5 % (v/v) bromophenol blue, 1 % SDS, 10 % (v/v) Glycerol and fresh addition before using of 100 mM DTT) . Made up to 10 mL with ddH₂O.

7.5.4. 10 x Running Gel Buffer

100 ml of Solution 10X (30 gm Tris, 144 gm Glycine and 10 gm SDS) Made up to 1 L with distilled water and adjustment at pH 8.3. Then, for use Running Gel Buffer diluted this solution 10 times by using ddH₂O.

7.5.5. Staining solution

Coomassie Brilliant Blue (CBB) G-250 the stain was used after running gel (8 % (w/v) of CBB G-250 and 0.3 % (v/v) of concentrated HCl). Stirring for 2-4 hrs. and stored in the dark place.

7.5.6. Buffers for Ni-NTA column

7.5.6.1. Regenerate Ni column

Ni-NTA column was washed by 5 times column volume by 500 mM EDTA (the throw out was collected in a separate bottle as Ni is very toxic to the environment and needs specialist waste disposal). Then, the column was washed by 20 column volume of water. Next, 3 column volumes of NiSO₄ 100 mM was loaded the column. Later, the column was washed by 10 times column volume of ddH₂O.

7.5.6.2. N1 buffer

25 mM Tris pH 7.5, 140 mM NaCl and 10 mM imidazole, (2 times of resin volume).

7.5.6.3. N2 buffer

25 mM Tris pH 7.5, 140 mM NaCl and 500 mM imidazole, adjusted pH to 7.5.

7.5.6.4. Dialysis buffer

50 mM NaCl, 20 mM Tris pH 7.5, 0.5 mM TCEP and 0.2 mM EDTA.

7.6. Gel Filtration

Gel filtration (size exclusion chromatography) was used to obtain a high purity protein by separating any impurities or other proteins that are not needed in the solution, and this insulation is according to the size of the different molecules in the solution. This is achieved by porous polymer beads consisting of agarose and dextrose, trapping smaller molecules and retaining them for a longer time compared to other molecules, which are too large to be trapped in the bead pores. The protein is pumped through the column at low pressure (~ 0.2 MPa) to protect the column media and the elution is detected via a UV-visible lamp.

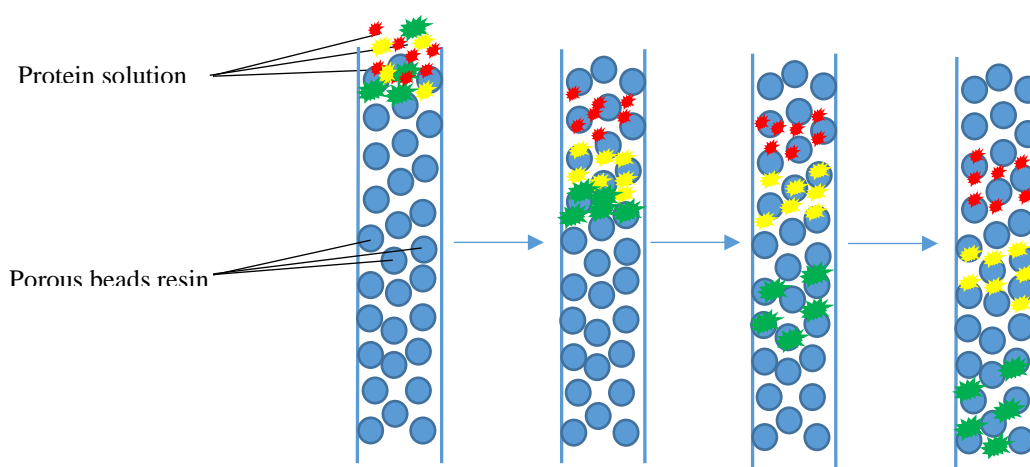


Figure 7-1 Schematic representation of size exclusion chromatography or gel filtration.

7.7. Size Exclusion Chromatography

In the final purification step the protein sample was concentrated and filtered through a $0.2 \mu\text{m}$ Supor® membrane to remove any insoluble particles. A size exclusion chromatography S200 column was mounted on a AKTA® purifier. The protein sample was then loaded onto the column and separated by elution. The components of the protein sample were then separated depending on their size. Larger molecules (such as the protein) are unable to enter the pores of the column matrix and therefore interact less with the column and thus are eluted faster. Elution is monitored by UV-vis absorbance at 280 nm. The fractions with the highest absorbance are collected and SDS-PAGE is run to measure the purity of the final protein sample.

7.8. Protocols

7.8.1. Competent cell preparation

Bacterial cells were spread on LB agar plate and incubated at 37°C for 12 hours. A single bacterial colony was used to inoculate LB broth (500 ml) and the media was incubated at 37°C until an OD 600 nm of 0.4 was achieved. The cultures were then placed on ice for 20 minutes before being spun down at 3000 g for 10 minutes. The rest of the cell preparation is carried out in a cold room set at (4 °C). The bacterial cell pellet was re-suspended in 60 ml CaCl₂ solution (0.1 mM) and incubated on ice for a further 30 minutes. The sample was spun down at 3000 g for 10 minutes. The bacterial cell pellet was re-suspended in 18 ml of CaCl₂ glycerol solution (0.1 mM; 15% Glycerol). 200 µl aliquots of competent cells were transferred into an Eppendorf and frozen in liquid nitrogen. Competent cells are stored at -80°C.

7.8.2. Cell Lysis

The lysis buffer is a solution of components designed to aid cell membrane disruption and prevent digestion of the target protein. It contains: lysozyme, deoxyribonuclease (DNase) and a protease inhibitor. Lysozyme is a glycoside hydrolase enzyme, it hydrolyses linkages in peptidoglycans (a polymer that forms the cell wall in *E. coli*) breaking down *E. coli* cell wall. DNase catalyses hydrolytic cleavage of phosphodiester linkages, breaking up the large bacterial DNA filaments into smaller fragments, lowering the viscosity of the solution and making it easier to remove the bacterial DNA. Protease inhibitors interact with the naturally occurring proteases found in *E. coli* preventing the proteolysis of the target protein during the purification procedure.

Sonication is a method of mechanically shearing the bacterial cell walls and DNA using sound energy in the ultra-sonic frequencies. It is carried out in short intervals under ice to prevent the sample from reaching a temperature high enough to denature the target protein or increase protease activity.

Once the cells were lysed the crude lysate was centrifuged and the resulting sample was split into the soluble fraction containing the proteins of interest and the insoluble fraction which was discarded.

7.8.3. Denaturing SDS-polyacrylamide gel electrophoresis (SDS-PAGE)

SDS-PAGE gels consisted of a 12% (w/v) polyacrylamide running gel and 4% (w/v) polyacrylamide stacking gel.

Protein samples (10 μ L) were prepared by mixing with an equal volume of sample buffer and boiling for 5 minutes. The samples were loaded onto the gel along with a pre-stained molecular marker (New England BioLabs). The gels were run at 180 V in running buffer until the dye-front reached the end of the gel. The gels were stained with Coomassie Blue staining solution for 60 minutes before being de-stained by soaking in de-staining solution overnight. First solution used for SDS-PAGE is Resolving gel (12% (w/v) acrylamide, 375 mM Tris-HCl with pH 8.8, 1 % (v/v) of SDS, 0.5 % (v/v) of APS and 0.1 % (v/v) TEMED). The second solution is Stacking gel (4 % (w/v) acrylamide, 125 mM Tris-HCl with pH 6.8, 1 % (v/v) of SDS, 0.5 % (v/v) of APS and 0.1 % (v/v) TEMED).

7.8.4. SDS-PAGE gel silver stain protocol

SDS-PAGE gel silver stain protocol was used to investigate the protein (dPER-PAS-A and dPER-PAS-B) after purification (in first and second trials). In silver staining, the gel is impregnated with soluble silver ions and developed by treatment with formaldehyde, which reduces silver ions to form an insoluble brown precipitate of metallic silver. This reduction is promoted by protein.

Gel was transfer to container containing fixative solution (100 ml of methanol, 100 ml of ddH₂O and 100 μ L of formaldehyde (Formaldehyde is added freshly each time using)) on a shaker for 2 hr under cover. Then, the gel was rinse with ddH₂O. After that, gel was kept on the shaker covered by DTT solution (10 μ g/ml) for 30-45 min. Gel was rinse once with 200 ml ddH₂O. Then, 200 ml ddH₂O with 1.5 ml of 20% silver nitrate was added and lifted on the shaker for 30-45 min. Next, gel was washed by 200 ml of ddH₂O to completely remove the silver nitrate. And immersed in 125 mL of 4% sodium carbonate with formaldehyde solution. 2.5 M of citric acid was added to gel to stop the reaction after the development of bands. Finally, gel was washed by ddH₂O.

In this work there isn't big difference between the protein (no tag-dPER-PAS-B) band in gel stained by silver or gel stained by Coomassie blue (Figure 7-2 and 7-3). Therefore, coomassie blue was used with all SDS- PAGE in this work because it is more safety and cheaper.

Table 7-1 Extinction coefficient and pI value for dPER-PAS-A, dPER-PAS-B and dPER-PAS-AB.

No.	Domain	pI value	Extinction Coefficient ϵ ($M^{-1} cm^{-1}$)	Classified trail
1.	dPER-PAS-A	5.23	8250	1 st trail
2.	dPER-PAS-B	8.43	17780	1 st trail
3.	dPER-PAS-AB	6.56	31150	1 st trail
4.	dPER-PAS-A	6.46	21620	2 nd Trail
5.	dPER-PAS-A	5.69	19060	2 nd Trail
6.	dPER-PAS-B	7.23	17780	2 nd Trail
7.	dPER-PAS-AB	6.84	39400	2 nd Trail
8.	dPER-PAS-AB	6.66	36840	2 nd Trail
9.	dPER-PAS-A	8.48	12090	3 rd trail
10.	dPER-PAS-B	8.9	17780	3 rd trail
11.	dPER-PAS-AB	8.69	31150	3 rd trail
12.	dPER-PAS-B α	7.23	17780	3 rd trail
13.	dPER-PAS-AB α	7.68	31150	3 rd trail

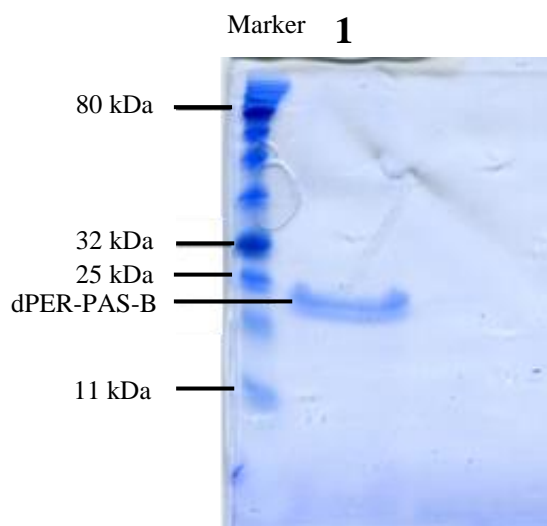


Figure 7-2 SDS-PAGE no tag-dPER-PAS-B colored by Coomassie blue stain. M: protein marker 1: dPER-PAS-B before refolding, 2: dPER-PAS-B after refolding, 3: flow through of dPER-PAS-B, 4: wash, 5: first fraction eluted by 100 mM of NaCl and 20 mM of Tris pH= 7.5, second fraction eluted by 200 mM of NaCl and 20 mM of Tris pH= 7.5, third fraction eluted by 300 mM of NaCl and 20 mM of Tris pH= 7.5, Fourth fraction eluted by 500 mM of NaCl and 20 mM of Tris pH= 7.5, Fifth fraction eluted by 1 M of NaCl and 20 mM of Tris pH= 7.5.

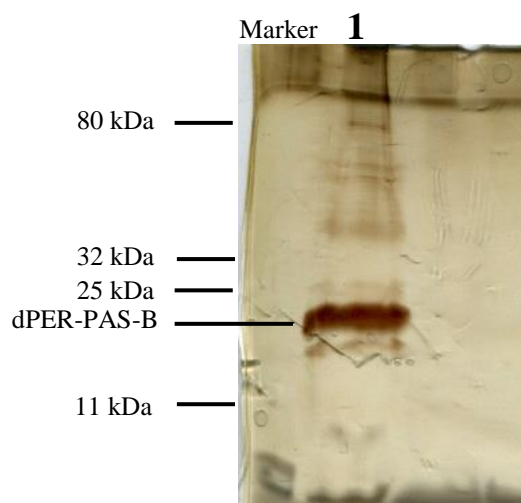


Figure 7-3 SDS-PAGE no tag-dPER-PAS-B colored by silver stain. M: protein marker 1: dPER-PAS-B before refolding, 2: dPER-PAS-B after refolding, 3: flow through of dPER-PAS-B, 4: wash, 5: first fraction eluted by 100 mM of NaCl and 20 mM of Tris pH= 7.5, second fraction eluted by 200 mM of NaCl and 20 mM of Tris pH= 7.5, third fraction eluted by 300 mM of NaCl and 20 mM of Tris pH= 7.5, Fourth fraction eluted by 500 mM of NaCl and 20 mM of Tris pH= 7.5, Fifth fraction eluted by 1 M of NaCl and 20 mM of Tris pH= 7.5.

7.8.5. Tag Cleavage

After the SDS-PAGE gel has shown the eluted fractions to be sufficiently pure, TEV protease was added. The sample was then loaded into a dialysis membrane and stored in dialysis buffer in a cold room overnight. The TEV protease has high sequence specificity; it is only able to bind the TEV protease binding site on the protein and therefore, directed cleavage will remove the tag should be capital H and leave the rest of the protein intact. It is important to cleave the tag because of the possibility of being able to bind to the heme iron and hence interfere with our heme binding studies. The protein was then separated from the cleaved tag by running another Ni-NTA column or GST column or any column was used according the tag's type. After approximately sixteen hours, the protein solution was removed from the membrane and buffer exchanged to remove any trace amounts of EDTA and DTT which can displace/reduce the nickel column respectively. Successful cleavage and removal of the tag was determined by assessment of the size of the protein with SDS-PAGE.

7.8.6. Measure of Protein Concentration

7.8.6.1. Bio-Rad Protein assay day reagent concentrate

One of the different ways to measure protein concentration was measured using a Bio-Rad Protein assay day reagent concentrate on Cat. #500-0006 Bio-Rad® UV/Vis spectrometer. 2 µL of protein sample was mixed with 1 ml of Bio-Rad (which diluted 1 to 5) dye that contains Coomassie Brilliant Blue G-250™ in the tubes vortexed and incubated at room temperature for 30 minutes. The samples were then transferred to plastic cuvettes. And the change in absorbance is recorded at 595 nm. The reading of spectrometer multiply by 17 and the result would be the concentration of protein in mg per ml. This way more convenient for solution with low concentration of protein because in high concentration the color of mixture (Bio-rad pigment with protein) will be deep and maybe give wrong reading. The Coomassie Brilliant Blue G-250™ dye is in equilibrium between red and blue forms. The change in absorbance is due to the shift in the red/blue dye equilibrium as a result of protein binding to the blue form of the dye.

7.9. Vectors

7.9.1. pLEICS-07

Amino acid tag: N-terminal 6 x His-tag, S-tag and then a TEV protease cleavage site.

Antibiotic resistance: Kanamycin.

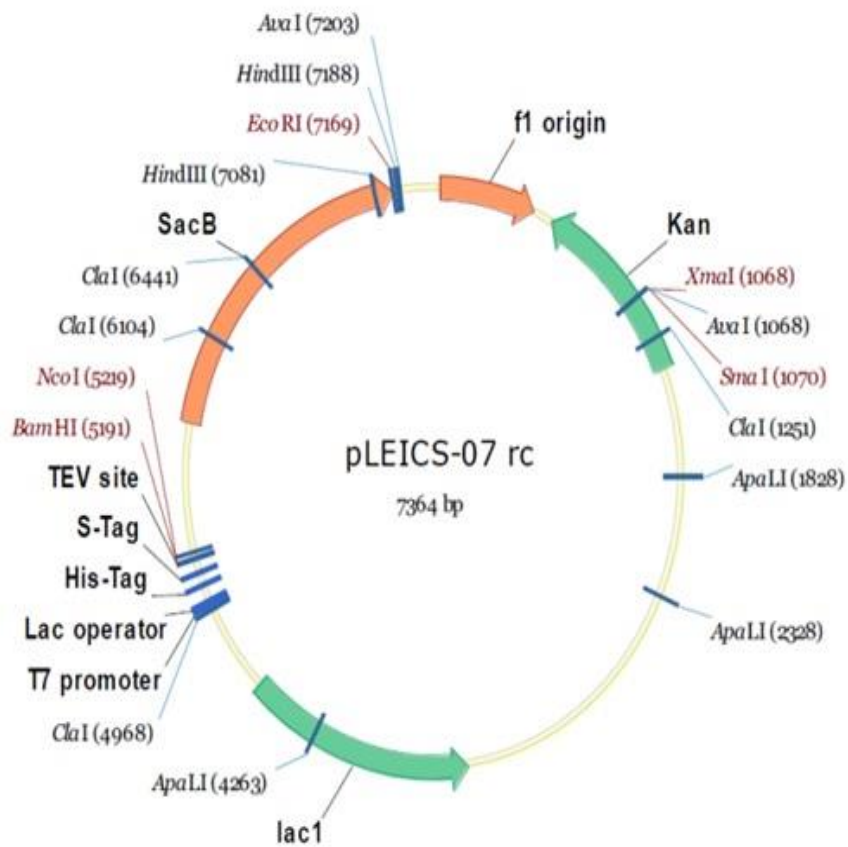


Figure 7-4 Plasmid map of the pLEICS-07 expression vector.

7.9.2. pLEICS-14

Amino acid tag: N-terminal GST-tag, a TEV protease cleavage site.

Antibiotic resistance: Ampicillin.

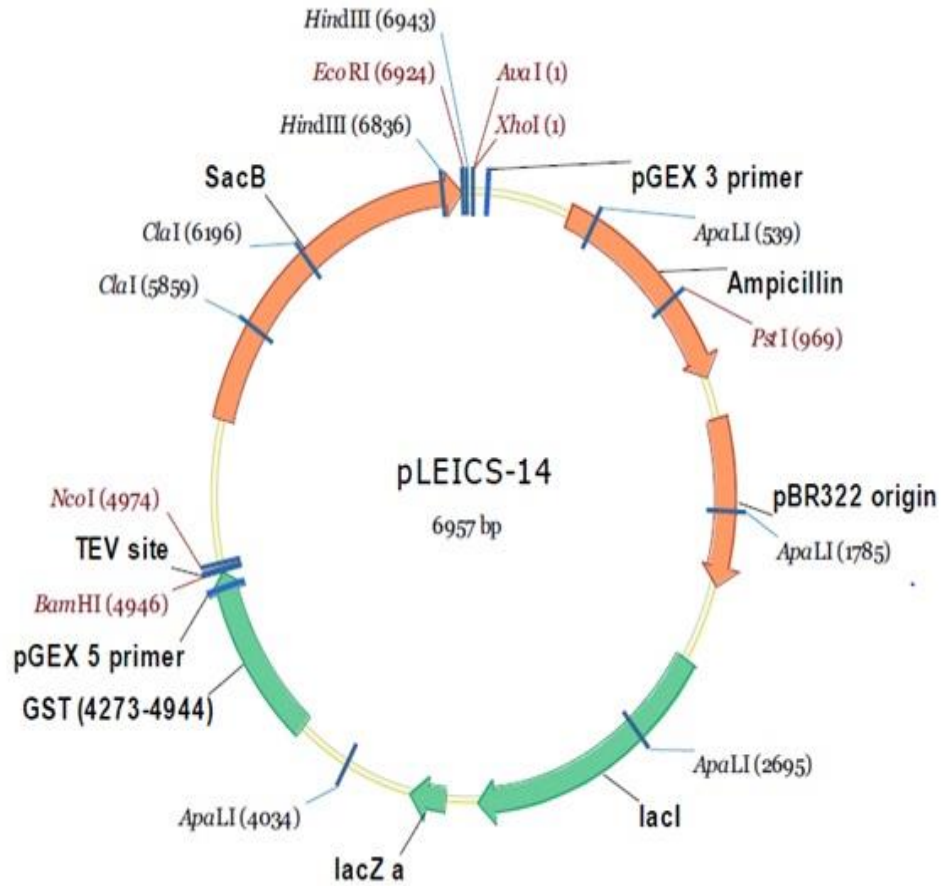


Figure 7-5 Plasmid map of the pLEICS-14 expression vector.

7.9.3.pLEICS-05

Amino acid tag: N-terminal 6 x His-tag.

Antibiotic resistance: Ampicillin.

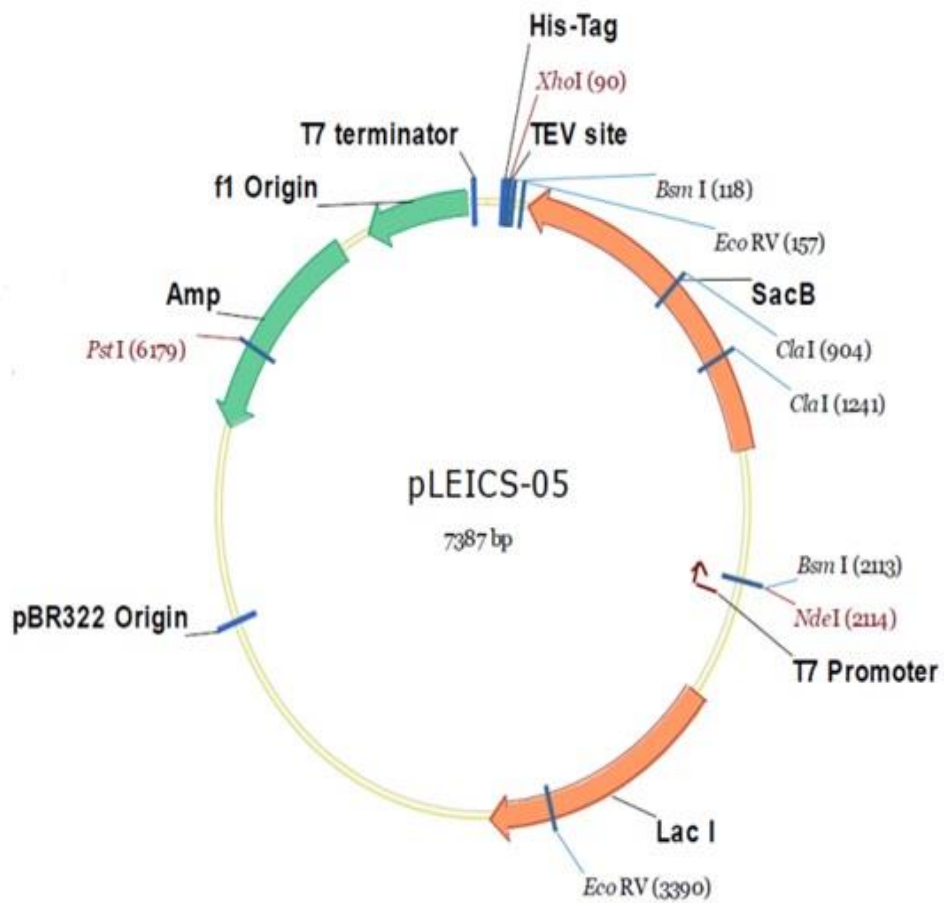


Figure 7-6 Plasmid map of the pLEIS-5 expression vector.

7.9.4.pLEICS-10

Amino acid tag: N-terminal MBP-tag.

Antibiotic resistance: Ampicillin.

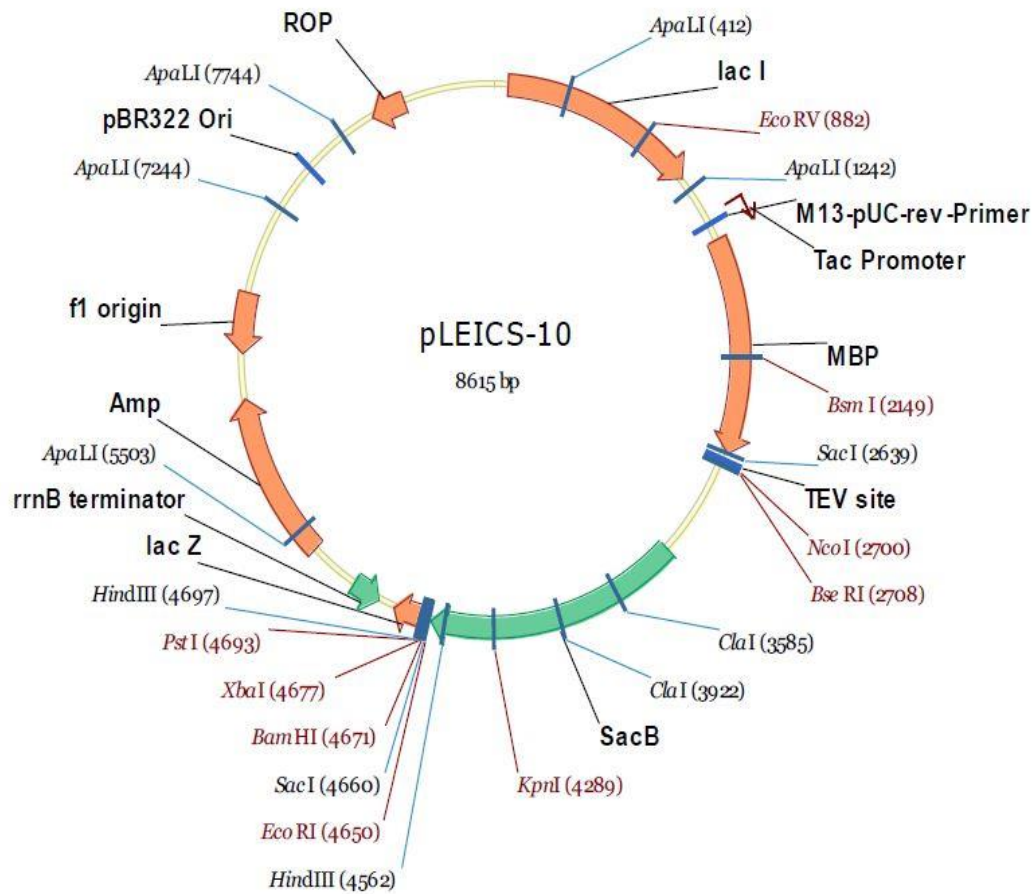


Figure 7-7 Plasmid map of the pLEICS-10 expression vector.

7.9.5.pLEICS-92

Amino acid tag: N-terminal GST-tag, a TEV protease cleavage site.

Antibiotic resistance: Ampicillin.

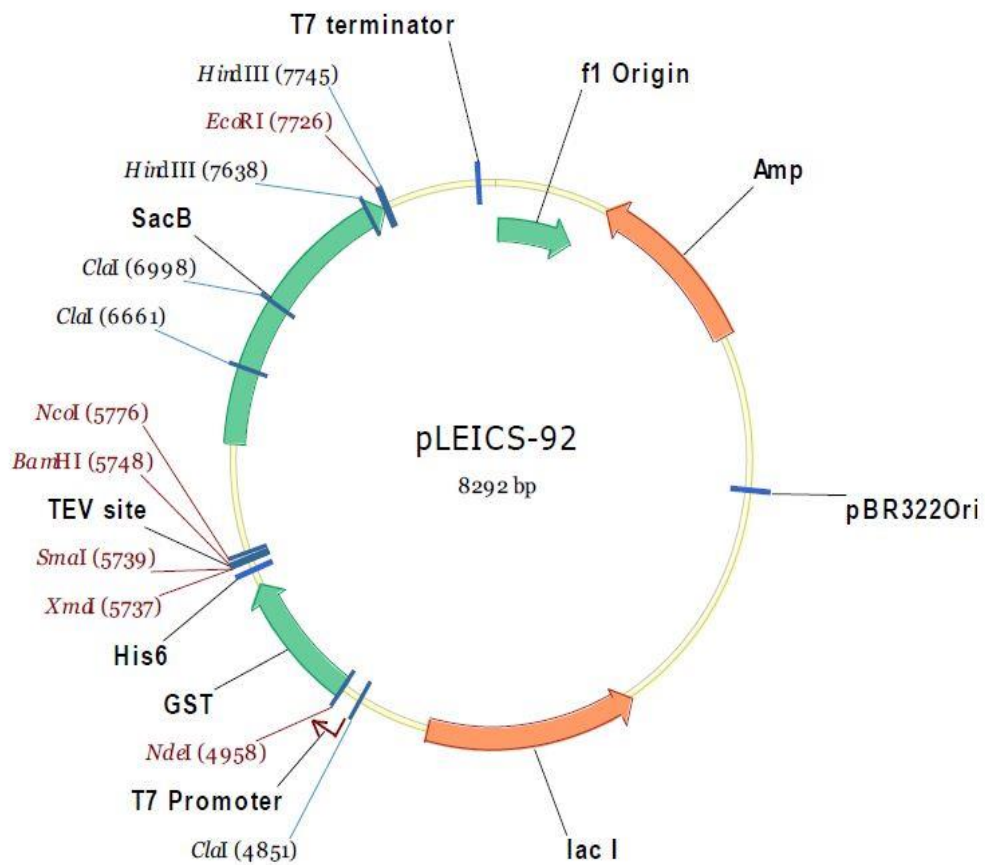


Figure 7-8 Plasmid map of the pLEICS-92 expression vector.

7.9.6.pLEICS-93

Amino acid tag: N-terminal 6 x His-tag.

Antibiotic resistance: Ampicillin.

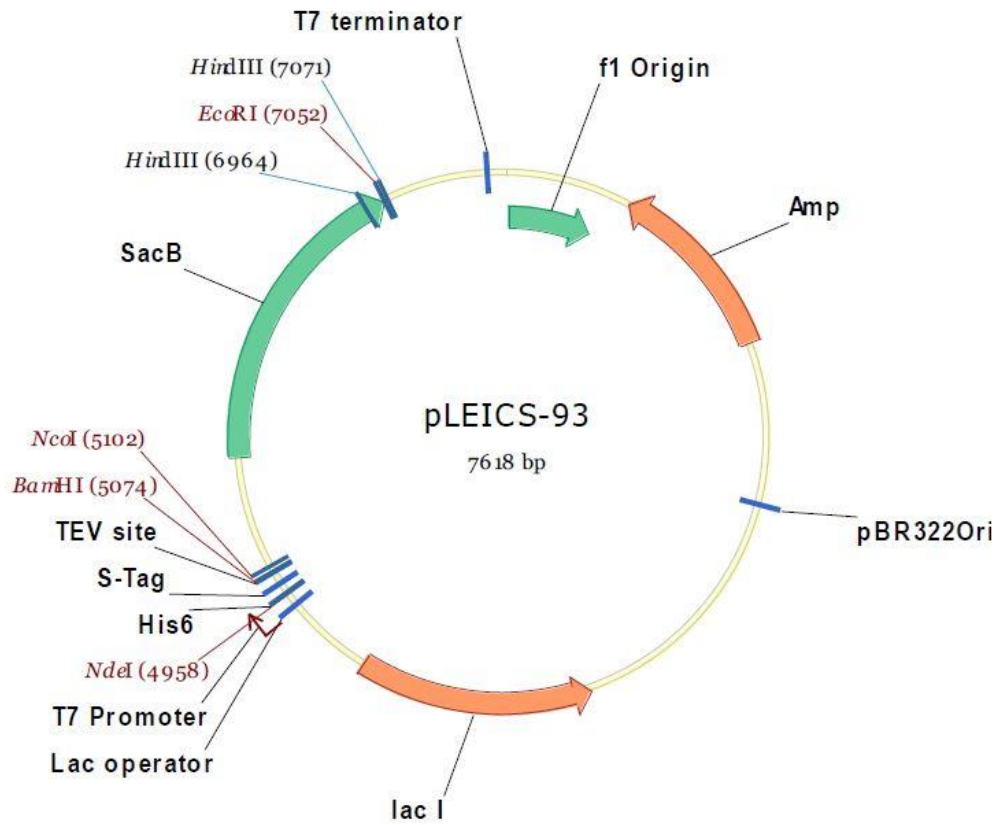


Figure 7-9 Plasmid map of the pLEICS-93 expression vector.

7.9.7.pLEICS-04

Amino acid tag: N-terminal GST-tag, a TEV protease cleavage site.

Antibiotic resistance: Kanamycin.

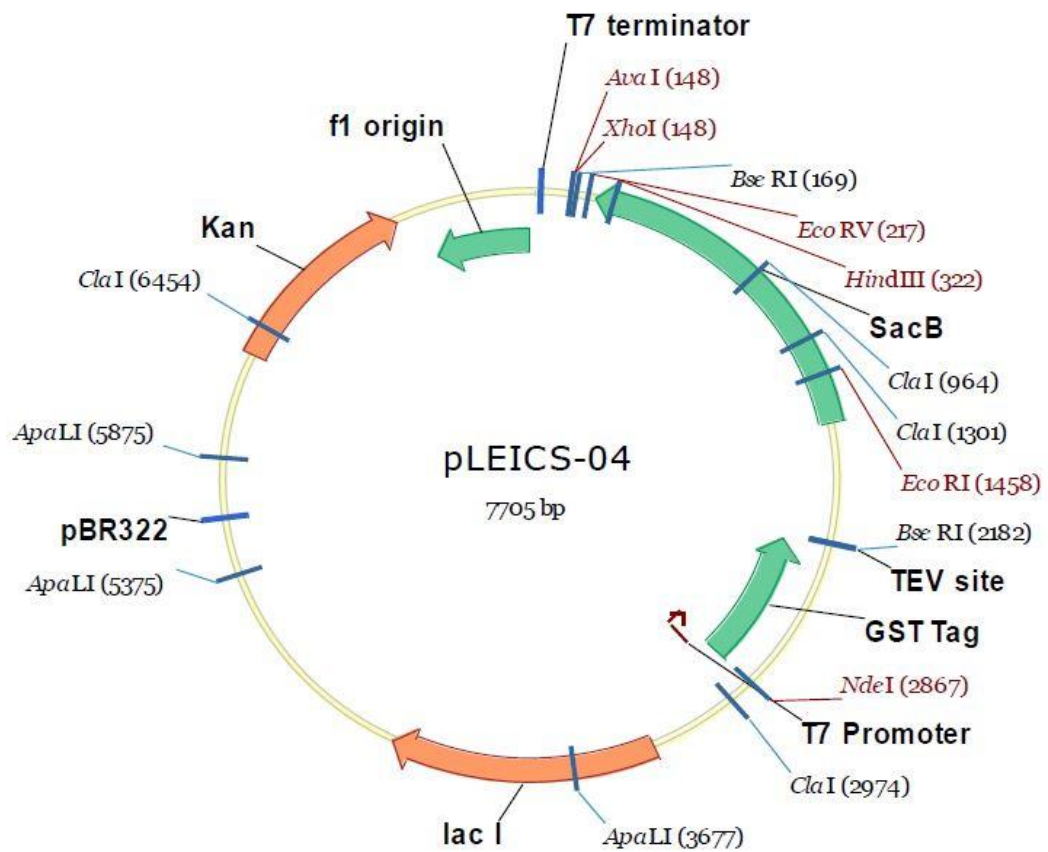


Figure 7-10 Plasmid map of the pLEICS-04 expression vector.

7.9.8. pLEICS-03

Amino acid tag: N-terminal 6 x His-tag.

Antibiotic resistance: Kanamycin.

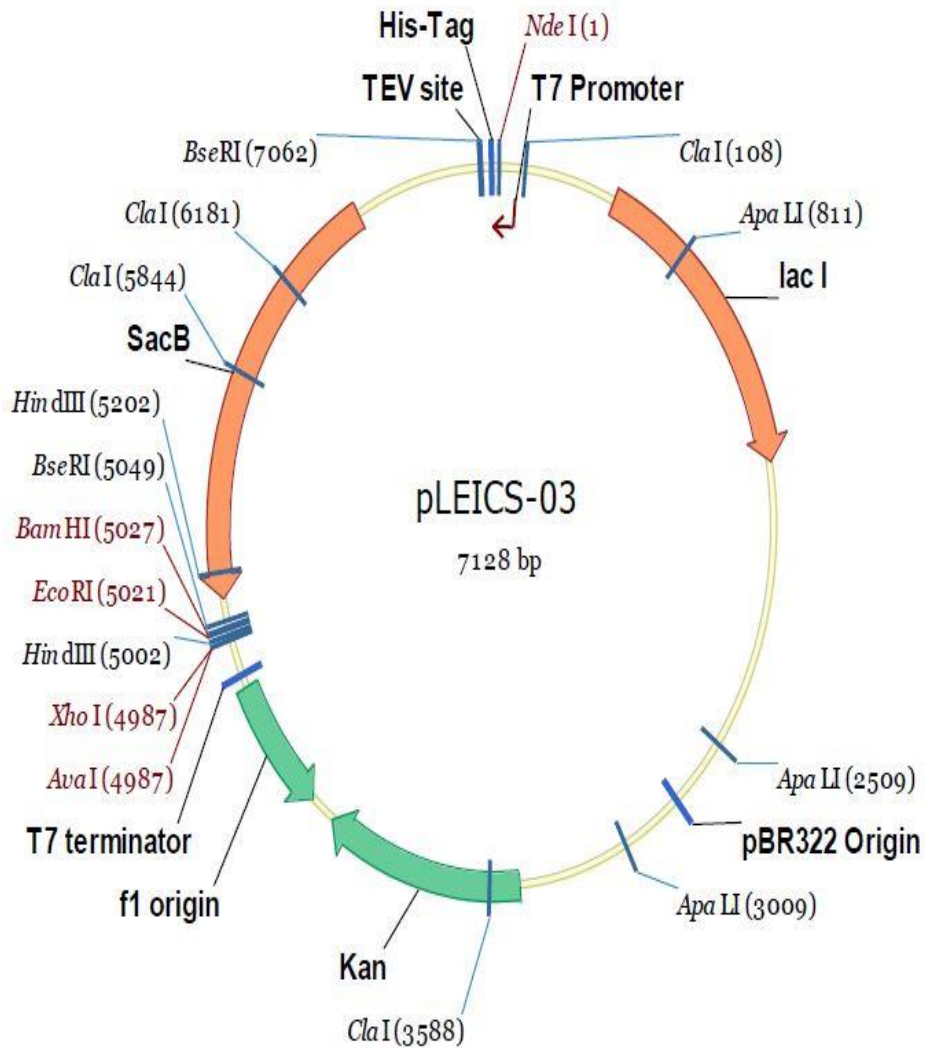


Figure 7-11 Plasmid map of the pLEICS-03 expression vector.

7.9.9.pLEICS-01

Amino acid tag: N-terminal 6 x His-tag.

Antibiotic resistance: Ampicillin.

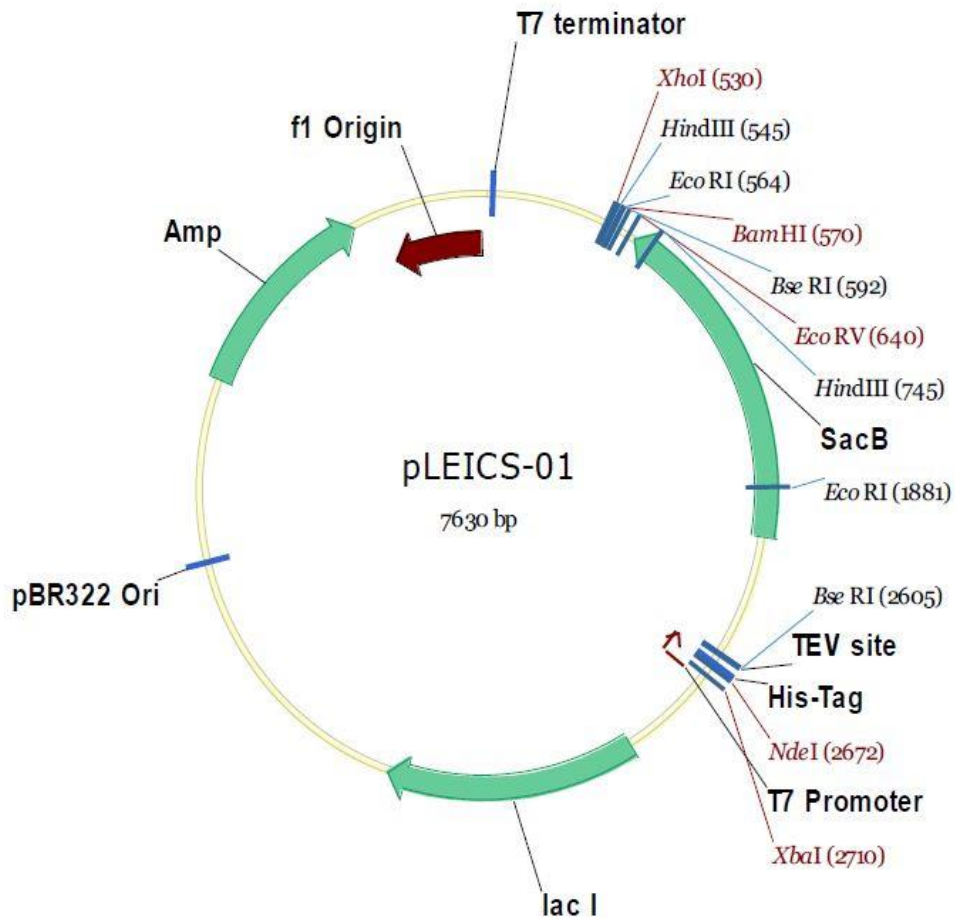


Figure 7-12 Plasmid map of the pLEICS-01 expression vector.

Table 7-2 Type and concentration of antibiotic for each vector was used.

No.	Vectors	Antibiotic resistance	final concentration
1.	pLEICS-01	Ampicillin	100 µg/ml.
2.	pLEICS-03	Kanamycin	50 µg/ml
3.	pLEICS-04	Kanamycin	50 µg/ml
4.	pLEICS-05	Ampicillin	100 µg/ml
5.	pLEICS-07	Kanamycin	50 µg/ml
6.	pLEICS-10	Ampicillin	100 µg/ml.
7.	pLEICS-14	Ampicillin	100 µg/ml.
8.	pLEICS-92	Ampicillin	100 µg/ml
9.	pLEICS-93	Ampicillin	100 µg/ml

